Molecular analyses of host-microbe interactions in the ancient metazoan *Hydra*

Dissertation

zur Erlangung des Doktorgrades
der Mathematisch-Naturwissenschaftlichen Fakultät
der Christian-Albrechts-Universität
zu Kiel

vorgelegt von

Katja Schröder

Kiel, im November 2018

Erster Gutachter: Prof. Dr. Dr. h.c. Thomas C. G. Bosch

Zweiter Gutachter: Prof. Dr. Thomas Roeder

Tag der mündlichen Prüfung: 20. Dezember 2018

„Honor thy symbionts“

(Xu & Gordon 2003)

Summary

All animals are holobionts consisting of a multicellular host and its associated microbiota. The microbiota occupies different niches within a host and benefits the health of the host in various ways. The mechanisms shaping the composition and the spatial distribution of the microbiota to maintain homeostasis within a holobiont are not well understood. In this thesis different aspects of symbiotic interactions in the holobiont *Hydra* were investigated.

As a member of the ancient phylum Cnidaria, *Hydra*'s entire body is formed of an epithelial bilayer. The ectodermal epithelium facing the aquatic environment is covered by a multilayered glycocalyx. In this thesis the outer mucus-like layer of *Hydra*'s glycocalyx was identified as the natural habitat of the bacterial microbiota. To investigate the molecular composition of the glycocalyx an integrative transcriptomic and proteomic approach was applied and resulted in the identification of 79 candidate genes. Among these a family of putative antimicrobial peptides (AMPs) was identified and further characterized.

Antimicrobial activity is not restricted to epithelium-derived peptides in *Hydra*. Members of all major neuropeptide classes were shown to possess antimicrobial activity. In particular, a specific neuropeptide, termed NDA-1, was shown to affect the spatial distribution of *Hydra*'s main colonizer, the Gram-negative *Curvibacter* sp., suggesting a role for distinct nerve cells in the spatial organization of the microbiota along the *Hydra*'s body axis.

The green hydra, *Hydra viridissima*, is not only host to bacteria, but in addition harbors unicellular photosynthetic algae of the genus *Chlorella* in its endodermal epithelial cells. Genome sequencing of *Chlorella* sp. A99 revealed a degenerated nitrate assimilation pathway and a large number of amino acid transporters suggesting that the alga depends on the import of host-derived amino acids as a nitrogen source. Indeed, *in vitro* growth of otherwise obligate symbiotic *Chlorella* was supported by supplementing the medium with glutamine. Microarray transcriptional profiling of the hydra host identified, among others, a glutamine synthetase that is specifically up-regulated by photosynthetic activity of *Chlorella* as well as by supplying exogenous maltose. These results indicate a metabolic co-dependence with *Chlorella* providing the photosynthetic product maltose to *Hydra*, which in turn up-regulates glutamine synthetase expression to supply the algae with nitrogen in form of glutamine.

Interestingly, photosynthesis activity of *Chlorella* seems to affect not only host gene expression, but also the bacterial microbiota. This work provides the first detailed description of the *H. viridissima* microbiota and shows that the bacterial community composition fluctuates in light-dependent manner indicating that the photosynthetic activity of endosymbiotic *Chlorella* algae modulates the bacterial microbiota in the green *Hydra* holobiont.

Zusammenfassung

Alle Tiere sind Holobionten bestehend aus einem multizellulärem Wirt und der mit ihm assoziierten Mikrobiota. Die Mikrobiota besetzt verschiedene Nischen im Wirt und unterstützt seinen Gesundheitszustand auf verschiedenste Weise. Die Mechanismen, die die Zusammensetzung und räumliche Verteilung der Mikrobiota modellieren, um die Homöostase im Holobionten zu wahren, sind nicht komplett verstanden. In dieser Arbeit wurden verschieden Aspekte symbiotischer Interaktionen im Holobiont *Hydra* untersucht.

Als Mitglied des Phylums Cnidaria besteht der gesamte Körperbau von *Hydra* aus zwei Epithelien. Das ektodermale Epithelium steht in Kontakt mit der aquatischen Umwelt und ist von einer mehrschichtigen Glykokalyx bedeckt. In dieser Arbeit wurde die äußere, Mukus-ähnliche Schicht als das natürliche Habitat der bakteriellen Mikrobiota identifiziert. Um die molekulare Zusammensetzung der Glykokalyx zu ermitteln, wurde eine kombinierte Transkriptom- und Proteom-Analyse durchgeführt, die zur Identifizierung von 79 Kandidatengenen führte. Unter diesen wurde eine Familie putativer antimikrobieller Peptide charakterisiert.

Antimikrobielle Aktivität beschränkt sich in *Hydra* nicht nur auf epitheliale Peptide. Es konnte gezeigt werden, dass Mitglieder aller Hauptklassen von Neuropeptiden antimikrobielle Aktivität besitzen und ein spezielles Neuropeptid, NDA-1, die räumliche Verteilung des Gram-negativen Hauptkolonisierers *Curvibacter* sp. beeinflusst. Dies deutet auf eine Funktion von Neuronen bei der räumlichen Organisation der Mikrobiota entlang der *Hydra* Körperachse hin.

Die grüne Hydra, *Hydra viridissima*, ist nicht nur Wirt für Bakterien, sondern beherbergt auch einzellige, photosynthetische Algen der Art *Chlorella* in den endodermalen Epithelzellen. Die Genomsequenzierung von *Chlorella* sp. A99 zeigte, dass einerseits die Gene für den Stoffwechselweg der Stickstoff-Assimilation unvollständig sind und anderseits eine große Anzahl von Aminosäuretransporter-Genen vorliegt. Dies könnte darauf hinweisen, dass die Alge auf den Import von Aminosäuren als Stickstoffquelle angewiesen ist. Tatsächlich wurde gezeigt, dass die Supplementierung des Mediums mit Glutamin die *in vitro* Kultivierung der obligat symbiotischen Alge unterstützt. Die Transkriptionsanalyse (Microarray-Analyse) des *Hydra* Wirts identifizierte u.a. eine Glutaminsynthetase, die in Abhängigkeit der photosynthetischen Aktivität von *Chlorella* sowie durch exogene Zugabe von Maltose spezifisch hochreguliert wird. Diese Ergebnisse weisen auf eine metabolische Abhängigkeit hin, wobei *Chlorella* das Photosyntheseprodukt Maltose an *Hydra* liefert, woraufhin der Polyp die Glutaminsynthetase-Expression hochreguliert, um die Alge mit Stickstoff in Form von Glutamin zu versorgen.

Interessanterweise beeinflusst die photosynthetische Aktivität von *Chlorella* nicht nur die Genexpression des *Hydra* Wirts, sondern auch die bakterielle Mikrobiota. Diese Arbeit beinhaltet die erste detaillierte Beschreibung der *H. viridissima* Mikrobiota, wobei die bakterielle Zusammensetzung Licht-abhängigen Fluktuationen unterliegt. Dies deutet darauf hin, dass die photosynthetische Aktivität der endosymbiotischen Alge die bakterielle Mikrobiota im *H. viridissima* Holobiont moduliert.

General Introduction

From foes to friends: Rethinking host-microbe interactions

Approximately 350 years ago, the invention of primitive microscopes enabled two men, Robert Hooke and Antoni van Leeuwenhoek, to observe microorganisms for the first time (Gest, 2004). The discovery that there were forms of life, which are invisible to the naked eye, opened the door to a whole new microscopic world: the field of microbiology was born.

In 1835 the Italian entomologist Agostino Bassi discovered that the white muscardine disease of silkworms was caused by a small, parasitic fungus and thereby, gave the first proof that microorganisms are capable of causing disease. Bassi suggested that similar living agents might cause other contagious diseases. However, the idea of tiny invisible organisms in the air was considered to be a fanciful tale and although supported by the work of Bassi and others such as Edward Jenner, John Snow, and Ignaz Semmelweis the emerging 'germ theory of disease' was mostly rejected. It was only in the 1860s that the 'germ theory of disease' was strongly promoted by the experiments of Louis Pasteur, followed by the pioneering studies of Robert Koch and Joseph Lister. Pasteur demonstrated that fermentation of wine and souring of milk are caused by living microorganisms, thereby disproving the doctrine of spontaneous generation. With the discovery of the roots of food spoilage Pasteur adopted a related view on the cause of diseases. He proposed that hindering microorganisms from entering the human body may prevent certain diseases. Based on this idea Joseph Lister promoted the concept of antiseptic surgery and successfully introduced carbolic acid to clean wounds and sterilize surgical instruments. In 1876 Robert Koch discovered the bacterium *Bacillus anthracis* as the causative agent of anthrax and with the publication of his findings the 'golden age' of bacteriology had begun. In a span of just 30 years the principal bacterial pathogens of human infectious disease were isolated including anthrax, gonorrhea, typhus, tuberculosis, cholera, diphteria, tetanus, plague and syphilis (Blevins and Bronze, 2010). In 1905 Robert Koch received the Nobel Prize in medicine for his research on tuberculosis, which led him to frame his famous postulates that have guided the understanding of the nature of infectious diseases.

There is no doubt, that the eminent contributions of Louis Pasteur, Robert Koch and their fellow scientists revolutionized the medical field and had important implications for the way in which people cleaned their homes, selected and prepared food. However, the identification of microbes as causative agents of disease and food spoilage also paved the way for the idea that healthy organisms are defined as living entities free of bacteria and viruses.

Suspicion and mostly irrational fear of microbes have sustained until today, when many people regularly use antibacterial products such as soaps, detergents and hand sanitizers that claim to kill microbes on telephones, keyboards, doorknobs and even in the air. At the end of the 19th century the relationship between microbes and man was declared as a battlefront and the development of vaccines and in particular the discovery of antibiotics in the 20th century were anticipated to herald the end of infectious disease. Nowadays, we are aware that this assumption was overoptimistic and premature, thereby underestimating the outstanding ability of microorganisms to evolve effective strategies to escape drug lethality. Excessive overuse and misuse of antibiotics in medicine as well as the use of antibiotics for non-therapeutic purposes in food-producing animals promoted the emerge of multidrug-resistant bacteria. Today, many decades after the first patients were treated with antibiotics, resistance has been observed for almost all antibiotics that have been developed and bacterial infections have become a major public health threat again. Furthermore, we face the emerge of complex diseases such as irritable bowel syndrome, ulcerative colitis, Crohn's disease, and atopic dermatitis. Intriguingly, these disorders cannot be attributed to a newly arrived pathogen, instead they are accompanied by an imbalance in the ever-present bacteria, a condition termed 'dysbiosis' (Petersen and Round, 2014). Indeed, when we draw the battle line between 'them' (the microbes) and 'us' (the host) in the early 20th century an important fact was overlooked: we are inhabited by trillions of microorganisms and only a tiny fraction of them act as pathogens, while most are innocuous and even beneficial to us.

Bacteria were colonizing the earth already for 2 billion years, when first multicellular eukaryotes emerged and thus, metazoan evolution took place in a 'bacterial suspension' (Knoll, 2011; McFall-Ngai et al., 2013). From this point of view, it comes not as a surprise that strong interactions evolved between multicellular organisms and microbes and clearly, these coevolutionary relationships encompass not only parasitism and pathogenicity, but also mutualism and commensalism. Today, it is widely recognized that all animals are colonized by host-specific microbial communities including bacteria, archaea, fungi, algae, protozoa and, although not an organism in the strictest sense, viruses (Fraune and Bosch, 2007; Ley et al., 2008; Ochman et al., 2010; McFall-Ngai et al., 2013). All microbes associated with a distinct host at a given timepoint are summarized as microbiota (Lederberg and McCray, 2001), while the entirety of their genetic material is defined as microbiome. The microbiota colonizes the oral cavity, the skin or specialized organs, such as female reproductive tissues (Funkhouser and Bordenstein, 2013), the surface mucus of reef-building corals, the light organ of the Hawaiian bobtail squid *Euprymna scolopes*, and other surfaces exposed to the environment, with the

gastrointestinal tract reaching the highest bacterial densities in mammals (Turnbaugh et al., 2007; Schloissnig et al., 2013).

Over the last two decades, numerous studies in a wide range of animals have revealed that the microbiota is involved in essential physiological processes including organ development and morphogenesis (Sommer and Bäckhed, 2013), digestion (Hooper et al., 2001), metabolism (Nicholson et al., 2012; Tremaroli and Bäckhed, 2012) and immunity (Hooper and MacPherson, 2010). For instance, larval settlement and further development in many marine invertebrates is regulated by biofilm bacteria (Hadfield, 2011; Freckelton et al., 2017). In zebrafish and mice the gut microbiota was shown to be essential for proper morphogenesis of the digestive tract (Bates et al., 2006; Smith et al., 2007), while in the squid *Euprymna scolopes*, the development of the light organ is triggered by the presence of lipopolysaccharide (LPS) and peptidoglycan fragments of the bacterial symbiont *Vibrio fisheri* (Koropatnick et al., 2004). In amphibians such as salamanders the skin microbiota secretes antimycotic compounds, thereby protecting the host against fungal infection (Harris et al., 2006). Many invertebrates have intracellular bacterial symbionts, whose genes encode metabolic capabilities lacking in animals, such as the synthesis of essential amino acids (Baumann, 2005), photosynthesis (Venn et al., 2008), or chemosynthesis (Dubilier et al., 2008). Similarly, the extracellularly located mammalian gut microbiota provides an extensive repertoire of enzymes (Gill et al., 2006) and determines the host capacity to harvest energy from the diet (Ley et al., 2006; Turnbaugh et al., 2006, 2008, 2009). In addition, several studies have revealed the central role of microbial symbiosis in the normal development and maturation of the mammalian immune system (Mazmanian et al., 2005; Bouskra et al., 2008; Round and Mazmanian, 2009; Salzman, 2011; Olszak et al., 2012).

More than 50 years ago, Abrams and Bishop reported that mice devoid of live microbes show a decreased gut motility, thereby providing the first hint of a link between the intestinal microbiota and the enteric nervous system (Abrams and Bishop, 1967). However, neuroscientists have only recently revealed that the gut microbiota is indeed involved in normal development (Collins et al., 2014; Kabouridis and Pachnis, 2015) and function (Mao et al., 2013; McVey Neufeld et al., 2013) of the enteric nervous system. Within the past decade several microbial metabolites with neuroactive properties have been described (Bienenstock and Collins, 2010; Nicholson et al., 2012) and there is accumulating evidence that the influence of the gut microbiota reaches far beyond the gastrointestinal tract and affects the host's central nervous system (Sampson and Mazmanian, 2015; Vuong et al., 2017). Studies in germ-free

mice have demonstrated that these animals display significant differences in brain development and neurochemistry accompanied with an increased stress response and reduced anxiety-like behavior, indicating that the gut microbiota is involved in shaping behavioral phenotypes of the host (Sudo et al., 2004; Heijtz et al., 2011; Neufeld et al., 2011a, 2011b). These insights led to the concept of the 'microbiota-gut-brain axis', a multifaceted bidirectional communication system involving neural, endocrine, immune, and metabolic signaling as well as epigenetic regulation (Stilling et al., 2014; Carabotti et al., 2015).

Disturbances in the microbial community composition, in particular the loss of microbial and metabolic diversity, have been associated with a large array of human diseases including inflammatory bowel diseases (IBD) (Laing et al., 2018), irritable bowel syndrome (IBS) (Kennedy et al., 2014), metabolic diseases such obesity and type 2 diabetes (Hur and Lee, 2015), asthma and allergic disease (Bisgaard et al., 2011) and recently also neurological and psychiatric disorders such as multiple sclerosis (Jangi et al., 2016), Parkinson's disease (Sampson et al., 2016), autism (Mayer et al., 2014) and depression (Foster and McVey Neufeld, 2013). However, yet it remains unclear whether dysbiosis manifests as a direct cause or merely as a consequence of these diseases. There is accumulating evidence that dysbiosis can be promoted by diet (David et al., 2014), antibiotic exposure (Dethlefsen and Relman, 2011), disruption of circadian rhythm (Thaiss et al., 2014) and other environmental factors. It is proposed that resilience, the ability of a bacterial community to resist or compensate perturbations and return to the stable state, is tightly connected to the development of dysbiosis-related diseases (Greenhalgh et al., 2016; Sommer et al., 2017). The molecular mechanisms that underlie resilience of the microbiota are unknown so far, but host genetics and the individual microbiota composition, which varies across different stages of life are thought to play a role (Yatsunenko et al., 2012; Raymond et al., 2016). For example, the human gut microbiota appears to be particularly vulnerable to antibiotic-induced perturbations during the first two years of infancy, which is the time before a stable adult-like microbial community has developed (Cox et al., 2014; Zeissig and Blumberg, 2014; Scott et al., 2016). Therefore, overuse of antibiotics not only increases the risk of emerging resistance, but also may have lasting effects on the symbiotic partnership with our commensal bacteria.

In summary, research of the last two decades revealed that a homeostatic interaction with the microbiota is essential for many aspects of host fitness and a complete understanding of the biology of any eukaryotic organism requires knowledge of its microbiome. Advances in sequencing tools, such as high-throughput genomics, transcriptomics and metabolomics, have

been major drivers of progress in microbiome research. Combined with the study of germ-free animal models they provided some of the most persuasive evidence for the role of the microbiota in health and disease. However, there are still many challenges, In addition, the proposed multifactorial origin of dysbiosis-related diseases necessitates new considerations for the development of therapies and preventive treatments that target the microbiota to restore and maintain human health.

The vast majority of work investigating microbial communities has been carried out in humans or in mice as a proxy. However, investigating the biology of simpler model organisms may allow us to answer questions that are unreachable in human or mice due to the complexity of their microbiomes. A number of non-mammalian model systems have provided major insights of general significance such as the squid for integration of microbial function into the host circadian rhythm (Heath-Heckman et al., 2013), *Hydra* for the role of interactions between commensal bacteria in colonization resistance (Fraune et al., 2015) and the killifish for microbial determinants of lifespan (Smith et al., 2017).

Taken together, the long-held notion that most microbes are pathogens changed dramatically with the realization that fundamental physiological processes rely on the symbiotic partnership with them. Since the discovery of microorganisms in the 17th century, our knowledge on them extended substantially and reached a new peak with the emerge of powerful sequencing tools. The microbiome field has come a long way in a short time, but despite extensive gains in knowledge, we are only just beginning to untangle the complex interactions that connect our microbial partners inextricably to our health. The challenge of future research will be to identify the mechanistic concepts that underlie the complex relationship between the host and its microbiome, and how they change due to early-life antibiotic exposure, Western diet, shift work and stress of our fast-paced, modern lifestyle.

The holobiont / metaorganism concept

In 2006 Reshef and colleagues observed that certain corals can acquire pathogen resistance by incorporating a new bacterium into their microbiota (Reshef et al., 2006). This led them to propose the ‘coral probiotic hypothesis’, stating an important biological principle: adjusting their associated microbiota allows organisms to adapt much faster to changing environmental conditions than by genetic mutation or recombination of the host alone (Reshef et al., 2006; Rosenberg et al., 2007). Considering host-microbe interactions as significant drivers of animal evolution led to the development of the ‘hologenome theory of evolution’

implying that instead of a single animal organism an ecological consortium consisting of the multicellular host and its associated microbiota is interacting with the environment and therefore, represents a unit of natural selection (Zilber-Rosenberg and Rosenberg, 2008).

The multipartite entity of a host and its associated microbial communities is termed 'holobiont' (Rohwer et al., 2002; Zilber-Rosenberg and Rosenberg, 2008) or synonymously 'metaorganism' (Bosch and McFall-Ngai, 2011). A holobiont displays a dynamic assemblage in which microbes can be constantly or inconstantly associated with the host and colonize different niches depending on developmental stage, diet or other environmental factors (Zilber-Rosenberg and Rosenberg, 2008). The traits that microbes encode are context-dependent and may result in benefit, damage, or no consequence to the holobiont (Theis et al., 2016). Clearly, the holobiont arises not solely from cooperation and neither excludes competition and cheating between its members.

The genetic information provided by the host, united with the genomes of its microbiota are collectively defined as the hologenome (Rosenberg and Zilber-Rosenberg, 2013; Bordenstein and Theis, 2015), which is several fold more complex than the genomes of the single organisms (Bäckhed et al., 2004). Variation in the hologenome can arise by mutation and recombination in the host and the microbiome, but also by changes in microbial abundance, horizontal gene transfer among microbes, loss of symbionts, and acquisition of new microbial strains from the environment. Thus, the dynamic attributes of a holobiont translate directly to the hologenome (**Figure 1**).

The microbiome can be vertically and horizontally transmitted or selected from the environment. Although most animals and plants come in contact with billions of microorganisms during their life time, only few become stably incorporated in the holobiont. Thereby, the underlying mechanisms of accurate transmission and selection that ensure the continuity of partnerships over generations of holobionts still remain a mystery.

Recent discourse on the hologenome theory of evolution is mainly founded on the statement that 'a holobiont forms a unit of selection in evolution' (Moran and Sloan, 2015; Douglas and Werren, 2016). Indeed, the holobiont is posited to be a unit of selection (Zilber-Rosenberg and Rosenberg, 2008), but notably not the only or necessarily primary unit of selection. Not all microbes of a holobiont share an evolutionary history with the host and large parts of both the host genome and the microbiome can evolve neutrally or be in conflict (Rosenberg and Zilber-Rosenberg, 2013; Bordenstein and Theis, 2015). The members of a holobiont face and respond to environmental pressures as individuals and as a community and

thus, holobionts can be formed through neutral processes and through selection at multiple levels (Douglas and Werren, 2016; Theis et al., 2016).

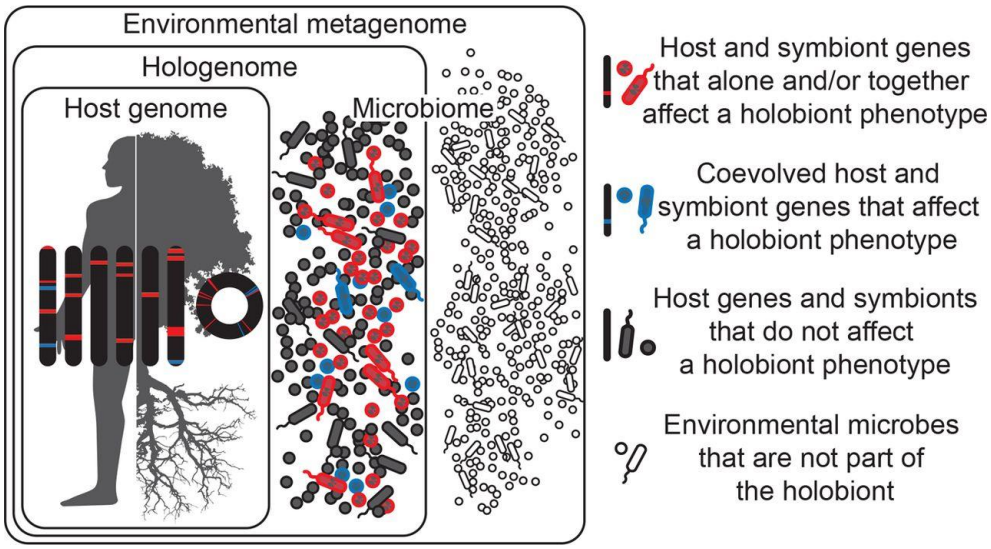

Figure 1. The hologenome concept.
Holobionts are dynamic entities comprised of an individual host and its microbial community, including cellular microorganisms and viruses. Thereby, both microbes that have coevolved with host (blue) and those which have not (red) can affect the holobiont's phenotype, while others again do not affect the holobiont's phenotype at all (gray). Microbial symbionts can be vertically or horizontally transmitted, can be constant or inconstant and therefore, the holobiont phenotype can change as microbes come into and out. Microbes in the environment are not part of the holobiont (white).
Hologenomes encompass the genomes of the host and all of its microbes at any given time point, with individual genomes and genes falling into the same three functional categories of blue, red, and gray. Taken from (Theis et al., 2016).

Innate immunity and the microbiota

For each living organism self-nonself discrimination is of tremendous importance to recognize invading microbes or degenerated cells and subsequently initiate defense strategies that ensure the reproductive success and survival of the species (Khalturin and Bosch, 2007; Rosenstiel et al., 2009). However, the recent advances in the microbiome field have shown that all animals are stably associated with a specific and diverse microbiota, which has fundamental impact on many aspects of host fitness and normally does not trigger inflammation (Bäckhed et al., 2005; Dethlefsen et al., 2007; Nyholm and Graf, 2012; McFall-Ngai et al., 2013). In this framework, it is clear that the immune system must allow a certain amount of tolerance towards the microbiota to avoid constant activation and chronic inflammation. Therefore, the healthy immune system must be able to distinguish not only between ‚self' and ‚nonself', but also between ‚friend' and ‚foe'.

An introduction to immunity

In the broadest sense the immune system displays a mechanism that allows organisms to discriminate between ‚self' and ‚non-self'. In jawed vertebrates including humans two immunologic subsystems are distinguished; the innate and the adaptive (acquired) immune system. The adaptive immune system responses relatively slow but mediates a long-term memory of past infections that protects the organism against attacks of the same pathogen in the future (Cooper and Alder, 2006). Thereby, the somatic rearrangement of antigen receptor genes allows the generation of highly-specific receptors for virtually any protein or carbohydrate. Since invertebrates lack adaptive immunity, they exclusively rely on the primordial defense strategies comprised by the innate immune system (Beutler, 2004). The innate immune system is activated fast and encompasses the non-specific barrier function of epithelia, recognition of microbes *via* germline-encoded receptors, activation of phagocytes and humoral components such as the complement system and antimicrobial peptides (AMPs) (Takeuchi and Akira, 2010).

A critical first step in initiating an innate immune response is the sensing of microbes, which is mediated by germline-encoded pattern recognition receptors (PRRs) present in the extracellular milieu and endosomal compartments of immune and non-immune cells. PRRs encompass structurally divergent proteins, which are divided into five families based on protein domain homology: the Toll-like receptors (TLRs), the C-type lectin receptors (CLRs), the retinoic acid-inducible gene (RIG)-I-like receptors (RLRs), the nucleotide-binding oligomerization domain (NOD)-like receptors (NLRs) and the absent in melanoma 2 (AIM2)-like receptors (ALRs) (Takeuchi and Akira, 2010). Each of these receptor families detects conserved microbe-associated molecular patterns (MAMPs) such as lipopolysaccharide (LPS), flagellin, peptidoglycans and CpG DNA in a multicellular host and triggers different intracellular signaling cascades leading to transcriptional expression of inflammatory mediators that coordinate the elimination of invading microbes and infected cells. In addition to MAMPs, some PRRs are capable to sense damage associated molecular patterns (DAMPs), which display endogenous molecules released from damaged cells such as histones, genomic and mitochondrial DNA, ATP and heat-shock proteins (Matzinger, 2002; Takeuchi and Akira, 2010). Thus, an innate immune response can also be initiated in absence of microbes, resulting in so-called ‘sterile inflammation’ that arises from non-physiological cell death, damage, or stress (Kono and Rock, 2008; Rock and Kono, 2008).

Beyond pathogen defense – innate immunity in homeostasis and tolerance

When exploring symbiotic host-microbe interactions in the past decade, much has been learned about the organization and function of the immune system. Intruigingly, the microbiota was shown to play a fundamental role in the development, maturation and normal function of the host immune system (Belkaid and Hand, 2014). For instance, studies in mice revealed that the microbiota promotes lymphoid organogenesis, activates regulatory T cells and balances pro- and anti-inflammatory cytokines (Mazmanian et al., 2005; Round and Mazmanian, 2009; Round et al., 2011). Furthermore, key players of the innate immune system, such as PRRs and AMPs appear to act not only in pathogen defense, but also in establishment of a homeostatic relationship between the host and its microbiota. For example, TLR-signaling was shown to play a critical role in the maintenance of intestinal homeostasis (Rakoff-Nahoum et al., 2004; Lee et al., 2006; Mukherji et al., 2013). Knockout of the key adaptor protein MyD88 in mice led to impaired antimicrobial activity, diminished mucus levels, differences in the microbial composition, bacterial translocation and increased colitis susceptibility (Frantz et al., 2012). MAMPs display ubiquitous molecular signatures present in pathogenic as well as in commensal microorganisms and thus, should trigger the same response in both cases (Pasare and Medzhitov, 2005; Akira et al., 2006; Medzhitov, 2007). However, it was shown that the permanent recognition of the microbiota by TLRs induces tolerance instead of inflammation, which is crucial for intestinal homeostasis (Rakoff-Nahoum et al., 2004; Lee et al., 2006). The underlying mechanisms of this phenomenon are not completely understood, but research of the last decade has shed light on some aspects of it. One strategy in promoting microbial tolerance is the compartmentalization of TLR expression to specific cell types and locations in the gut (Cario, 2008, 2010; Yu and Gao, 2015). For instance, in the human colon TLR3 and TLR5 are abundantly expressed, while TLR2 and TLR4 expression is low, but inducible (Cario, 2008, 2010). In addition, individual TLRs induce different sets of cytokines, thus there are many levels of regulation that allow fine-tuning of the immune response.

Taken together, animal host have developed an array of immune responses that on the one hand allow establishing a profitable homeostatic coexistence with thousands of different microbes, while on the other hand enable effective combating of pathogen invasion. In addition, the microbiota itself seems to contribute to immune tolerance. Numerous members of the order *Bacteroidales,* which display the dominant Gram-negative bacteria in the healthy human gut microbiota, produce antagonistic forms of LPS that inhibit TLR-4 signaling and thus, dampen innate immune activation (Vatanen et al., 2016; d'Hennezel et al., 2017).

Antimicrobial peptides – small molecules with many faces

Antimicrobial peptides (AMPs) are evolutionarily ancient components of the innate immune system that are produced by almost all plants and animals and show direct microbiocidal activity against Gram-positive and Gram-negative bacteria (Zasloff, 2002), viruses (Albiol Matanic and Castilla, 2004) or fungi (De Lucca and Walsh, 1999) in micromolar concentrations (Matsuzaki, 1999; Jenssen et al., 2006). In vertebrates, most AMPs are produced by epithelial cells of the respiratory, gastrointestinal and urogenital tract, keratinocytes of the skin and immune cells such as macrophages and neutrophils (McCormick and Weinberg, 2010). The temporal and spatial expression of different AMPs is tightly regulated with some being constitutively produced, while others are only expressed at high levels upon activation of PRRs during infection (Cash et al., 2006). Some AMP families are widely conserved throughout evolution, such as the defensins that are found in a several phyla including vertebrates, mollusks, arthropods, plants and fungi (Wong et al., 2007). However, most AMPs are considered as taxonomically restricted genes (TRGs) (Khalturin et al., 2009) meaning that they are present only in a few species belonging to close phylogenetic groups, which indicates that they have undergone an extensive co-evolution with the diverse world of microorganisms. AMPs are extremely variable in amino acid composition and show a wide range of secondary structures with β-sheets, α-helices, loop structures, and extended structures being the most prominent (Jenssen et al., 2006) (**Figure 2**). Nevertheless, classical AMPs share similar characteristic features such as small size (6 to 59 amino acids), positive charge, and amphipathic secondary structures, i.e. molecular conformations with both hydrophilic and hydrophobic domains. Most eukaryotic AMPs are synthesized as prepropeptides and stored in secretory vesicles as inactive propeptides after removal of the signal peptide. The mature AMP is finally generated through a second proteolytic cleavage. Thereby, the microbicidal activities of many AMPs are limited under physiological salt concentrations (Scott and Hancock, 2000), but are exerted on the external surfaces of the skin and the mucosal epithelia lining the gut, the respiratory and reproductive tract (Ganz and Lehrer, 1998).

The mechanism of antimicrobial action is often due to large cationic patches on the molecular surface of AMPs, which enables electrostatic interaction with the anionic phospholipids of the microbial cell membrane (Epand and Epand, 2009). Thereby, many AMPs permeabilize the membrane by pore formation leading to collapse of the transmembrane potential and finally resulting in cell death (Hale and Hancock, 2007; Wimley, 2010). For this reason, they are less likely to induce resistance in microbes (Hale and Hancock, 2007) than

conventional pharmaceutical antibiotics, which are typically directed towards single, mostly enzymatic targets (Nguyen et al., 2011; Fjell et al., 2012). In addition, multicellular organisms simultaneously produce various AMPs that belong to multiple structural classes and exhibit different modes of action. Thus, the development of a single resistance mechanism, most likely is not sufficient to avoid the lethal assault of a diverse group of AMPs (Zasloff, 2002). In addition, AMPs can accumulate at infection sites to extremely high local concentrations, which cannot be completely overcome by most microbial resistance strategies (Diamond et al., 2000; Ghosh et al., 2002).

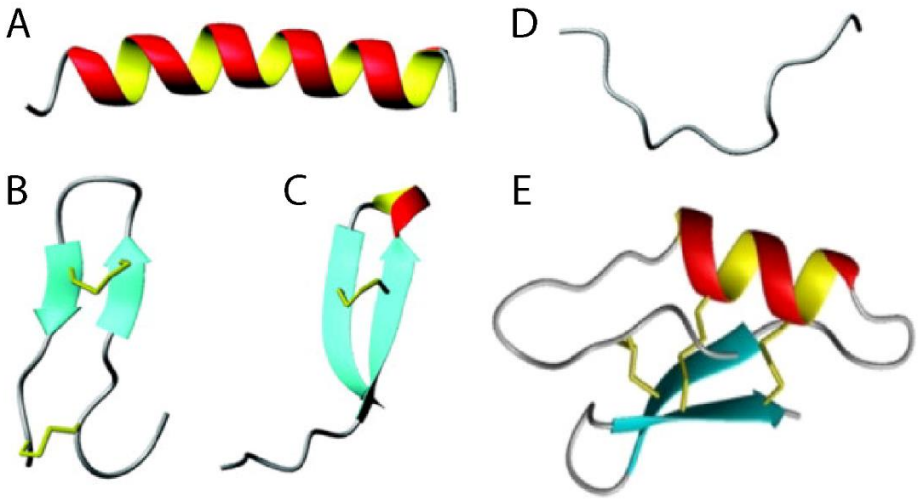

Figure 2. Common structural classes of antimicrobial peptides.
(A) α-helical magainin-2. (B) β-sheeted polyphemusin. (C) looped cathelicidin LL-37. (D) extended indolicidin. (E) mixed secondary structure of plectasin. Disulfide linkages are indicated by yellow bonds. Taken from (Jenssen, 2009; Ong et al., 2014).

Although AMPs were initially recognized as potent natural antibiotics determined to kill pathogens, it is becoming clear that they also play an essential role in shaping the composition and location of the commensal microbiota (Bevins and Salzman, 2011; Nakatsuji and Gallo, 2012). Several studies provide compelling evidence that experimental manipulation of AMPs affects the resident microbiota by changing their composition (Vaishnava et al., 2008; Salzman et al., 2010; Franzenburg et al., 2013b) or behavior (Login et al., 2011). Furthermore, AMPs such as the mammalian antibacterial lectin RegIIIγ were shown to regulate the spatial relationship between the microbiota and the host (Vaishnava et al., 2011). In a healthy gut environment with bacteria restricted to the outer mucus layer, while RegIIIγ is localized in the bacteria-free inner mucus layer. RegIIIγ defiency results in loss of this spatial separation between bacteria and the intestinal surface, which is reflected by a dramatic increase in bacterial translocation and chronic intestinal inflammation (Vaishnava et al., 2011; Loonen et al., 2014).

Interestingly, several studies have shown that the microbiota itself promotes the production of AMPs (Hooper et al., 2003; Schauber et al., 2003; Cash et al., 2006; Brandl et al., 2007; Vaishnava et al., 2008). For instance, studies on the skin innate immune system revealed that secreted factors of the cutaneous microbiota induce AMP expression *via* TLR-2 and NF-κB activation (Wanke et al., 2011). These data indicate that the commensal microbiota is involved in maintenance of AMP steady-state production and thus, enhances the antimicrobial shield that provides resistance to infection and overgrowth of pathogens. Strikingly, the predominant members of the human gut microbiota were shown to have an increased tolerance to host AMPs compared with foreign bacteria, which likely contributes to the temporal stability of the resident gut microbiota during host inflammatory response (Cullen et al., 2015; Kwong et al., 2017).

Furthermore, there is increasing evidence that AMPs are pleiotropic, multifunctional molecules with immunomodulatory properties. Several mammalian AMPs were shown to interact with various receptors, thereby influencing cellular processes in the host (Lai and Gallo, 2009). For example, some AMPs were shown to modulate TLR-dependent inflammatory responses (Biragyn et al., 2002; Mookherjee et al., 2006; Di Nardo et al., 2007) and promote wound healing (Mangoni et al., 2016). Furthermore, the mammalian AMPs of the cathelicidin as well as the α- and β-defensin families were shown to have chemotactic function on monocytes, immature dendritic cells and T cells (Yang et al., 1999, 2000; De Yang et al., 2000; García et al., 2001; Rohrl et al., 2010). While micromolar concentrations exert the antimicrobial activity against invasive microorganisms, nanomolar concentrations of distinct AMPs may form a gradient in the tissue to attract phagocytes to endangered sites and thus, amplify the immune response by calling for help. The multiple indirect functions of AMPs not only complement their antimicrobial action but may be important for limiting the evolution of microbial resistance. Conventional pharmaceutic antibiotics are acting through a single approach and thus, can be completely evaded by a single resistance system. In contrast, AMPs may have retained their efficacy over evolutionary time scales because their role in host defense is much broader than that of endogenous antibiotics. Clearly, many pathogens succeeded in developing resistance against the direct antimicrobial activity of AMPs (Gruenheid and Le Moual, 2012; Nawrocki et al., 2014). However, these AMPs may still contribute to host defense by triggering recruitment and activation of various immune cells to favor resolution of infection and repair of damaged epithelia.

Numerous studies have provided compelling evidence that AMPs play a role in a variety of human diseases, including atopic dermatitis, psoriasis, cystic fibrosis and inflammatory bowel diseases (IBD) (Zaiou, 2007). However, it is important to note that until today not a single disease has been proven to be directly caused by AMP deficiency, dysregulation or overproduction. Instead, it seems to require multiple genetic lesions that target other immune mechanisms in addition to the defects in AMP production. To gain a better understanding of how AMPs are involved in complex inflammatory diseases, it will be crucial to acknowledge not only their antimicrobial action, but also their role as multifunctional mediators, which act in shaping the commensal microbiota and influence diverse processes including cytokine release, chemotaxis and wound healing and adaptive immune induction.

The freshwater polyp *Hydra*

Hydra was introduced as model organism in developmental biology as early as 1744 (Trembley, 1744). Its enormous regeneration capacity together with its simplistic anatomy described below predestined the polyp to study axial patterning, neurogenesis, cell differentiation, stem cell function, endosymbiosis and recently also host-microbe interactions. In 2010 the genome of *Hydra magnipapillata* was sequenced (Chapman et al., 2010) revealing that *Hydra* possesses most of the gene families found in bilaterians and therefore has retained many ancestral genes that have been lost in model ecdysozoan species like *D. melanogaster* and *Caenorhabditis elegans* (Miller et al., 2005; Technau et al., 2005).

Phylogeny of *Hydra*

The freshwater polyp *Hydra* belongs to the oldest eumetazoan phylum, the diploblastically organized Cnidaria. The phylum consists of approximately 9,000 species and is the proposed sister group of the Bilateria, which are composed of three blastodermic layers (Wainright et al., 1993; Medina et al., 2001; Schierwater et al., 2009) (**Figure 3**). The Cnidaria separate from the Parazoa (Porifera and Placozoa) by the possession of a nervous system and epithelia of polarized cells, which are connected by septate junctions (Faurot, 1895, 1903; Cleave and Hyman, 1940; Jägersten, 1955; Schierwater et al., 2009). The members of the phylum are distinguished from all other animals by possession of a specific stinging cell, the nematocyte (cnidocyte), which can be used for predation, adhesion or defense (Holstein, 1981; Tardent and Holstein, 1982; Lengfeld et al., 2009) and is considered to be one of the most complex cell types in animal kingdom (Tardent, 1995).The phylum Cnidaria is subdivided into

five classes; the Anthozoa including corals and sea anemones, followed by the classes of Staurozoa, Scyphozoa, Cubozoa and Hydrozoa (Collins et al., 2006).

The genus *Hydra* belongs to the Hydrozoa and was, based on their morphology, divided into four species groups: the *viridissima* group ('green' hydra), the *braueri* group ('gracile' hydra), the *oligactis* group ('stalked' hydra) and the *vulgaris* group ('common' hydra) (Campbell, 1987). Only members of the *viridissima* group live in a stable endosymbiosis with unicellular algae of the genus *Chlorella*, while members of the other three groups do not harbor intracellular algae and are summarized as 'brown' *Hydra*. Sequence analyses of mitochondrial and nuclear marker genes support the four groups proposed and unraveled the phylogenetic relationships of *Hydra* species within the distinct groups (Hemmrich et al., 2007a; Schwentner and Bosch, 2015) (**Figure 3**). The 'green' *Hydra* of the *viridissima* group appeared to be the most ancestral group followed by the *braueri* group. The *vulgaris* group was identified to be the most derived as well as the most diverse group within the genus *Hydra* (**Figure 3**) (Martínez et al., 2010; Schwentner and Bosch, 2015). The laboratory strain *Hydra vulgaris* (AEP), which is utilized for the generation of stable transgenic animals (Wittlieb et al., 2006), was shown to be conspecific with *H. carnea* (Hemmrich et al., 2007a; Schwentner and Bosch, 2015).

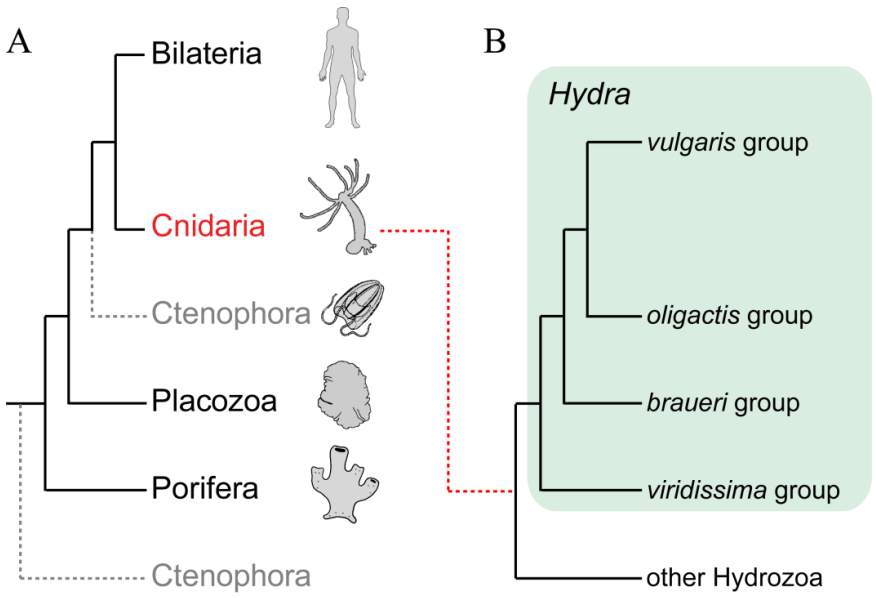

Figure 3. Phylogenetic classification of *Hydra*.
(A) Schematic representation of an eumetazoan phylogenetic tree. Cnidaria are shown as the sister group to the Bilateria. The phyolgentic position of the Ctenophora is still discussed (Pisani et al., 2015). Modified from (Murillo-Rincon et al., 2017). (B) Phylogenetic tree of the genus *Hydra* based on genomic analyses. Illustrated after (Schwentner and Bosch, 2015).

Biology and reproduction of *Hydra*

While most hydrozoans reside in marine environments, polyps of the genus *Hydra* are exclusively found in freshwater ponds or lakes, where they attach to substratum of organic and anorganic material. *Hydra* polyps are globally distributed in the temperate and tropical regions of the Northern and Southern Hemisphere with sometimes multiple species living in same location in close proximity (Martínez et al., 2010). While all *Hydra* species are sensitive to salt, some species are tolerant to huge temperature shifts and survive temperatures between 5 °C and 30 °C (Schroeder and Callaghan, 1981). The polyps feed on small crustaceans, nematodes and insect larvae, which they capture with their nematocytes equipped tentacles (Trembley, 1744). The prey is ingested through the mouth opening into the gastric cavity, where extracellular digestion *via* peristalsis and proteolytic enzymes released by the gland cells begins. Finally, the endodermal epithelial cells take up the pre-digested food through phago- and pinocytosis. Indigestible material is ejected through the mouth opening 6 to 9 hours after feeding (Shimizu et al., 2004).

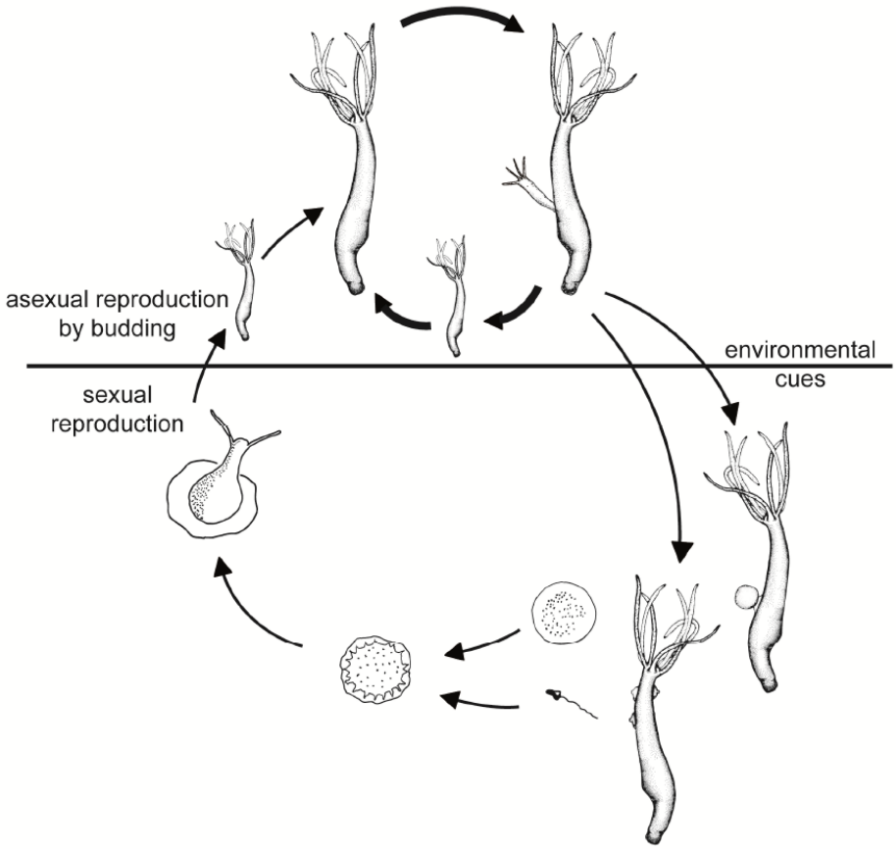

Figure 4. The life cycle of *Hydra*.
Asexual reproduction takes place by budding, while gamete formation is triggered by different environmental cues. Modified from (Bosch, 2012).

Hydra reproduces mainly asexually but can also form eggs and sperms for sexual reproduction (Bosch and David, 1987). Asexual reproduction by budding is tightly linked to food supply (**Figure 4**). Under well-fed conditions the doubling time of a single polyp can reach three to four days, facilitating clonal propagation of laboratory cultures (David and Campbell, 1972; Bosch and David, 1984). Sexual reproduction is induced by different environmental cues, e. g. temperature decrease in *H. oligactis* or a starvation period in *H. viridissima* and *H. vulgaris* (AEP) (Littlefield et al., 1991). Concerning the determination and maintenance of sex various strategies can be observed in different *Hydra* species. While *H. viridissima* polyps are hermaphrodites and develop testes and eggs at the same time, other species such as *H. oligactis* are gonochoric (exclusively male or female). *H. magnipapillata* and *H. vulgaris* are designated as unstable gonochoric, since they can spontaneously change their sex (Bosch and David, 1986). During sexual reproduction testes and egg patches are formed on the external wall of the body column of the polyp (**Figure 5B**). An egg patch contains thousands of germ cells with only one cell giving rise to the oocyte, while the rest differentiates into nurse cells (Miller et al., 2000). The oocyte is fertilized by free-swimming sperm that are released from the testes into the surrounding water. The embryo stays attached to the mother polyp in the early phase of embryogenesis, but usually detaches before gastrulation is completed. Gastrulation is followed by a cuticle stage, which is characterized by a thick outer layer protecting the embryo from the external environment (Martin et al., 1997). Under laboratory conditions hatching occurs two to four weeks after fertilization. However, protected by the thick cuticle, embryos can overwinter unfavorable conditions in a period of dormancy up to 52 weeks (Martin et al., 1997). Finally, a small *Hydra* polyp hatches directly from the cuticle stage without the occurrence of any larval stage. The young polyps are able to capture, uptake and digest prey immediately after hatching and rapidly grow to adult size.

Morphology and histology of *Hydra*

The 0.5 cm sized *Hydra* polyps show a simple radially symmetric body plan, which can be subdivided into three regions along the oral-aboral body axis: head, body column and foot (**Figure 5A**). The oral pole contains the head structures with the dome-shaped hypostome, which is surrounded by a ring of 4 to 12 tentacles used to capture prey (Liu and Chang, 1946). The center of the hypostome harbors the mouth opening, which is used for both food uptake as well as excretion of waste products of digestion. In contrast to most animals, the mouth of *Hydra* is not a permanent opening, but when closed, it presents a continuous epithelial sheet

sealed with septate junctions (Campbell, 1987). The tube-like body column encloses the gastric cavity and represents the zone of gonad and bud formation. The aboral foot consists of a stalk region and the basal disc with the mucus-producing cells that allows the polyps to attach to different substrates. Although *Hydra*'s gastric cavity is commonly believed to display a blind sac with only one opening at the oral pole, there is also a narrow opening in the center of the basal disc at the aboral pole (Shimizu et al., 2007). The function of the so-called aboral pore remains unclear.

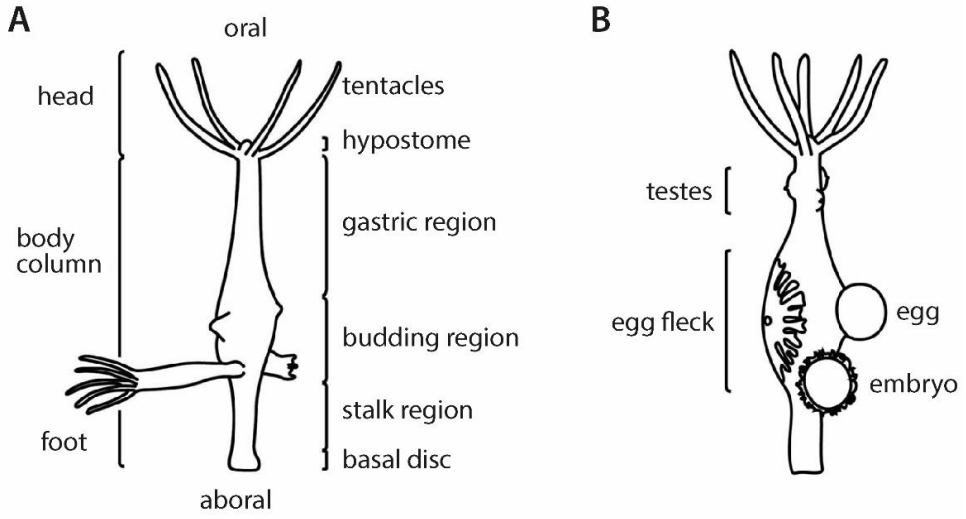

Figure 5. The morphology of *Hydra*.
Schematic drawing of *Hydra* polyps**.** (A) Asexual phenotype. (B) Sexual phenotype. Modified after (Campbell and Bode, 1983).

The cnidarian body plan is diploblastically organized, thereby consisting of only two germ layers; the endoderm and the ectoderm. A third germ layer, the mesoderm, is a characteristic feature of the Bilateria and thus, not present. The cnidarian endoderm and ectoderm represent epithelial monolayers with the endoderm lining the gastric cavity and the ectoderm facing the external environment. They are separated by an extracellular matrix, termed mesoglea, which functions as a basal lamina. The mesoglea is secreted by both epithelial layers and allows ecto–endodermal cell contacts through small pores (Shimizu et al., 2002, 2008; Seybold et al., 2016).

The whole *Hydra* polyp is built up by about 100,000 cells, which comprise approximately 20 cell types that are derived from three stem cell lineages (Bosch, 2009; Hemmrich et al., 2012). Two separate lineages of stem cells give rise to the ectodermal and endodermal epitheliomuscular tissue, which harbor contractile myofibrils at their basal part, while they are connected to neighboring cells by apical junctional belts and exhibit the

characteristic apical-basal polarity of epithelial cells. In the ectoderm the myofibrils run parallel to the oral-aboral body axis and thus form a longitudinal muscle for contraction of the body, whereas the endodermal myofibrils are oriented circumferentially functioning as a ring muscle. The third stem cell lineage is represented by a population of multipotent interstitial cells (i-cells) interspersed among the ectodermal epithelium throughout the gastric region. The multipotent i-cell stem cell lineage gives rise to several different cell types (David and Murphy, 1977; Bode et al., 1987); (i) the neurons, which are interspersed among both epithelial layers forming a net within the entire body (Bode et al., 1973). (ii) the endodermally located gland cells that secrete mucus and digestive enzymes into the gastric cavity. (iii) the ectodermally located proliferating nematoblasts, which form clusters of 4, 8 or 16 cells and terminally differentiate into nematocytes when reaching the tentacles, where they are incorporated into differentiated ectodermal epithelial cells, so-called battery cells (Slautterback and Fawcett, 1959; Dübel et al., 1987). (iv) the ectodermally located germ cells, whose formation is triggered by different environmental cues (**Figure 5B and Figure 6A**). Consequently, there is no separate germ line in *Hydra* (Bosch and David, 1987; Bosch, 2007).

All three stem cell lineages are permanently proliferating and conform to a well-defined spatial distribution across the whole body column, which can be considered as *Hydra*'s stem cell niche. Thus, there is a continuous cell flow from the body column to the head, the foot and to the developing bud. Excessive cells are sloughed off at the basal disc, the hypostome and the tips of the tentacles (**Figure 6A**) (Campbell, 1967; Holstein et al., 1991; Bosch, 2003). Depending on their position along the body axis the cells differentiate and change in morphology and function, e. g. ectodermal epitheliomuscular cells transdifferentiate into mucus-secreting cells at the basal disc, whereas they form battery cells when reaching the tentacles.

A characteristic feature of most animal epithelial cells is a dense forest of highly diverse and constantly renewed transmembrane glycoproteins, proteoglycans and glycolipids at the apical cell surface, referred to as the glycocalyx (Moran et al., 2011; Ouwerkerk et al., 2013). In *Hydra* only the ectodermal apical surface is covered by a glycocalyx, while the endoderm does not possess a comparable structure. Instead, endodermal epithelial cells are ciliated with pseudopod-like protrusions on the apical surface reflecting their phagocytotic function (**Figure 6B**). The ectodermally derived glycocalyx extends up to 1.5 µm from the cell surface and is composed of at least five morphologically distinguishable layers (**Figure 6C**) (Holstein et al., 2010; Böttger et al., 2012). All layers as well as the large secretory vesicles underneath

the apical membrane, were shown to be highly periodic acid-Schiff stain (PAS) reactive, indicating a high carbohydrate content (Böttger et al., 2012). Although the structure was initially termed glycocalyx, the characteristic feature of being membrane-bound does not account for all of its parts. The outer layer, which accounts for more than 50% of the glycocalyx, is made of a loose meshwork that can be removed completely by a hypertonic salt wash, whereas the four inner layers display a dense composition and are firmly attached to the epithelial surface (Böttger et al., 2012). Therefore, the outer layer of *Hydra*'s glycocalyx has mucus-like properties rather than being a part of the membrane-anchored glycocalyx.

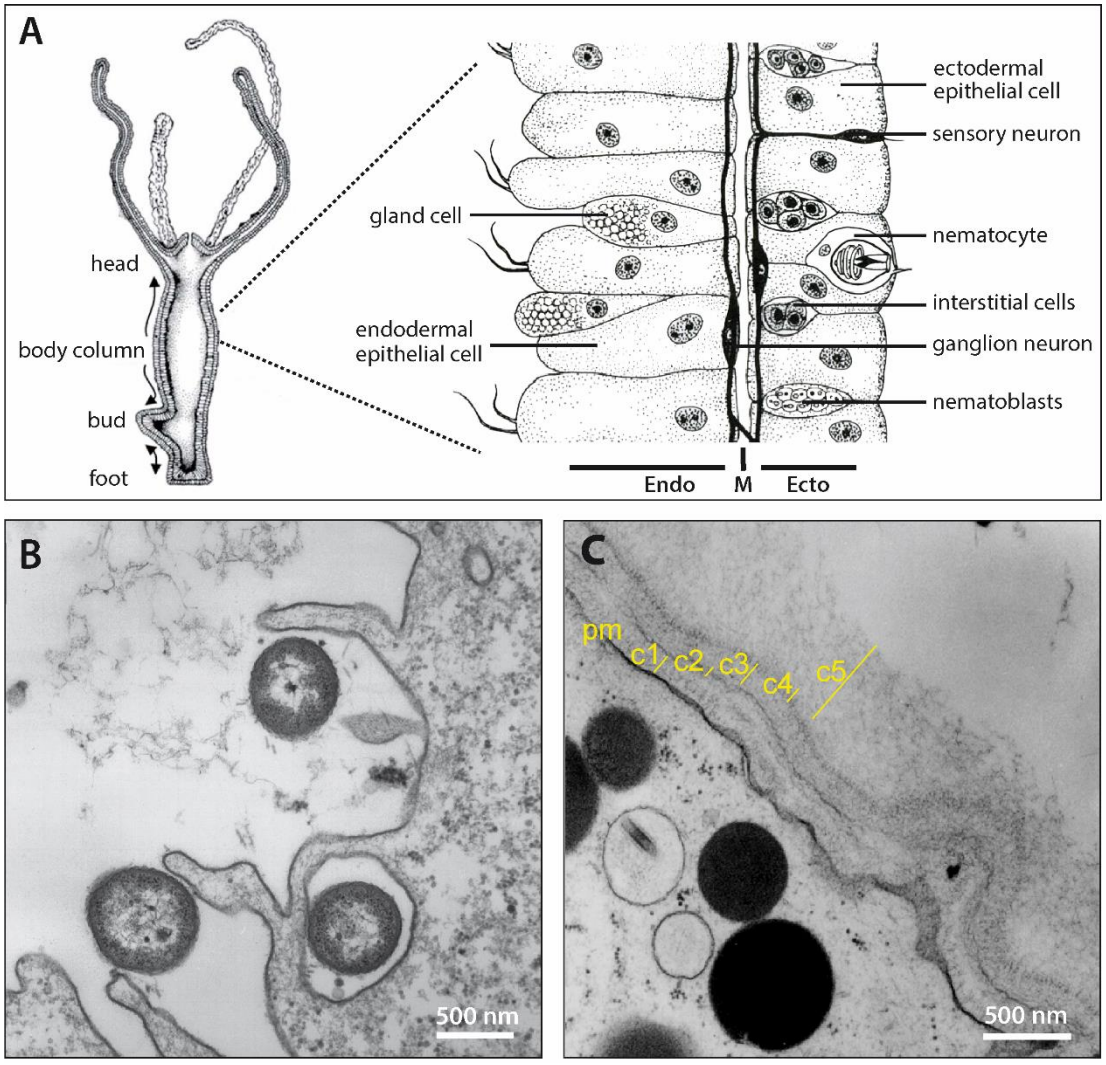

Figure 6. *Hydra*'s diploblastic body plan.
(A) Schematic longitudinal cross section of a *Hydra* polyp showing the cellular composition of the epithelial bilayer of the body column. Arrows indicate the direction of tissue displacement. Endo, endodermal epithelium; M, mesoglea; Ecto, ectodermal epithelium. Modified after (Holstein and Emschermann, 1995; Bosch, 2007). (B) Transmission electron microscopy (TEM) graph of the apical surface of an endodermal epithelial cell engulfing bacteria. Modified after (Bosch et al., 2009). (C) TEM graph showing the ectodermal epithelium. The apical surface is covered by a glycocalyx composed of five distint layers (c1-c5). Pm, plasma membrane. Modified after (Fraune et al., 2015).

Innate immunity in *Hydra*

Many components of the innate immune system were shown to be conserved throughout metazoan evolution (Hibino et al., 2006; Hemmrich et al., 2007b; Rosenstiel et al., 2009) and in the last decade *Hydra* has been proved as a valuable and genetically tractable model to study the basic principles of epithelial defense. As a limnic organism *Hydra* is permanently surrounded by microorganisms like bacteria, protists, fungi, oomycetes and viruses. Despite the absence of motile immune effector cells *Hydra* has developed an effective innate immune system including physical and chemical barriers as well as humoral and cell-mediated components.

The first line of defense is represented by the epithelial cells, which are tightly interconnected by septate junctions and act as a physical barrier. Microbial-epithelial interactions may differ between the ectodermal and endodermal epithelium due to morphological differences. Noteworthy, the ectoderm is protected from direct contact with microbes by a multilayered glycocalyx that extends up to 1.5 µm from the cell surface (Holstein et al., 2010; Böttger et al., 2012). Upon exposure to filtrates of adherent grown *Pseudomonas aeruginosa*, ectodermal cells form numerous blebs at the apical surface and secretory vesicles underneath the cell membrane strongly increase (Bosch et al., 2009). Thus, *Hydra*'s ectodermal epithelial cells respond to microbial stimuli by cytoskeletal rearrangement and increased secretory activity, most likely reinforcing the mucosal barrier represented by the glycocalyx. In contrast, the endoderm does not possess a comparable structure that restricts microbial access to the epithelium and thus, directly faces various kinds of microbes, which are ingested together with the polyp's prey. The endodermal epithelial cells act as stationary phagocytes and engulf not only pre-digested food particles, but also bacteria and unicellular algae present in the gastric cavity (Bosch et al., 2009). Beside phagocytosis, the cellular innate immune mechanisms in *Hydra* include tissue repair, regeneration and apoptotic reactions (Bosch et al., 2009).

The detection of microbes in *Hydra* is mediated *via* pattern recognition receptors (PRRs). All conserved components of the vertebrate TLR signaling cascade were identified in *Hydra* including the key adaptor protein MyD88 and NF-κB (Hemmrich et al., 2007b; Miller et al., 2007). Noteworthy, the TLR identified in *Hydra* is not a *bona fide* one, since it is composed of two proteins; an intracellular TIR-transmembrane domain protein hyTRR-1 and an extracellular hyLRR-2 domain protein. Using a HEK293 cell based *in vitro* assay it was shown that hyTRR-1 and hyLRR-2 can form a functional unit upon stimulation with flagellin (Bosch et al., 2009). Finally, *in vivo* experiments using transgenic MyD88 knockdown polyps

demonstrated that TLR signaling in *Hydra* is involved in bacterial recognition, thereby mediating both defense against bacterial pathogens as well as host-mediated recolonization by commensal bacteria (Franzenburg et al., 2012).

In the cytosol the presence of MAMPs and DAMPs is detected by NOD-like receptors (NLRs), which induce the formation of different multimeric protein complexes termed inflammasomes (Fritz et al., 2006; Meylan et al., 2006). Despite the presence of a large and complex repertoire of putative NRLs, their role in *Hydra*'s immunity is still discussed. In the *H. magnipapillata* genome 290 nucleotide binding domain (NBD) containing loci were identified, but none of the putative proteins contains a C-terminal ligand-binding region composed of leucine-rich repeats (LRRs) present in classical NLRs (Lange et al., 2011). However, *in vitro* studies using a heterologous expression system demonstrated that HyNLR type 1 protein is able to recruit two *Hydra* caspases suggesting a potential role in apoptosis regulation downstream of NLR activation (Lange et al., 2011). Nevertheless, further investigations are required to elucidate if *Hydra*'s NLRs contribute to a cytosolic MAMP-sensing system capable of modulating the host cell survival.

The humoral immune response in *Hydra* involves the secretion of a variety of antimicrobial peptides (AMPs), which are almost exclusively produced in the endoderm (Augustin et al., 2009a; Bosch et al., 2009; Jung et al., 2009; Fraune et al., 2010). In addition, zymogen gland cells, which are interspersed in the endodermal epithelium releases kazal 2-type serine protease inhibitors with bactericidal activity (Augustin et al., 2009b). Until today, three families of potent AMPs have been identified in *Hydra*; the hydramacins, the periculins and the arminins. Whereas the hydramacins show a high degree of sequence identity with two other AMPs in leech, namely theromacin and neuromacin (Tasiemski et al., 2004; Schikorski et al., 2008), the members of the arminin and periculin AMP families do not show any homology with other peptides. Therefore, they are classified as taxonomically restricted genes (TRGs), a feature that applies to many immune effector molecules (Khalturin et al., 2009).

The first AMP isolated from *Hydra* was hydramacin-1, which comprises a 60 amino acid long, secreted cationic peptide containing eight cysteines (Jung et al., 2009). *Hydramacin-1* is expressed in endodermal epithelial cells and becomes up-regulated by LPS in a concentration dependent manner (Bosch et al., 2009). The peptide was shown to be potently active against a wide range of Gram-positive and Gram-negative bacteria at concentrations lower than 1 µM.

Another *Hydra* AMP is periculin-1, which was initially identified among up-regulated genes in a suppression subtractive hybridization (SSH) comparing polyps exposed to filtrate of

adherent grown *Pseudomonas aeruginosa* with control polyps. In both *H. magnipapillata* and *H. vulgaris* (AEP) the periculin peptide family is represented by five paralogues. All members are synthetized as prepropeptides of 129–158 amino acids containing a signal peptide, an anionic N-terminal and a highly conserved cationic C-terminal region, that includes eight cysteine residues. After proteolytic cleavage the cationic C-terminal fragment is released and was shown to possess bactericidal activity. *Periculin-1* is expressed in the endodermal epithelium as well as in a distinct population of i-cells that resembles the egg-fleck, which gives rise to the female germ line. Male polyps show no *Periculin*-1 expression in the i-cell lineage (Bosch et al., 2009; Fraune et al., 2010). Exogenous signals such as LPS, flagellin and viral dsRNA lead to an up-regulation of *Periculin-1* expression (Bosch et al., 2009). Different *Periculin* paralogues are sequentially expressed during oogenesis and embryogenesis. Periculin-1 is produced by the nurse cells of the developing egg and is secreted immediately after fertilization forming a chemical barrier on the epithelial surface of the early embryo. After mid-blastula transition zygotic expression of *Periculin-2b* starts and complements the maternally derived periculin-1. In *Hydra* the embryo develops outside the mother polyp and thus, is directly exposed to the environment and potentially pathogenic microbes before the cuticle layer has formed. The periculin peptides are proposed to have a protective function against invading bacteria when expressed in the endodermal epithelium as well as during oogenesis and embryonic development. In addition to their role in host defense, they might be involved in shaping the microbial community colonizing the embryonic cuticle (Fraune et al., 2010).

The third and largest AMP family in *Hydra* is represented by the arminin peptides. Like the periculins, the arminins are short, secreted peptides with a negatively charged N-terminal part and a highly cationic C-terminal region, which is predicted to be cleaved off. The synthetically produced C-terminal fragment of arminin-1a was shown to exhibit broad-spectrum activity against several bacteria, including multiresistant human pathogenic strains in concentrations equal or lower than 0.4 μM (Augustin et al., 2009a). Interestingly, each *Hydra* species is equipped with a unique repertoire of arminin peptides, which is represented by ten paralogues in *H. magnipapillata*, nine in *H. vulgaris* (AEP), six in *H. oligactis* and four in *H. viridissima*. In contrast to the periculins, the C-terminal region of different arminins shows a high sequence variability, which may result in differential bactericidal activity. Except for one paralogue that is ectodermally expressed, in *H. vulgaris* (AEP) all arminins were shown to be expressed in the endodermal epithelium of the body column (Franzenburg et al., 2013b). Thus, like the hydramacin and periculin peptides, the arminins are likely to be secreted into the

gastric cavity. Some arminins show a remarkably high expression level, which even exceeds the expression of the housekeeping gene *β-actin*, indicating the biological relevance of this gene family in *Hydra* (Franzenburg et al., 2013b).

Interestingly, humoral immunity in *Hydra* is interconnected with the stem cell transcription factor forkhead box O (FoxO). FoxO is highly conserved across metazoans and plays an important role in life-span extension by contributing to cell survival, stem cell control and tissue homeostasis in various organisms (Monsalve and Olmos, 2011; Webb et al., 2016). Besides its well-known function as major tissue regulator, FoxO was also shown to be involved in transcriptional modulation of immune effector molecules such as AMPs in many model organisms including *C. elegans* (Libina et al., 2003), *Drosophila* (Becker et al., 2010), mouse (Seiler et al., 2013) and *Hydra* (Boehm et al., 2012). In the latter, it was demonstrated that knockdown of FoxO in the endodermal epithelium led to down-regulation of distinct AMPs and the Kazal-2 serine protease inhibitors (Boehm et al., 2012; Mortzfeld et al., 2018). As a phenotypic consequence the FoxO knockdown polyps were impaired in selecting for bacteria resembling the native microbiota and more susceptible to colonization by foreign bacteria (Mortzfeld et al., 2018).

The holobiont *Hydra*

Understanding the mechanisms of establishment and maintenance of bacterial communities in complex systems could have far-reaching applications, ranging from coral reef conservation and restoration to the improvement of human health. Untangling the complex interactions to elucidate the fundamental principles requires well-established, genetically tractable animal models, which are colonized by a limited number of bacteria. One such model is the freshwater polyp *Hydra*.

Hydra's career as a model for host-bacteria interactions started in 2007 with the discovery that polyps of various species differ greatly in their microbiota, although they have been cultivated for more than 20 years in the laboratory at constant temperature and with identical food (Fraune and Bosch, 2007). 16S rRNA gene sequencing of seven different *Hydra* species revealed that all of them are colonized by distinct bacterial communities, which are remarkably stable even during co-cultivation with other *Hydra* species (Fraune and Bosch, 2007; Franzenburg et al., 2013b). Furthermore, the bacterial community composition mirrors the phylogenetic relationship of their hosts (**Figure 7**) (Franzenburg et al., 2013b), a pattern termed phylosymbiosis (Brucker and Bordenstein, 2013). In all *Hydra* species the microbiota

is dominated by Gram-negative bacteria, which mostly belong to different orders of the *Betaproteobacteria* (Fraune and Bosch, 2007; Franzenburg et al., 2013b). Compared to mammals, *Hydra*'s bacterial communities show a relatively low complexity with approximately 100 phylotypes present in *H. vulgaris* (AEP) and notably, most of them can be cultivated (Franzenburg et al., 2013a; Fraune et al., 2015).

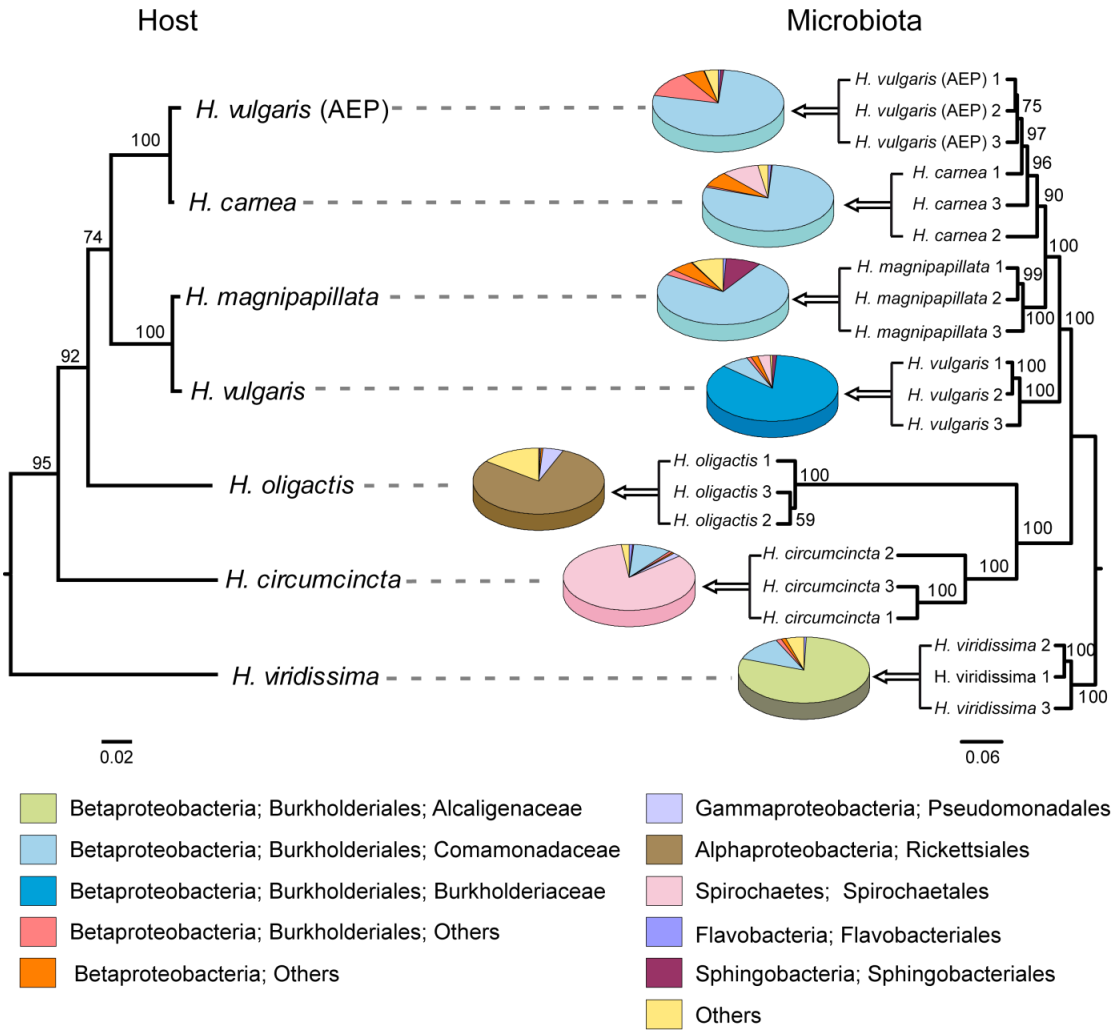

Figure 7. *Hydra*'s species-specific microbiota.
(Left) Phylogenetic tree of *Hydra* species. (Right) Environment cluster tree of 21 bacterial communities of seven different *Hydra* species. Pie charts represent mean relative abundances of bacterial orders. Note that the phylogenetic tree of the *Hydra* species resembles the phylogenetic relations of the associated microbiota. Modified from (Franzenburg et al., 2013b).

Commensal microbes provide a variety of benefits to their host and among the longest known is the ability of an uncompromised microbiota to prevent pathogen infections, a phenomenon termed 'colonization resistance' (Stecher and Hardt, 2008). Germ-free *Hydra* polyps were shown to be prone to lethal fungal infection indicating that the commensal microbiota displays an integral part of antifungal immunity and supports survival of the polyps

(Fraune et al., 2015). The protection from fungal infections could be restored in germ-free polyps by re-introducing the complex microbiota, but not by addition of single bacterial isolates indicating that additive and synergistic interactions of commensal bacteria are contributing to full fungal resistance.

To preserve colonization resistance the host needs to control the proper establishment and maintenance of its specific microbiota. Profiling of the assembly of *Hydra*'s bacterial community after hatching revealed that the colonization process follows a robust, temporal pattern with distinct and reproducible stages (Franzenburg et al., 2013a). Thereby, a high diversity and interindividual variability in the first week is followed by the transient occurrence an adult-like profile, which disappears again in the third week. From week four on the progressive emergence of the stable adult-like pattern begins, which is characterized by low species diversity and the preponderance of the Betaproteobacterium *Curvibacter*. Interestingly, a similar pattern with a transient adult-like microbiota profile was observed when profiling the postnatal bacterial colonization of the human gut (Palmer et al., 2007).

The arising question, which factors and rules influence the community assembly, composition and diversity was subsequently addressed using a mathematical modeling approach, which suggested that both frequency-dependent bacteria-bacteria interactions and host factors are shaping the succession of microbial colonization in *Hydra* (Franzenburg et al., 2013a). One such host factor is comprised by the AMPs of the arminin family, which show a unique composition and expression profile in each *Hydra* species (Franzenburg et al., 2013b). Transgenic polyps with simultaneous decreased expression of several arminins showed impaired ability to select for bacteria resembling their native microbiota strongly indicating a role for the arminin AMPs in shaping *Hydra*'s species-specific bacterial communities (Franzenburg et al., 2013b). Besides epithelial-derived host factors, a previous study in *Hydra* indicated a potential role for neurons in host-microbe interactions (Fraune et al., 2009). Thereby, it was demonstrated that the depletion of nerve cells is accompanied with significant changes in *Hydra*'s microbiota, while the absence of interstitial stem cells and nematocytes had no effect on the bacterial composition. Indeed, neurons possess an elaborate secretion system and thus, some of their products may be involved in host-microbe cross-talk.

Furthermore, a recent study provided evidence that the hydra host not only influences the composition of its microbiota, but also the bacterial behavior (Pietschke et al., 2017). More precisely, it was shown that *Hydra* can modify quorum sensing signals of its bacterial colonizers, which leads to repression of bacterial motility and promotes the production of

bioactive compounds by the commensal bacteria (Pietschke et al., 2017). While *Hydra* appears to be capable of manipulating the bacterial behavior, it was shown that vice versa the microbiota affects the spontaneous contractile behavior of their host (Murillo-Rincon et al., 2017). Thereby, germ-free polyps show reduced and less regular contraction frequencies, an effect that could be partially rescued by restoring the native microbiota, which demonstrates a direct impact of bacterial colonization on the neural activity of *Hydra* (Murillo-Rincon et al., 2017).

Finally, besides host factors and bacteria-bacteria interactions, bacteriophages have been suggested as a potential regulator of *Hydra*'s bacterial microbiota. The analysis of the viral communities in different *Hydra* species revealed that the viromes are species-specific and majorly consist of bacteriophages (Grasis et al., 2014). Strikingly, the predicted bacterial host range of these bacteriophages consisted mainly of Gamma- and Betaproteobacteria classes, which dominate the microbiota of most *Hydra* species. Therefore, a role for bacteriophages in the establishment and maintenance of *Hydra*'s bacterial microbiota was proposed (Grasis et al., 2014).

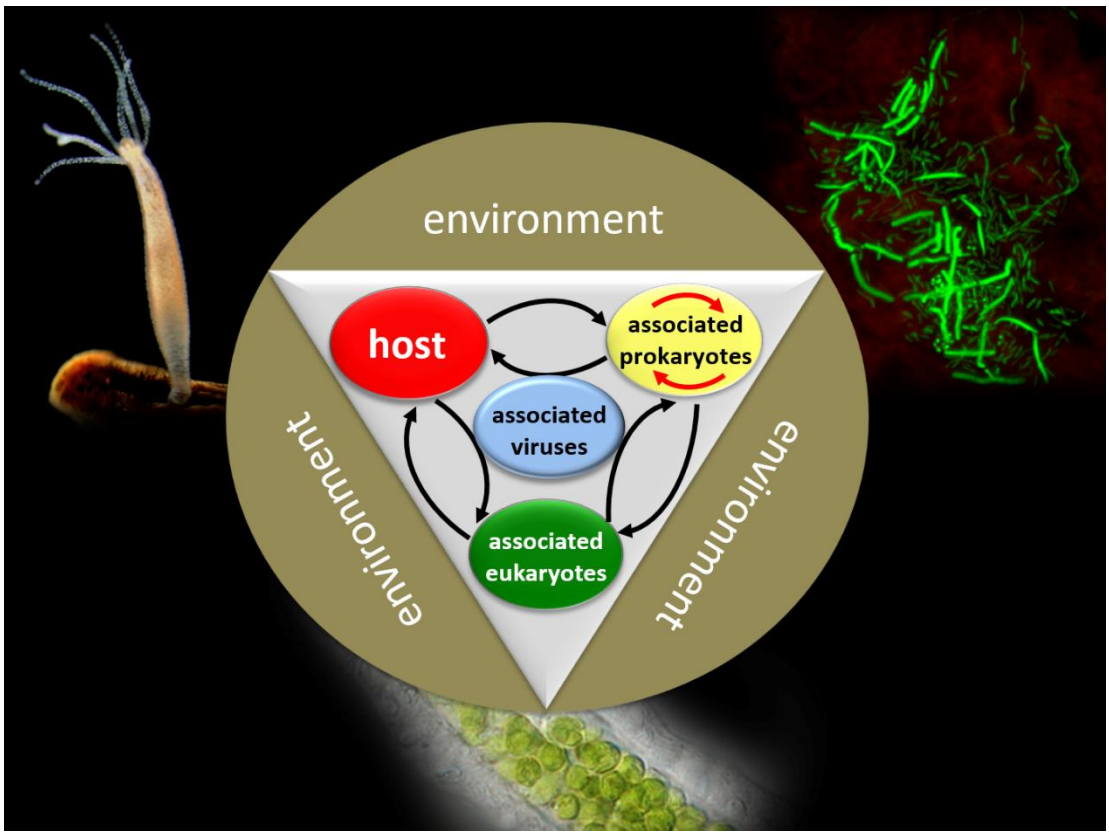

Figure 8. Interactions in the *Hydra* holobiont.
The holobiont consists of the *Hydra* host and its associated bacteria, viruses and, in case of *Hydra viridissima*, eukaryotic unicellular algae of the genus *Chlorella*. This consortium is liable to selection and constantly interacting with the environment (Zilber-Rosenberg and Rosenberg, 2008; Bosch and McFall-Ngai, 2011; Fraune et al., 2011). Figure modified from (Bosch, 2013).

Taken together, *Hydra* has been proven to be a valuable model to analyze host-microbe interactions in the last decade. The low complexity and high stability of *Hydra*'s species-specific microbiota together with the availability of transgenic and germ-free polyps as well as the cultivability of the bacterial colonizers result in an attractive experimental system to decipher the contribution from each partner in the holobiont. As an evolutionary ancient metazoan, *Hydra* can provide insights into the basic molecular toolkit required for establishment and maintenance of a holobiont and thus, may help to elucidate the mechanisms in more complex systems such as the mammalian gut.

The *Hydra viridissima* – *Chlorella* endosymbiosis

The *Hydra viridissima* holobiont involves not only the animal host and its associated bacterial and viral communities, but also unicellular photosynthetic algae, which are harboured in the endodermal epithelial cells. Among the four species groups within the genus *Hydra*, algal stable endosymbiosis only occurs in the most ancestral *viridissima* group, which was recently shown to comprise at least five different phylogenetic species, that are all referred to as *H. viridissima* (Martínez et al., 2010; Schwentner and Bosch, 2015). Since there is no report on a naturally occurring algae-free *H. viridissima* strain, algal endosymbiosis has been considered as the key characteristic of the *viridissima* group (Campbell, 1983). Indeed, recent phylogenetic analyses indicate that algal symbiosis was established after the divergence from non-symbiotic 'brown' *Hydra* (Martínez et al., 2010; Schwentner and Bosch, 2015). Based on morphological observation and molecular phylogenetic analyses the unicellular photosynthetic algae associated with green hydra are attributed to the genus *Chlorella*, which are small (2-10 μm), nonmotile, unicellular organisms of spherical or elliptical shape (Douglas and Huss, 1986; Huss et al., 1999; Lewis and Muller-Parker, 2004; Pröschold et al., 2011; Kawaida et al., 2013). *Chlorella* algae typically harbor a single chloroplast and reproduce exclusively asexual by the formation of so-called autospores. Most *Chlorella* species are free-living in freshwater environments as well as on land, while some species occur as endosymbionts of ciliates, freshwater sponges, bivalves and cnidarians (Smith, 1991; Venn et al., 2008).

The *Hydra-Chlorella* endosymbiosis is characterized by the persistent residence of *Chlorella* algae at the basal part of the endodermal epithelial cells with each algal cell being enclosed within an individual perialgal vacuolar membrane termed 'symbiosome' (Muscatine et al., 1975; Jolley and Smith, 1980). The number of algae per host cell stays relatively constant with each endodermal cell containing 20 to 40 endosymbionts, thereby the cells in the gastric

region contain more algae then endodermal cells in the head and foot region (Pardy and Muscatine, 1973; Pardy, 1974a; Habetha et al., 2003). All endosymbiotic algae found in a single host polyp are clonal and a recent phylogenetic analysis of six different green hydra strains and their symbiotic *Chlorella* algae revealed that the phylogenetic trees of the *Hydra* hosts and the algal symbionts are congruent indicating co-speciation (Kawaida et al., 2013). Yet, *Hydra*'s symbiotic algae such as *Chlorella* strain A99 could not be cultivated outside the host (Muscatine, 1965; Park et al., 1967) indicating loss of autonomy and thus, are assumed to be obligate endosymbionts, which are vertically transmitted to the next generation of *Hydra* (Habetha et al., 2003). In asexually reproducing polyps the endosymbionts are inherited by budding while during sexual reproduction the *Chlorella* algae are maternally transmitted. Thereby, the endosymbiont leaves the endoderm *via* exocytosis and transmigrates through the mesoglea to reach the oocyte before fertilization (Muscatine and McAuley, 1982; Campbell, 1990). Since it was shown that algae increase in the endoderm underneath the ovary, it was suggested that the ovary secrets a chemoattractant that is sensed by endodermal cells and induces the exocytosis of the algae (Campbell, 1990).

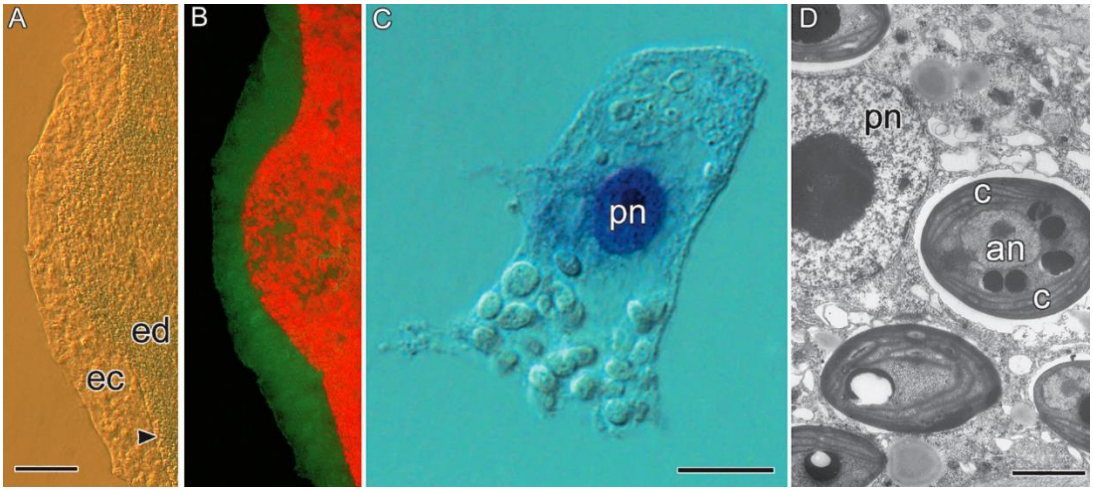

Figure 9. Morphological features of the *Hydra viridissima*-*Chlorella* endosymbiosis.
(A) Phase-contrast micrograph of a polyp's budding zone. The arrow head marks the mesoglea which separates ectoderm from endoderm. Scale bar, 0.1 mm. Flourescence microscopy of the same area shown in A. Algae appear red, *Hydra* tissue green. (C) Phase contrast micrograph of a single mazerated endodermal epithelial cell containig symbiotic algae in the basal part below the nucleus (stained blue). Scale bar, 5 µm. (D) Electron micrograph of symbiotic *Chlorella* within an endodermal epithelial cell. Scale bar, 1 µm. an, nucleus of alga; c, chloroplast; ec, ectoderm; ed endoderm; pn, nucleus of the polyp's cell.

Although algae-free *H. viridissima* have never been observed in nature, they can be artificially generated by strong light exposure and incubation with the photosynthesis inhibitor 3-(3,4-dichlorophenyl)-1,1-dimethylurea (DCMU) (Pardy, 1976; Habetha et al., 2003). These

so-called aposymbiotic animals show the same morphology as symbiotic animals and can be easily maintained under laboratory conditions, thereby providing a useful tool to study the *Hydra-Chlorella* symbiosis. Despite rare cases of polyps hatching without algae have been reported (Pardy and Muscatine, 1973; Muscatine and McAuley, 1982), aposymbiotic *H. viridissima* apparently do not occur naturally indicating that there is a fitness benefit for polyps hosting the algal endosymbiont (Smith et al., 1969). Indeed, comparison of aposymbiotic and symbiotic polyps revealed that the presence of *Chlorella* has a profound impact on *Hydra´*s fitness with regard to growth rate and sexual reproduction. While symbiotic and aposymbiotic animals show the same budding rate during daily feeding, aposymbiotic polyps form significantly less buds at low feeding regime and thus, symbiotic animals are more tolerant to starvation (Muscatine and Lenhoff, 1965; Habetha et al., 2003). Furthermore, sexual reproduction in *H. viridissima* is induced by starvation, thereby aposymbiotic polyps were shown to form significantly less oocytes than symbiotic animals, whereas spermatogenesis was not impaired by the absence of *Chlorella* algae (Habetha et al., 2003).

Furthermore, it is possible to reinfect aposymbiotic polyps by injecting suspensions of *Chlorella* algae into the gastric cavity. The recolonization of the endodermal epithelium by native symbiotic *Chlorella* involves four stages (Pardy and Muscatine, 1973); (i) phagocytosis of symbionts at the apical side of the endodermal epithelial cells, (ii) avoidance of digestion by inhibition of phagosome-lysosome fusion (‘sorting’) (Hohman et al., 1982), (iii) migration of algae-containing endosomes to the basal part of the cell (iv) restoration of the normal number of algae per host cell (Muscatine et al., 1975). It is still debated whether the initial engulfment occurs nonspecifically or if the take-up of symbiotic algae is enhanced by a recognition mechanism at the cell surface such as lectin-glycan interaction (Pool, 1979; Jolley and Smith, 1980; Meints and Pardy, 1980). However, only potential symbionts pass the sorting and migration phases (McAuley and Smith, 1982), whereas non-symbiotic algae usually become digested or expelled within a few days (Jolley and Smith, 1980). Notably, a few heterologous *Chlorella* strains, which are symbionts of other invertebrates such as the ciliate *Paramecium bursaria*, can form stable associations with *Hydra* that persist indefinitely (Douglas and Smith, 1984). Nevertheless, it remains unclear to which extent these associations resemble the physiological interrelationship of *H. viridissima* and its native *Chlorella* endosymbiont.

Beyond the initial steps of algal recognition, sorting and migration, there must be a complex series of interactions that regulate the long-term harmonious co-existence of the host and the endosymbiotic algae. Pioneering studies in the 1960s and 1980s provided evidence that

a mutually beneficial metabolic interrelationship occurs between *Hydra* and *Chlorella*. Thereby, the endosymbiont supplies *H. viridissima* with photosynthetically fixed carbon in form of maltose, enabling its host to survive periods of starvation (Muscatine and Lenhoff, 1963, 1965; Roffman and Lenhoff, 1969; Habetha et al., 2003). In the meanwhile, the algae benefit from the predator-free zone within the hydra cell and are supplied with both organic (Thorington and Margulis, 1981) and inorganic (Cook, 1981) nutrients from the host. Yet, despite over 40 years of research, the exact molecular mechanisms mediating the metabolic exchange between *Hydra* and *Chlorella* have not been determined.

The maintenance of a stable symbiont / host cell ratio is crucial for a homeostatic co-existence with an intracellular symbiont. If the algal endosymbiont proliferates too fast, it may overgrow and finally kill the host. On the other hand, the symbiont may be diluted out, if its growth rate falls behind that of the host. Since the *Chlorella* endosymbionts produce not two but four autospores with each division (Oschman, 1967), a synchronous cell replication of the endosymbiont and *Hydra* would result in overgrowth of the host. During host cell division the algal symbionts are partitioned randomly and unevenly between the two daughter cells, but ultimately attain similar densities with maximal 40 algae per cell (McAuley, 1990; McAuley and Darrah, 1990). Thus, there must be regulatory mechanism to equilibrate the proliferation rate of *Hydra* and the *Chlorella* algae. It was suggested that host-derived factors may regulate algal mitosis or cell division in a density-dependent manner (Pardy, 1974b, 1974a; McAuley, 1981). Thereby, the algal cell cycle would be diminished in host cells with a full complement of symbionts, whereas inhibition would be diminished in recently divided host cells with fewer symbionts. Besides a mechanism directly interfering with algal mitosis, several studies indicated that algal proliferation might be regulated by the availability of host-derived inorganic nutrients such as nitrogen (McAuley, 1986, 1987; McAuley and Muscatine, 1986; Rees, 1986, 1989, 1990a, 1990b; Rees and Ellard, 1989; Rees et al., 1989). Furthermore, expulsion or digestion of algae as well as the production of a density-dependent inhibitor by the algae themselves were discussed as regulatory mechanisms (Muscatine and Pool, 1979; Muscatine and Neckelmann, 1981; McAuley, 1982). Nevertheless, the question by which mechanism algal proliferation is regulated remains unanswered so far.

Taken together, previous studies of the *Hydra-Chlorella* endosymbiosis have clearly shown that there is a great deal of adaptation and specificity between the two partners. The selection of a suitable symbiont seems to involve much more than the recognition of a single algal character, but rather depends upon a number of algal properties that enable a successful

interplay with the host. Like all animals *H. viridissima* is also host to a distinct bacterial microbiota (Franzenburg et al., 2013b), a fact that has been widely neglected in previous research, but makes the *H. viridissima* holobiont an attractive model to study tripartite interkingdom associations between an animal host, bacterial colonizers and endosymbiotic algae.

Aims of the study

A holobiont can be considered a dynamic ecological unit consisting of the host and a multitude of associated microorganisms. Maintenance of the delicate homeostasis within this system requires an elaborate cross talk between the host and microbes. Despite its simple body plan and the lack of adaptive immunity, *Hydra* has developed complex mechanisms that regulate the establishment and maintaince of a specific and diverse bacterial community (Fraune and Bosch, 2007; Franzenburg et al., 2012, 2013a, 2013b).

Research of the last decade has shown that all *Hydra* species are associated with specific bacterial communities, which are remarkably stable even during co-cultivation with other *Hydra* species (Fraune and Bosch, 2007; Franzenburg et al., 2013b). However, the exact localization of *Hydra*'s microbiota remained unknown. Several attempts to visualize the bacterial colonizers by confocal and electron microscopy failed, likely due to ineffective fixation methods. Therefore, the first aim of this study was (i) the localization of *Hydra*'s microbiota and further on characterization of their habitat.

As a member of the ancient phylum Cnidaria, *Hydra*'s entire body is formed of an epithelial bilayer interspersed by one of the anatomically simplest nervous systems. Interestingly, a previous study indicated that the depletion of neurons in *Hydra* leads to disturbances in the bacterial community (Fraune et al., 2009). Since some neuropeptides have been shown to possess a direct antimicrobial activity *in vitro* (Minter et al., 2005; Hansen et al., 2006; El Karim et al., 2008; Holzer and Farzi, 2014), the question arose whether or not the absence of neuropeptides was responsible for the observed microbial shift in nerve-cell depleted *Hydra*. Therefore, in the second part of this thesis (ii) the antimicrobial activity of *Hydra*'s neuropeptides and their role in shaping the microbial composition was investigated.

The green hydra, *Hydra viridissima*, is not only colonized by a distinct bacterial microbiota, but in addition harbors unicellular photosynthetic algae of the genus *Chlorella* in its endodermal epithelial cells. Although the *H. viridissima-Chlorella* endosymbiosis has been

a focus of research for many decades, little is known on the underlying molecular mechanisms (Habetha and Bosch, 2005). In the third chapter of this thesis (iii) the molecular basis of symbiotic adaptations in the *Hydra-Chlorella* relationship was investigated by genome sequencing of the native endosymbiont *Chlorella* sp. A99 and by microarray transcriptional profiling of symbiotic and aposymbiotic polyps.

While host-algal interactions in the *H. viridissima* holobiont have been extensively studied in the past, the role of the bacterial microbiota has been widely neglected in the past. In the fourth part of this study the *H. viridissima* holobiont was used to investigate symbiotic interactions in a tripartite animal–algal–bacterial model system, thereby addressing the question (iv) if the presence of intracellular photosynthetic algae affects the composition of the bacterial microbiota.

References

Abrams GD and Bishop JE (1967) Effect of the Normal Microbial Flora on Gastrointestinal Motility. *Exp. Biol. Med.* **126**(1). 301–304. doi:10.3181/00379727-126-32430.

Akira S, Uematsu S and Takeuchi O (2006) Pathogen Recognition and Innate Immunity. *Cell* **124**(4). 783–801.

Albiol Matanic VC and Castilla V (2004) Antiviral activity of antimicrobial cationic peptides against Junin virus and herpes simplex virus. *Int. J. Antimicrob. Agents* **23**(4). 382–389. doi:10.1016/j.ijantimicag.2003.07.022.

Augustin R, Anton-Erxleben F, Jungnickel S, Hemmrich G, Spudy B, Podschun R, et al. (2009a) Activity of the novel peptide arminin against multiresistant human pathogens shows the considerable potential of phylogenetically ancient organisms as drug sources. *Antimicrob. Agents Chemother.* **53**(12). 5245–50. doi:10.1128/AAC.00826-09.

Augustin R, Siebert S and Bosch TCG (2009b) Identification of a kazal-type serine protease inhibitor with potent anti-staphylococcal activity as part of Hydra's innate immune system. *Dev. Comp. Immunol.* **33**(7). 830–7. doi:10.1016/j.dci.2009.01.009.

Bäckhed F, Ding H, Wang T, Hooper L V, Koh GY, Nagy A, et al. (2004) The gut microbiota as an environmental factor that regulates fat storage. *Proc. Natl. Acad. Sci. U. S. A.* **101**(44). 15718–23. doi:10.1073/pnas.0407076101.

Bäckhed F, Ley RE, Sonnenburg JL, Peterson DA and Gordon JI (2005) Host-bacterial mutualism in the human intestine. *Science* **307**(5717). 1915–20. doi:10.1126/science.1104816.

Bates JM, Mittge E, Kuhlman J, Baden KN, Cheesman SE and Guillemin K (2006) Distinct signals from the microbiota promote different aspects of zebrafish gut differentiation. *Dev. Biol.* **297**(2). 374–86. doi:10.1016/j.ydbio.2006.05.006.

Baumann P (2005) Biology of bacteriocyte-associated endosymbionts of plant sap-sucking insects. *Annu. Rev. Microbiol.* **59**(1). 155–189. doi:10.1146/annurev.micro.59.030804.121041.

Becker T, Loch G, Beyer M, Zinke I, Aschenbrenner AC, Carrera P, et al. (2010) FOXO-dependent regulation of innate immune homeostasis. *Nature* **463**(7279). 369–73. doi:10.1038/nature08698.

Belkaid Y and Hand TW (2014) Role of the microbiota in immunity and inflammation. *Cell*, 121–141. doi:10.1016/j.cell.2014.03.011.

Beutler B (2004) Innate immunity: an overview. *Mol. Immunol.* **40**(12). 845–59.

Bevins CL and Salzman NH (2011) The potter's wheel: the host's role in sculpting its microbiota. *Cell. Mol. Life Sci.* **68**(22). 3675–3685. doi:10.1007/s00018-011-0830-3.

Bienenstock J and Collins S (2010) 99th Dahlem Conference on Infection, Inflammation and Chronic Inflammatory Disorders: Psycho-neuroimmunology and the intestinal microbiota: clinical observations and basic mechanisms. *Clin. Exp. Immunol.* **160**(1). 85–91. doi:10.1111/j.1365-2249.2010.04124.x.

Biragyn A, Ruffini PA, Leifer CA, Klyushnenkova E, Shakhov A, Chertov O, et al. (2002) Toll-like receptor 4-dependent activation of dendritic cells by β-defensin 2. *Science (80-.).* **298**(5595). 1025–1029. doi:10.1126/science.1075565.

Bisgaard H, Li N, Bonnelykke K, Chawes BLK, Skov T, Paludan-Müller G, et al. (2011) Reduced diversity of the intestinal microbiota during infancy is associated with increased risk of allergic disease at school age. *J. Allergy Clin. Immunol.* **128**(3). 646–652.e5. doi:10.1016/j.jaci.2011.04.060.

Blevins SM and Bronze MS (2010) Robert Koch and the "golden age" of bacteriology. *Int. J. Infect. Dis.*, e744–e751. doi:10.1016/j.ijid.2009.12.003.

Bode H, Berking S, David CN, Gierer A, Schaller H and Trenkner E (1973) Quantitative analysis of cell types during growth and morphogenesis in Hydra. *Wilhelm Roux Arch. für Entwicklungsmechanik der Org.* **171**(4). 269–285. doi:10.1007/BF00577725.

Bode HR, Heimfeld S, Chow MA and Huang LW (1987) Gland cells arise by differentiation from interstitial cells in Hydra attenuata. *Dev. Biol.* **122**(2). 577–585. doi:10.1016/0012-1606(87)90321-6.

Boehm A-M, Khalturin K, Anton-Erxleben F, Hemmrich G, Klostermeier UC, Lopez-Quintero JA, et al. (2012) FoxO is a critical regulator of stem cell maintenance in immortal Hydra. *Proc. Natl. Acad. Sci. U. S. A.* **109**(48). 19697–702. doi:10.1073/pnas.1209714109.

Bordenstein SR and Theis KR (2015) Host biology in light of the microbiome: Ten principles of holobionts and hologenomes. *PLoS Biol.* **13**(8). e1002226. doi:10.1371/journal.pbio.1002226.

Bosch TC and David CN (1986) Male and female stem cells and sex reversal in Hydra polyps. *Proc. Natl. Acad. Sci. U. S. A.* **83**(24). 9478–9482. doi:10.1073/pnas.83.24.9478.

Bosch TCG (2003) Ancient signals: Peptides and the interpretation of positional information in ancestral metazoans. *Comp. Biochem. Physiol. - B Biochem. Mol. Biol.*, 185–196. doi:10.1016/S1096-4959(03)00226-4.

Bosch TCG (2007) Why polyps regenerate and we don't: Towards a cellular and molecular framework for Hydra regeneration. *Dev. Biol.* **303**(2). 421–433.

Bosch TCG (2009) Hydra and the evolution of stem cells. *BioEssays* **31**(4). 478–486. doi:10.1002/bies.200800183.

Bosch TCG (2012) What Hydra Has to Say About the Role and Origin of Symbiotic Interactions. *Biol. Bull.* **223**(1). 78–84.

Bosch TCG (2013) Cnidarian-Microbe Interactions and the Origin of Innate Immunity in Metazoans. *Annu. Rev. Microbiol.* **67**(1). 499–518. doi:10.1146/annurev-micro-092412-155626.

Bosch TCG, Augustin R, Anton-Erxleben F, Fraune S, Hemmrich G, Zill H, et al. (2009) Uncovering the evolutionary history of innate immunity: The simple metazoan Hydra uses epithelial cells for host defence. *Dev. Comp. Immunol.* **33**(4). 559–569.

Bosch TCG and David CN (1984) Growth regulation in Hydra: Relationship between epithelial cell cycle length and growth rate. *Dev. Biol.* **104**(1). 161–171.

Bosch TCG and David CN (1987) Stem cells of Hydra magnipapillata can differentiate into somatic cells and germ line cells. *Dev. Biol.* **121**(1). 182–191.

Bosch TCG and McFall-Ngai MJ (2011) Metaorganisms as the new frontier. *Zoology* **114**(4). 185–190.

Böttger A, Doxey AC, Hess MW, Pfaller K, Salvenmoser W, Deutzmann R, et al. (2012) Horizontal gene transfer contributed to the evolution of extracellular surface structures: the freshwater polyp Hydra is covered by a complex fibrous cuticle containing glycosaminoglycans and proteins of the PPOD and SWT (sweet tooth) families. *PLoS One* **7**(12). e52278. doi:10.1371/journal.pone.0052278.

Bouskra D, Brézillon C, Bérard M, Werts C, Varona R, Boneca IG, et al. (2008) Lymphoid tissue genesis induced by commensals through NOD1 regulates intestinal homeostasis. *Nature* **456**(7221). 507–510. doi:10.1038/nature07450.

Brandl K, Plitas G, Schnabl B, DeMatteo RP and Pamer EG (2007) MyD88-mediated signals induce the bactericidal lectin RegIIIγ and protect mice against intestinal Listeria monocytogenes infection. *J. Exp. Med.* **204**(8). 1891–1900. doi:10.1084/jem.20070563.

Brucker RM and Bordenstein SR (2013) The hologenomic basis of speciation: gut bacteria cause hybrid lethality in the genus Nasonia. *Science* **341**(6146). 667–9. doi:10.1126/science.1240659.

Campbell R (1983) Identifying Hydra Species. *Hydra Res. Methods SE - 4*, 19–28. doi:10.1007/978-1-4757-0596-6_4.

Campbell RD (1967) Tissue dynamics of steady state growth inHydra littoralis. II. Patterns of tissue movement. *J. Morphol.* **121**(1). 19–28. doi:10.1002/jmor.1051210103.

Campbell RD (1987) A new species of Hydra (Cnidaria: Hydrozoa) from North America with comments on species clusters within the genus. *Zool. J. Linn. Soc.*, 253–263. doi:10.1111/j.1096-3642.1987.tb01510a.x.

Campbell RD (1990) Transmission of symbiotic algae through sexual reproduction in hydra: Movement of algae into the oocyte. *Tissue Cell* **22**(2). 137–147. doi:10.1016/0040-8166(90)90017-4.

Campbell RD and Bode HR (1983) Terminology for Morphology and Cell Types. *H.M- Lenhoff Hydra Res. Methods* 5–6. doi:10.1007/978-1-4757-0596-6_2.

Carabotti M, Scirocco A, Maselli MA and Severi C (2015) The gut-brain axis: interactions between enteric microbiota, central and enteric nervous systems. *Ann. Gastroenterol.* **28**(2). 203–209.

Cario E (2008) Barrier-protective function of intestinal epithelial toll-like receptor 2. *Mucosal Immunol.*, 62–66. doi:10.1038/mi.2008.47.

Cario E (2010) Toll-like receptors in inflammatory bowel diseases: A decade later. *Inflamm. Bowel Dis.*, 1583–1597. doi:10.1002/ibd.21282.

Cash HL, Whitham C V, Behrendt CL and Hooper L V (2006) Symbiotic bacteria direct expression of an intestinal bactericidal lectin. *Science* **313**(5790). 1126–30. doi:10.1126/science.1127119.

Chapman J a, Kirkness EF, Simakov O, Hampson SE, Mitros T, Weinmaier T, et al. (2010) The dynamic genome of Hydra. *Nature* **464**(7288). 592–6. doi:10.1038/nature08830.

Cleave HJ Van and Hyman LH (1940) The Invertebrates: Protozoa Through Ctenophora. *Am. Midl. Nat.* **24**(2). 499. doi:10.2307/2420952.

Collins A, Schuchert P, Marques A, Jankowski T, Medina M and Schierwater B (2006) Medusozoan phylogeny and character evolution clarified by new large and small subunit rDNA data and an assessment of the utility of phylogenetic mixture models. *Syst. Biol.* **55**(1). 97–115. doi:10.1080/10635150500433615.

Collins J, Borojevic R, Verdu EF, Huizinga JD and Ratcliffe EM (2014) Intestinal microbiota influence the early postnatal development of the enteric nervous system. *Neurogastroenterol. Motil.* **26**(1). 98–107. doi:10.1111/nmo.12236.

Cook CB (1981) Adaptations to endosymbiosis in green hydra. *Ann. N. Y. Acad. Sci.* **361**(1). 273–283. doi:10.1111/j.1749-6632.1981.tb54370.x.

Cooper MD and Alder MN (2006) The evolution of adaptive immune systems. *Cell*, 815–822. doi:10.1016/j.cell.2006.02.001.

Cox LM, Yamanishi S, Sohn J, Alekseyenko A V., Leung JM, Cho I, et al. (2014) Altering the intestinal microbiota during a critical developmental window has lasting metabolic consequences. *Cell* **158**(4). 705–721. doi:10.1016/j.cell.2014.05.052.

Cullen TW, Schofield WB, Barry NA, Putnam EE, Rundell EA, Trent MS, et al. (2015) Antimicrobial peptide resistance mediates resilience of prominent gut commensals during inflammation. *Science (80-.).* **347**(6218). 170–175. doi:10.1126/science.1260580.

d'Hennezel E, Abubucker S, Murphy LO and Cullen TW (2017) Total Lipopolysaccharide from the Human Gut Microbiome Silences Toll-Like Receptor Signaling. *mSystems* **2**(6). e00046-17. doi:10.1128/mSystems.00046-17.

David CN and Campbell RD (1972) Cell cycle kinetics and development of Hydra attenuata. *J. Cell Sci.* **11**(2). 557–568.

David CN and Murphy S (1977) Characterization of interstitial stem cells in hydra by cloning. *Dev. Biol.* **58**(2). 372–383. doi:10.1016/0012-1606(77)90098-7.

David LA, Maurice CF, Carmody RN, Gootenberg DB, Button JE, Wolfe BE, et al. (2014) Diet rapidly and reproducibly alters the human gut microbiome. *Nature* **505**(7484). 559–63. doi:10.1038/nature12820.

De Lucca AJ and Walsh TJ (1999) Antifungal peptides: novel therapeutic compounds against emerging pathogens. *Antimicrob. Agents Chemother.* **43**(1). 1–11.

De Yang, Chen Q, Schmidt AP, Anderson GM, Wang JM, Wooters J, et al. (2000) Ll-37, the Neutrophil Granule–And Epithelial Cell–Derived Cathelicidin, Utilizes Formyl Peptide Receptor–Like 1 (Fprl1) as a Receptor to Chemoattract Human Peripheral Blood Neutrophils, Monocytes, and T Cells. *J. Exp. Med.* **192**(7). 1069–1074. doi:10.1084/jem.192.7.1069.

Dethlefsen L, McFall-Ngai M and Relman DA (2007) An ecological and evolutionary perspective on humang-microbe mutualism and disease. *Nature*, 811–818. doi:10.1038/nature06245.

Dethlefsen L and Relman DA (2011) Incomplete recovery and individualized responses of the human distal gut microbiota to repeated antibiotic perturbation. *Proc. Natl. Acad. Sci.* **108**(Supplement_1). 4554–4561. doi:10.1073/pnas.1000087107.

Di Nardo A, Braff MH, Taylor KR, Na C, Granstein RD, McInturff JE, et al. (2007) Cathelicidin antimicrobial peptides block dendritic cell TLR4 activation and allergic contact sensitization. *J. Immunol.* **178**(3). 1829–34.

Diamond G, Kaiser V, Rhodes J, Russell JP and Bevins CL (2000) Transcriptional regulation of beta-defensin gene expression in tracheal epithelial cells. *Infect. Immun.* **68**(1). 113–9.

Douglas A and Smith DC (1984) The Green Hydra Symbiosis. VIII. Mechanisms in Symbiont Regulation. *Proc. R. Soc. B Biol. Sci.* **221**(1224). 291–319. doi:10.1098/rspb.1984.0035.

Douglas AE and Huss VAR (1986) On the characteristics and taxonomic position of symbiotic Chlorella. *Arch. Microbiol.* **145**(1). 80–84. doi:10.1007/BF00413031.

Douglas AE and Werren JH (2016) Holes in the hologenome: Why host-microbe symbioses are not holobionts. *MBio*, e02099. doi:10.1128/mBio.02099-15.

Dübel S, Hoffmeister S a. H and Schaller HC (1987) Differentiation pathways of ectodermal epithelial cells in hydra. *Differentiation* **35**(3). 181–189. doi:10.1111/j.1432-0436.1987.tb00167.x.

Dubilier N, Bergin C and Lott C (2008) Symbiotic diversity in marine animals: The art of harnessing chemosynthesis. *Nat. Rev. Microbiol.*, 725–740. doi:10.1038/nrmicro1992.

El Karim IA, Linden GJ, Orr DF and Lundy FT (2008) Antimicrobial activity of neuropeptides against a range of micro-organisms from skin, oral, respiratory and gastrointestinal tract sites. *J. Neuroimmunol.* **200**(1). 11–16. doi:10.1016/j.jneuroim.2008.05.014.

Epand RM and Epand RF (2009) Biochimica et Biophysica Acta Lipid domains in bacterial membranes and the action of antimicrobial agents. *BBA - Biomembr.* **1788**(1). 289–294. doi:10.1016/j.bbamem.2008.08.023.

Faurot L (1895) Etudes sur l'anatomie, l'histologie et le développement des Actinies. *Arch. Zool. Exp. Gén. Sér.* **3**(3). 43–262.

Faurot L (1903) Développement du pharynx des couples et des paires de cloisons chez les Hexactinies. *Arch. Zool. Exp. Gén. Sér.* **3**(1). 359–399.

Fjell CD, Hiss JA, Hancock REW and Schneider G (2012) Designing antimicrobial peptides: form follows function. *Nat. Rev. Drug Discov.* **11**(1). 37–51. doi:10.1038/nrd3591.

Foster JA and McVey Neufeld KA (2013) Gut-brain axis: How the microbiome influences anxiety and depression. *Trends Neurosci.*, 305–312. doi:10.1016/j.tins.2013.01.005.

Frantz AL, Rogier EW, Weber CR, Shen L, Cohen DA, Fenton LA, et al. (2012) Targeted deletion of MyD88 in intestinal epithelial cells results in compromised antibacterial immunity associated with downregulation of polymeric immunoglobulin receptor, mucin-2, and antibacterial peptides. *Mucosal Immunol.* **5**(5). 501–12. doi:10.1038/mi.2012.23.

Franzenburg S, Fraune S, Altrock PM, Künzel S, Baines JF, Traulsen A, et al. (2013a) Bacterial colonization of Hydra hatchlings follows a robust temporal pattern. *ISME J.* **7**(4). 781–90. doi:10.1038/ismej.2012.156.

Franzenburg S, Fraune S, Künzel S, Baines JF, Domazet-Loso T and Bosch TCG (2012) MyD88-deficient Hydra reveal an ancient function of TLR signaling in sensing bacterial colonizers. *Proc. Natl. Acad. Sci. U. S. A.* **109**(47). 19374–9. doi:10.1073/pnas.1213110109.

Franzenburg S, Walter J, Künzel S, Wang J, Baines JF, Bosch TCG, et al. (2013b) Distinct antimicrobial peptide expression determines host species-specific bacterial associations. *Proc. Natl. Acad. Sci. U. S. A.* **110**(39). E3730-8. doi:10.1073/pnas.1304960110.

Fraune S, Abe Y and Bosch TCG (2009) Disturbing epithelial homeostasis in the metazoan Hydra leads to drastic changes in associated microbiota. *Environ. Microbiol.* **11**(9). 2361–9. doi:10.1111/j.1462-2920.2009.01963.x.

Fraune S, Anton-Erxleben F, Augustin R, Franzenburg S, Knop M, Schröder K, et al. (2015) Bacteria-bacteria interactions within the microbiota of the ancestral metazoan Hydra contribute to fungal resistance. *ISME J.* **9**(7). 1543–56. doi:10.1038/ismej.2014.239.

Fraune S, Augustin R, Anton-Erxleben F, Wittlieb J, Gelhaus C, Klimovich VB, et al. (2010) In an early branching metazoan, bacterial colonization of the embryo is controlled by maternal antimicrobial peptides. *Proc. Natl. Acad. Sci. U. S. A.* **107**(42). 18067–72. doi:10.1073/pnas.1008573107.

Fraune S and Bosch TCG (2007) Long-term maintenance of species-specific bacterial microbiota in the basal metazoan Hydra. *Proc. Natl. Acad. Sci. U. S. A.* **104**(32). 13146–51. doi:10.1073/pnas.0703375104.

Fraune S, Franzenburg S, Augustin R and Bosch TCG (2011) Das Prinzip Metaorganismus. *BIOspektrum* **17**(6). 634–636. doi:10.1007/s12268-011-0101-8.

Freckelton ML, Nedved BT and Hadfield MG (2017) Induction of Invertebrate Larval Settlement; Different Bacteria, Different Mechanisms? *Sci. Rep.* **7**. 42557. doi:10.1038/srep42557.

Fritz JH, Ferrero RL, Philpott DJ and Girardin SE (2006) Nod-like proteins in immunity, inflammation and disease. *Nat. Immunol.* **7**(12). 1250–1257. doi:10.1038/ni1412.

Funkhouser LJ and Bordenstein SR (2013) Mom Knows Best: The Universality of Maternal Microbial Transmission. *PLoS Biol.* **11**(8). e1001631. doi:10.1371/journal.pbio.1001631.

Ganz T and Lehrer RI (1998) Antimicrobial peptides of vertebrates. *Curr. Opin. Immunol.*, 41–44. doi:10.1016/S0952-7915(98)80029-0.

García J-R, Jaumann F, Schulz S, Krause A, Rodríguez-Jiménez J, Forssmann U, et al. (2001) Identification of a novel, multifunctional *-defensin (human *-defensin 3) with specific antimicrobial activity. *Cell Tissue Res.* **306**(2). 257–264. doi:10.1007/s004410100433.

Gest H (2004) The discovery of microorganisms by Robert Hooke and Antoni van Leeuwenhoek, fellows of the Royal Society. *Notes Rec. R. Soc.*, 187–201. doi:10.1098/rsnr.2004.0055.

Ghosh D, Porter E, Shen B, Lee SK, Wilk D, Drazba J, et al. (2002) Paneth cell trypsin is the processing enzyme for human defensin-5. *Nat. Immunol.* **3**(6). 583–590. doi:10.1038/ni797.

Gill SR, Pop M, Deboy RT, Eckburg PB, Turnbaugh PJ, Samuel BS, et al. (2006) Metagenomic analysis of the human distal gut microbiome. *Science* **312**(5778). 1355–9. doi:10.1126/science.1124234.

Grasis JA, Lachnit T, Anton-Erxleben F, Lim YW, Schmieder R, Fraune S, et al. (2014) Species-specific viromes in the ancestral holobiont Hydra. *PLoS One* **9**(10). e109952. doi:10.1371/journal.pone.0109952.

Greenhalgh K, Meyer KM, Aagaard KM and Wilmes P (2016) The human gut microbiome in health: establishment and resilience of microbiota over a lifetime. *Environ. Microbiol.*, 2103–2116. doi:10.1111/1462-2920.13318.

Gruenheid S and Le Moual H (2012) Resistance to antimicrobial peptides in Gram-negative bacteria. *FEMS Microbiol. Lett.*, 81–89. doi:10.1111/j.1574-6968.2012.02528.x.

Habetha M, Anton-Erxleben F, Neumann K and Bosch TCG (2003) The Hydra viridis / Chlorella symbiosis. Growth and sexual differentiation in polyps without symbionts. *Zoology* **106**(2). 101–108.

Hadfield MG (2011) Biofilms and Marine Invertebrate Larvae: What Bacteria Produce That Larvae Use to Choose Settlement Sites. *Ann. Rev. Mar. Sci.* **3**(1). 453–470. doi:10.1146/annurev-marine-120709-142753.

Hale JD and Hancock RE (2007) Alternative mechanisms of action of cationic antimicrobial peptides on bacteria. *Expert Rev. Anti. Infect. Ther.* **5**(6). 951–959. doi:10.1586/14787210.5.6.951.

Hansen CJ, Burnell KK and Brogden KA (2006) *Antimicrobial activity of Substance P and Neuropeptide Y against laboratory strains of bacteria and oral microorganisms*. *J. Neuroimmunol.* doi:10.1016/j.jneuroim.2006.05.011.

Harris RN, James TY, Lauer A, Simon MA and Patel A (2006) Amphibian pathogen Batrachochytrium dendrobatidis is inhibited by the cutaneous bacteria of amphibian species. *Ecohealth* **3**(1). 53–56. doi:10.1007/s10393-005-0009-1.

Heath-Heckman EAC, Peyer SM, Whistler CA, Apicella MA, Goldman WE and McFall-Ngai MJ (2013) Bacterial bioluminescence regulates expression of a host cryptochrome gene in the squid-vibrio symbiosis. *MBio* **4**(2). e00167-13. doi:10.1128/mBio.00167-13.

Heijtz RD, Wang S, Anuar F, Qian Y, Bjorkholm B, Samuelsson A, et al. (2011) Normal gut microbiota modulates brain development and behavior. *Proc. Natl. Acad. Sci.* **108**(7). 3047–3052. doi:10.1073/pnas.1010529108.

Hemmrich G, Anokhin B, Zacharias H and Bosch TCG (2007a) Molecular phylogenetics in Hydra, a classical model in evolutionary developmental biology. *Mol. Phylogenet. Evol.* **44**(1). 281–290. doi:10.1016/j.ympev.2006.10.031.

Hemmrich G, Khalturin K, Boehm A-M, Puchert M, Anton-Erxleben F, Wittlieb J, et al. (2012) Molecular signatures of the three stem cell lineages in hydra and the emergence of stem cell function at the base of multicellularity. *Mol. Biol. Evol.* **29**(11). 3267–80. doi:10.1093/molbev/mss134.

Hemmrich G, Miller DJ and Bosch TCG (2007b) The evolution of immunity: a low-life perspective. *Trends Immunol.* **28**(10). 449–454. doi:10.1016/j.it.2007.08.003.

Hibino T, Loza-Coll M, Messier C, Majeske AJ, Cohen AH, Terwilliger DP, et al. (2006) The immune gene repertoire encoded in the purple sea urchin genome. *Dev. Biol.* **300**(1). 349–365. doi:10.1016/j.ydbio.2006.08.065.

Hohman TC, McNeil PL and Muscatine L (1982) Phagosome-lysosome fusion inhibited by algal symbionts of hydra Viridis. *J. Cell Biol.* **94**(1). 56–63. doi:10.1083/jcb.94.1.56.

Holstein T (1981) The morphogenesis of nematocytes in Hydra and Forskalia: an ultrastructural study. *J. Ultrastruct. Res* **75**. 276–290. doi:10.1016/s0022-5320(81)80085-8.

Holstein T and Emschermann P (1995) *Cnidaria: Hydrozoa, Kamptozoa*. .

Holstein TW, Hess MW and Salvenmoser W (2010) *Preparation techniques for transmission electron microscopy of Hydra. Methods Cell Biol.* doi:10.1016/S0091-679X(10)96013-5.

Holstein TW, Hobmayer E and David CN (1991) Pattern of epithelial cell cycling in hydra. *Dev. Biol.* **148**(2). 602–11.

Holzer P and Farzi A (2014) Neuropeptides and the microbiota- Gut-brain axis. *Adv. Exp. Med. Biol.* **817**. 196–219. doi:10.1007/978-1-4939-0897-4_9.

Hooper L V. and MacPherson AJ (2010) Immune adaptations that maintain homeostasis with the intestinal microbiota. *Nat. Rev. Immunol.*, 159–169. doi:10.1038/nri2710.

Hooper L V., Stappenbeck TS, Hong C V. and Gordon JI (2003) Angiogenins: A new class of microbicidal proteins involved in innate immunity. *Nat. Immunol.* **4**(3). 269–273. doi:10.1038/ni888.

Hooper L V., Wong MH, Thelin A, Hansson L, Falk PG and Gordon JI (2001) Molecular analysis of commensal host-microbial relationships in the intestine. *Science (80-.).* **291**(5505). 881–884. doi:10.1126/science.291.5505.881.

Hur KY and Lee MS (2015) Gut microbiota and metabolic disorders. *Diabetes Metab. J.* **39**(3). 198–203. doi:10.4093/dmj.2015.39.3.198.

Huss VAR, Frank C, Hartmann EC, Hirmer M, Kloboucek A, Seidel BM, et al. (1999) Biochemical taxonomy and molecular phylogeny of the genus Chlorella sensu lato (Chlorophyta). *J. Phycol.* **35**(3). 587–598. doi:10.1046/j.1529-8817.1999.3530587.x.

Jägersten G (1955) On the early phylogeny of the Bilateria. *Zool. Bidr. Uppsala* **30**. 321–354.

Jangi S, Gandhi R, Cox LM, Li N, Von Glehn F, Yan R, et al. (2016) Alterations of the human gut microbiome in multiple sclerosis. *Nat. Commun.* **7**. 12015. doi:10.1038/ncomms12015.

Jenssen H (2009) Therapeutic approaches using host defence peptides to tackle herpes virus infections. *Viruses*, 939–964. doi:10.3390/v1030939.

Jenssen H, Hamill P and Hancock REW (2006) Peptide antimicrobial agents. *Clin. Microbiol. Rev.* **19**(3). 491–511. doi:10.1128/CMR.00056-05.

Jolley E and Smith DC (1980) The Green Hydra Symbiosis. II. The Biology of the Establishment of the Association. *Proc. R. Soc. B Biol. Sci.* **207**(1168). 311–333. doi:10.1098/rspb.1980.0026.

Jung S, Dingley AJ, Augustin R, Anton-Erxleben F, Stanisak M, Gelhaus C, et al. (2009) Hydramacin-1, structure and antibacterial activity of a protein from the basal metazoan Hydra. *J. Biol. Chem.* **284**(3). 1896–905. doi:10.1074/jbc.M804713200.

Kabouridis PS and Pachnis V (2015) Emerging roles of gut microbiota and the immune system in the development of the enteric nervous system. *J. Clin. Invest.*, 956–964. doi:10.1172/JCI76308.

Kawaida H, Ohba K, Koutake Y, Shimizu H, Tachida H and Kobayakawa Y (2013) Symbiosis between hydra and chlorella: Molecular phylogenetic analysis and experimental study provide insight into its origin and evolution. *Mol. Phylogenet. Evol.* **66**(3). 906–914. doi:10.1016/j.ympev.2012.11.018.

Kennedy PJ, Cryan JF, Dinan TG and Clarke G (2014) Irritable bowel syndrome: a microbiome-gut-brain axis disorder? *World J. Gastroenterol.* **20**(39). 14105–25. doi:10.3748/wjg.v20.i39.14105.

Khalturin K and Bosch TC (2007) Self/nonself discrimination at the basis of chordate evolution: limits on molecular conservation. *Curr. Opin. Immunol.*, 4–9. doi:10.1016/j.coi.2006.11.001.

Khalturin K, Hemmrich G, Fraune S, Augustin R and Bosch TCG (2009) More than just orphans: are taxonomically-restricted genes important in evolution? *Trends Genet.* **25**(9). 404–413.

Knoll AH (2011) The Multiple Origins of Complex Multicellularity. *Annu. Rev. Earth Planet. Sci.* **39**(1). 217–239. doi:10.1146/annurev.earth.031208.100209.

Kono H and Rock KL (2008) How dying cells alert the immune system to danger. *Nat. Rev. Immunol.* **8**(4). 279–89. doi:10.1038/nri2215.

Koropatnick TA, Engle JT, Apicella MA, Stabb E V, Goldman WE and McFall-Ngai MJ (2004) Microbial factor-mediated development in a host-bacterial mutualism. *Science (80-.).* **306**(5699). 1186–1188. doi:10.1126/science.1102218.

Kwong WK, Mancenido AL and Moran NA (2017) Immune system stimulation by the native gut microbiota of honey bees. *R. Soc. Open Sci.* **4**(2). 170003. doi:10.1098/rsos.170003.

Lai Y and Gallo RL (2009) AMPed up immunity: how antimicrobial peptides have multiple roles in immune defense. *Trends Immunol.* **30**(3). 131–41. doi:10.1016/j.it.2008.12.003.

Laing B, Barnett MPG, Marlow G, Nasef NA and Ferguson LR (2018) An update on the role of gut microbiota in chronic inflammatory diseases, and potential therapeutic targets. *Expert Rev. Gastroenterol. Hepatol.* **12**(10). 1–15. doi:10.1080/17474124.2018.1505497.

Lange C, Hemmrich G, Klostermeier UC, López-Quintero JA, Miller DJ, Rahn T, et al. (2011) Defining the origins of the NOD-like receptor system at the base of animal evolution. *Mol. Biol. Evol.* **28**(5). 1687–702. doi:10.1093/molbev/msq349.

Lederberg BJ and McCray AT (2001) ' Ome Sweet ' Omics-- A Genealogical Treasury of Words. *Sci.* **15**(7). 8.

Lee J, Mo J-H, Katakura K, Alkalay I, Rucker AN, Liu Y-T, et al. (2006) Maintenance of colonic homeostasis by distinctive apical TLR9 signalling in intestinal epithelial cells. *Nat. Cell Biol.* **8**(12). 1327–1336. doi:10.1038/ncb1500.

Lengfeld T, Watanabe H, Simakov O, Lindgens D, Gee L, Law L, et al. (2009) Multiple Wnts are involved in Hydra organizer formation and regeneration. *Dev. Biol.* **330**(1). 186–199. doi:10.1016/j.ydbio.2009.02.004.

Lewis LA and Muller-Parker G (2004) Phylogenetic Placement of "Zoochlorellae" (Chlorophyta), Algal Symbiont of the Temperate Sea Anemone *Anthopleura elegantissima*. *Biol. Bull.* **207**(2). 87–92. doi:10.2307/1543583.

Ley RE, Lozupone CA, Hamady M, Knight R and Gordon JI (2008) Worlds within worlds: evolution of the vertebrate gut microbiota. *Nat. Rev. Microbiol.* **6**(10). 776–88. doi:10.1038/nrmicro1978.

Ley RE, Turnbaugh PJ, Klein S and Gordon JI (2006) Microbial ecology: human gut microbes associated with obesity. *Nature* **444**(7122). 1022–3. doi:10.1038/4441022a.

Libina N, Berman JR and Kenyon C (2003) Tissue-Specific Activities of C. elegans DAF-16 in the Regulation of Lifespan. *Cell* **115**(4). 489–502. doi:10.1016/S0092-8674(03)00889-4.

Littlefield CL, Finkemeier C and Bode HR (1991) Spermatogenesis in Hydra oligactis. II. How temperature controls the reciprocity of sexual and asexual reproduction. *Dev. Biol.* **146**(2). 292–300. doi:10.1016/0012-1606(91)90231-Q.

Liu TT and Chang JT (1946) Number of Tentacles in Hydra vulgaris as a Genetic Character. *Nature* **157**(3996). 728. doi:10.1038/157728b0.

Login FH, Balmand S, Vallier A, Vincent-Monégat C, Vigneron A, Weiss-Gayet M, et al. (2011) Antimicrobial peptides keep insect endosymbionts under control. *Science* **334**(6054). 362–5. doi:10.1126/science.1209728.

Loonen LM, Stolte EH, Jaklofsky MT, Meijerink M, Dekker J, Van Baarlen P, et al. (2014) REG3γ-deficient mice have altered mucus distribution and increased mucosal inflammatory responses to the microbiota and enteric pathogens in the ileum. *Mucosal Immunol.* **7**(4). 939–947. doi:10.1038/mi.2013.109.

Mangoni ML, Mcdermott AM and Zasloff M (2016) Antimicrobial peptides and wound healing: Biological and therapeutic considerations. *Exp. Dermatol.* **25**(3). 167–173. doi:10.1111/exd.12929.

Mao YK, Kasper DL, Wang B, Forsythe P, Bienenstock J and Kunze WA (2013) Bacteroides fragilis polysaccharide A is necessary and sufficient for acute activation of intestinal sensory neurons. *Nat. Commun.* **4**(1). 1465. doi:10.1038/ncomms2478.

Martin VJ, Littlefield CL, Archer WE and Bode HR (1997) Embryogenesis in hydra. *Biol. Bull.* **192**(3). 345–363. doi:10.2307/1542745.

Martínez DE, Iñiguez AR, Percell KM, Willner JB, Signorovitch J and Campbell RD (2010) Phylogeny and biogeography of Hydra (Cnidaria: Hydridae) using mitochondrial and nuclear DNA sequences. *Mol. Phylogenet. Evol.* **57**(1). 403–410. doi:10.1016/j.ympev.2010.06.016.

Matsuzaki K (1999) Why and how are peptide–lipid interactions utilized for self-defense? Magainins and tachyplesins as archetypes. *Biochim. Biophys. Acta - Biomembr.* **1462**(1). 1–10.

Matzinger P (2002) The danger model: A renewed sense of self. *Science (80-.).*, 301–305. doi:10.1126/science.1071059.

Mayer EA, Padua D and Tillisch K (2014) Altered brain-gut axis in autism: Comorbidity or causative mechanisms? *BioEssays* **36**(10). 933–939. doi:10.1002/bies.201400075.

Mazmanian SK, Cui HL, Tzianabos AO and Kasper DL (2005) An immunomodulatory molecule of symbiotic bacteria directs maturation of the host immune system. *Cell* **122**(1). 107–118. doi:10.1016/j.cell.2005.05.007.

McAuley PJ (1981) Control of cell division of the intracellular Chlorella symbionts in green Hydra. *J. Cell Sci.* **47**. 197–206.

McAuley PJ (1982) Temporal relationships of host cell and algal mitosis in the green hydra symbiosis. *J. Cell Sci.* **58**. 423–31.

McAuley PJ (1986) Uptake of amino acids by cultured and freshly isolated symbiotic Chlorella. *New Phytol.* **104**(3). 415–427. doi:10.1111/j.1469-8137.1986.tb02909.x.

McAuley PJ (1987) Nitrogen limitation and amino-acid metabolism of Chlorella symbiotic with green hydra. *Planta* **171**(4). 532–538. doi:10.1007/BF00392303.

McAuley PJ (1990) Partitioning of Symbiotic Chlorella at Host Cell Telophase in the Green Hydra Symbiosis. *Philos. Trans. R. Soc. B Biol. Sci.* **329**(1252). 47–53. doi:10.1098/rstb.1990.0148.

McAuley PJ and Darrah PR (1990) Regulation of numbers of symbiotic Chlorella by density-dependent division. *Philos. Trans. - R. Soc. London, B* **329**(1252). 55–63. doi:10.1098/rstb.1990.0149.

McAuley PJ and Muscatine L (1986) The cell cycle of symbiotic Chlorella. IV. DNA content of algae slowly increases during host starvation of green hydra. *J. Cell Sci.* **85**. 73–84.

McAuley PJ and Smith DC (1982) The Green Hydra Symbiosis. V. Stages in the Intracellular Recognition of Algal Symbionts by Digestive Cells. *Proc. R. Soc. B Biol. Sci.* **216**(1202). 7–23. doi:10.1098/rspb.1982.0058.

McCormick TS and Weinberg A (2010) Epithelial cell-derived antimicrobial peptides are multifunctional agents that bridge innate and adaptive immunity. *Periodontol. 2000* **54**(1). 195–206. doi:10.1111/j.1600-0757.2010.00373.x.

McFall-Ngai M, Hadfield MG, Bosch TCG, Carey H V, Domazet-Lošo T, Douglas AE, et al. (2013) Animals in a bacterial world, a new imperative for the life sciences. *Proc. Natl. Acad. Sci. U. S. A.* **110**(9). 3229–36. doi:10.1073/pnas.1218525110.

McVey Neufeld KA, Mao YK, Bienenstock J, Foster JA and Kunze WA (2013) The microbiome is essential for normal gut intrinsic primary afferent neuron excitability in the mouse. *Neurogastroenterol. Motil.* **25**(2). 183-e88. doi:10.1111/nmo.12049.

Medina M, Collins a G, Silberman JD and Sogin ML (2001) Evaluating hypotheses of basal animal phylogeny using complete sequences of large and small subunit rRNA. *Proc. Natl. Acad. Sci.* **98**(17). 9707–9712. doi:10.1073/pnas.171316998.

Medzhitov R (2007) Recognition of microorganisms and activation of the immune response. *Nature* **449**(7164). 819–826. doi:10.1038/nature06246.

Meints RH and Pardy RL (1980) Quantitative demonstration of cell surface involvement in a plant-animal symbiosis: lectin inhibition of reassociation. *J. Cell Sci.* **43**(1). 239–51.

Meylan E, Tschopp J and Karin M (2006) Intracellular pattern recognition receptors in the host response. *Nature* **442**(7098). 39–44. doi:10.1038/nature04946.

Miller DJ, Ball EE and Technau U (2005) Cnidarians and ancestral genetic complexity in the animal kingdom. *Trends Genet.*, 536–539. doi:10.1016/j.tig.2005.08.002.

Miller DJ, Hemmrich G, Ball EE, Hayward DC, Khalturin K, Funayama N, et al. (2007) The innate immune repertoire in cnidaria--ancestral complexity and stochastic gene loss. *Genome Biol.* **8**(4). R59. doi:10.1186/gb-2007-8-4-r59.

Miller MA, Technau U, Smith KM and Steele RE (2000) Oocyte development in Hydra involves selection from competent precursor cells. *Dev. Biol.* **224**(2). 326–338. doi:10.1006/dbio.2000.9790.

Minter LM, Turley DM, Das P, Shin HM, Joshi I, Lawlor RG, et al. (2005) Inhibitors of γ-secretase block in vivo and in vitro T helper type 1 polarization by preventing Notch upregulation of Tbx21. *Nat. Immunol.* **6**(7). 680–688. doi:10.1038/ni1209.

Monsalve M and Olmos Y (2011) The complex biology of FOXO. *Curr. Drug Targets* **12**(9). 1322–50.

Mookherjee N, Brown KL, Bowdish DME, Doria S, Falsafi R, Hokamp K, et al. (2006) Modulation of the TLR-mediated inflammatory response by the endogenous human host defense peptide LL-37. *J. Immunol.* **176**(4). 2455–64.

Moran a P, Gupta a and Joshi L (2011) Sweet-talk: role of host glycosylation in bacterial pathogenesis of the gastrointestinal tract. *Gut* **60**(10). 1412–25. doi:10.1136/gut.2010.212704.

Moran NA and Sloan DB (2015) The Hologenome Concept: Helpful or Hollow? *PLoS Biol.* **13**(12). e1002311. doi:10.1371/journal.pbio.1002311.

Mortzfeld BM, Taubenheim J, Fraune S, Klimovich A V and Bosch TCG (2018) Stem Cell Transcription Factor FoxO Controls Microbiome Resilience in Hydra. *Front. Microbiol.* **9**. 629. doi:10.3389/fmicb.2018.00629.

Mukherji A, Kobiita A, Ye T and Chambon P (2013) Homeostasis in intestinal epithelium is orchestrated by the circadian clock and microbiota cues transduced by TLRs. *Cell* **153**(4). 812–827. doi:10.1016/j.cell.2013.04.020.

Murillo-Rincon AP, Klimovich A, Pemöller E, Taubenheim J, Mortzfeld B, Augustin R, et al. (2017) Spontaneous body contractions are modulated by the microbiome of Hydra. *Sci. Rep.* **7**(1). 15937. doi:10.1038/s41598-017-16191-x.

Muscatine L (1965) Symbiosis of hydra and algae—III. Extracellular products of the algae. *Comp. Biochem. Physiol.* **16**(1). 77–92. doi:10.1016/0010-406X(65)90165-9.

Muscatine L, Cook CB, Pardy RL and Pool RR (1975) Uptake, recognition and maintenance of symbiotic Chlorella by Hydra viridis. *Symp. Soc. Exp. Biol.* (29). 175–203.

Muscatine L and Lenhoff HM (1963) Symbiosis: On the role of algae symbiotic with hydra. *Science (80-.).* **142**(3594). 956–958. doi:10.1126/science.142.3594.956.

Muscatine L and Lenhoff HM (1965) Symbiosis of Hydra and Algae. II. Effects of Limited Food and Starvation on Growth of Symbiotic and Aposymbiotic Hydra. *Biol. Bull.* **129**(2). 316. doi:10.2307/1539848.

Muscatine L and McAuley PJ (1982) Transmission of symbiotic algae to eggs of green hydra. *Cytobios* **33**(130). 111–124.

Muscatine L and Neckelmann N (1981) Regulation of Numbers of Algae in the Hydra-Chlorella Symbiosis. *Ber. Dtsch. Bot. Ges.* **94**(1). 571–582. doi:10.1111/j.1438-8677.1981.tb03428.x.

Muscatine L and Pool RR (1979) Regulation of numbers of intracellular algae. *Proc. R. Soc. London - Biol. Sci.* **204**(1155). 131–139. doi:10.1098/rspb.1979.0018.

Nakatsuji T and Gallo RL (2012) Antimicrobial Peptides: Old Molecules with New Ideas. *J. Invest. Dermatol.* **132**(3). 887–895. doi:10.1038/jid.2011.387.

Nawrocki KL, Crispell EK and McBride SM (2014) Antimicrobial peptide resistance mechanisms of gram-positive bacteria. *Antibiot.* **3**(4). 461–492. doi:10.3390/antibiotics3040461.

Neufeld K-AM, Kang N, Bienenstock J and Foster JA (2011a) Effects of intestinal microbiota on anxiety-like behavior. *Commun. Integr. Biol.* **4**(4). 492–4. doi:10.4161/cib.4.4.15702.

Neufeld KM, Kang N, Bienenstock J and Foster JA (2011b) Reduced anxiety-like behavior and central neurochemical change in germ-free mice. *Neurogastroenterol. Motil.* **23**(3). 255-e119. doi:10.1111/j.1365-2982.2010.01620.x.

Nguyen LT, Haney EF and Vogel HJ (2011) The expanding scope of antimicrobial peptide structures and their modes of action. *Trends Biotechnol.* **29**(9). 464–472. doi:10.1016/j.tibtech.2011.05.001.

Nicholson JK, Holmes E, Kinross J, Burcelin R, Gibson G, Jia W, et al. (2012) Host-gut microbiota metabolic interactions. *Science (80-.).*, 1262–1267. doi:10.1126/science.1223813.

Nyholm S V and Graf J (2012) Knowing your friends: Invertebrate innate immunity fosters beneficial bacterial symbioses. *Nat. Rev. Microbiol.*, 815–827. doi:10.1038/nrmicro2894.

Ochman H, Worobey M, Kuo C-H, Ndjango J-BN, Peeters M, Hahn BH, et al. (2010) Evolutionary relationships of wild hominids recapitulated by gut microbial communities. *PLoS Biol.* **8**(11). e1000546. doi:10.1371/journal.pbio.1000546.

Olszak T, An D, Zeissig S, Vera MP, Richter J, Franke A, et al. (2012) Microbial exposure during early life has persistent effects on natural killer T cell function. *Science (80-.).* **336**(6080). 489–493. doi:10.1126/science.1219328.

Ong ZY, Wiradharma N and Yang YY (2014) Strategies employed in the design and optimization of synthetic antimicrobial peptide amphiphiles with enhanced therapeutic potentials. *Adv. Drug Deliv. Rev.*, 28–45. doi:10.1016/j.addr.2014.10.013.

Oschman JL (1967) Structure and reproduction of the algal symbionts of Hydra viridis. *J. Phycol.* **3**(4). 221–228. doi:10.1111/j.1529-8817.1967.tb04660.x.

Ouwerkerk JP, de Vos WM and Belzer C (2013) Glycobiome: bacteria and mucus at the epithelial interface. *Best Pract. Res. Clin. Gastroenterol.* **27**(1). 25–38. doi:10.1016/j.bpg.2013.03.001.

Palmer C, Bik EM, DiGiulio DB, Relman DA and Brown PO (2007) Development of the human infant intestinal microbiota. *PLoS Biol.* **5**(7). 1556–1573. doi:10.1371/journal.pbio.0050177.

Pardy RL (1974a) Some factors affecting the growth and distribution of the algal endosymbionts of Hydraviridis. *Biol. Bull.* **147**(1). 105–118. doi:10.2307/1540572.

Pardy RL (1974b) Regulation of the endosymbiotic algae in Hydra viridis by digestive cells and tissue growth. *Am. Zool.* **14**(2). 583–588.

Pardy RL (1976) The production of aposymbiotic hydra by the photodestruction of green hydra zoochlorellae. *Biol. Bull.* **151**(1). 225–235. doi:10.2307/1540716.

Pardy RL and Muscatine L (1973) Recognition of symbiotic algae by Hydra viridis. A quantitative study of the uptake of living algae by aposymbiotic H. viridis. *Biol. Bull.* **145**(3). 565–579. doi:10.2307/1540637.

Park HD, Greenblatt CL, Mattern CFT and Merril CR (1967) Some relationships between Chlorohydra, its symbionts and some other chlorophyllous forms. *J. Exp. Zool.* **164**(2). 141–161. doi:10.1002/jez.1401640203.

Pasare C and Medzhitov R (2005) Toll-like receptors: linking innate and adaptive immunity. *Adv Exp Med Biol* **560**. 11–18. doi:10.1007/0-387-24180-9_2.

Petersen C and Round JL (2014) Defining dysbiosis and its influence on host immunity and disease. *Cell. Microbiol.*, 1024–1033. doi:10.1111/cmi.12308.

Pietschke C, Treitz C, Forêt S, Schultze A, Künzel S, Tholey A, et al. (2017) Host modification of a bacterial quorum-sensing signal induces a phenotypic switch in bacterial symbionts. *Proc. Natl. Acad. Sci.* **114**(40). E8488–E8497. doi:10.1073/pnas.1706879114.

Pisani D, Pett W, Dohrmann M, Feuda R, Rota-Stabelli O, Philippe H, et al. (2015) Genomic data do not support comb jellies as the sister group to all other animals. *Proc. Natl. Acad. Sci.* **112**(50). 15402–15407. doi:10.1073/pnas.1518127112.

Pool RR (1979) The role of algal antigenic determinants in the recognition of potential algal symbionts by cells of Chlorohydra. *J. Cell Sci.* **35**. 367–79.

Pröschold T, Darienko T, Silva PC, Reisser W and Krienitz L (2011) The systematics of Zoochlorella revisited employing an integrative approach. *Environ. Microbiol.* **13**(2). 350–364. doi:10.1111/j.1462-2920.2010.02333.x.

Rakoff-Nahoum S, Paglino J, Eslami-Varzaneh F, Edberg S and Medzhitov R (2004) Recognition of commensal microflora by toll-like receptors is required for intestinal homeostasis. *Cell* **118**(2). 229–241. doi:10.1016/j.cell.2004.07.002.

Raymond F, Ouameur AA, Déraspe M, Iqbal N, Gingras H, Dridi B, et al. (2016) The initial state of the human gut microbiome determines its reshaping by antibiotics. *ISME J.* **10**(3). 707–720. doi:10.1038/ismej.2015.148.

Rees TAV (1990a) The green hydra symbiosis and ammonium III. Characteristics of ammonium release by a high maltose-releasing symbiotic strain of Chlorella. *Proc. R. Soc. B Biol. Sci.* **242**(1305). 249–253. doi:10.1098/rspb.1990.0131.

Rees TAV (1990b) The green hydra symbiosis and ammonium IV. Methylammonium uptake by freshly isolated symbionts and cultured algae; evidence for low-ammonium concentration in the perialgal space. *Proc. R. Soc. B Biol. Sci.* **242**(1305). 255–259. doi:10.1098/rspb.1990.0132.

Rees TAV and Ellard FM (1989) Nitrogen conservation and the green hydra symbiosis. *Proc. - R. Soc. London, B* **236**(1283). 203–212. doi:10.1098/rspb.1989.0021.

Rees TA V. (1986) The Green Hydra Symbiosis and Ammonium I. The Role of the Host in Ammonium Assimilation and its Possible Regulatory Significance. *Proc. R. Soc. B Biol. Sci.* **229**(1256). 299–314. doi:10.1098/rspb.1986.0087.

Rees TA V. (1989) The Green Hydra Symbiosis and Ammonium II. Ammonium Assimilation and Release by Freshly Isolated Symbionts and Cultured Algae. *Proc. R. Soc. B Biol. Sci.* **235**(1281). 365–382. doi:10.1098/rspb.1989.0005.

Rees TA V., Shah N and Stewart GR (1989) Glutamine synthetase isoforms in the green hydra symbiosis. *New Phytol.* **111**(4). 621–623. doi:10.1111/j.1469-8137.1989.tb02355.x.

Reshef L, Koren O, Loya Y, Zilber-Rosenberg I and Rosenberg E (2006) The coral probiotic hypothesis. *Environ. Microbiol.* **8**(12). 2068–73. doi:10.1111/j.1462-2920.2006.01148.x.

Rock KL and Kono H (2008) The Inflammatory Response to Cell Death. *Annu. Rev. Pathol. Mech. Dis.* **3**(1). 99–126. doi:10.1146/annurev.pathmechdis.3.121806.151456.

Roffman B and Lenhoff HM (1969) Formation of polysaccharides by hydra from substrates produced by their endosymbiotic algae. *Nature* **221**(5178). 381–2.

Rohrl J, Yang D, Oppenheim JJ and Hehlgans T (2010) Human -Defensin 2 and 3 and Their Mouse Orthologs Induce Chemotaxis through Interaction with CCR2. *J. Immunol.* **184**(12). 6688–6694. doi:10.4049/jimmunol.0903984.

Rohwer F, Seguritan V, Azam F and Knowlton N (2002) Diversity and distribution of coral-associated bacteria. *Mar. Ecol. Prog. Ser.* **243**. 1–10. doi:10.3354/meps243001.

Rosenberg E, Koren O, Reshef L, Efrony R and Zilber-Rosenberg I (2007) The role of microorganisms in coral health, disease and evolution. *Nat. Rev. Microbiol.* **5**(5). 355–362. doi:10.1038/nrmicro1635.

Rosenberg E and Zilber-Rosenberg I (2013) *The hologenome concept: Human, animal and plant microbiota*. *Hologenome Concept Human, Anim. Plant Microbiota*. doi:10.1007/978-3-319-04241-1.

Rosenstiel P, Philipp EER, Schreiber S and Bosch TCG (2009) Evolution and function of innate immune receptors--insights from marine invertebrates. *J. Innate Immun.* **1**(4). 291–300. doi:10.1159/000211193.

Round JL, Lee SM, Li J, Tran G, Jabri B, Chatila TA, et al. (2011) The Toll-like receptor 2 pathway establishes colonization by a commensal of the human microbiota. *Science* **332**(6032). 974–7. doi:10.1126/science.1206095.

Round JL and Mazmanian SK (2009) The gut microbiota shapes intestinal immune responses during health and disease. *Nat. Rev. Immunol.* **9**(5). 313–23. doi:10.1038/nri2515.

Salzman NH (2011) Microbiota-immune system interaction: An uneasy alliance. *Curr. Opin. Microbiol.*, 99–105. doi:10.1016/j.mib.2010.09.018.

Salzman NH, Hung K, Haribhai D, Chu H, Karlsson-Sjöberg J, Amir E, et al. (2010) Enteric defensins are essential regulators of intestinal microbial ecology. *Nat. Immunol.* **11**(1). 76–83. doi:10.1038/ni.1825.

Sampson TR, Debelius JW, Thron T, Janssen S, Shastri GG, Ilhan ZE, et al. (2016) Gut Microbiota Regulate Motor Deficits and Neuroinflammation in a Model of Parkinson's Disease. *Cell* **167**(6). 1469–1480.e12. doi:10.1016/j.cell.2016.11.018.

Sampson TR and Mazmanian SK (2015) Control of brain development, function, and behavior by the microbiome. *Cell Host Microbe*, 565–576. doi:10.1016/j.chom.2015.04.011.

Schauber J, Svanholm C, Term??n S, Iffland K, Menzel T, Scheppach W, et al. (2003) Expression of the cathelicidin LL-37 is modulated by short chain fatty acids in colonocytes: Relevance of signalling pathways. *Gut* **52**(5). 735–741. doi:10.1136/gut.52.5.735.

Schierwater B, Eitel M, Jakob W, Osigus HJ, Hadrys H, Dellaporta SL, et al. (2009) Concatenated analysis sheds light on early metazoan evolution and fuels a modern "urmetazoon" hypothesis. *PLoS Biol.* **7**(1). 36–44. doi:10.1371/journal.pbio.1000020.

Schikorski D, Cuvillier-Hot V, Leippe M, Boidin-Wichlacz C, Slomianny C, Macagno E, et al. (2008) Microbial challenge promotes the regenerative process of the injured central nervous system of the medicinal leech by inducing the synthesis of antimicrobial peptides in neurons and microglia. *J. Immunol.* **181**(2). 1083–95. doi:10.4049/JIMMUNOL.181.2.1083.

Schloissnig S, Arumugam M, Sunagawa S, Mitreva M, Tap J, Zhu A, et al. (2013) Genomic variation landscape of the human gut microbiome. *Nature* **493**(7430). 45–50. doi:10.1038/nature11711.

Schroeder LA and Callaghan WM (1981) Thermal tolerance and acclimation of two species of Hydra. *Limnol. Ocean.* **26**(4). 690–696. doi:10.4319/lo.1981.26.4.0690.

Schwentner M and Bosch TCG (2015) Revisiting the age, evolutionary history and species level diversity of the genus Hydra (Cnidaria: Hydrozoa). *Mol. Phylogenet. Evol.* **91**. 41–55. doi:10.1016/j.ympev.2015.05.013.

Scott FI, Horton DB, Mamtani R, Haynes K, Goldberg DS, Lee DY, et al. (2016) Administration of Antibiotics to Children Before Age 2 Years Increases Risk for Childhood Obesity. *Gastroenterology* **151**(1). 120–129.e5. doi:10.1053/j.gastro.2016.03.006.

Scott MG and Hancock RE (2000) Cationic antimicrobial peptides and their multifunctional role in the immune system. *Crit Rev Immunol* **20**(5). 407–431.

Seiler F, Hellberg J, Lepper PM, Kamyschnikow A, Herr C, Bischoff M, et al. (2013) FOXO Transcription Factors Regulate Innate Immune Mechanisms in Respiratory Epithelial Cells. *J. Immunol.* **190**(4). 1603–1613. doi:10.4049/jimmunol.1200596.

Seybold A, Salvenmoser W and Hobmayer B (2016) Sequential development of apical-basal and planar polarities in aggregating epitheliomuscular cells of Hydra. *Dev. Biol.* **412**(1). 148–159. doi:10.1016/j.ydbio.2016.02.022.

Shimizu H, Aufschnaiter R, Li L, Sarras MP, Borza DB, Abrahamson DR, et al. (2008) The extracellular matrix of hydra is a porous sheet and contains type IV collagen. *Zoology* **111**(5). 410–418. doi:10.1016/j.zool.2007.11.004.

Shimizu H, Koizumi O and Fujisawa T (2004) Three digestive movements in Hydra regulated by the diffuse nerve net in the body column. *J. Comp. Physiol. A* **190**(8). 623–30. doi:10.1007/s00359-004-0518-3.

Shimizu H, Takaku Y, Zhang X and Fujisawa T (2007) The aboral pore of hydra: Evidence that the digestive tract of hydra is a tube not a sac. *Dev. Genes Evol.* **217**(8). 563–568. doi:10.1007/s00427-007-0165-0.

Shimizu H, Zhang X, Zhang J, Leontovich A, Fei K, Yan L, et al. (2002) Epithelial morphogenesis in hydra requires de novo expression of extracellular matrix components and matrix metalloproteinases. *Development* **129**(6). 1521–1532.

Slautterback DB and Fawcett DW (1959) The Development of the Cnidoblasts of Hydra An Electron Microscope Study of Cell Differentiation. *J Biophys Biochem Cytol* **5**(3). 441–452.

Smith D, L M and Lewis D (1969) Carbohydrate movement from autotrophs to heterotrophs in parasitic and mutualistic symbiosis. *Biol. Rev. Camb. Philos. Soc.* **44**(1). 17–90. doi:10.1111/j.1469-185X.1969.tb00821.x.

Smith DC (1991) Why do so few animals form endosymbiotic associations with photosynthetic microbes? *Philos. Trans. R. Soc. London. Ser. B Biol. Sci.* **333**(1267). 225–230. doi:10.1098/rstb.1991.0071.

Smith K, McCoy KD and Macpherson AJ (2007) Use of axenic animals in studying the adaptation of mammals to their commensal intestinal microbiota. *Semin. Immunol.* **19**(2). 59–69. doi:10.1016/J.SMIM.2006.10.002.

Smith P, Willemsen D, Popkes M, Metge F, Gandiwa E, Reichard M, et al. (2017) Regulation of life span by the gut microbiota in the short-lived african turquoise killifish. *Elife* **6**. doi:10.7554/eLife.27014.

Sommer F, Anderson JM, Bharti R, Raes J and Rosenstiel P (2017) The resilience of the intestinal microbiota influences health and disease. *Nat. Rev. Microbiol.* **15**(10). 630–638. doi:10.1038/nrmicro.2017.58.

Sommer F and Bäckhed F (2013) The gut microbiota-masters of host development and physiology. *Nat. Rev. Microbiol.*, 227–238. doi:10.1038/nrmicro2974.

Stecher B and Hardt WD (2008) The role of microbiota in infectious disease. *Trends Microbiol.* **16**(3). 107–114. doi:10.1016/j.tim.2007.12.008.

Stilling RM, Dinan TG and Cryan JF (2014) Microbial genes, brain & behaviour - epigenetic regulation of the gut-brain axis. *Genes, Brain Behav.* **13**(1). 69–86. doi:10.1111/gbb.12109.

Sudo N, Chida Y, Aiba Y, Sonoda J, Oyama N, Yu X-N, et al. (2004) Postnatal microbial colonization programs the hypothalamic-pituitary-adrenal system for stress response in mice. *J. Physiol.* **558**(Pt 1). 263–75. doi:10.1113/jphysiol.2004.063388.

Takeuchi O and Akira S (2010) Pattern Recognition Receptors and Inflammation. *Cell* **140**(6). 805–820. doi:10.1016/j.cell.2010.01.022.

Tardent P (1995) The cnidarian cnidocyte, a hightech cellular weaponry. *BioEssays* **17**(4). 351–362. doi:10.1002/bies.950170411.

Tardent P and Holstein T (1982) Morphology and morphodynamics of the stenotele nematocyst of Hydra attenuata Pall. (Hydrozoa, Cnidaria). *Cell Tissue Res.* **224**(2). 269–290. doi:10.1007/BF00216873.

Tasiemski A, Vandenbulcke F, Mitta G, Lemoine J, Lefebvre C, Sautière P-E, et al. (2004) Molecular characterization of two novel antibacterial peptides inducible upon bacterial challenge in an annelid, the leech Theromyzon tessulatum. *J. Biol. Chem.* **279**(30). 30973–82. doi:10.1074/jbc.M312156200.

Technau U, Rudd S, Maxwell P, Gordon PMK, Saina M, Grasso LC, et al. (2005) Maintenance of ancestral complexity and non-metazoan genes in two basal cnidarians. *Trends Genet.* **21**(12). 633–9. doi:10.1016/j.tig.2005.09.007.

Thaiss CA, Zeevi D, Levy M, Zilberman-Schapira G, Suez J, Tengeler AC, et al. (2014) Transkingdom control of microbiota diurnal oscillations promotes metabolic homeostasis. *Cell* **159**(3). 514–29. doi:10.1016/j.cell.2014.09.048.

Theis KR, Dheilly NM, Klassen JL, Brucker RM, Baines JF, Bosch TCG, et al. (2016) Getting the Hologenome Concept Right: an Eco-Evolutionary Framework for Hosts and Their Microbiomes. *mSystems* **1**(2). e00028-16. doi:10.1128/mSystems.00028-16.

Thorington G and Margulis L (1981) Hydra viridis: transfer of metabolites between Hydra and symbiotic algae. *Biol. Bull.* **160**(1). 175–188. doi:10.2307/1540911.

Tremaroli V and Bäckhed F (2012) Functional interactions between the gut microbiota and host metabolism. *Nature* **489**(7415). 242–9. doi:10.1038/nature11552.

Trembley A (1744) *Mémoires pour servir à l'histoire d'un genre de polypes d'eau douce, à bras en forme de cornes*. . doi:10.5962/bhl.title.64073.

Turnbaugh PJ, Bäckhed F, Fulton L and Gordon JI (2008) Diet-Induced Obesity Is Linked to Marked but Reversible Alterations in the Mouse Distal Gut Microbiome. *Cell Host Microbe* **3**(4). 213–223. doi:10.1016/j.chom.2008.02.015.

Turnbaugh PJ, Hamady M, Yatsunenko T, Cantarel BL, Duncan A, Ley RE, et al. (2009) A core gut microbiome in obese and lean twins. *Nature* **457**(7228). 480–484. doi:10.1038/nature07540.

Turnbaugh PJ, Ley RE, Hamady M, Fraser-Liggett CM, Knight R and Gordon JI (2007) The human microbiome project. *Nature* **449**(7164). 804–10. doi:10.1038/nature06244.

Turnbaugh PJ, Ley RE, Mahowald MA, Magrini V, Mardis ER and Gordon JI (2006) An obesity-associated gut microbiome with increased capacity for energy harvest. *Nature* **444**(7122). 1027–31. doi:10.1038/nature05414.

Vaishnava S, Behrendt CL, Ismail AS, Eckmann L and Hooper L V. (2008) Paneth cells directly sense gut commensals and maintain homeostasis at the intestinal host-microbial interface. *Proc. Natl. Acad. Sci.* **105**(52). 20858–20863. doi:10.1073/pnas.0808723105.

Vaishnava S, Yamamoto M, Severson KM, Ruhn KA, Yu X, Koren O, et al. (2011) The antibacterial lectin RegIIIgamma promotes the spatial segregation of microbiota and host in the intestine. *Science* **334**(6053). 255–8. doi:10.1126/science.1209791.

Vatanen T, Kostic AD, D'Hennezel E, Siljander H, Franzosa EA, Yassour M, et al. (2016) Variation in Microbiome LPS Immunogenicity Contributes to Autoimmunity in Humans. *Cell* **165**(4). 842–853. doi:10.1016/j.cell.2016.04.007.

Venn AA, Loram JE and Douglas AE (2008) Photosynthetic symbioses in animals. *J. Exp. Bot.* **59**(5). 1069–1080. doi:10.1093/jxb/erm328.

Vuong HE, Yano JM, Fung TC and Hsiao EY (2017) The Microbiome and Host Behavior. *Annu. Rev. Neurosci.* **40**(1). 21–49. doi:10.1146/annurev-neuro-072116-031347.

Wainright PO, Hinkle G, Sogin ML and Stickel SK (1993) Monophyletic origins of the metazoa: an evolutionary link with fungi. *Science (80-.).* **260**(5106). 340–342. doi:10.1126/science.8469985.

Wanke I, Steffen H, Christ C, Krismer B, Götz F, Peschel A, et al. (2011) Skin Commensals Amplify the Innate Immune Response to Pathogens by Activation of Distinct Signaling Pathways. *J. Invest. Dermatol.* **131**(2). 382–390. doi:10.1038/jid.2010.328.

Webb AE, Kundaje A and Brunet A (2016) Characterization of the direct targets of FOXO transcription factors throughout evolution. *Aging Cell* **15**(4). 673–685. doi:10.1111/acel.12479.

Wimley WC (2010) Describing the mechanism of antimicrobial peptide action with the interfacial activity model. *ACS Chem. Biol.*, 905–917. doi:10.1021/cb1001558.

Wittlieb J, Khalturin K, Lohmann JU, Anton-Erxleben F and Bosch TCG (2006) Transgenic Hydra allow in vivo tracking of individual stem cells during morphogenesis. *Proc. Natl. Acad. Sci.* **103**(16). 6208–6211. doi:10.1073/pnas.0510163103.

Wong JH, Xia L and Ng TB (2007) A review of defensins of diverse origins. *Curr. Protein Pept. Sci.* **8**(5). 446–59.

Yang D, Chen Q, Chertov O and Oppenheim JJ (2000) Human neutrophil defensins selectively chemoattract naive T and immature dendritic cells. *J. Leukoc. Biol.* **68**(1). 9–14.

Yang D, Chertov O, Bykovskaia SN, Chen Q, Buffo MJ, Shogan J, et al. (1999) ??-Defensins: Linking innate and adaptive immunity through dendritic and T cell CCR6. *Science (80-.).* **286**(5439). 525–528. doi:10.1126/science.286.5439.525.

Yatsunenko T, Rey FE, Manary MJ, Trehan I, Dominguez-Bello MG, Contreras M, et al. (2012) Human gut microbiome viewed across age and geography. *Nature* **486**(7402). 222–7. doi:10.1038/nature11053.

Yu S and Gao N (2015) Compartmentalizing intestinal epithelial cell toll-like receptors for immune surveillance. *Cell. Mol. Life Sci.*, 3343–3353. doi:10.1007/s00018-015-1931-1.

Zaiou M (2007) Multifunctional antimicrobial peptides: Therapeutic targets in several human diseases. *J. Mol. Med.*, 317–329. doi:10.1007/s00109-006-0143-4.

Zasloff M (2002) Antimicrobial peptides of multicellular organisms. *Nature* **415**(6870). 389–95. doi:10.1038/415389a.

Zeissig S and Blumberg RS (2014) Life at the beginning: Perturbation of the microbiota by antibiotics in early life and its role in health and disease. *Nat. Immunol.*, 307–310. doi:10.1038/ni.2847.

Zilber-Rosenberg I and Rosenberg E (2008) Role of microorganisms in the evolution of animals and plants: The hologenome theory of evolution. *FEMS Microbiol. Rev.*, 723–735. doi:10.1111/j.1574-6976.2008.00123.x.

Chapter I

Hydra's glycocalyx:
A bacterial habitat and a barrier

Parts of the results in this chapter have been published in

- **Schröder K**, Bosch TCG "The origin of mucosal immunity: lessons from the holobiont *Hydra*"

  mBio: published online 1st of November 2016
  doi:10.1128/mBio.01184-16

- Fraune S, Anton-Erxleben F, Augustin R, Franzenburg S, Knop M, **Schröder K**, Willoweit-Ohl D, Bosch TCG "Bacteria-bacteria interactions within the microbiota of the ancestral metazoan *Hydra* contribute to fungal resistance"

  The ISME Journal: accepted 13th of November 2014
  doi: 10.1038/ismej.2014.239.

Abstract

Epithelial tissues serve as protective barriers and as interfaces with the environment including the microbiota. As a member of the phylum Cnidaria, the entire body plan of *Hydra* is organized as an epithelial bilayer composed of an ectoderm and an endoderm. The ectodermal epithelium is covered by a complex multi-layered glycocalyx extending up to 1.5 µm from the cell surface. The visualization of *Hydra*'s glycocalyx has been challenging due to its fragile organization that is highly sensitive to preparation procedures for electron microscopy analysis. In a methodological approach a chemical fixation was developed, which preserves details of the glycocalyx architecture previously detected only by high-pressure freezing/freeze substitution fixation (HPF/FS). This study provides the first description of how the glycocalyx is formed during ontogenetic development and shows that *Hydra* polyps hatch without a glycocalyx. Within 48 h posthatching a fully structured glycocalyx will be formed. Microscopic analysis identified the outer mucus-like layer of *Hydra*'s glycocalyx as the habitat of a diverse bacterial community. To characterize the glycocalyx as bacterial habitat the aim of this study was to identify protein components of the glycocalyx with a combined approach of gel-enhanced liquid chromatography-tandem mass spectrometry (GeLC-MS/MS) and cell line-specific transcriptome analysis. This integrative approach resulted in the identification of 79 candidate genes / proteins. Among those, the members of a cysteine-rich peptide family were identified as putative antimicrobial peptides and have been characterized with regards to gene expression patterns, protein localization and antimicrobial activity.

Introduction

All animals are holobionts consisting of a multicellular hosts and its associated bacteria, archaea, protozoa, algae, fungi, and viruses, collectively termed microbiota (Zilber-Rosenberg and Rosenberg, 2008; Bosch and McFall-Ngai, 2011; McFall-Ngai et al., 2013). The microbiota occupies different niches within a host, thereby colonizing the external and internal epithelial surfaces of various body parts. Sometimes the host organism has developed specialized cells, tissues or organs to harbor distinct microbial partners, e.g. the bacteriocytes in the aphid–*Buchnera* symbiosis (Moran et al., 2008; Douglas, 2009) and the light organ in the bobtail squid–*Vibrio* symbiosis (Nyholm and McFall-Ngai, 2004; Visick and Ruby, 2006). While intracellular symbioses with bacteria or photosynthetic algae are widespread in invertebrates, vertebrates host their microbes exclusively extracellular with one known exception of beneficial algae that live inside salamander cells (Kerney et al., 2011).

The best-characterized microbial habitat is the vertebrate gut where trillions of microbes live in a symbiotic relationship with their host. The epithelial surface in the gastrointestinal tract is covered by a highly hydrated mucus gel that protects the underlying epithelium against chemical, enzymatic, microbial and mechanical insults. By shielding the underlying epithelium from luminal bacteria and food antigens permanent overactivation of the immune system is prevented and thus, mucus plays a critical role in the maintenance of gut homeostasis (Shan et al., 2013). The intestinal tract contains a number of distinct microbial habitats that differ in mucus structure and select for heterogeneous spatial and functional organization of the microbiota (Tropini et al., 2017). The density and diversity of bacteria increase along the longitudinal axis of the gut, with the small intestine favoring facultative anaerobic, proteolytic bacteria, and the colon favoring anaerobic, saccharolytic bacteria (Turnbaugh et al., 2009; Faith et al., 2013; Gu et al., 2013; Seedorf et al., 2014). Along the transverse axis, the mucus gel can be divided into two layers: a loosely associated layer that forms the natural habitat for bacteria and a firmly attached layer, which is impenetrable for bacteria in the healthy gut (Johansson et al., 2008, 2010). Underneath the mucus layers cells present a dense 'forest' of highly diverse glycoproteins and glycolipids, which form the glycocalyx.

The muscus gel is formed by high-molecular-mass oligomeric glycoproteins referred to as mucins. Mucins are responsible for the viscous properties of the mucus gel and provide an adhesive matrix for a diverse array of antimicrobial molecules like defensins, lysozyme, lactoferrin and RegIIIγ (Vaishnava et al., 2011; Antoni et al., 2013). The positively charged antimicrobial peptides remain attached to the negatively charged mucin glycoproteins and generate a gradient within the mucus layer restricting their bactericidal action mostly to bacteria coming too close to the epithelial surface (Meyer-Hoffert et al., 2008; Vaishnava et al., 2011; Dupont et al., 2015). The segregation of antimicrobial activity within the mucus is important to enable the colonization of the outer mucus layer by the microbiota, which is crucial to inhibit the persistence or growth of pathogenic bacteria, which is referred to as 'colonization resistance' (Stecher and Hardt, 2008). Taken together, the mucus represents not only the first line of defense between bacteria and the epithelium, but also serves as the interface for host-microbe interactions.

As a member of the Cnidaria, *Hydra*'s entire body plan is formed by an epithelial bilayer composed of the endoderm lining the gastric cavity and the ectoderm permanently exposed to the aquatic environment. The endodermal epithelial cells are ciliated with pseudopod-like protrusions reflecting their phagocytotic function, while the apical surface of the ectodermal

epithelium is covered by a fibrous multi-layered structure extending up to 1.5 µm from the cell surface. Based on its ultrastructural similarity with the extracellular surface coats of mammalian epithelia lining the intestine and the lumina of blood vessels, this extracellular layer was termed glycocalyx (Kuznetsov et al., 2002). *Hydra*'s glycocalyx is composed of at least five morphologically distinguishable layers (Holstein et al., 2010), which were shown to be highly reactive to periodic acid-Schiff stain (PAS), indicating a high carbohydrate content (Böttger et al., 2012). Although the entire structure is termed glycocalyx, the characteristic feature of being membrane bound does not account for all of its layers. The outer layer that builds up more than 50% of *Hydra*'s glycocalyx consists of a loose meshwork that can be removed completely by a hypertonic salt wash (Böttger et al., 2012). Therefore, the outer layer of *Hydra*'s glycocalyx was proposed to have mucus-like properties rather than being a part of the membrane-anchored glycocalyx (Schröder and Bosch, 2016).

Research of the last decade has shown that all *Hydra* species are associated with distinct bacterial communities, which are remarkably stable even during co-cultivation with other *Hydra* species (Fraune and Bosch, 2007; Franzenburg et al., 2013). However, the exact localization of *Hydra*'s microbiota remained unknown. Spirochaetes were reported to colonize the mesoglea occasionally (Davis and Haynes, 1968; Hufnagel and Myhal, 1977), but this seems to be the exception rather than the rule, because mostly there are no bacteria present in the mesoglea. While *H. oligactis* harbors bacteria within the ectodermal epithelial cells (Fraune and Bosch, 2007), *H. vulgaris* (AEP) and *H. magnipapillata* do not possess intracellular bacteria suggesting an extracellular localization for the colonizing bacteria. However, so far several attempts to visualize *Hydra*'s extracellular bacterial colonizers by electron microscopy failed, which may be due to ineffective fixation methods. Therefore, the aims of this study were the localization of *Hydra*'s microbiota and, subsequently, the characterization of their habitat.

Results

Microscopic analyses of *Hydra*'s glycocalyx

The ectodermal epithelial surface of *Hydra* is covered by a multi-layered glycocalyx (Holstein et al., 2010; Böttger et al., 2012). In the past, electron microscopic (EM) visualization of the glycocalyx has been challenging with conventional chemical fixation. In paraformaldehyde-fixed preparations, and even after fixation with glutaraldehyde and osmium tetroxide, the outer layer of the glycocalyx was found collapsed, fragmented or detached from

the ectodermal surface. So far, the complex multi-layered structure was demonstrated only bythe highly sophisticated and technically challenging high-pressure freezing / freeze-substitution (HPF/FS) fixation (‘cryo-fixation’) (Holstein et al., 2010).

As a first attempt to improve the structural integrity of the glycocalyx during chemical fixation 0.15% ruthenium red (RR) was included in the conventional fixative, which contains 3.5% glutaraldehyde in 50 mM sodium cacodylate buffer (pH 7.4). RR is a hexavalent cationic dye with high affinity for anionic mucopolysaccharides and generates a detectable electron density in the presence of osmium tetroxide. Prior to fixation *Hydra* polyps were relaxed by 2 min incubation in 2% urethane, a commonly used invertebrate anesthetic (Macklin, 1976). Analysis of thin sections by transmission EM (TEM) showed that although the RR treatment provided a good contrast enhancement, the glycocalyx still appeared to be poorly preserved. While the outer loose layer of the glycocalyx was almost completely absent, the firmly attached inner layers were still present extending ~300 nm from the plasma membrane (**Figure 1A**). Strikingly, when polyps were not subjected to urethane treatment before fixation the outer glycocalyx layer was preserved and appeared as a filamentous mesh-like structure (**Figure 1B**). Thus, the urethane relaxation step prior fixation is responsible for almost complete loss of the outer glycocalyx layer. Therefore, in further investigations the urethane treatment was omitted, while the addition of RR was maintained to improve the contrast.

Although the outer glycocalyx layer was detectable when omitting the urethane step, it appeared as a sparse filamentous mesh-like structure (**Figure 1B**) rather than the fluffy layer observed in cryo-fixed samples (**Figure 1F**). Furthermore, the outer layer strongly varied in dimension ranging from 300 nm to 700 µm width indicating that the altered fixation conditions were suboptimal. Next, chemical fixation was performed using ‚Karnovsky‘s fixative‘ consisting of 2.5% glutaraldehyde and 2% paraformaldehyd (Karnovsky, 1965). TEM analysis revealed outer glycocalyx layers with a width of ≥700 nm consistently, which is in line with the results form cryo-fixation. In addition, a considerable increase in fibrous material in the outer layer was observed (**Figure 1C**). However condensed structures with large electron-lucid spaces in between were seen (**Figure 1C**), which are absent in the cryo-fixed glycocalyx (**Figure 1F**). To overcome this limitation Karnovsky’s fixative was supplemented with 75 mM L-lysine, which has been successfully used to visualize the fibrous anionic matrix of bacterial glycocalyces (Jacques and Graham, 1989). Together with glutaraldehyde the diamine L-lysine can form large polymers of various length by crosslinkages and therefore, may improve the preservation of the outer glycocalyx layer architecture. Indeed, hydra tissue treated with this

fixative formulation revealed in TEM analysis a homogenous, fluffy appearance of the outer glycocalyx layer (**Figure 1D**) comparable to cryo-fixed samples (**Figure 1F**). The average width of the total glycocalyx varied from 1 µm to 1.5 µm, which is in line with previous results from cryofixation (Holstein et al., 2010; Böttger et al., 2012). Notably, the addition of RR is not required for stabilization of the outer glycocalyx layer, but enhances the contrast (**Figure 1D and E**).

A limitation of glutaraldehyde as a fixing agent is that it forms irreversible cross-links, which often affect the accessibility of epitopes and hence impair the binding of antibodies. Indeed, immunohistochemistry using actin staining by phalloidin and eGFP antibodies was not compatible with Karnovsky's fixative. Therefore, the here-introduced formulation of the fixative should be chosen primarily if the visualization of the tissue morphology without further staining is of prime interest.

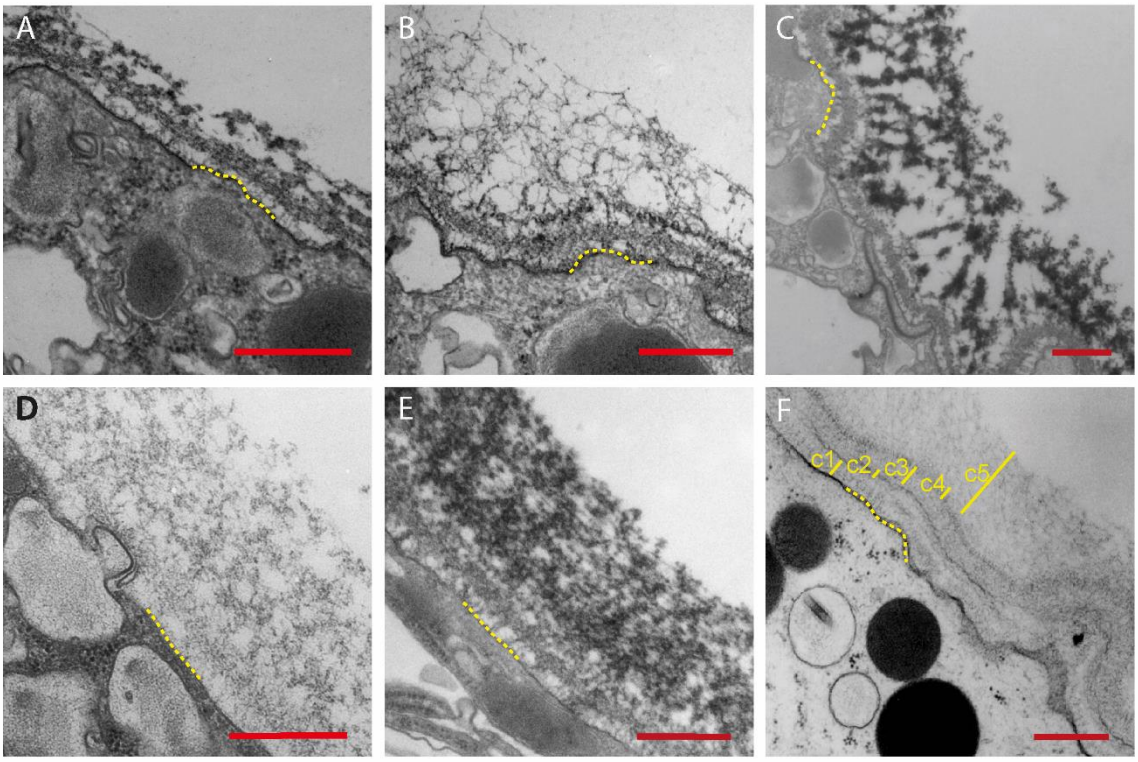

Figure 1. Preservation of *Hydra*'s glycocalyx under different chemical fixation methods.
Transmission electron microscopy (TEM) of the ectodermal surface. (A) Urethane treatment prior fixation. Fixative containing 3.5% glutaraldehyde and 0.15% ruthenium red (RR). (B-F) no urethane treatment prior fixation. (B) Fixative containing 3.5% glutaraldehyde and 0.15% RR. (C) Karnovsky's fixative (2.5% glutaraldehyde, 2% paraformaldehyde) containing 0.15% RR. (D) Karnovsky's fixative containing 75 mM L-lysine. Note the increase in fibrous material in the outer layer. (E) Karnovsky's fixative containing 75 mM L-lysine and 0.15% RR. (F) For comparison a TEM graph of high-pressure freezing / freeze substitution (HPF/FS) fixation is shown. Note the excellent preservation of five distinct layers (c1–c5). Modified from (Fraune et al., 2015). Scale bars 500 nm. Dashed yellow line indicates the plasma membrane.

As a next step scanning EM (SEM) was performed on *Hydra* polyps fixed with Karnovsky's fixative including L-lysine and RR. SEM analysis revealed that the glycocalyx appears as a homogenous coat covering the entire surface of the polyp with the exception of the aboral end of the polyp. Notably, the ectodermal epithelial cells of the peduncle (the region between the basal disc and the budding zone) are completely covered by the glycocalyx, which then abruptly ends by forming a sharp border to the cells of the basal disc (**Figure 2A and B**). The basal disc is formed by glandulomuscular cells that arise from ectodermal epithelial cells of the peduncle region as a result of terminal differentiation under tight positional control (Campbell, 1967; Bode et al., 1986; Dübel et al., 1987; Böttger and Hassel, 2012). The cells of the basal disc are known to produce a sticky mucus allowing *Hydra* to attach to the surface of different substrates (Rodrigues et al., 2016). The foot mucus was shown to contain acidic mucopolysaccharides and differs in histochemical properties from the vesicles of the ectodermal body wall that secrete the glycocalyx (Burnett, 1966; Davis, 1973).

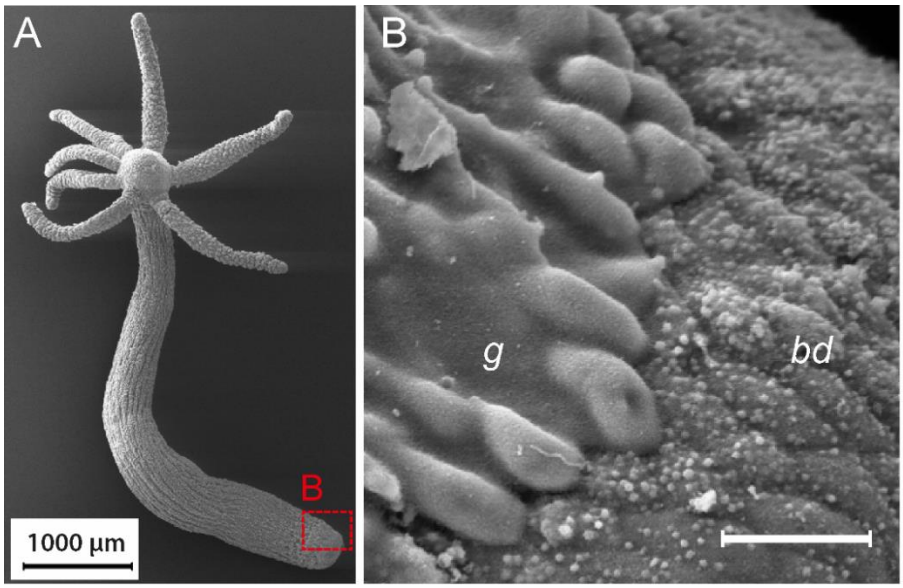

Figure 2. *Hydra*'s glycocalyx ends with a sharp border at the basal disc.
(A) Scanning electron microscopy of a *Hydra* polyp. Red box indicates the foot region shown in (B). Note the abrupt ending of glycocalyx coated ectodermal cells (g) and numerous apical blebs at the surface of basal disc cells (bd) indicating their secretory function. Scale bar 20 µm.

Bacteria colonize the outer mucus-like layer of *Hydra*'s glycocalyx

The first aim of this study was the localization of *Hydra*'s microbiota. Indeed, the successful establishment of a chemical fixation method preserving *Hydra*'s multi-layered glycocalyx revealed that bacteria colonize the loose outer layer (c5) of the glycocalyx (**Figure 3A**). Strikingly, bacteria were observed to penetrate the inner layers of the glycocalyx

(c1–4) indicating that these firmly attached layers may function as a protective barrier for the epithelial cell surface. Confocal laser scanning microscopy (CLSM) using SYBR Gold staining as well as scanning EM (SEM) uncovered a dense and morphologically heterogeneous community of bacteria colonizing the outer surface of the ectodermal epithelium (**Figure 3B-D**). In all specimens examined, rod-shaped as well as cocci bacteria were found attached to the ectodermal epithelial cells.

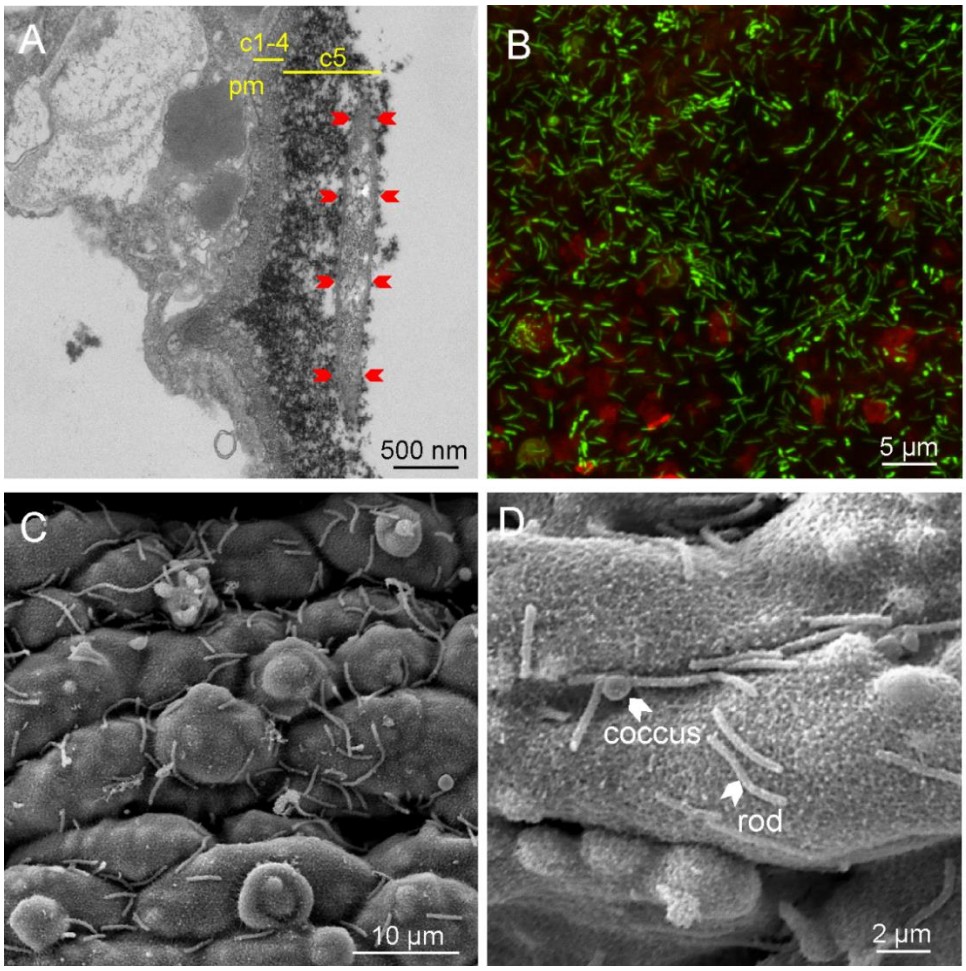

Figure 3. *Hydra*'s glycocalyx is colonized by a complex bacterial community.
(A) Transmission electron micrograph of a rod-shaped bacterium (red arrows) located within the outer layer (c5) of the glycocalyx covering ectodermal epithelium. (B) Total bacterial community colonizing the surface of the ectodermal epithelium in *Hydra* stained with SYBR gold. (C and D) Scanning electron microscopy (SEM) analysis of *Hydra*'s ectodermal. Pictures have been published in (Fraune et al., 2015).

Furthermore, the same microscopic techniques (TEM, SEM and CLSM) were used to examine the endodermal epithelium lining *Hydra*'s gastric cavity. Whereas the ectodermal epithelium appears to be protected from direct contact with bacteria by the glycocalyx the endodermal epithelium does not possess a comparable glycocalyx-like structure (**Figure 4A)**.

Instead, the endodermal cells are ciliated and the surface exhibits pseudopod-like structures pointing to their phagocytotic function where a dense glycocalyx would be detrimental (**Figure 4B and C**). Despite the use of various fixation and preparation techniques, so far no evidence that bacteria stably colonize the endodermal epithelial surface. As it seems, *Hydra*'s digestive system might not possess a stable bacterial community.

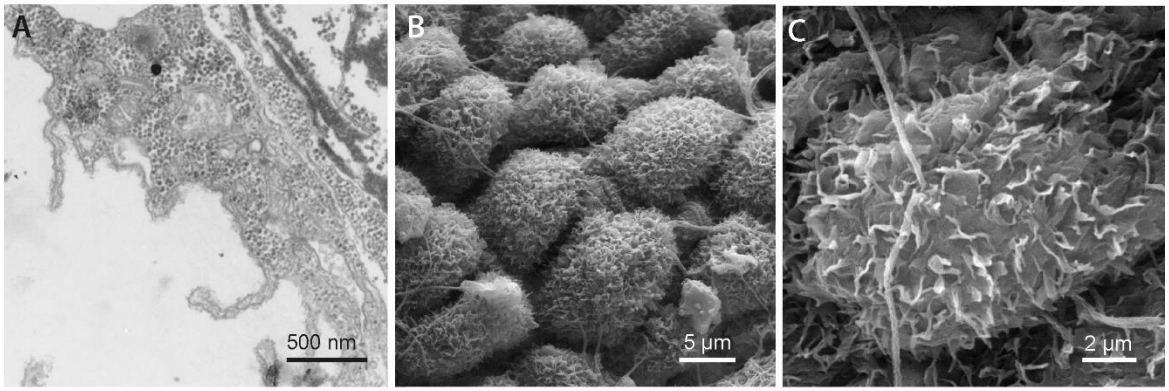

Figure 4. Electron microscopic analysis of *Hydra*'s endoderm.
(A) Transmission electron microscopy of the endodermal cell surface. Note the absence of a glycocalyx. (B and C) Scanning electron microscopy of the endodermal surface in the gastric cavity. Panel B and C have been published in (Schröder and Bosch, 2016).

Hydra polyps hatch without a glycocalyx

The successful development of a chemical fixation method preserving the fragile structure of *Hydra*'s glycocalyx revealed that the outer mucus-like layer is the habitat for bacteria, while the firmly attached inner layers act as a barrier separating bacteria from direct contact with the epithelial cells. Since there are no reports on the development of *Hydra*'s glycocalyx during embryogenesis, the question arose when does the formation of the interface for host-microbe cross-talk take place during ontogenetic development.

Although *Hydra* mainly propagates asexually by budding, the animals also go through seasonal sexual phases with eggs and sperm produced from interstitial stem cells (Bosch and David, 1987). *Hydra*'s embryonic development begins with radial cleavages forming a coeloblastula about 8 hours after fertilization followed by gastrulation, which is completed approximately 24 hours postfertilization. At that time, cells of the outer epithelial layer develop filopodia and finally secrete cuticular material, which forms a thick protective layer, referred to as embryotheca (Martin et al., 1997). The embryo stays in the so-called cuticle stage during a variable time of dormancy, in *H. vulgaris* (AEP) usually ranging from 2 to 6 weeks, until a young polyp hatches. During the last two days before hatching specification of the three cell

lineages occurs, the gastric cavity forms and the interstitial stem cells proliferate and differentiate into neurons, nematocytes, and secretory cells (Martin et al., 1997). Finally, the embryotheca cracks and the young polyp hatches with the head end appearing first.

To address the question, if *Hydra* polyps already possess a glycocalyx when they hatch, embryos were collected and monitored to capture the beginning of the hatching process that becomes visible by breaking of the thick outer shell of the embryotheca. *In vivo* observation of hatching *Hydra* revealed that young polyps remain enveloped by a delicate, transparent membrane during the hatching process (**Figure 5A and B**). The thin envelope remains for approximately 6 to 12 hours and will be pierced eventually by the elongating polyp leaving the embryotheca.

Some of the hatching polyps were subjected to chemical fixation for subsequent TEM analysis. The embryotheca that surrounds the young polyp is a 10 µm thick multi-layered structure that can be roughly separated into two parts, the thick outer shell and an inner part of about 2 µm (**Figure 5C and D**). At the beginning of the hatching process the inner part of the embryotheca is in close contact to the ectodermal epithelium of the polyp and comprises five distinguishable layers, which differ morphologically from the glycocalyx of adult *Hydra* (**Figure 5C and D**). The thick outer shell of the embryotheca cracks at the beginning of the hatching process and detaches from the inner part of the embryotheca, which starts to swell and detaches from the ectodermal epithelium that is devoid of a glycocalyx (**Figure 5E and F**). TEM analysis revealed that the swollen inner part of the embryotheca forms the delicate envelope surrounding the hatchling, which was previously observed *in vivo* (**Figure 5A, B and F**). Notably, bacteria were frequently seen attached to the surface of the membranous envelope (data not shown), but never inside suggesting that it represents a protective barrier for the young polyp that is devoid of a glycocalyx at this time point (**Figure 5F**).

As a next step the ectodermal surface of young polyps was analyzed by TEM to examine when glycocalyx formation takes place. A few hours after polyps had liberated completely from the embryotheca the ectodermal epithelium shows a thin extracellular coat of approximately 150 nm width without any stratification (**Figure 6A**). A morphological correlate of the multi-layered glycocalyx was observed 48 hours after hatching. Comparable to adult *Hydra* the four inner layers of the glycocalyx exhibit about 200 nm (**Figure 6B and C**). Notably, the outer mucus-like layer is significantly thinner than in adult polyps suggesting that the formation of the glycocalyx has not completed at this time point (**Figure 6B and C**).

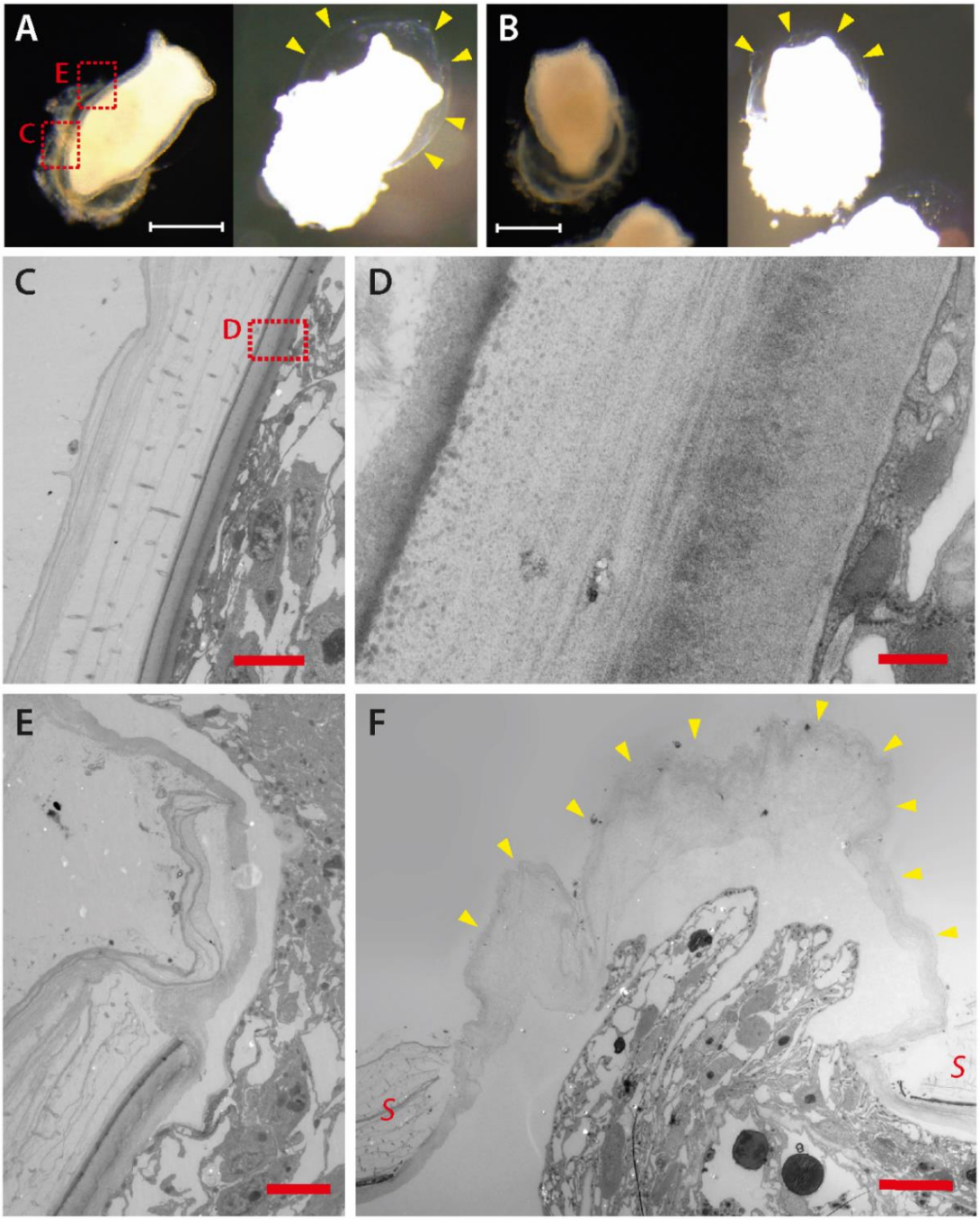

Figure 5. The ectodermal surface in hatching *Hydra* polyps.
(A and B) Hatching *Hydra* polyps. Light overexposure reveals that the thick outer shell of the embryotheca has cracked, while the polyp is still covered by a thin membrane (yellow arrow heads). Red boxes indicate the regions analyzed by transmission electron microscopy (TEM). Scale bars 0.5 mm. (C) TEM graph of the cuticle. The polyp's ectodermal epithelium is in close contact to the inner part of the embryotheca (yellow line), which presents a ~2 µm thick multi-layered structure morphologically distinct from the glycocalyx of adult polyps. Scale bar 5 µm, red box indicates the region depicted in (D) High-resolution TEM graph of the ectodermal surface. Scale bar 300 nm. (E) TEM graph showing the edge of the breaking embryotheca. Note that the inner part completely detaches from the ectodermal surface, which is devoid of a glycocalyx. Scale bar 5 µm. (F). TEM graph of a polyp starting to hatch through a crack of the thick outer shell (os). Yellow arrow heads mark the delicate membrane (see A and B) that originates from the inner part of the embryotheca, which start swelling after removal of the thick embryotheca shell. Scale bar 8 µm.

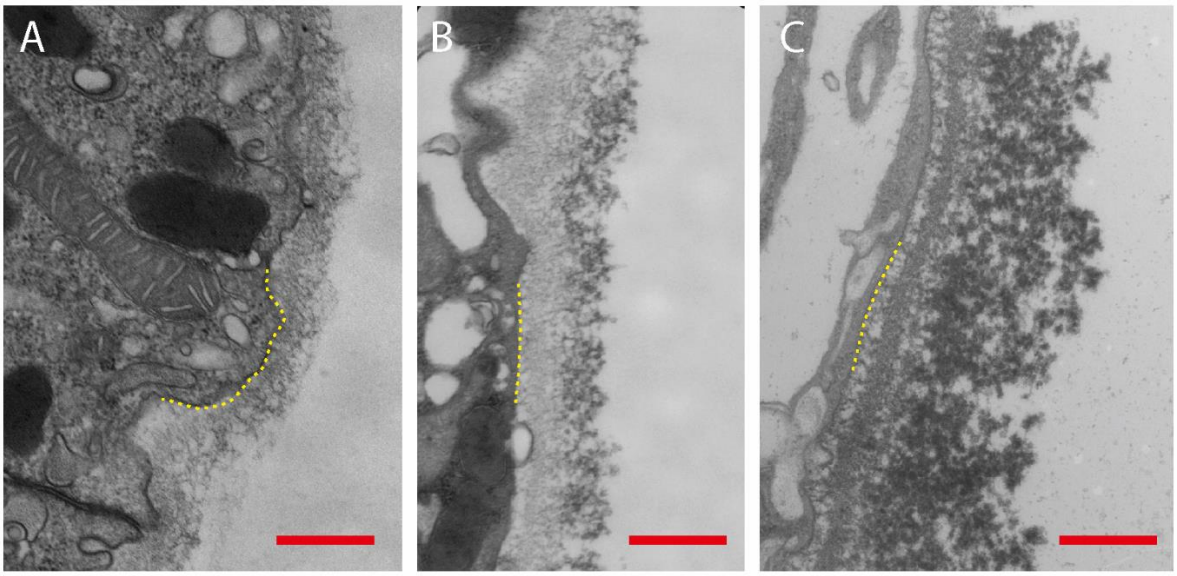

Figure 6. The ectodermal surface in young *Hydra* polyps after hatching.
Transmission electron microscopy analysis of the ectodermal surface. (A) A few hours after hatching the ectoderm is covered by a ~250 nm thick structure lacking distinguishable separate layers. (B) 48 h after hatching the dense inner layers of the glycocalyx have appeared and the outer mucus-like layer starts to form, although still thinner than in adult polyps. (C) The glycocalyx of an adult polyp with ~1 µm in height. The yellow dashed line marks the plasma membrane. Scale bars 500 nm.

Taken together, hatching *Hydra* polyps are devoid of a glycocalyx and instead covered by a delicate membranous structure during the first 6 to 12 hours after hatching. A few hours after the polyp left the embryotheca the ectodermal epithelium starts to secret extracellular material, which forms into a morphological correlate of the adult glycocalyx after 48 hours.

Mass-spectrometric analysis of the glycocalyx – a candidate gene approach

Microscopic analysis demonstrated that *Hydra*'s glycocalyx is colonized by bacteria and thus, displays an interface for host-microbe cross-talk. Little is known about the molecular composition of the glycocalyx. A previous study demonstrated the presence of chondroitin and chondroitin-6-sulfate as well as few proteins such as PPODs (putative peroxidases) in the glycocalyx of *H. magnipapillata* (Böttger et al., 2012).

To further investigate the protein components of *Hydra*'s glycocalyx, a mass spectrometry approach was conducted using the species *H. vulgaris* (AEP), which in contrast to *H. magnipapillata* is genetically tractable and allows gain- and loss-of-function studies of candidate genes. For glycocalyx extraction *Hydra* polyps were subjected to a hypertonic salt wash, which did not injure the animals and essentially all of them recovered after a few minutes. Subsequent EM analysis revealed the extensive removal of the outer glycocalyx layer

(**Figure 7**). In contrast, the four inner glycocalyx layers are not released by the salt wash, but stay firmly attached to the cell surface. However, soluble components of the inner layer may still be extracted.

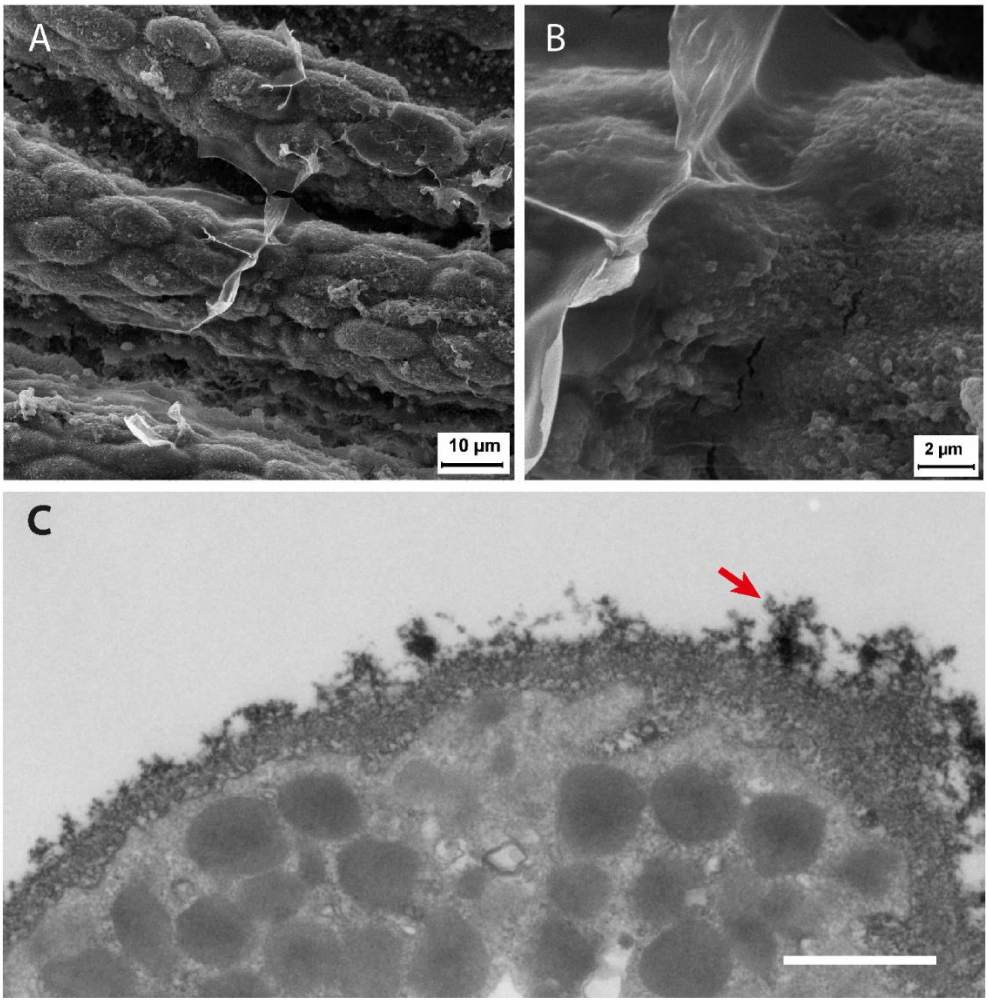

Figure 7. Removal of the outer layer of the glycocalyx by a hypertonic salt wash.
(A) Scanning electron micrograph (SEM) of the ectodermal surface after the salt wash. (B) Higher magnification of (A) for detailed structures. (C) Transmission electron micrograph (TEM) of the ectodermal surface after the salt wash. The loose outer layer of the glycocalyx has been almost completely removed. Red arrow indicates small remaining parts of the outer mucus-like layer. Scale bar 1 µm.

To identify the glycocalyx proteins released by the salt wash gel-enhanced liquid chromatography-tandem mass spectrometry (GeLC-MS/MS) was performed in collaboration with Dr. Christian Treitz and Prof. Dr. Andreas Tholey of the Institute for Experimental Medicine of the Christian Albrechts University of Kiel. For analysis of the LC–MS/MS data a protein database was constructed by translation of the *H. vulgaris* (AEP) transcriptome. The database search was performed with help of the proteome discoverer 1.4 using the Mascot, SEQUEST-HT and MS Amanda algorithms, which resulted in the identification of 4451

peptide hits. The high number of peptide hits most likely does not reflect the protein compexity of *Hydra*'s glycocalyx. The protein pool obtained by the primary analysis contains as well cytosolic proteins, which could be explained by the fact that *Hydra* polyps constantly slought off excessive tissue at the basal disc, the hypostome and the tips of the tentacles and therefore those cells and cellular fragments are present in the salt wash fraction. To overcome this limitation a rigorous filtering method was apllied to the primary mass spectrometry results using as a key element cell line-specific transcriptome data.

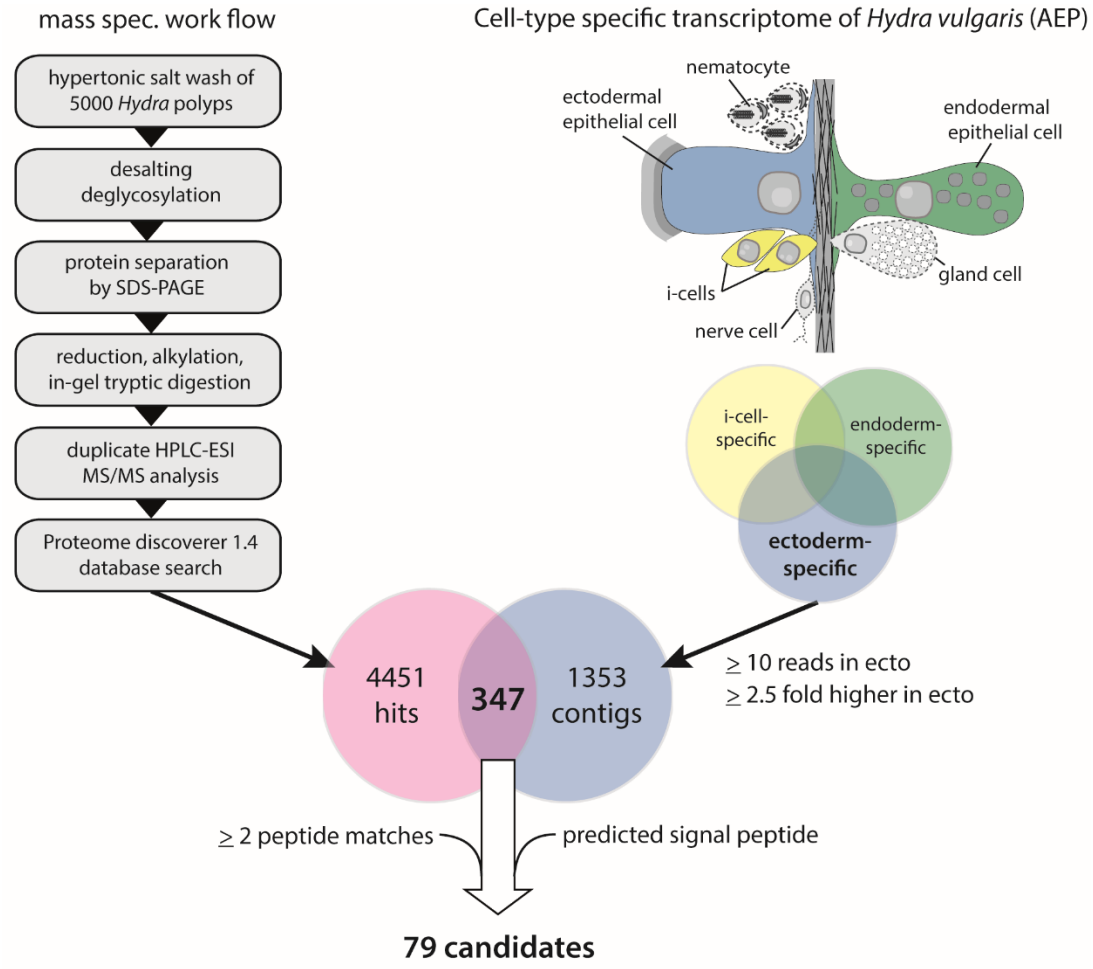

Figure 8. Identification of glycocalyx candidate genes by an integrative transcriptomic and proteomic approach.
Hydra's glycocalyx was removed by a hypertonic salt wash and subjected to high-performance liquid chromatograph-electrospray ionization tandem mass spectrometry (HPLC-ESI MS/MS) analysis resulting in 4451 peptide hits. In a previous study cell-line specific transcriptomes of *H. vulgaris* (AEP) were generated (Hemmrich et al., 2012), which allowed to filter the 4451 hits from the primary mass spectrometry analysis for ectoderm-specific expression (at least 10 reads and ≥2.5-fold higher gene expression than in the endodermal and i-cell lineages). The resulting 347 ectoderm-specific hits were filtered for two parameters; the presence of at least two peptide hits and a signal peptide. This resulted in the identification of 79 candidate genes.

In a previous study by Hemmrich et al. cell line-specific transcriptomes of *H. vulgaris* (AEP) were generated providing information on the expression level of each contig in the ectodermal, endodermal and interstitial stem cell lineage (**Figure 8**) (Hemmrich et al., 2012). Since the glycocalyx is produced by the ectodermal epithelium all contigs matching one of the 4451 peptide hits were filtered for predominant expression in the ectoderm (≥ 10 reads in the ectoderm and ≥2.5-fold higher expression in the ectoderm than in the endodermal and i-cell lineage). This resulted in 347 ectoderm-specific contigs exhibiting at least one peptide hit in the mass spectrometry analysis. The glycocalyx components are supposed to be membrane-bound and soluble extracellular proteins requiring a signal peptide in most cases. Thus, the 347 contigs were filtered for signal peptide prediction using the SignalP 4.1 server. Contigs that were not full-length at the 5'-end were validated, if possible, by screening the corresponding orthologue in the *H. magnipapillata* genome or otherwise retained in the candidate list. Conservative criteria recommend that ≥2 unique peptides need to be identified within a single protein for its positive identification ('double-hit rule') (Carr et al., 2004; Omenn et al., 2005). However, in this study a translated transcriptome was used as database, which involves the presence of several nearly-identical sequences and proteins, respectively. Due to contig redundancy it is likely that many proteins will not to fulfill the double-hit rule, which therefore was alleviated to ≥2 peptides instead of ≥2 unique peptides. Finally, 79 contigs were identified as candidates for glycocalyx constituents (**Figure 8**).

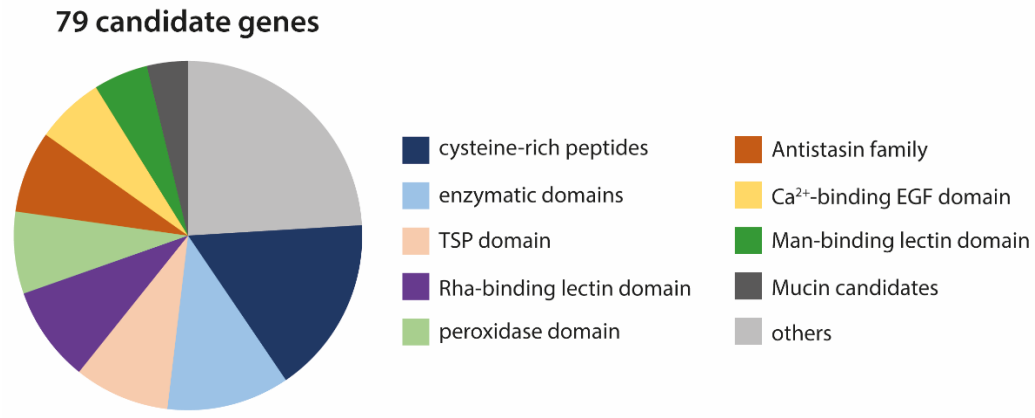

Figure 9. Protein domains and families in the glycocalyx candidate genes.
Pie chart representing the distribution of protein domains and families predicted by HMM Pfam in the 79 glycocalyx candidate genes. TSP, thrombospondine; Rha, rhamnose; Man, mannose.

Most of the 79 identified glycocalyx candidates represent contigs of unknown functionality with no homologue detected in other species than *Hydra* and thus, can be assigned

as taxonomical restricted genes (TRGs) (**Table 1**). For more than 26% of the candidate proteins no protein domain or domains of unknown function (DUF) could be detected. Interestingly, the remaining contigs (>73%) were enriched for distinct protein domains such as galactose-binding and mannose-binding lectin domains, calcium-binding EGF domains and thrombospondine domains (**Figure 9**). Three contigs contained regions with high proportions of proline, threonine and serine, referred to as PTS-regions, which were interspersed by short cysteine-rich domains. Due to these characteristic features the three contigs were assigned as mucin protein candidates. Furthermore, the candidate genes also included PPOD (putative peroxidase) proteins, which have been previously identified as glycocalyx constituents and serve as an extraction control in this approach (Böttger et al., 2012).

Table 1. List of glycocalyx candidate genes.
The contig ID corresponds to the H. vulgaris (AEP) transcriptome database (haep_t-cds_v02_ID). AA, amino acids; SP, signal peptide (Yes / No); pI, predicted isoelectric point; HmmDesc, protein domains / families identified by HMM (Hidden Markov Model) search; gene expression was calculated by number of reads. ECT, ectoderm; END, endoderm; ICE, i cell lineage. Number of peptides identified in mass spectrometry.

	Protein properties			BLAST annotation	HmmDesc	Gene expression			Identified peptides	
ID	AA	SP	pI			ECT	END	ICE	unique	total
Thromobospindin domain										
10	580	N	6,1	PREDICT: similar to HyTSR1 protein [Hmag] ref|XP_002158380.1|	Thrombospondin type 1 domain	1873	31	103	17	25
4144	354	N	6,2	PREDICT: similar to HyTSR1 protein [Hmag] ref|XP_002158380.1|	Thrombospondin type 1 domain	481	1	21	1	6
4164	531	N	5,1	PREDICT: similar to HyTSR1 protein [Hmag] ref|XP_002158380.1|	Thrombospondin type 1 domain	182	0	13	11	18
42213	273	Y	4,9	PREDICT: similar to HyTSR1 protein [Hmag] ref|XP_002158380.1|	von Willebrand factor type A domain	108	2	7	7	13
11	68	N	7,1	PREDICT: similar to HyTSR1 protein [Hmag] ref|XP_002158380.1|	Thrombospondin type 1 domain	21	1	2	0	3
4156	323	N	6,2	PREDICT: similar to HyTSR1 protein, partial [Hmag] ref|XP_002160421.1|	Thrombospondin type 1 domain	466	2	32	1	6
5189	230	Y	6,1	PREDICT: similar to HyTSR1 protein [Hmag] ref|XP_002154802.1|	Thrombospondin type 1 domain	26	0	6	2	8
Calcium binding EGF domain										
32	900	Y	5,7	PREDICT: similar to fibrillin 2 [Hmag] ref|XP_002154154.1|	Calcium binding EGF domain	765	4	55	15	16
4493	465	Y	5,4	PREDICT: similar to fibrillin 1 [Hmag] ref|XP_002169192.1|	Calcium binding EGF domain	414	1	15	4	4
4547	583	Y	5,3	PREDICT: similar to FiBrilliN homolog family member (fbn-1) [Hmag] ref|XP_002161135.1|	Calcium binding EGF domain	320	1	25	6	9
80	1552	N	5,4	PREDICT: similar to Latent-transforming growth factor beta-binding protein, isoform 1S precursor (LTBP-1), partial [Hmag] ref|XP_002156630.1|	Calcium binding EGF domain	170	2	25	6	7
5798	713	Y	4,6	PREDICT: similar to fibrillin 1, partial [Hmag] ref|XP_002156630.1|	Calcium binding EGF domain	48	0	8	7	7
Putative peroxidases (PPODs)										
4813	269	N	8,8	PPOD1 peroxidase [Hvul] gb|AAZ31364.1|	Fascin domain	617	27	18	9	29
4731	222	N	9,1	PPOD1 peroxidase [Hvul] gb|AAZ31364.1|	Fascin domain	563	96	13	6	16
4296	108	Y	9,2	PPOD1 peroxidase [Hvul] gb|AAZ31364.1|	Domain of unknown function (DUF1971)	378	4	10	1	8
4781	108	Y	9,2	PPOD1 peroxidase [Hvul] gb|AAZ31364.1|	Domain of unknown function (DUF1971)	210	11	7	0	8
5274	372	Y	8,6	PREDICT: similar to putative ascorbate peroxidase [Hmag] ref|XP_002154085.1|	Peroxidase	324	2	1	2	3
6037	372	Y	5,5	PREDICT: similar to putative ascorbate peroxidase [Hmag] ref|XP_002157274.1|	Peroxidase	68	2	0	2	2

	Protein properties			BLAST annotation	HmmDesc	Gene expression			Identified peptides	
ID	AA	SP	pI			ECT	END	ICE	unique	total
Antistasin family										
7012	181	Y	7,0	PREDICT: similar to antistasin [Hmag] ref|XP_002166012.1|	Antistasin family	373	1	5	0	4
5328	241	Y	8,1	PREDICT: similar to antistasin [Hmag] ref|XP_002156680.1|	Antistasin family	265	2	14	0	10
5338	236	Y	8,2	PREDICT: similar to antistasin [Hmag] ref|XP_002156680.1|	Antistasin family	265	4	6	2	14
7051	237	Y	8,5	PREDICT: similar to antistasin [Hmag] ref|XP_002166370.1|	Antistasin family	78	0	3	6	10
43346	78	N	8,4	PREDICT: similar to antistasin [Hmag] ref|XP_002161397.1|	Antistasin family	39	5	0	0	6
45439	178	Y	5,0	PREDICT: similar to antistasin [Hmag] ref|XP_002166012.1|	Antistasin family	22	0	1	1	4
Mucin candidates										
4441	547	N	5,3	PREDICT: mucin-5AC-like, partial [Hvul] ref| XP_002159997.2|		708	11	70	15	17
5331	499	N	4,1	PREDICT: mucin-2-like [Hvul]◘ ref|XP_012562846.1|		140	2	5	2	2
705	959	Y	3,7	PREDICT: mucin-2-like [Hvul]◘ ref|XP_012562846.1|		62	1	1	2	2
Rhamnose-binding lectin domain										
4499	402	Y	8,6	PREDICT: rhamnose-binding lectin-like [Hvul] ref|XP_002166914.1|	Galactose binding lectin domain	1410	8	15	12	20
5472	234	N	8,4	PREDICT: similar to predicted protein [Hmag] ref|XP_002166604.1|	Galactose binding lectin domain	808	7	15	4	8
4332	606	N	7,8	PREDICT: rhamnose-binding lectin-like [Hvul] ref|XP_012565931.1|	Galactose binding lectin domain	451	1	13	12	18
4906	185	N	8,2	PREDICT: rhamnose-binding lectin-like [Hvul] ref|XP_012560383.1|	Galactose binding lectin domain	106	2	0	0	11
5925	193	Y	8,5	PREDICT: rhamnose-binding lectin-like [Hvul] ref|XP_012560383.1 |	Galactose binding lectin domain	85	7	2	5	16
4905	186	N	8,2	PREDICT: rhamnose-binding lectin-like [Hvul] ref|XP_012560383.1 |	Galactose binding lectin domain	50	18	6	1	15
6032	175	N	7,9	PREDICT: rhamnose-binding lectin-like [Hvul] ref|XP_012560383.1 |	Galactose binding lectin domain	20	7	0	0	10
Mannose-binding lectin domain										
6332	206	Y	9,9	PREDICT: hypothetical protein [Hmag] ref|XP_002166268.1|	D-mannose binding lectin	334	4	2	0	6
5400	206	Y	9,7	PREDICT: hypothetical protein [Hmag] 002166268.1|	D-mannose binding lectin	312	9	5	0	7
5209	209	Y	8,8	PREDICT: hypothetical protein [Hmag] ref|XP_002166268.1|	D-mannose binding lectin	291	7	14	6	13
43905	206	Y	9,6	PREDICT: hypothetical protein [Hmag] ref|XP_002166268.1|	D-mannose binding lectin	51	11	4	5	7

	Protein properties			BLAST annotation	HmmDesc	Gene expression			Identified peptides	
ID	AA	SP	pI			ECT	END	ICE	unique	total
Cysteine-rich peptide family 1										
6017	125	Y	8,0	hypothetical protein CGI_10013165 [Crassostrea gigas] ref|EKC32775.1|		854	19	16	0	14
5608	109	N	7,7	hypothetical protein CGI_10013165 [Crassostrea gigas] ref|EKC32775.1|		800	5	3	0	14
2345	107	Y	8,6	hypothetical protein CGI_10013165 [Crassostrea gigas] ref|EKC32775.1|		327	1	8	0	11
47542	127	Y	8,2	hypothetical protein CGI_10013165 [Crassostrea gigas] ref|EKC32775.1|		284	11	1	3	8
1506	43	N	9,6	hypothetical protein CGI_10005739 [Crassostrea gigas] ref|EKC30560.1|		28	2	0	0	5
Cysteine-rich peptide family 2										
6618	84	Y	7,9			739	3	18	0	4
7483	81	Y	7,9			89	0	3	0	4
902	65	Y	8,8			32	0	1	0	4
1324	79	Y	8,2			31	0	1	0	4
Cysteine-rich peptide family 3										
7160	101	Y	7,5	PREDICT: hypothetical protein [Hmag] ref|XP_002164839.1|	Protein of unknown function (DUF2005)	314	12	1	3	5
11229	121	N	8,3	PREDICT: hypothetical protein isoform 2 [Hmag] ref|XP_002159115.1|		78	2	0	4	4
2075	101	Y	7,1	PREDICT: hypothetical protein isoform 2 [Hmag] ref|XP_002159115.1|	Eukaryotic protein of unknown function	11	0	1	0	3
Domains with predicted enzymatic activity										
168	387	Y	5,7	PREDICT: similar to Porphyromonas-type peptidyl-arginine deiminase family protein [Hmag] ref|XP_002159393.1|	Porphyromonas-type peptidyl-arginine	782	9	7	31	36
128	415	N	5,6	alpha-N-acetylgalactosaminidase, putative [Pediculus humanus corporis] ref|XP_002423479.1|	Melibiase	413	57	48	13	13
4301	680	Y	9,0	PREDICT: similar to 8(R)-lipoxygenase [Hmag] ref|XP_002167264.1|	Lipoxygenase	233	4	6	5	5
43319	361	Y	5,7	PREDICT: similar to Zinc metalloproteinase nas-4 [Hmag] ref|XP_002165364.1|	Astacin (Peptidase family M12A)	84	30	11	2	2
48316	130	Y	9,1	PREDICT: similar to Alpha-1,6-mannosylglycoprotein 6-beta-N-acetylglucosaminyltransferase A [Hmag] ref|XP_002156958.1|	SFI toxin family	84	4	5	4	4
43485	427	Y	7,6	PREDICT: similar to predicted protein [Hmag] ref|XP_002155319.1|	Prolyl-tRNA synthetase, C-terminal	67	0	4	1	7
46784	456	Y	5,5	PREDICT: similar to predicted protein [Hmag] ref|XP_002158014.1|	Alpha-L-fucosidase	63	11	5	3	3
43383	325	Y	6,2	PREDICT: similar to Carboxypeptidase D [Hmag] ref|XP_002159473.1|	Zinc carboxypeptidase	57	21	11	3	3
11449	271	Y	6,3	Gamma-glutamyl hydrolase A-like [Hvul] ref|XP_012559207.1|	Peptidase C26, gamma-glutamyl hydrolase	18	2	2	4	4

	Protein properties			BLAST annotation	HmmDesc	Gene expression			Identified peptides	
ID	AA	SP	pI			ECT	END	ICE	unique	total
others										
4171	735	Y	5,8	PREDICT: similar to NIDogen (basement membrane protein family member (nid-1) [Hmag] ref|XP_002166874.1|	EGF-like domain	3046	26	212	25	27
4194	448	Y	7,4	PREDICT: similar to apextrin [Hmag] ref|XP_002165837.1|	MAC/Perforin domain	828	45	172	6	8
5722	186	Y	9,0	PREDICT: hypothetical protein [Hmag] ref|XP_002159291.1|	LytB protein	450	11	11	6	6
4578	619	Y	7,5	PREDICT: similar to tyrosine kinase receptor [Hmag] ref|XP_002162719.1|	Domain of unknown function (DUF1966)	205	2	15	1	6
47148	166	Y	8,6	PREDICT: hypothetical protein [Hmag] ref|XP_002156459.1|		196	5	6	5	5
6452	155	Y	7,2	PREDICT: similar to predicted protein [Hmag] ref|XP_002163343.1|		185	2	36	0	7
4819	664	Y	5,6	PREDICT: hypothetical protein [Hmag] ref|XP_002157739.1|	La domain	157	19	20	3	4
8354	258	Y	8,5	PREDICT: similar to GLI pathogenesis-related 2 [Hmag] ref|XP_002165977.1|	SCP-like extracellular protein	110	8	1	5	7
6991	458	Y	7,9	PREDICT: hypothetical protein [Hmag] ref|XP_002157212.1|	Fibronectin type III domain	108	15	14	2	3
6138	161	N	6,3	PREDICT: similar to predicted protein [Hmag] ref|XP_002163343.1|	Domain of unknown function (DUF1899)	102	1	23	2	11
44345	259	Y	6,7	PREDICT: similar to predicted protein [Hmag] ref|XP_002166617.1|	EMI domain	88	2	1	1	2
4690	333	Y	8,0	uncharacterized protein LOC100205981, partial [Hvul] ref|012558233.1|	V4R domain	80	1	10	0	9
5893	559	Y	8,2	PREDICT: similar to predicted protein, partial [Hmag] ref|XP_002169416.1|	Laminin G domain	72	3	12	2	2
43476	662	Y	6,3	PREDICT: similar to predicted protein, partial [Hmag] ref|XP_002169931.1|	Protein of unknown function (DUF1367)	54	9	8	8	10
48199	192	Y	9,4	PREDICT: similar to predicted protein [Hmag] ref|XP_002165249.1|	Lipocalin-like domain	51	3	2	2	2
5471	74	N	8,5	PREDICT: similar to predicted protein [Hmag] ref|XP_002155588.1|		28	0	1	0	3
44626	1309	Y	4,7	PREDICTED: similar to Protocadherin Fat 4 [Hmag] ref|XP_002156380.1|	Cadherin domain	25	0	2	4	4
45825	124	Y	7,1	PREDICT: hypothetical protein [Hmag] ref|XP_002164839.1|	Eukaryotic protein of unknown function	21	0	3	0	4
5497	62	N	4,7	PREDICT: similar to calcium-binding protein [Hmag] ref|XP_002158871.1|		18	1	5	0	10
8387	62	Y	5,1	PREDICT: hypothetical protein [Hmag] ref|XP_00216991481358851.1|		14	5	1	0	5

Identification of a putative antimicrobial peptide family

Among the glycocalyx candidate genes a significant proportion (16%) was represented by small cysteine-rich peptides (CRPs) (**Figure 9 and Table 1**). CRPs encompass a large and widespread group of secreted molecules, heterogeneous in primary sequence and structural arrangement, and with different functional roles (Gruber et al., 2007; Taylor et al., 2008; Marshall et al., 2011). However, invertebrate CRPs have been frequently related to immune defense with many of them representing AMPs (Dimarcq et al., 1998; Mitta et al., 2000; Bulet et al., 2004). Mucosal interfaces often represent a reservoir for host AMPs, a phenomenon not only observed in the mammalian gut (Antoni et al., 2013), but also in the epidermal mucus of fish and frogs (Subramanian et al., 2009; Grazia et al., 2015). Interestingly, so far almost all AMP genes identified in *Hydra* were expressed in the endodermal epithelium lining the gastric cavity (Augustin et al., 2009b, 2009a; Bosch et al., 2009; Franzenburg et al., 2013). To examine the possibility that ectoderm-derived AMPs are secreted into *Hydra*'s glycocalyx, the CRPs identified in this study were screened for characteristic features of AMPs.

Among the glycocalyx candidate genes 13 CRPs were identified, which form three distinct families (**Table 1**). One of these peptide families, CRP family 1, stands out by remarkably high expression levels of its members (**Table 1**). Sequence analysis revealed the presence of a signal peptide followed by 110 amino acids resulting in a predicted molecular weight of 12.7 kDa. The peptides contain six cysteine residues with the potential to form three disulfide bonds. The strongly positively charged C-terminus (pI 9.7) is separated from the signal peptide by a negatively charged N-terminal region (**Figure 10A**). This domain architecture comprising a signal peptide, a negatively charged pro-region, and the positively charged mature peptide has been described for many AMPs including the arminins and periculins of *Hydra* (Augustin et al., 2009a; Bosch et al., 2009; Fraune et al., 2010). Thus, the members of CRP family 1 display promising candidates for AMPs and were termed ‚custodins' with regard to their putative function (latin 'custos'= guard).

Further analysis revealed that the five contigs identified in the mass spectrometric analysis can be assigned to three custodin peptide isoforms (contig 6017 and 5608 represent custodin-1a, contig 2345 and 1506 represent custodin-1c and contig 47542 represents custodin-2). In addition, EST data bank search identified a fourth peptide, custodin-1b, which was not detected in the glycocalyx of *H. vulgaris* (AEP). Screening the *H. magnipapillata* genome and transcriptomes of *H. oligactis* and *H. viridissima* revealed the presence of four custodin orthologues in *H. magnipapillata*, two in *H. oligactis* and one in *H. viridissima*. An

amino acid alignment of all custodin paralogues showed that they share the domain composition described above (**Figure 10A and B**).

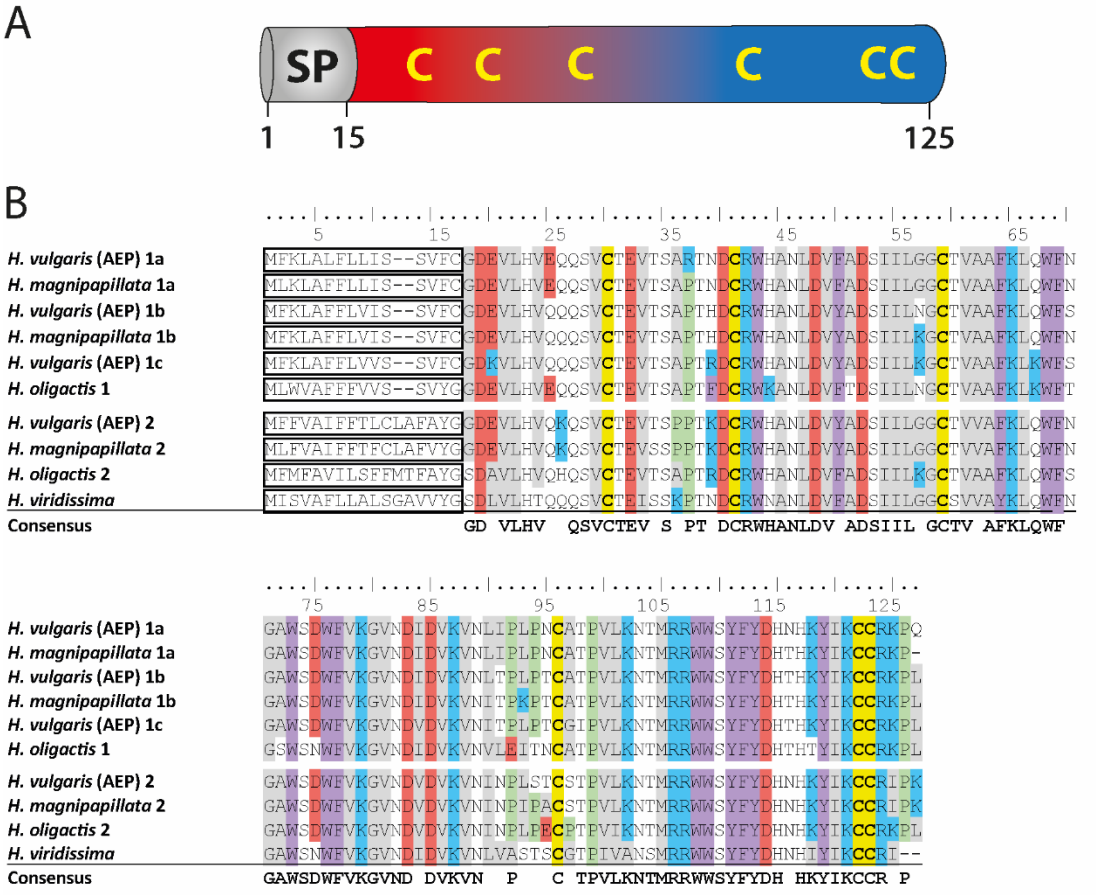

Figure 10. Protein sequence alignment of the custodin peptides.
Clustal-W alignment of the custodin protein sequences of *H. vulgaris* (AEP), *H. magnipapillata*, *H. oligactis* und *H. viridissima*. The consensus sequence has been calculated with a threshold of 80%. The predicted signal peptide is framed and the six cysteine residues are highlighted in yellow. Other amino acids are highlighted in blue (positively charged), red (negatively charged), grey (hydrophobic), purple (aromatic) and green (helix-breaking).

A phylogenetic tree based on the amino acid sequence alignment places the members of custodin peptide family in two isoform groups, the custodin-1 group and the custodin-2 group (**Figure 11**). *H. vulgaris* (AEP) possesses three isoforms that cluster in the custodin-1 group, while *H. magnipapillata* exhibits two custodin-1 isoforms and *H. oligactis* only one. The two isoforms of custodin-1a and custodin-1b of *H. magnipapillata* and *H. vulgaris* (AEP) form two distinct clades. The custodin-2 group is formed by one isoform of *H. vulgaris* (AEP), *H. magnipapillata* and *H. oligactis* each. *H. viridissima* possesses only one custodin homologue, which forms an outgroup.

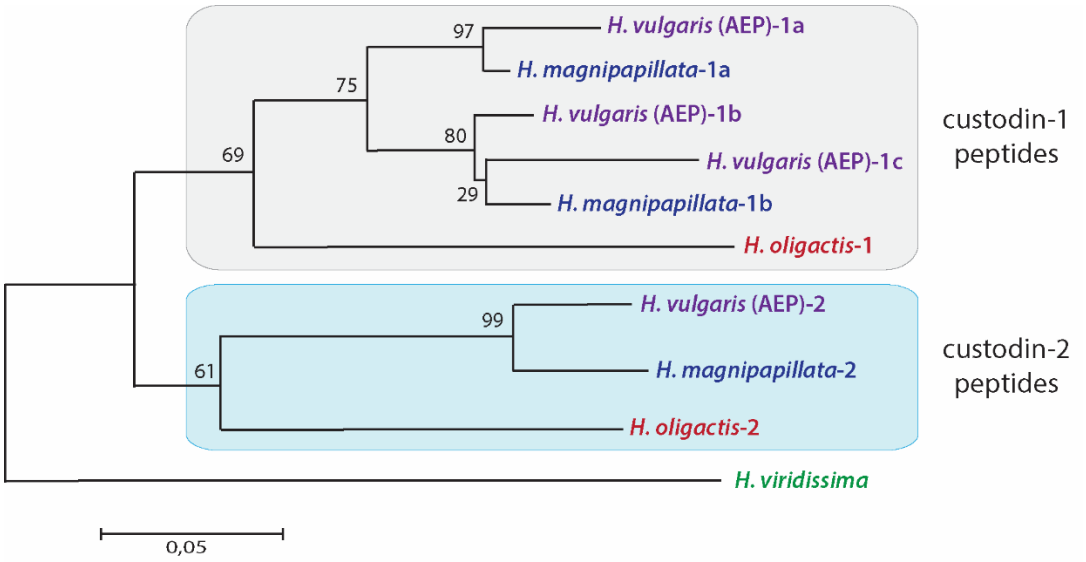

Figure 11. The custodin peptides, a novel gene family in *Hydra*.
Phylogenetic analysis of the custodin peptide family in four *Hydra* species. The custodin peptides can be divided in two groups, the custodin-1 peptides (highlighted in grey) and the custodin-2 peptides (highlighted in blue). Hydra viridissima exhibits only one custodin paralogue that forms an outgroup.

Characterization of custodin expression patterns in different *Hydra* species

To verify the proposed ectodermal gene expression of the custodin genes whole mount *in situ* hybridization was performed with species-specific RNA probes for *H. vulgaris* (AEP), *H. oligactis* and *H. viridissima*. In *H. vulgaris* (AEP) *custodin-1a* is expressed in the ectodermal epithelium including the basal disc and the bud (**Figure 12A**). The expression patterns of *custodin-1b* and *custodin-1c* could not be analyzed separately due to high nucleotide sequence identities and the probe designed for custodin-1c most likely detects both transcripts. *Custodin-1b/c* were found to be expressed in ectodermal epithelial cells along the body column, but in contrast to *custodin-1a*, the basal disc and the bud showed no expression (**Figure 12B**). *H. oligactis* possesses only one *custodin-1* isoform, which is expressed in the ectodermal epithelial cells of the stalk region (**Figure 13A**). Interestingly, some individuals showed increased *custodin-1* expression that gradually expands in direction of the oral pole (**Figure 13B and C**). No expression was detected in the basal disc and tentacles.

Interestingly, in both *H. vulgaris* (AEP) and *H. oligactis*, the *custodin-2* transcript was exclusively detected in the ectodermal cells of the basal disc (**Figure 14A**). Analysis of polyps in various stages of budding demonstrates that *custodin-2* transcripts are also detectable in the foot region of late buds (**Figure 14B**). Shortly after bud detachment the mother polyp still shows strong *custodin-2* expression at the bud detachment site (**Figure 14C**).

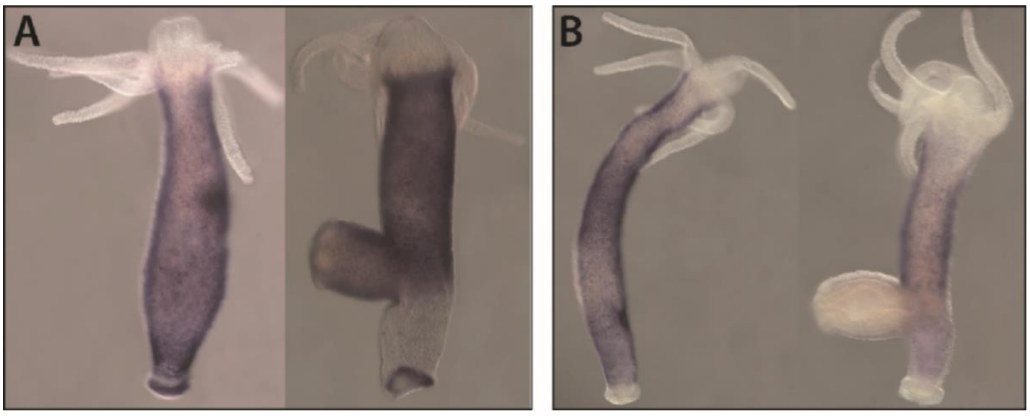

Figure 12. Expression of custodin-1a and custodin-1b/c in *H. vulgaris* (AEP).
(A) Custodin-1a is strongly expressed in the ectodermal epithelium along the body column including the basal disc and the bud. In the head region and tentacles no signal was detected. (B) Custodin-1b/c are expressed in the ectodermal epithelium along the body column, but in contrast to custodin-1a in the basal disc and in the bud no expression of custodin-1b/c was detected.

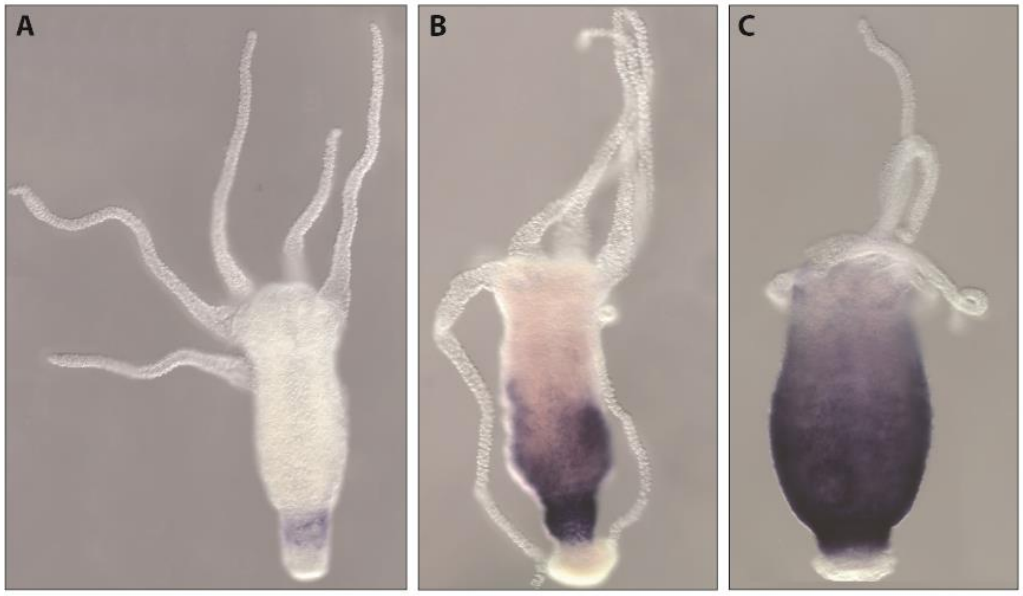

Figure 13. Expression of custodin-1 in *H. oligactis.*
H. oligactis possesses a single Custodin-1 homologue, which is expressed in ectodermal epithelial cells along the body column with significant inter-individual differences. (A) Custodin-1 expression exclusively in the stalk region. (B) Strong expression in the stalk region and weaker gradual expression in the lower half of the body column. (C) Strongest expression in the stalk, which gradually weakens along the entire body column. In the basal disc, the head region and tentacles no expression was detected.

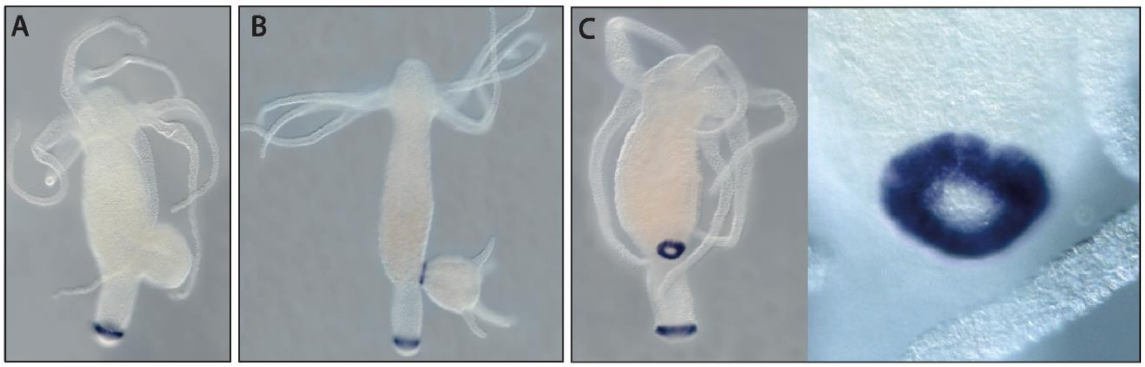

Figure 14. Expression of custodin-2 in *H. oligactis* and *H. vulgaris* (AEP).
(A) Custodin-2 expression in ectodermal cells of the basal disc. (B) Custodin-2 expression in the basal disc of the mother polyps and in the developing basal disc of the bud. (C) Mother polyp shortly after the bud dropped off showing strong custodin-2 expression at the bud detachment site. The custodin-2 expression pattern was identical in *H. vulgaris* (AEP) and *H. oligatis* (depicted here).

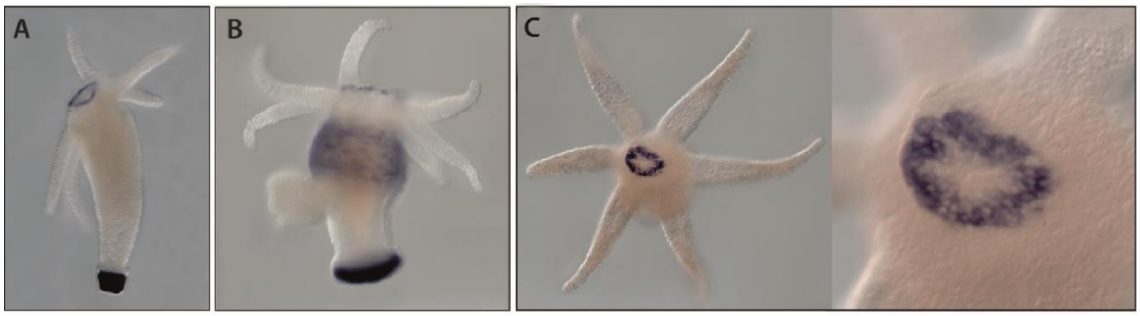

Figure 15. Expression of the only custodin paralogue in *H. viridissima.*
H. viridissima possesses a single custodin homologue that cannot be assigned to the custodin-1 or custodin-2 group. (A) Custodin expression in ectodermal cells of in the basal disc and around the hypostome. (B) Some polyps show additional expression in ectodermal tissue of the gastric region. (C) Custodin expression in a ring of ectodermal epithelial cells around the hypostome.

In contrast to the other *Hydra* species investigated, *H. viridissima* exhibits only one *custodin* isoform, that was neither assigned to custodin-1 group nor to the custodin-2 group in the previous phylogenetic analysis (**Figure 11**). *In situ* hybridization revealed a unique expression pattern of the *H. viridissima custodin* with strong expression in the basal disc and in a ring of ectodermal epithelial cells around the hypostome (**Figure 15**). In addition, some polyps showed *custodin* expression in the ectoderm along the body column (**Figure 15B**). Thus, on one hand the *H. viridissima custodin* shares the expression in the basal disc with the custodin-2 group, while on the other hand the observed expression in the ectoderm of gastric region is a common feature with the *custodin-1* group.

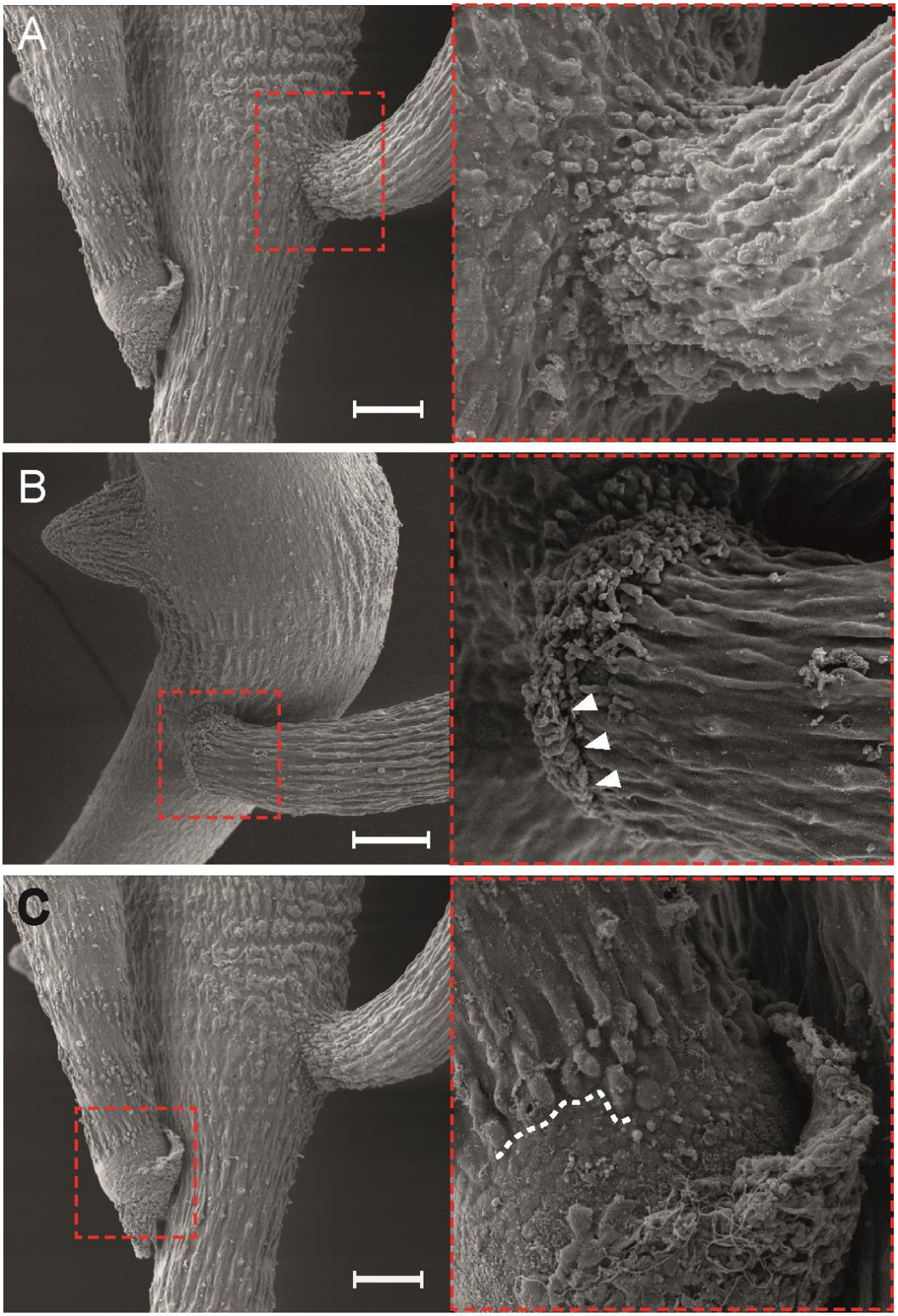

Figure 16. Secretion of foot mucus by glandulomuscular cells of the basal disc during budding. Scanning electron microscopy (SEM). Red boxes indicate the section depicted in higher magnification images to right. Scale bars 250 µm. (A) Bud with beginning differentiation of the basal disc. All cells are covered by the glycocalyx. (B) Bud starts pinching off the mother polyp. Cells at the lowest part of the foot start secreting mucus and form a sharp border (white arrow heads). (C) Bud shortly before detaching from the mother polyp. Ectodermal cells of the basal disc have already produced significant amounts of mucus. The glycocalyx-ends with a sharp border before the basal disc (dashed white line).

Taken together, all *custodin* paralogues are expressed exclusively in ectodermal epithelial cells, thus likely being secreted into the glycocalyx or into the foot mucus, respectively. While the expression patterns of the custodin-1 group showed much variation between distinct *custodin-1* isoforms as well as between different *Hydra* species (**Figures 12 and 13**), the strong expression of *custodin-2* in the basal disc is conserved in all *Hydra* species (**Figures 14 and 15**). The polyps use the basal disc to attach to various substrates such as the surfaces of plants and stones, which are colonized by microorganisms. Therefore, the basal disc may be particularly vulnerable to invasion of foreign microbes and may require different antimicrobial defense molecules than the ectodermal surface exposed to the surrounding water only. Notably, expression of *custodin-2* was already detected in buds at the beginning of the differentiation of the basal disc. Indeed, SEM analysis of polyps in various stages of budding demonstrates that foot mucus secretion by glandulomuscular cells of the basal disc already starts before the bud detaches from the mother polyp (**Figure 16A-C**).

Localization of custodin-1c:eGFP fusion protein in transgenic *Hydra*

To assess whether custodin-1c is secreted into the glycocalyx at the apical surface transgenic polyps that express custodin-1c in epithelial cells were generated. *Hydra* embryos were microinjected with an expression construct in which two copies of the full-length custodin-1c gene were fused to eGFP under the control of the *Hydra* β-actin promoter (**Figure 17A**). The first copy of custodin-1c includes the signal peptide and was fused in front of the eGFP reporter gene, allowing *in vivo* tracing of the fusion protein. A second copy of custodin-1c was fused behind the eGFP gene to allow the putative proteolytic release of the C-terminal peptide. Transgenic founder polyps expressed the custodin-1c:eGFP fusion protein in both ectodermal and endodermal epithelial cells (**Figure 17B and C**). In the ectoderm the custodin-1c:eGFP fusion protein was detected in small vesicles, which accumulated below the apical cell surface, likely being secreted into the glycocalyx (**Figure 17C and D**). Interestingly, in endodermal epithelial cells the custodin-1c:eGFP containing vesicles did not accumulate below the apical cell surface, but were detected evenly distributed in the whole cell indicating that the targeting signals for apical sorting differ between ectoderm and endoderm in *Hydra* (**Figure 17C**).

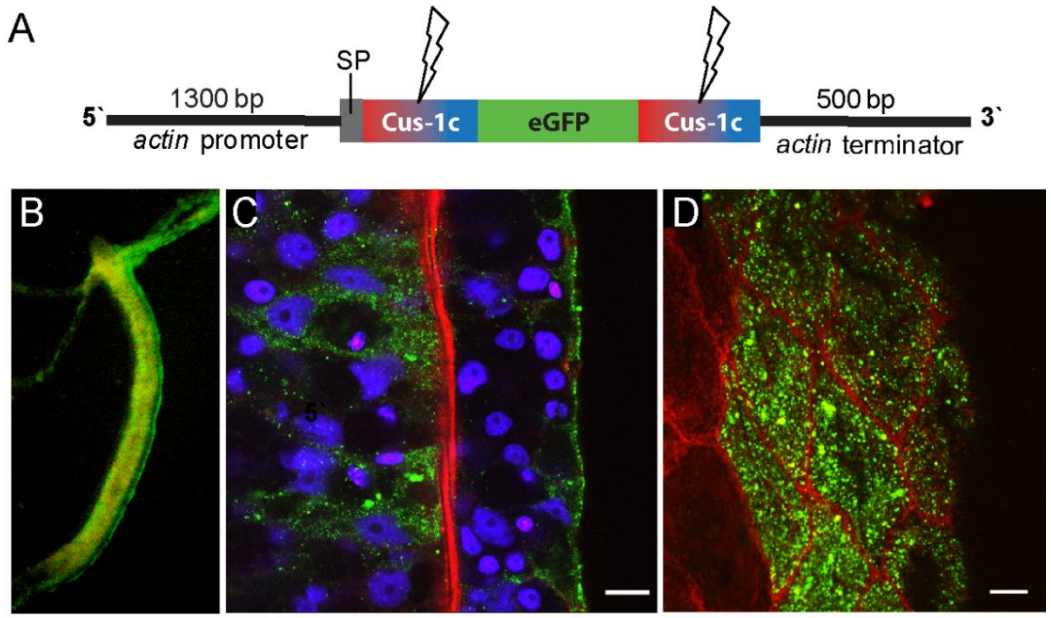

Figure 17. Custodin-1c:eGFP overexpression in *H. vulgaris* (AEP).
(A) Expression construct for generation of transgenic *Hydra*. The construct contains custodin-1c including the signal peptide fused in frame of the 5'end of the eGFP reporter gene and custodin-1c lacking the signal peptide fused to the 3'end of eGFP. Lightening bolt indicates a putative cleavage site. (B) *in vivo* image of a transgenic *H. vulgaris* (AEP) polyp expressing custodin-1c:eGFP in the ectodermal epithelium. (C and D) Confocal laser scanning microscope (CLSM) analysis. Green custodin-1c:eGFP; red, phalloidin staining of actin filaments; blue, TO-PRO DNA stain. (C) Transgenic polyp expressing eGFP:custodin-1c in endodermal and ectodermal epithelial cells. Scale bar 10.6 µm. (D) Surface of custodin-1c:eGFP expressing ectodermal epithelial cells. Notice the custodin-1c:eGFP localization in secretory vesicles. Scale bar 8.7 µm.

A first evaluation of the antibacterial activity of recombinant custodin-1c

To assess whether custodin-1c had antimicrobial activity, the peptide was heterologously expressed in *E. coli*. The sequence of mature custodin-1c containing 110 amino acids was cloned into the pET28a(+) expression vector and fused to a C-terminal hexa histidine-tag (6x His-tag) to allow detection and purification of the recombinant protein. Although custodin-1c was found to be expressed as insoluble aggregates, so-called inclusion bodies, the induction of custodin-1c expression resulted in an immediate growth stagnation of *E. coli* (**Figure 18A**). This may indicate that a small fraction of custodin-1c is produced in soluble form and exerts an antibacterial / growth retardation effect on the *E. coli* cells. Purification of custodin-1c inclusion bodies was analyzed by SDS-PAGE and Western blot revealing one predominant protein band at the expected size of ~14 kDa with >80% purity (**Figure 18B and C**). After solubilization and refolding custodin-1c was purified by C_{18} reverse-phase chromatography and subsequently used for microdilution susceptibility assays to determine the minimal inhibitory concentration (MIC) against the Gram-positive *Bacillus megaterium*

ATCC 14581 as a primary test assay. Recombinant custodin-1c showed strong bactericidal activity and affected the growth of *B. megaterium* at a concentration of 400 nM. However, for conclusive evidence custodin-1c needs to be tested on additional bacterial specimen. Here, it would be of particular interest whether the indigenous *Hydra* bacteria such as *Curvibacter* sp. are sensitive to custodin-1c. In conclusion, the results of this study form the basis for further characterization of the antimicrobial activity within the custodin peptide family.

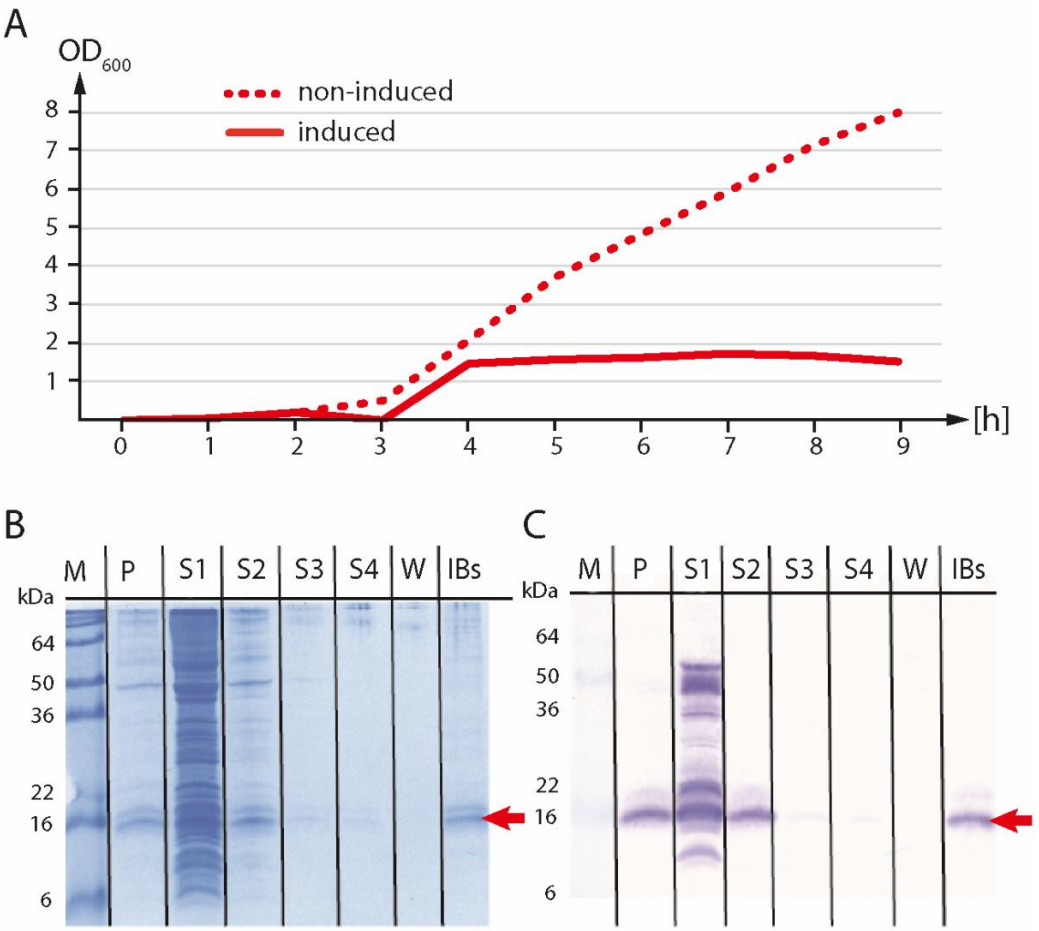

Figure 18. Purification of custodin-1c inclusion bodies expressed in *E. coli*.
(A) Bacterial growth curve of *E. coli* Rosetta(DE3) containing the pET28a(+)-custodin-1c vector. Expression of His-tagged custodin-1c in was induced at 4 h with 0.5 mM IPTG (red line). Note the growth stagnation after induction compared to the non-induced control (dashed line). Custodin-1c was expressed in inclusion bodies, which were purified before solubilization and refolding. Purification of inclusion body purification was analyzed by (B) SDS-PAGE and (C) Western Blot using anti-His tag antibody. 10 µl sample volume were loaded per lane. M, molecular weight marker SeeBlue® Plus2 Pre-stained Protein Standard; P, pellet after cell lysis; S1-4, supernatant 1-4; W, washing buffer; IBs, inclusion bodies. Red arrows indicate the predicted molecular weight of 14 kDa for recombinant custodin-1c.

Discussion

In this study, the outer mucus-like layer of *Hydra*'s glycocalyx was identified as a bacterial habitat. Notably, bacteria were never found penetrating the firmly attached inner layers of *Hydra*'s glycocalyx. Thus, the glycocalyx on the one hand seems to separate the bacteria from direct contact to the ectodermal epithelium and on the other hand provides a habitat for the microbiota. This dual role of representing both, a barrier and a habitat for symbiotic bacteria was previously described for the mucosal surface of the mammalian colon, where bacteria are restricted to the outer loose mucus layer, whereas the inner mucus is impervious for bacteria and thus, prevents excessive immune activation (Johansson et al., 2008, 2011; Johansson and Hansson, 2016). This work provides first evidence, that the principle of separating a mucosal surface into a barrier and a habitat can be traced back to the ancestral metazoan *Hydra* and apparently displays a conserved feature.

An integrative transcriptomic and proteomic approach led to the identification of 79 glycocalyx candidate genes including a putative AMP family, the custodins. The custodin peptides display the first candidates for ectoderm-derived AMPs in *Hydra*, since all other AMPs identified so far are expressed in the endodermal epithelium (Augustin et al., 2009a, 2009b; Bosch et al., 2009; Jung et al., 2009; Franzenburg et al., 2013). In this study transgenic *Hydra* were generated that express a custodin-eGFP fusion protein, which was localized in secretory vesicles below the ectodermal apical cell surface strongly indicating that the protein is secreted into the glycocalyx. Unfortunately, the exact localization of the protein in the glycocalyx could not be detected due to the lack of a suitable fixation method. The chemical fixative developed in this work provides a good preservation of the glycocalyx, but contains glutaraldehyde, which affects the antigenicity of the eGFP epitope and thus, is not compatible with immunohistochemistry. However, it would be of particular interest whether the custodin peptides accumulate to high concentrations within *Hydra*'s glycocalyx and thus, may contribute to the barrier function. In the mammalian gut it was shown that mucus represents a reservoir for AMPs, which form a gradient from the epithelium toward the lumen (Antoni et al., 2013). In particular, the antibacterial lectin RegIIIγ has been shown to play an critical role in maintaining gut homeostasis through spatially segregating bacteria (Brandl et al., 2007; Vaishnava et al., 2011). Interestingly, RegIIIγ is considerably larger (15 kDa) than classical AMPs such as the α-defensins (~3 kDa) and it was speculated that the increased size is involved in preventing rapid diffusion through the mucus layer (Vaishnava et al., 2011). Notably, the custodin peptides are significantly larger (13 kDa) than the endodermally expressed AMPs, *e.g.*

mature arminin-1a has a predicted molecular mass of 3.9 kDa (Augustin et al., 2009a). Indeed, the issue of preventing loss of AMPs by diffusion most likely does not pertain to the endoderm, since *Hydra*'s mouth is not a permanent opening and when closed, it presents a continuous epithelial sheet sealed with septate junctions (Campbell, 1987). Therefore, small peptides secreted into the gastric cavity such as the arminins are likely to reach high concentrations without the risk of dilution.

An interesting feature of the custodin peptide family are the species-specific expression patterns. While the custodin-1 group shows a great deal of variation between distinct *custodin-1* isoforms as well as between different species, the strong expression of *custodin-2* in the basal disc is conserved in all *Hydra* species. In their natural habitat polyps attach with the basal disc to various substrates such as the surfaces of plants and stones, which are colonized by different microorganisms than present the surrounding water. Therefore, the foot mucus of the basal disc may require different AMPs than the ectodermal surface to efficiently combat invasion by foreign microbes. Furthermore, the variable expression patterns of the custodin-1 peptides between different *Hydra* species arise the question whether the custodins contribute to a species-specific spatial organization of the microbiota along the body column. However, the hypothesis that distinct custodin isoforms display differential antimicrobial activity needs further investigation. Until today the examination of the spatial distribution of *Hydra*'s microbiota by fluorescence *in situ* hybridization (FISH) failed due to the lack of a suitable fixation method. The fragile glycocalyx (and the bacteria attached to it) do not withstand the heat and harsh chemicals involved in the FISH procedure.

The essential components of mucus are the heavily glycosylated mucin proteins, which are divided into two structurally different families: the secreted gel-forming and the membrane (cell surface)-associated mucins. Gel-forming-mucin type of proteins have been identified in several invertebrates including Cnidaria, Porifera and Ctenophora indicating that mucins were present early in metazoan evolution (Lang et al., 2007, 2016). In the present study we used a hypertonic salt wash to remove the outer layer of *Hydra*'s glycocalyx, while the inner layers remained firmly attached to plasma membrane. Therefore, only secreted mucins are likely to be identified in the subsequent mass spectrometric analysis. Indeed, three contigs identified by mass spectrometry show similarity to genes annotated as 'mucin-2-like' and 'mucin-5AC-like' in the *Hydra vulgaris* genome (formerly *H. magnipapillata*). Mucin-2 and mucin-5AC represent the predominant secreted gel-forming mucins in the mammalian gut and respiratory tract (Tytgat et al., 1996; Rose, 2006). Recently, the generation of transgenic mice expressing

a GFP-tagged gel-forming mucin was reported (Portal et al., 2017). Such an approach provides an attractive model to study the mechanisms that regulate mucus production and secretion and thus, would be desirable experimental set-up to investigate *Hydra*'s glycocalyx. Unfortunately, the identified contigs of the *H. vulgaris* (AEP) transcriptome are not full-length, while *H. magnipapillata* is not genetically tractable, which hampered the generation of transgenic *Hydra* so far. However, efforts in sequencing methods may overcome these problems in future.

Besides mucin candidates and putative AMPs, a significant proportion (14%) of the glycocalyx candidate genes in *Hydra* comprised proteins containing lectin domains. Lectins are widely distributed both in the animal and plant kingdoms and recognize carbohydrate structures and agglutinate various cells by binding to cell-surface glycoconjugates. They are often involved in pattern recognition by binding to MAMPs including glucan, mannose, and LPS among others (Arason, 1996; Marques and Barracco, 2000; Hanington et al., 2010; Yang et al., 2015). Most known animal lectins are located internally, but some are also found in the skin mucus of several animal species, especially in fish (Muramoto et al., 1999; Okamoto et al., 2005; Nakamura et al., 2006; Tsutsui et al., 2006, 2009, 2011, 2016, 2018; Ng et al., 2015; Huang et al., 2016). The largest family of lectins identified in *Hydra* display putative L-rhamnose-binding lectins (RBLs). RBLs are animal lectins that bind specifically to L-rhamnose or D-galactose (Kilpatrick, 2002) and have been identified in more than 25 species of teleost fish, annelids, bivalves, and in the ascidian *Botryllus schlosseri* (Ogawa et al., 2011). Some of these RBLs have been shown to bind to glycolipids and glycoproteins of a parasitic microsporidian (Watanabe et al., 2008), while others appear to recognize lipoteichoic acid of Gram-positive bacteria as well as LPS of Gram-negative bacteria, thereby displaying preferential affinity for distinct types of LPS (Tateno et al., 2002). Recently, a RBL of the stony coral *Pocillopora damicornis* was shown to bind bacterial Lipid A and LPS as well as symbiotic zooxanthellae (Zhou et al., 2017). Notably, the coral RBL shares highest amino acid sequence similarity (55%) with *Hydra vulgaris*. However, the RBLs identified in *Hydra* are still awaiting their functional characterization to elucidate a potential role in immunity.

Taken together, the integrative transcriptomic and proteomic approach of this study has provided a list of glycocalyx candidate genes that are awaiting future validation and follow-up experiments. Of particular interest are proteins that may be involved in shaping *Hydra*'s species-specific microbiota, such as AMPs and lectins. Furthermore, transgenic reporter or knockdown lines for mucin candidates genes may expand our understanding on the function and relevance of *Hydra*'s glycocalyx.

Materials and Methods

Chemical fixation of the glycocalyx

Polyps were fixed in 2% paraformaldehyde, 2.5% glutaraldehyde, 75 mM L-lysine and 0.05% ruthenium red in 50 mM cacodylate buffer, pH 7.4, for 18 h at 4 °C. After washing with 75 mM cacodylate buffer for 30 min, postfixation was carried out with 1% OsO_4 and 0.05% ruthenium red in 75 mM cacodylate buffer for 2 h at 4 °C. After washing with 75 mM cacodylate buffer for 30 min, tissue was dehydrated in ethanol. For scanning electron microscopy, animals were critical point dried in an ethanol–carbon dioxide mixture (CPD030; Bal-Tec), sputter coated (SCD050; Bal-Tec) and viewed at 10 kV using S420 scanning electron microscope (LEO, Leica).

For transmission electron microscopy, animals were embedded in Agar 100 resin (Agar Scientific, Ltd, Stansted, UK). Ultrathin sections were contrasted with 2.5% uranyl acetate for 5 min and lead citrate solution (freshly prepared from lead acetate and sodium citrate) for 2 min and were analyzed using a Tecnai G2 Spirit BioTWIN transmission electron microscope (FEI Company).

Confocal microscopy

Laser-scanning confocal data were acquired by using a Leica TCS SP5 confocal laser scanning microscope. Detection of eGFP in whole mounts was performed following standard procedures (Wittlieb et al., 2006). In brief, polyps were relaxed in 2% urethane before fixation in 4% (v/v) paraformaldehyde for 30 min. After removal of fixative and permeabilization with 0.5% Triton X-100 in PBS, polyps were incubated in blocking solution containing 1% bovine serum albumin (BSA). Polyclonal rabbit anti-GFP antibodies (Millipore) were diluted 1:500 in blocking buffer and incubated at 4 °C overnight. After four washing steps with blocking solution for 10 min each, immunostaining was followed by secondary goat anti-rabbit 488 IgG antibodies (Invitrogen). F-actin was stained by rhodamin-phalloidin and nuclear DNA by TO-PRO3 iodide AlexaFluor633 (Invitrogen) as described previously (Anton-Erxleben et al., 2009).

For visualization of bacteria urethane treatment prior fixation was omitted and polyps were fixed in 2% paraformaldehyde, 2.5% glutaraldehyde and 75 mM L-lysine in 50 mM cacodylate buffer, pH 7.4, for 18 h at 4 °C. Animals were washed six times for 10 min in phosphate-buffered saline. After washing, polyps were stained with SYBR Gold (Life

Technologies GmbH) for 5 min. Before embedding in Mowiol/DABCO (Sigma-Aldrich), animals were rinsed for 10 min in phosphate-buffered saline.

Whole-mount *in situ* hybridization

In situ nucleotide hybridization in hydra polyps whole-mounts was performed as previously described (Augustin et al., 2006). A digoxigenin (DIG)-labeled antisense RNA probe was designed to recognize specifically the sequence of *Hydra* gene products. Primers are liste below in **Table 2**. DIG-labeled sense probes (targeting the same sequences as the antisense probes) were used as a control.

Table 2. Oligonucleotides for generation of custodin *in situ* hybrization probes.

gene / species	name	sequence (5‘ → 3‘)	T_m [°C]
Custodin-1a *H. vulgaris* (AEP)	AEP_6017_F2	GCTCCAATGGTTTAACGGT	54,5
	AEP_6017_R2	CTTGATTCTTCCCAAATATTCG	54,7
Custodin-1b/c *H. vulgaris* (AEP)	KS_2345_ISH_F	GTTGTAATATTTATTAGGAAATAG	51,2
	AEP_2345_R5	CTTATTTCTACGATCATACGC	50,8
Custodin-2 *H. vulgaris* (AEP)	Haep_47542_F	GTAGCAATATTTTTCACTCTTTGTTTG	57,4
	Haep_47542_R	TAAAAACTTTACGAGGACTTGACC	57,6
Custodin-1 *H. oligactis*	Holi_14192_F	GGGTTGCTTTCTTTTTTGTAGTTTC	58,1
	Holi_14192_R	GTCCTCCATTAAAAAATAAAATGACAG	57,4
Custodin-2 *H. oligactis*	KS_Holi_2_F2	GAGTTGTAGCCGAATATTTAAG	54,7
	KS_Holi_2_R2	CCAATGCATGTGTTCATTTAC	54,0
Custodin *H. viridissima*	Hvir_1527_F	GGTGTTGAGATCGCTGAGGA	59,4
	Hvir_1527_R	CATCACCTTGTCAATTCTAATACAAAAAG	59,6

Glycocalyx extraction and sample processing for HPLC-ESI MS/MS

For glycocalyx extraction 5000 *H. vulgaris* (AEP) polyps were used. To avoid massive bacterial contamination the culture medium (S-medium) was supplemented with 50 µg/ml of ampicillin, rifampicin, streptomycin, neomycin and spectinomycin each for five days. Polyps were not fed during the experiment to avoid contamination by food particles. One day prior glycocalyx extraction animals were placed in sterile S-medium without antibiotics. For glycocalyx extraction the animals were gently rocked in 150 ml phophate buffered-saline with 1 mM EDTA for 5 min. The medium was taken off, filled into sterile 50 ml tubes and frozen in liquid nitrogen. Samples were stored for 1 h at -80 °C and subsequently subjected to lyophilization to reduce the sample volume to about 30 ml. Concentration, desalting and buffer exchange were carried out in centrifugation filters (Amicon® Ultra-15, 3000 MWCO,

Millipore) at 3000×*g* and 4 °C. After the first cetrifugation the flow-through was collected, desalted on a SepPak® C18 Vac 6 cc column (Waters), eluted with 84% acetonitrile (ACN) and lyophilized to dryness. The sample was stored at -20 °C for later in-solution digestion (see in-gel tryptic digestion).

The remaining sample was washed with 0.1 M ammonium bicarbonate twice and concentrated to volume of 1 ml, which frozen at -80 °C and subsequently lyophilized to dryness. The lyophilized sample was dissolved in water and divided into two parts. One part was supplemented with SDS-sample buffer with 100 mM DTT, while the other part was subjected to deglycosylation before adding the SDS-sample buffer. Deglycosylation was carried out using the Protein Deglycosylation Mix (New England Biolabs) according to the manufacturer's protocol. The Protein Deglycosylation Mix contains PNGase F, β-*N*-acetylglucosaminidase, β-1-4 galactosidase, neuraminidase (sialidase) and, *O*-Glycosidase to simultaneously remove *N*-glycans and some *O*-glycans (Koutsioulis et al., 2008). Proteins were separated by 1D-SDS-PAGE using a 4-15% gradient precast gel. The gel was subsequently stained with Coomassie Brilliant Blue.

Analysis of glycocalyx protein extracts via 1D-gel LC-ESI MS/MS

In-gel tryptic digestion

Gel slices were cut from stained SDS-PAGE gel lanes using a sterile scapel blade and transferred to 1.5 ml reaction tubes. Each gel slice was vortexted in 200 µl H_2O. The supernatant was discarded and gel slices were washed for 15 min with 200 µl of 1:1 aqueous ACN / H_2O using a thermo mixer (20 °C, 7500 rpm). Supernatant was removed and the step was repeated. After removal of supernatant gel slices were reduced in 100 µl 0.1 M TEAB buffer (triethylammonium bicarbonate) and 5 mM TCEP (tris(2-carboxyethyl)-phosphine on a thermo mixer for 1 h at 60 °C and 7500 rpm. The supernatant was removed and alkylation was performed by incubation with 100 mM TEAB, 10 mM MMTS (S-Methly methanethiosulfonate) at room temperature for 20 min. Supernatant was removed and gel pieces were dried, then covered with 100 mM TEAB, 50 ng trypsin and digested overnight (16 h) on a thermo mixer at 37 °C. Peptides were extracted from gel pieces by washing with 30 µl of 60% ACN, 0.1% trifluoroacetic acid (TFA) for 20 min (7500 rpm), then with 60 µl 100% ACN (20 min, 700 rpm). After each step samples were sonicated for 1 min and the supernatants were combined, lyophilized and resolved in 0.1% aqueous TFA for LC-MS/MS analysis. The flow through from Amicon filters was desalted on a SepPack, eluted and

lyophilized to dryness. In-solution digest of the flow through fraction was performed in 200 µl TEAB as described for in-gel digest.

LC-ESI MS/MS

LC-MS/MS analysis of each of the ten extracted gel slices was performed in duplicate. For the LC-ESI MS/MS analysis a Dionex Ultimate 3000 HPLC system, equipped with an Acclaim PepMap100 nano-column (75 µm x 15 cm, 3 µm, 100 Å, Dionex), was coupled to an LTQ Orbitrap velos mass spectrometer (Thermo). IP-RP-HPLC separation was performed with a gradient of eluent A (Milli-Q water with 0.1% formic acid) and eluent B (80% ACN, 0.1% formic acid). Injecting 6 µl of the ten first dimensional fractions. Peptides were washed for 10 min on a PepMap C18 guard column (300 µm x 10 mm) with 0.1% aqueous TFA at a flow rate of 30 µl/min and separated by a gradient from 5 to 60% B in 120 min at a flow rate of 250 nl/min, followed by a sharp increase to 95% in 10 min and a 5 min washing step. The column was then equilibrated with 5% B for 15 min. UV detection was performed at 214 nm. HPLC-flow was coupled to the LTQ Orbitrap velos (Thermo) using a nanospray ion source with 1.3 kV spray voltage and 197 °C capillary temperature with a 30 µm PicoTip emitter (New Objective). After a delay time of 35 min full scans of 300–2000 m/z range were recorded in profile mode with a resolution of 30.000 for 155 min (AGC target 1E6; maximum inject time 500 ms, preview mode for FTMS master scans and Wideband activation were used). Top 5 precursors (minimum signal intensity 500 and rejecting charge state 1) were selected for both CID fragmentation and HCD fragmentation with a repeat count of 2 and a repeat duration of 20 s and subsequent dynamic exclusion of a 5 ppm mass window around the selected m/z values for 90 s. The CID isolation window was set to 3 Da, the AGC target was 1E4 with a maximum inject time of 400 ms, activation time of 10 ms and an activation q value of 0.25. Normalized collision energy for CID fragmentation was set to 35%. The isolation window for HCD precursors was set to 3 Da, AGC target was 1E5 with a maximum inject time of 500 ms, activation time of 0.1 ms. Normalized collision energy of 40% was used for fragmentation and HCD spectra were acquired with a resolution of 15.000. All MS2 spectra were recorded in centroid mode.

After one point recalibration with Recal-offline, using the polysiloxane contaminant peak 445.12003, raw-files were subjected to database search using Proteome Discoverer Software (v1.4). The hydra database was supplemented with common contaminants. Mascot (v2.1), SequestHT and MS Amanda search algorithms were used to search HCD-FT and CID-IT spectra with a fragment mass accuracy of 0.02 and 0.5 Da respectively. Parent-mass

accuracy for all spectra was set to 6 ppm with semi-trypsin specified as protease allowing for two missed cleavages. Methylthiolation of cysteine was set as static modification and deamidation of asparagine which occurs in concert with deglycosylation of N-glycans by PNGaseF (protein N-glycosidase F) as well as oxidation of methionine were allowed as variable modifications. Percolator (v 1.2) was used for posterior error calculation combining the results of the database searches with a false discovery rate restricted to 0.01 by q-value. Single peptide identifications were excluded and protein groups were assigned using strict parsimony rules.

Generation of transgenic *Hydra vulgaris* (AEP) expressing eGFP:custodin-1c

For generation of *H. vulgaris* (AEP) eGFP:custodin-1c transgenics, the custodin-1c sequence coding for the full-length protein including signal peptide was amplified from *H. vulgaris* (AEP) cDNA using Platinum High Fidelity polymerase (Invitrogen). The cDNA was cloned into the LigAF-1 vector at the 5'-end of the eGFP gene. The second custodin-1c was amplified without signal peptide and cloned into the expression vector at the 3′ end of eGFP. The resulting construct was sequenced and plasmid DNA was purified using Qiagen MidiPrep Kit and injected into *H. vulgaris* (AEP) embryos as previously described (Wittlieb et al., 2006). Founder polyps showing stable eGFP:custodin-1c expression in the ectodermal epithelium were expanded further by clonal propagation. *In vivo* observations were documented using Olympus SZX16 stereomicroscope and an Olympus DP71 digital camera.

Recombinant expression of custodin-1c in *E. coli*

A nucleotide fragment corresponding to amino acid residues 16 to 126 of custodin-1c was cloned into pET28a(+) vector (Novagen). An overnight culture of *E. coli* Rosetta 2(DE3) (Novagen) with the plasmid was diluted 1:100 in 1 L LB medium with kanamycin. After the culture reached an OD_{600} of 0.6, the expression of custodin-1c was induced by addition of 0.5 mM IPTG. The culture was incubated for 3 h at 37 °C.

Refolding of inclusion bodies and purification of recombinant custodin-1c

Recombinant bacteria were lysed at 0 °C with 50 mM Tris-HCl, 0.1 M NaCl, 5 mM EDTA, 0.5% (v/v) Triton-X100, 1 mM dithiothreitol (DTT), pH 8.0 using interval sonication (5 s impulse, 10 s pause) for 3 min. The suspension was centrifuged at 20,000×*g* for 10 min and after three repeated sonication/centrifugation steps the pellet (containing rCustodin-1c) was washed with lysis buffer without Triton X-100 and DTT and stored at -20 °C. The denatured rCustodin-1c was refolded by rapid dilution as follows. The inclusion body pellet

was solubilized at 0 °C in solubilization buffer (8.5 M urea, 0.1 M Tris-base, 50 mM glycine, 0.1 M DTT, pH 8.0) by interval sonication for 1 min (5 s impulse, 5 s pause). Protein was concentrated by 20,000×*g* centrifugation and drop-wise diluted to a final concentration of 100 µg/mL (as estimated by A280 absorption) into refolding buffer (0.1 M Tris-base, 50 mM glycine, 10% (v/v) glycerin, 0.4 mM L-arginine, 5 mM glutathione red, 0.5 mM glutathione oxi, 1 mM EDTA, 0.1 mM PMSF, pH 8.0) under moderate stirring at room temperature. The solution was stirred overnight at room temperature in the dark after which it was dialyzed (MWCO 3500, ThermoFisher Scientific) at 4 °C against 0.1 M Tris-base, 0.15 M NaCl, pH 8.0. Any precipitated protein was removed by centrifugation at 20,000×*g* for 30 min at 4 °C. The supernatant containing water-soluble rCustodin-1c peptide was again dialyzed overnight at 4 °C and finally stored at 4 °C. The dialysate was further purified with two consecutive reverse phase chromatography procedures. To decrease the volume and as a pre-purification step, the dialysate was bound to a SepPak® C18 Vac 6 cc column (Waters) and eluted with 84% ACN. The eluate was lyophilized and stored at -20 °C. The dried rCustodin-1c peptide was solubilized in 0.05% TFA and bound to an Xselect® CSH C18 reverse phase HPLC column (Waters, Eschborn, Germany) after which a linear gradient of 1.2% ACN/min for 60 min was used for eluation. The peptide-containing fractions were pooled, lyophilized, solubilized in 0.05% (v/v) TFA and stored at -20 °C to be further used in a microdilution susceptibility assay.

MIC determination of recombinant Custodin-1c

Minimal inhibitory concentraction (MIC) assays was performed with *Bacillus megaterium* ATCC 14581 obtained from ATCC. Microdilution susceptibility assays were performed in 96-well microtiter plates that were pre-coated with sterile 0.1% BSA for 10 min. After removal of BSA the wells were filled with a twofold dilution series of rCustodin-1c. Incubation with an inoculum of approximately 100 CFU per well was performed in 10 mM Na_2HPO_4 buffer (pH 6.2). Following overnight incubation at 37 °C in a moisture chamber the MIC was determined as the lowest serial dilution showing absence of a bacterial cell pellet. The experiment was carried out in triplicate.

References

Anton-Erxleben F, Thomas A, Wittlieb J, Fraune S and Bosch TCG (2009) Plasticity of epithelial cell shape in response to upstream signals: A whole-organism study using transgenic Hydra. *Zoology* **112**(3). 185–194. doi:10.1016/j.zool.2008.09.002.

Antoni L, Nuding S, Weller D, Gersemann M, Ott G, Wehkamp J, et al. (2013) Human colonic mucus is a reservoir for antimicrobial peptides. *J. Crohn's Colitis* **7**(12). e652–e664.

Arason GJ (1996) Lectins as defence molecules in vertebrates and invertebrates. *Fish Shellfish Immunol.* **6**(4). 277–289. doi:10.1006/fsim.1996.0029.

Augustin R, Anton-Erxleben F, Jungnickel S, Hemmrich G, Spudy B, Podschun R, et al. (2009a) Activity of the novel peptide arminin against multiresistant human pathogens shows the considerable potential of phylogenetically ancient organisms as drug sources. *Antimicrob. Agents Chemother.* **53**(12). 5245–50. doi:10.1128/AAC.00826-09.

Augustin R, Franke A, Khalturin K, Kiko R, Siebert S, Hemmrich G, et al. (2006) Dickkopf related genes are components of the positional value gradient in Hydra. *Dev. Biol.* **296**(1). 62–70. doi:10.1016/j.ydbio.2006.04.003.

Augustin R, Siebert S and Bosch TCG (2009b) Identification of a kazal-type serine protease inhibitor with potent anti-staphylococcal activity as part of Hydra's innate immune system. *Dev. Comp. Immunol.* **33**(7). 830–7. doi:10.1016/j.dci.2009.01.009.

Bode H, Dunne J, Heimfeld S, Huang L, Javois L, Koizumi O, et al. (1986) Transdifferentiation occurs continuously in adult hydra. *Curr. Top. Dev. Biol.* **20**. 257–80.

Bosch TCG, Augustin R, Anton-Erxleben F, Fraune S, Hemmrich G, Zill H, et al. (2009) Uncovering the evolutionary history of innate immunity: The simple metazoan Hydra uses epithelial cells for host defence. *Dev. Comp. Immunol.* **33**(4). 559–569.

Bosch TCG and David CN (1987) Stem cells of Hydra magnipapillata can differentiate into somatic cells and germ line cells. *Dev. Biol.* **121**(1). 182–191.

Bosch TCG and McFall-Ngai MJ (2011) Metaorganisms as the new frontier. *Zoology (Jena).* **114**(4). 185–90. doi:10.1016/j.zool.2011.04.001.

Böttger A, Doxey AC, Hess MW, Pfaller K, Salvenmoser W, Deutzmann R, et al. (2012) Horizontal gene transfer contributed to the evolution of extracellular surface structures: the freshwater polyp Hydra is covered by a complex fibrous cuticle containing glycosaminoglycans and proteins of the PPOD and SWT (sweet tooth) families. *PLoS One* **7**(12). e52278. doi:10.1371/journal.pone.0052278.

Böttger A and Hassel M (2012) Hydra, a model system to trace the emergence of boundaries in developing eumetazoans. *Int. J. Dev. Biol.* **56**(6–8). 583–591. doi:10.1387/ijdb.113454ab.

Brandl K, Plitas G, Schnabl B, DeMatteo RP and Pamer EG (2007) MyD88-mediated signals induce the bactericidal lectin RegIIIγ and protect mice against intestinal Listeria monocytogenes infection. *J. Exp. Med.* **204**(8). 1891–1900. doi:10.1084/jem.20070563.

Bulet P, Stöcklin R and Menin L (2004) Anti-microbial peptides: From invertebrates to vertebrates. *Immunol. Rev.*, 169–184. doi:10.1111/j.0105-2896.2004.0124.x.

Burnett AL (1966) A Model of Growth and Cell Differentiation in Hydra. *Am. Nat.* **100**(912). 165–189. doi:10.2307/2459475.

Campbell RD (1967) Tissue dynamics of steady state growth inHydra littoralis. II. Patterns of tissue movement. *J. Morphol.* **121**(1). 19–28. doi:10.1002/jmor.1051210103.

Campbell RD (1987) A new species of Hydra (Cnidaria: Hydrozoa) from North America with comments on species clusters within the genus. *Zool. J. Linn. Soc.*, 253–263. doi:10.1111/j.1096-3642.1987.tb01510a.x.

Carr S, Aebersold R, Baldwin M, Burlingame A, Clauser K and Nesvizhskii A (2004) The Need for Guidelines in Publication of Peptide and Protein Identification Data. *Mol. Cell. Proteomics* **3**(6). 531–533. doi:10.1074/mcp.T400006-MCP200.

Davis LE (1973) Histological and ultrastructural studies of the basal disk of Hydra - I. The glandulomuscular cell. *Zeitschrift für Zellforsch. und Mikroskopische Anat.* **139**(1). 1–27. doi:10.1007/BF00307458.

Davis LE and Haynes JF (1968) An ultrastructural examination of the mesoglea of Hydra. *Zeitschrift für Zellforsch. und Mikroskopische Anat. Zellforsch. und Mikroskopische Anat.* **92**(2). 149–158. doi:10.1007/BF00335643.

Dimarcq JL, Bulet P, Hetru C and Hoffmann J (1998) Cysteine-rich antimicrobial peptides in invertebrates. *Biopolymers* **47**(6). 465–77. doi:10.1002/(SICI)1097-0282(1998)47:6<465::AID-BIP5>3.0.CO;2-#.

Douglas AE (2009) The microbial dimension in insect nutritional ecology. *Funct. Ecol.*, 38–47. doi:10.1111/j.1365-2435.2008.01442.x.

Dübel S, Hoffmeister S a. H and Schaller HC (1987) Differentiation pathways of ectodermal epithelial cells in hydra. *Differentiation* **35**(3). 181–189. doi:10.1111/j.1432-0436.1987.tb00167.x.

Dupont A, Kaconis Y, Yang I, Albers T, Woltemate S, Heinbockel L, et al. (2015) Intestinal mucus affinity and biological activity of an orally administered antibacterial and anti-inflammatory peptide. *Gut* **64**(2). 222–232. doi:10.1136/gutjnl-2014-307150.

Faith JJ, Guruge JL, Charbonneau M, Subramanian S, Seedorf H, Goodman AL, et al. (2013) The long-term stability of the human gut microbiota. *Science (80-.).* **341**(6141). 1237439–1237439. doi:10.1126/science.1237439.

Franzenburg S, Walter J, Künzel S, Wang J, Baines JF, Bosch TCG, et al. (2013) Distinct antimicrobial peptide expression determines host species-specific bacterial associations. *Proc. Natl. Acad. Sci. U. S. A.* **110**(39). E3730-8. doi:10.1073/pnas.1304960110.

Fraune S, Anton-Erxleben F, Augustin R, Franzenburg S, Knop M, Schröder K, et al. (2015) Bacteria-bacteria interactions within the microbiota of the ancestral metazoan Hydra contribute to fungal resistance. *ISME J.* **9**(7). 1543–56. doi:10.1038/ismej.2014.239.

Fraune S, Augustin R, Anton-Erxleben F, Wittlieb J, Gelhaus C, Klimovich VB, et al. (2010) In an early branching metazoan, bacterial colonization of the embryo is controlled by maternal antimicrobial peptides. *Proc. Natl. Acad. Sci. U. S. A.* **107**(42). 18067–72. doi:10.1073/pnas.1008573107.

Fraune S and Bosch TCG (2007) Long-term maintenance of species-specific bacterial microbiota in the basal metazoan Hydra. *Proc. Natl. Acad. Sci. U. S. A.* **104**(32). 13146–51. doi:10.1073/pnas.0703375104.

Grazia A Di, Cappiello F, Imanishi A, Mastrofrancesco A, Picardo M, Paus R, et al. (2015) The frog skin-derived antimicrobial peptide esculentin-1α(1-21)NH2promotes the migration of human HaCaT keratinocytes in an EGF receptor-dependent manner: A novel promoter of human skin wound healing? *PLoS One* **10**(6). e0128663. doi:10.1371/journal.pone.0128663.

Gruber CW, Čemažar M, Anderson MA and Craik DJ (2007) Insecticidal plant cyclotides and related cystine knot toxins. *Toxicon*, 561–575. doi:10.1016/j.toxicon.2006.11.018.

Gu S, Chen D, Zhang JN, Lv X, Wang K, Duan LP, et al. (2013) Bacterial Community Mapping of the Mouse Gastrointestinal Tract. *PLoS One* **8**(10). e74957. doi:10.1371/journal.pone.0074957.

Hanington PC, Forys MA, Dragoo JW, Zhang S-M, Adema CM and Loker ES (2010) Role for a somatically diversified lectin in resistance of an invertebrate to parasite infection. *Proc. Natl. Acad. Sci.* **107**(49). 21087–21092. doi:10.1073/pnas.1011242107.

Hemmrich G, Khalturin K, Boehm AM, Puchert M, Anton-Erxleben F, Wittlieb J, et al. (2012) Molecular signatures of the three stem cell lineages in hydra and the emergence of stem cell function at the base of multicellularity. *Mol. Biol. Evol.* **29**(11). 3267–3280. doi:10.1093/molbev/mss134.

Hollingsworth M a and Swanson BJ (2004) Mucins in cancer: protection and control of the cell surface. *Nat. Rev. Cancer* **4**(1). 45–60. doi:10.1038/nrc1251.

Holstein TW, Hess MW and Salvenmoser W (2010) *Preparation techniques for transmission electron microscopy of Hydra. Methods Cell Biol.* doi:10.1016/S0091-679X(10)96013-5.

Huang Z, Ma A, Xia D, Wang X, Sun Z, Shang X, et al. (2016) Immunological characterization and expression of lily-type lectin in response to environmental stress in turbot (Scophthalmus maximus). *Fish Shellfish Immunol.* **58**. 323–331. doi:10.1016/j.fsi.2016.08.025.

Hufnagel LA and Myhal ML (1977) Observations on a Spirochaete Symbiotic in Hydra. *Trans. Am. Microsc. Soc.* **96**(3). 406. doi:10.2307/3225874.

Jacques M and Graham L (1989) Improved preservation of bacterila capsule for electron microscopy. *J. Electron Microsc. Tech.* **11**(2). 167–169. doi:10.1002/jemt.1060110212.

Johansson MEV and Hansson GC (2016) Immunological aspects of intestinal mucus and mucins. *Nat. Rev. Immunol.*, 639–649. doi:10.1038/nri.2016.88.

Johansson ME V, Ambort D, Pelaseyed T, Schütte A, Gustafsson JK, Ermund A, et al. (2011) Composition and functional role of the mucus layers in the intestine. *Cell. Mol. Life Sci.* **68**(22). 3635–41. doi:10.1007/s00018-011-0822-3.

Johansson ME V, Gustafsson JK, Sjöberg KE, Petersson J, Holm L, Sjövall H, et al. (2010) Bacteria penetrate the inner mucus layer before inflammation in the dextran sulfate colitis model. *PLoS One* **5**(8). e12238. doi:10.1371/journal.pone.0012238.

Johansson ME V, Phillipson M, Petersson J, Velcich A, Holm L and Hansson GC (2008) The inner of the two Muc2 mucin-dependent mucus layers in colon is devoid of bacteria. *Proc. Natl. Acad. Sci. U. S. A.* **105**(39). 15064–9. doi:10.1073/pnas.0803124105.

Jung S, Dingley AJ, Augustin R, Anton-Erxleben F, Stanisak M, Gelhaus C, et al. (2009) Hydramacin-1, structure and antibacterial activity of a protein from the basal metazoan Hydra. *J. Biol. Chem.* **284**(3). 1896–905. doi:10.1074/jbc.M804713200.

Karnovsky MJ (1965) A formaldehyde-glutaraldehyde fixative of high osmolarity for use in electron microscopy. *J. Cell Biol.* **27**. 137–138. doi:10.1038/srep27790.

Kerney R, Kim E, Hangarter RP, Heiss AA, Bishop CD and Hall BK (2011) Intracellular invasion of green algae in a salamander host. *Proc. Natl. Acad. Sci.* **108**(16). 6497–6502. doi:10.1073/pnas.1018259108.

Kilpatrick DC (2002) Animal lectins: A historical introduction and overview. *Biochim. Biophys. Acta - Gen. Subj.*, 187–197. doi:10.1016/S0304-4165(02)00308-2.

Koutsioulis D, Landry D and Guthrie EP (2008) Novel endo-α- N -acetylgalactosaminidases with broader substrate specificity. *Glycobiology* **18**(10). 799–805. doi:10.1093/glycob/cwn069.

Kuznetsov SG, Anton-Erxleben F and Bosch TCG (2002) Epithelial interactions in Hydra: apoptosis in interspecies grafts is induced by detachment from the extracellular matrix. *J. Exp. Biol.* **205**(24). 3809–3817.

Lang T, Hansson GC and Samuelsson T (2007) Gel-forming mucins appeared early in metazoan evolution. *Proc. Natl. Acad. Sci. U. S. A.* **104**(41). 16209–14. doi:10.1073/pnas.0705984104.

Lang T, Klasson S, Larsson E, Johansson MEV, Hansson GC and Samuelsson T (2016) Searching the evolutionary origin of epithelial mucus protein components – mucins and FCGBP. *Mol. Biol. Evol.* msw066. doi:10.1093/molbev/msw066.

Macklin M (1976) The effect of urethane on hydra. *Biol. Bull.* **150**(3). 442–452. doi:10.2307/1540684.

Marques MRF and Barracco MA (2000) Lectins, as non-self-recognition factors, in crustaceans. *Aquaculture* **191**(1–3). 23–44. doi:10.1016/S0044-8486(00)00417-8.

Marshall E, Costa LM and Gutierrez-Marcos J (2011) Cysteine-Rich Peptides (CRPs) mediate diverse aspects of cell-cell communication in plant reproduction and development. *J. Exp. Bot.* **62**(5). 1677–1686. doi:10.1093/jxb/err002.

Martin VJ, Littlefield CL, Archer WE and Bode HR (1997) Embryogenesis in hydra. *Biol. Bull.* **192**(3). 345–363. doi:10.2307/1542745.

McFall-Ngai M, Hadfield MG, Bosch TCG, Carey H V, Domazet-Lošo T, Douglas AE, et al. (2013) Animals in a bacterial world, a new imperative for the life sciences. *Proc. Natl. Acad. Sci. U. S. A.* **110**(9). 3229–36. doi:10.1073/pnas.1218525110.

Meyer-Hoffert U, Hornef MW, Henriques-Normark B, Axelsson L-G, Midtvedt T, Pütsep K, et al. (2008) Secreted enteric antimicrobial activity localises to the mucus surface layer. *Gut* **57**(6). 764–71. doi:10.1136/gut.2007.141481.

Mitta G, Vandenbulcke F, Noël T, Romestand B, Beauvillain JC, Salzet M, et al. (2000) Differential distribution and defence involvement of antimicrobial peptides in mussel. *J. Cell Sci.* **113**. 2759–2769.

Moniaux N (2001) Structural organization and classification of the human mucin genes. *Front. Biosci.* **6**(1). d1192. doi:10.2741/Moniaux.

Moran NA, McCutcheon JP and Nakabachi A (2008) Genomics and Evolution of Heritable Bacterial Symbionts. *Annu. Rev. Genet.* **42**(1). 165–190. doi:10.1146/annurev.genet.41.110306.130119.

Muramoto K, Kagawa D, Sato T, Ogawa T, Nishida Y and Kamiya H (1999) Functional and structural characterization of multiple galectins from the skin mucus of conger eel, Conger myriaster. *Comp. Biochem. Physiol. - B Biochem. Mol. Biol.* **123**(1). 33–45. doi:10.1016/S0305-0491(99)00037-1.

Nakamura O, Matsuoka H, Ogawa T, Muramoto K, Kamiya H and Watanabe T (2006) Opsonic effect of congerin, a mucosal galectin of the Japanese conger, Conger myriaster (Brevoort). *Fish Shellfish Immunol.* **20**(3). 433–435. doi:10.1016/j.fsi.2005.06.004.

Ng T, Fai Cheung R, Wing Ng C, Fang E and Wong J (2015) A Review of Fish Lectins. *Curr. Protein Pept. Sci.* **16**(4). 337–351. doi:10.2174/1389203716041504291608 50.

Nyholm S V. and McFall-Ngai M (2004) The winnowing: establishing the squid–vibrio symbiosis. *Nat. Rev. Microbiol.* **2**(8). 632–642. doi:10.1038/nrmicro957.

Ogawa T, Watanabe M, Naganuma T and Muramoto K (2011) Diversified Carbohydrate-Binding Lectins from Marine Resources. *J. Amino Acids* **2011**. 1–20. doi:10.4061/2011/838914.

Okamoto M, Tsutsui S, Tasumi S, Suetake H, Kikuchi K and Suzuki Y (2005) Tandem repeat l-rhamnose-binding lectin from the skin mucus of ponyfish, Leiognathus nuchalis. *Biochem. Biophys. Res. Commun.* **333**(2). 463–469. doi:10.1016/j.bbrc.2005.05.118.

Omenn GS, States DJ, Adamski M, Blackwell TW, Menon R, Hermjakob H, et al. (2005) Overview of the HUPO Plasma Proteome Project: Results from the pilot phase with 35 collaborating laboratories and multiple analytical groups, generating a core dataset of 3020 proteins and a publicly-available database. *Proteomics*, 3226–3245. doi:10.1002/pmic.200500358.

Perez-Vilar J and Hill RL (1999) The structure and assembly of secreted mucins. *J. Biol. Chem.* **274**(45). 31751–4.

Portal C, Gouyer V, Magnien M, Plet S, Gottrand F and Desseyn J-L (2017) In vivo imaging of the Muc5b gel-forming mucin. *Sci. Rep.* **7**. 44591. doi:10.1038/srep44591.

Rodrigues M, Leclère P, Flammang P, Hess MW, Salvenmoser W, Hobmayer B, et al. (2016) The cellular basis of bioadhesion of the freshwater polyp Hydra. *BMC Zool.* **1**(1). 3. doi:10.1186/s40850-016-0005-7.

Rose MC (2006) Respiratory Tract Mucin Genes and Mucin Glycoproteins in Health and Disease. *Physiol. Rev.* **86**(1). 245–278. doi:10.1152/physrev.00010.2005.

Schröder K and Bosch TCG (2016) The Origin of Mucosal Immunity: Lessons from the Holobiont Hydra. *MBio* **7**(6). e01184-16. doi:10.1128/mBio.01184-16.

Seedorf H, Griffin NW, Ridaura VK, Reyes A, Cheng J, Rey FE, et al. (2014) Bacteria from diverse habitats colonize and compete in the mouse gut. *Cell* **159**(2). 253–266. doi:10.1016/j.cell.2014.09.008.

Shan M, Gentile M, Yeiser JR, Walland AC, Bornstein VU, Chen K, et al. (2013) Mucus enhances gut homeostasis and oral tolerance by delivering immunoregulatory signals. *Science (80-.).* **342**(6157). 447–453. doi:10.1126/science.1237910.

Subramanian S, Ross NW and MacKinnon SL (2009) Myxinidin, A Novel Antimicrobial Peptide from the Epidermal Mucus of Hagfish, Myxine glutinosa L. *Mar. Biotechnol.* **11**(6). 748–757. doi:10.1007/s10126-009-9189-y.

Tateno H, Ogawa T, Muramoto K, Kamiya H and Saneyoshi M (2002) Rhamnose-binding Lectins from Steelhead Trout (Oncorhynchus mykiss) Eggs Recognize Bacterial Lipopolysaccharides and Lipoteichoic Acid. *Biosci. Biotechnol. Biochem.* **66**(3). 604–612. doi:10.1271/bbb.66.604.

Taylor K, Barran PE and Dorin JR (2008) Review: Structure-activity relationships in β-defensin peptides. *Biopolym. - Pept. Sci. Sect.*, 1–7. doi:10.1002/bip.20900.

Tian E and Ten Hagen KG (2009) Recent insights into the biological roles of mucin-type O-glycosylation. *Glycoconj. J.*, 325–334. doi:10.1007/s10719-008-9162-4.

Tropini C, Earle KA, Huang KC and Sonnenburg JL (2017) The Gut Microbiome: Connecting Spatial Organization to Function. *Cell Host Microbe*, 433–442. doi:10.1016/j.chom.2017.03.010.

Tsutsui S, Komatsu Y, Sugiura T, Araki K and Nakamura O (2011) A unique epidermal mucus lectin identified from catfish (Silurus asotus): First evidence of intelectin in fish skin slime. *J. Biochem.* **150**(5). 501–514. doi:10.1093/jb/mvr085.

Tsutsui S, Okamoto M, Tasumi S, Suetake H, Kikuchi K and Suzuki Y (2006) Novel mannose-specific lectins found in torafugu, Takifugu rubripes: A review. *Comp. Biochem. Physiol. Part D Genomics Proteomics* **1**(1). 122–127. doi:10.1016/j.cbd.2005.09.005.

Tsutsui S, Suzuki Y, Shibuya K and Nakamura O (2018) Sacciform cells in the epidermis of fugu (Takifugu rubripes) produce and secrete kalliklectin, a novel lectin found in teleosts. *Fish Shellfish Immunol.* **80**. 311–318. doi:10.1016/j.fsi.2018.06.017.

Tsutsui S, Yamaguchi M, Hirasawa A, Nakamura O and Watanabe T (2009) Common skate (Raja kenojei) secretes pentraxin into the cutaneous secretion: The first skin mucus lectin in cartilaginous fish. *J. Biochem.* **146**(2). 295–306. doi:10.1093/jb/mvp069.

Tsutsui S, Yoshinaga T, Komiya K, Yamashita H and Nakamura O (2016) Differential expression of skin mucus C-type lectin in two freshwater eel species, Anguilla marmorata and Anguilla japonica. *Dev. Comp. Immunol.* **61**. 154–160. doi:10.1016/j.dci.2016.03.027.

Turnbaugh PJ, Ridaura VK, Faith JJ, Rey FE, Knight R and Gordon JI (2009) The effect of diet on the human gut microbiome: A metagenomic analysis in humanized gnotobiotic mice. *Sci. Transl. Med.* **1**(6). 6ra14-6ra14. doi:10.1126/scitranslmed.3000322.

Tytgat KMAJ, Opdam FJM, Einerhand AWC, Büller HA and Dekker J (1996) MUC2 is the prominent colonic mucin expressed in ulcerative colitis. *Gut* **38**(4). 554–563. doi:10.1136/gut.38.4.554.

Vaishnava S, Yamamoto M, Severson KM, Ruhn KA, Yu X, Koren O, et al. (2011) The antibacterial lectin RegIIIgamma promotes the spatial segregation of microbiota and host in the intestine. *Science* **334**(6053). 255–8. doi:10.1126/science.1209791.

Visick KL and Ruby EG (2006) Vibrio fischeri and its host: it takes two to tango. *Curr. Opin. Microbiol.* **9**(6). 632–638. doi:10.1016/j.mib.2006.10.001.

Watanabe Y, Shiina N, Shinozaki F, Yokoyama H, Kominami J, Nakamura-Tsuruta S, et al. (2008) Isolation and characterization of l-rhamnose-binding lectin, which binds to microsporidian Glugea plecoglossi, from ayu (Plecoglossus altivelis) eggs. *Dev. Comp. Immunol.* **32**(5). 487–499. doi:10.1016/j.dci.2007.08.007.

Wittlieb J, Khalturin K, Lohmann JU, Anton-Erxleben F and Bosch TCG (2006) Transgenic Hydra allow in vivo tracking of individual stem cells during morphogenesis. *Proc. Natl. Acad. Sci.* **103**(16). 6208–6211. doi:10.1073/pnas.0510163103.

Yang J, Huang M, Zhang H, Wang L, Wang H, Wang L, et al. (2015) CfLec-3 from scallop: An entrance to non-self recognition mechanism of invertebrate C-type lectin. *Sci. Rep.* **5**. 10068. doi:10.1038/srep10068.

Zhou Z, Yu X, Tang J, Zhu Y, Chen G, Guo L, et al. (2017) Dual recognition activity of a rhamnose-binding lectin to pathogenic bacteria and zooxanthellae in stony coral Pocillopora damicornis. *Dev. Comp. Immunol.* **70**. 88–93. doi:10.1016/j.dci.2017.01.009.

Zilber-Rosenberg I and Rosenberg E (2008) Role of microorganisms in the evolution of animals and plants: The hologenome theory of evolution. *FEMS Microbiol. Rev.*, 723–735. doi:10.1111/j.1574-6976.2008.00123.x.

Chapter II

A secreted antibacterial neuropeptide shapes the microbiome of *Hydra*

***Nature Communications* (2017)**: accepted 13th of July 2017

doi: 10.1038/s41467-017-00625-1

nature COMMUNICATIONS

ARTICLE

DOI: 10.1038/s41467-017-00625-1 OPEN

A secreted antibacterial neuropeptide shapes the microbiome of *Hydra*

René Augustin[1], Katja Schröder[1], Andrea P. Murillo Rincón[1], Sebastian Fraune[1], Friederike Anton-Erxleben[1], Eva-Maria Herbst[1], Jörg Wittlieb[1], Martin Schwentner[1,4], Joachim Grötzinger[2], Trudy M. Wassenaar[3] & Thomas C.G. Bosch[1]

Colonization of body epithelial surfaces with a highly specific microbial community is a fundamental feature of all animals, yet the underlying mechanisms by which these communities are selected and maintained are not well understood. Here, we show that sensory and ganglion neurons in the ectodermal epithelium of the model organism hydra (a member of the animal phylum Cnidaria) secrete neuropeptides with antibacterial activity that may shape the microbiome on the body surface. In particular, a specific neuropeptide, which we call NDA-1, contributes to the reduction of Gram-positive bacteria during early development and thus to a spatial distribution of the main colonizer, the Gram-negative *Curvibacter* sp., along the body axis. Our findings warrant further research to test whether neuropeptides secreted by nerve cells contribute to the spatial structure of microbial communities in other organisms.

[1] Zoological Institute and Interdisciplinary Research Center Kiel Life Science, University of Kiel, 24098 Kiel, Germany. [2] Institute of Biochemistry, University of Kiel, 24098 Kiel, Germany. [3] Molecular Microbiology and Genomics Consultancy, 55576 Zotzenheim, Germany. [4] Present address: Museum of Comparative Zoology, Harvard University, Cambridge, MA 02138, USA. René Augustin and Katja Schröder contributed equally to this work. Correspondence and requests for materials should be addressed to T.C.G.B. (email: tbosch@zoologie.uni-kiel.de)

There is an increasing appreciation that homeostasis of any organism depends on a constant dialogue with the microorganisms that cover its surfaces[1–3] and this also applies to aquatic animals[4, 5]. Each organism maintains a specific microbiome, comprised of a stable core as well as variable components. However, how exactly the formation of a multi-level species microbiome is regulated, how the resultant holobiont operates as a functional unit, and by which mechanisms the host interacts with its microbiome, remains largely unknown.

Like all living organisms, animals are constantly being exposed to microbes; this applies to their external (skin, exoskeleton) as well as internal (respiratory, gastrointestinal) surfaces. Biologically active peptides provide bidirectional interactions between such host tissues and the microbiome. The body compartments of animals are innervated by a dense network of nerve cells that produce neuropeptides, which serve as messengers in the complex interactions within and between nerve cells and the connected body parts[6]. The microbiome interacts with nerve cell endings in surface tissues, for instance by inducing pain[7], while host-derived neuropeptides in turn have been proposed to interact with the microbiome[6–13]. However, the impact of neuropeptides on the composition of a host-specific microbiome has not been studied in detail.

Here, we tested the hypothesis that neuropeptides may be involved in the interaction and communication between the host and its natural array of microbes. For this we used the model organism hydra, a member of the animal phylum Cnidaria, to which corals, jellyfishes, and polyps belong. Cnidaria is the sister clade of Bilateria and among the first metazoans that contain neurons. Cnidarian nervous systems function as diffuse nerve nets of approximately 3000 neurons and offer great potential for understanding the basic design principles of a nervous system[14].

Hydra is covered by a microbiome that emerges progressively after hatching via a conserved temporal pattern, to reach a stable resident microbiome at adult stage[15]. The latter is characterized by Gram-negative bacterial species with a preponderance of *Curvibacter sp.*, a member of the β-Proteobacteria[15]. Disturbances or shifts in any of these bacterial colonizers can compromise the health of the whole animal[16].

In a previous study, we had observed that the absence of neurons affects the associated bacterial community and leads to an increase of Bacteroidetes and reduced levels of β-Proteobacteria, suggestive of neuron-mediated selective forces on the associated microbiota[17]. Here, we investigated whether such effects are due to neuropeptides, which we hypothesized to serve an antimicrobial, innate immune function that shapes the hydra's microbiome.

Results

Neuron development in Hydra coincides with decreasing Gram-positives. The formation of a functional nervous system during the development of hydra polyps from a hatching egg via juvenile to the adult polyp stage was quantified microscopically. Based on previous observations in *Hydra vulgaris* strain AEP[18], very few nerve cells (0.02 neurons per epithelial cell) are present in hatchlings. By 3 weeks a complete nervous system is present, with approximately 0.25 neurons per epithelial cell (Fig. 1a). The composition of the bacterial communities associated with hydra during ontogeny has been assessed previously by culture-independent pyrosequencing of bacterial DNA[15]. This resulted in the finding of dramatic changes in bacterial composition over time and a stable microbiome was observed 3 to 4 weeks after hatching[15]. Reanalysis of that data showed that the ratio of Gram-positive bacteria decreased approximately threefold within the first 2 weeks after hatching and continued to decrease, to comprise <1% of the microbial community at week 15 (Fig. 1b). This was accompanied by the establishment of a consistent bacterial composition dominated by *Curvibacter* sp.

The high variation in abundance of Gram-positive bacteria between week 3 and 6 (Fig. 1b) was shown previously[15] to be a characteristic feature of the maturation of the adult microbiome in hydra.

Locally expressed neuropeptide NDA-1 functions as an antimicrobial. When screening for hydra peptides with structural similarity to invertebrate cytokines, so-called astakines[19], we noticed a peptide, which we call NDA-1, that contains a signal sequence followed by a cationic 71 aa-long peptide containing ten conserved cysteine residues (Fig. 2a). A neighbor-joining phylogenetic tree was constructed but remained largely unresolved with regard to the relationship of the included prokineticins, astakines, dickkopf, and colipase gene families: apart from the cysteine pattern no congruence was observed between NDA-1 and the other peptides (Supplementary Fig. 1). An NDA-1 gene is present in the *Hydra magnipapillata* genome and in the transcriptome of three other hydra species including *H. vulgaris* AEP[20]. Since there are no identifiable orthologs to NDA-1 outside hydra, it is currently considered to represent a taxon-restricted gene (Supplementary Fig. 1).

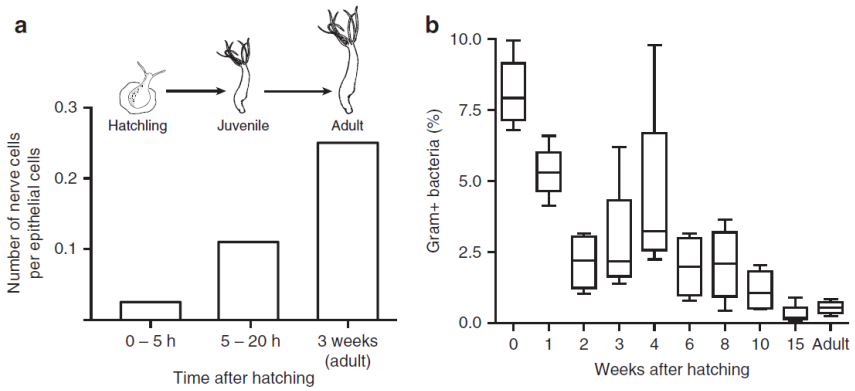

Fig. 1 Formation of a neural system and a microbiome during hydra development. **a** Quantitative assessment of the nervous system in three developmental stages; original data taken from ref. [18]. **b** Proportion of Gram-positive bacteria in the microbiome over time plotted as *box*- and *whisker*-plot with the *box* containing 25th to 75th percentiles, the *line* representing the *mean* and *whiskers* showing maximum and minimum values; original data taken from ref. [15]

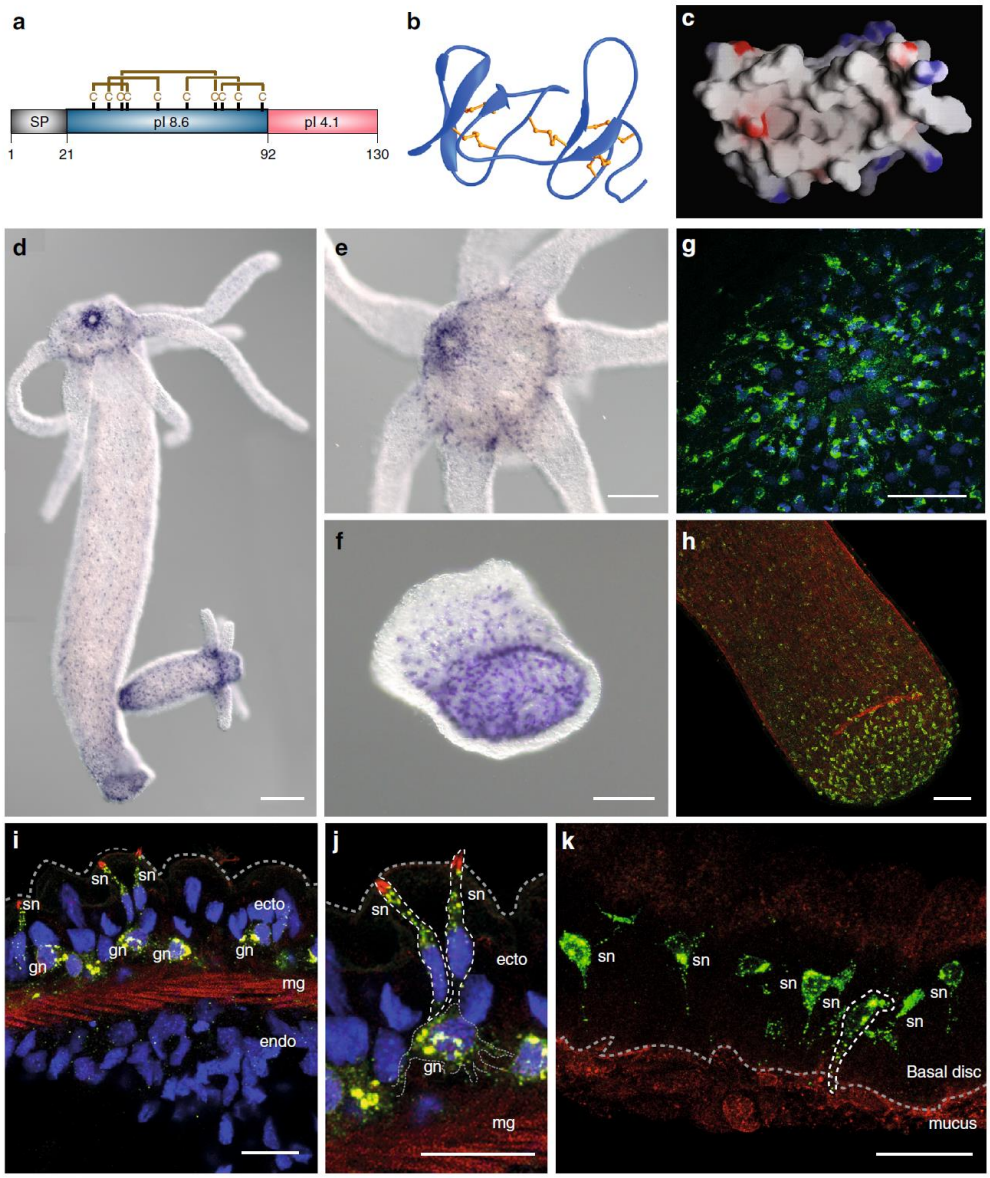

Fig. 2 Biochemical domains and expression of neuropeptide NDA-1. **a** Schematic representation of NDA-1 precursor peptide showing its signal peptide (*SP*), cysteine-rich cationic domain (*blue*) with predicted disulfide bonds indicated, and C-terminal domain (*red*). **b** Predicted tertiary structure of mature NDA-1 peptide. **c** Molecular surface presentation showing a hydrophobic pocket with localized anionic (*red*) and cationic (*blue*) residues. **d**–**f** In situ hybridization demonstrating gene expression of NDA-1 mRNA in the neurons of **d** an adult polyp, with high expression in **e** the head and **f** the foot. *Scale bar* **d**: 200 µm, **e**, **f**: 100 µm. **g**–**k** Immuno-cytochemistry of NDA-1 peptide (*green*) combined with TO-PRO3-stained cellular DNA (*blue*) and (except in **k**) rhodamin-phalloidin for F-actin (*red*). Dense population of NDA-1 positive neurons are located in **g** the head and **h** the foot. *Scale bar*: 50 µm. **i**–**k** Confocal laser scanning microscope showing intracellular location of NDA-1 peptide in **i**, **j** the hypostomal region of the head, where ganglion neurons (gn) and sensory neurons (sn) are located in the ectodermal (ecto) layer; mesoglea (mg), and endoderm (endo) are indicated. *Scale bar*: 16 µm. **k** Confocal laser scanning microscope showing intracellular location of NDA-1 peptide in sensory neurons of the foot, with 1A10-antibody detecting an ectodermal surface epitope (*red*). A sensory neuron expressing NDA-1 is marked by a *broken white line*. *Scale bar*: 20 µm

The predicted structure of the cationic domain of NDA-1 is shown in Fig. 2b. The signal peptide is followed by a segment containing two β-sheets that are separated by a long flexible loop and are held together by five disulfide bonds with similarity to a colipase fold. Molecular surface prediction indicates the formation of a strongly hydrophobic pocket (Fig. 2c). Taken together, the predicted structure, its charge distribution and the cysteine pattern all support the view that NDA-1 is produced as a precursor: cleavage of the 38 aa C-terminal would produce a mature peptide of 71 aa.

By means of in situ hybridization we determined that the gene for NDA-1 was expressed in neurons throughout the body

(Fig. 2d–f). High numbers of NDA-1 gene-expressing ganglion and sensory neurons are localized in the head (hypostome) and foot of the polyp, whereas in the body column fewer ganglion cells express the NDA-1 gene. To localize the peptide in hydra tissue a polyclonal antiserum was produced, which detected mature peptide in ganglion as well as sensory neurons interspersed in the ectodermal epithelial layer (Fig. 2g, h). Confocal laser scanning microscopy revealed that NDA-1 was located in the distal parts of the sensory neurons, facing the outer mucus layer (Fig. 2i, j). Similarly, in sensory neurons in the foot the peptide was detected in the protrusions reaching out to the ectodermal surface (Fig. 2k), suggesting that the peptide is secreted into the mucus layer.

Since the mucus layer is the habitat of most of the resident microbiome[16, 21], we next assessed whether the mature peptide had antimicrobial activity. For this, recombinant mature peptide (rNDA-1) was produced in *E. coli*. After partial purification, microdilution susceptibility assays were performed to determine the minimal inhibitory concentration (MIC) of rNDA-1 against a range of Gram-negative and Gram-positive bacteria. As summarized in Table 1, the peptide was highly toxic for the Gram-positive freshwater species *Bacillus megaterium*, *Trichococcus pasteurii*, and *Trichococcus collinsii*, whose growth was inhibited by concentrations below 1 µM. Growth of *B. megaterium* was affected at a concentration of 400 nM. In contrast, a strain of *Pseudomonas* sp. that had been isolated from a biofilm in hydra

Table 1 Minimal inhibitory concentration values of NDA-1 against a selection of Gram-positive and Gram-negative bacteria

	Bacterial strain	Habitat	NDA-1 MIC (µM)
Gram-positives	*Bacillus megaterium* ATCC 14581	Soil, fresh water	0.4
	Staphylococcus aureus ATCC 12600	Human skin, mucosal surfaces	23.1
	Bacillus subtilis DSM 10	Soil, fresh water	5.8
	Trichococcus pasteurii DSM 2381	Fresh water	0.9
	Trichococcus collinsii DSM 14526	Fresh water	0.4–0.9
Gram-negatives	*Escherichia coli* K12 MG1665	—	>14.0
	Curvibacter sp.	*H. vulgaris* AEP main colonizer	0.4
	Acinetobacter sp. (Biofilm 4)	*H. vulgaris* AEP culture dish	7.0
	Pseudomonas sp. (Biofilm 3)	*H. vulgaris* AEP culture dish	>20.9

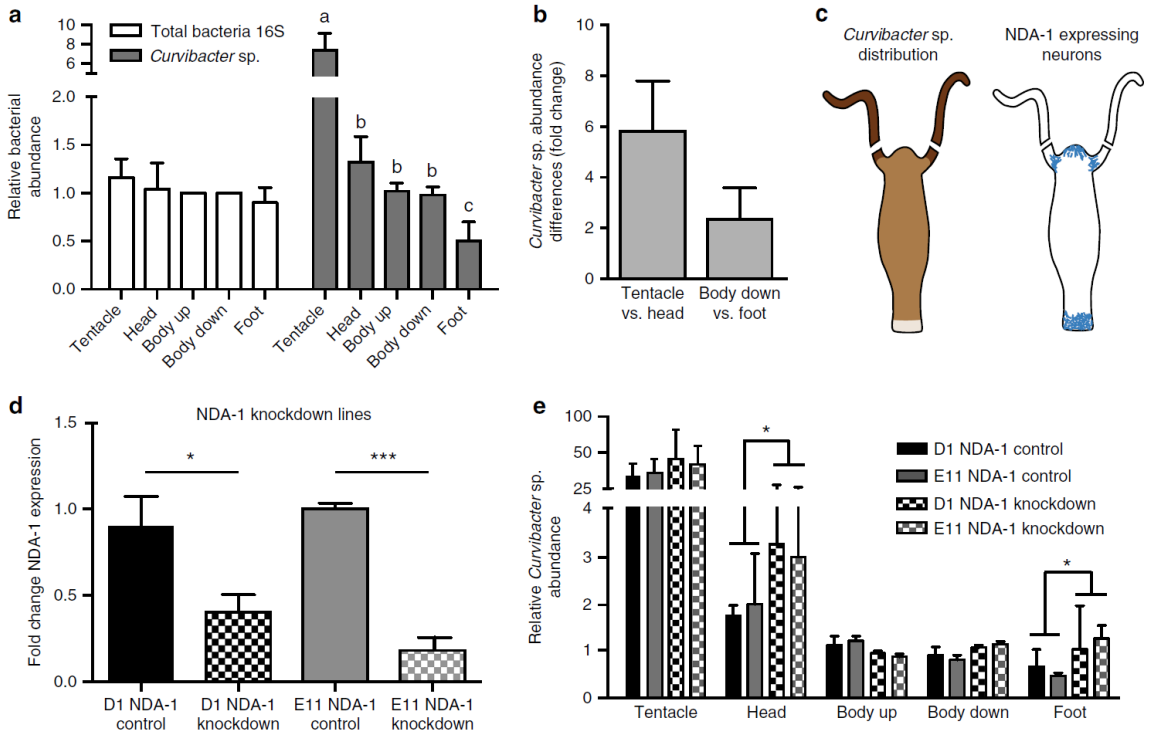

Fig. 3 Spatial distribution of *Curvibacter* is regulated by NDA-1. **a** Abundance of total bacterial loads (*white bars*) and *Curvibacter* sp. (*gray bars*) at various body parts, with standard errors of the mean. Statistical differences ($P < 0{,}001$, GLM; $n = 5$) are indicated by different letters. **b** Relative abundance of *Curvibacter* sp. on different body parts. **c** Schematic representation of the quantitative distribution of *Curvibacter* (*left*) and NDA-1-expressing sensory neurons (*right*). **d** NDA-1 expression in hydra knockdown lines D1 and E11 with their corresponding controls; statistical significance: $^{*}P < 0{,}05$, $^{***}P < 0{,}001$ ANOVA; $n = 3$. **e** Body site distribution of *Curvibacter* sp. in NDA-1 knockdown lines and controls (GLM; $n = 3$)

culture dish was not inhibited, though significant activity was observed against a likewise isolated biofilm-forming *Acinetobacter* sp. Interestingly, NDA-1 was particularly potent against *Curvibacter* sp., the main colonizer that can reach over 70% abundance in the hydra microbiome[16]. We speculate that the observed antimicrobial activity of the peptide is due to interactions of its hydrophobic pocket with bacterial membranes. Based on the observed expression pattern and antimicrobial activity, we propose that NDA-1 may regulate the composition of the hydra microbiome, both qualitatively (regulating the ratio between Gram-negative and Gram-positive bacteria) and quantitatively, by keeping the numbers of bacteria in check.

NDA-1 determines the spatial distribution of *Curvibacter* sp. The high antimicrobial activity against *Curvibacter* sp. raised the question about consequences with respect to the local distribution of this main colonizer along the body. Total bacterial load and *Curvibacter* abundance were determined for various body parts. While total bacterial load was found to be evenly distributed along the body column (Fig. 3a), *Curvibacter* had a higher mean abundance in the tentacles than in other body regions (Fig. 3a–c). An additional difference was observed between the lower body column and the foot tissue with very low abundance of *Curvibacter* in foot tissue (Fig. 3a–c). In head tissue, where NDA-1 is strongly expressed by sensory neurons around the hypostome and in the base of tentacles (as shown in Fig. 2e), a sixfold reduction in *Curvibacter* abundance is observed compared to tentacles (Fig. 3b). Conversely, when comparing body column and foot tissue, *Curvibacter* abundance is twofold lower in foot tissue, which has a high density of NDA-1-expressing and secreting neurons (Fig. 3b, c).

To elucidate whether there is a direct relationship between presence of NDA-1 secreting neurons and the drastic change in *Curvibacter* abundance in tentacle vs. head and body column vs. foot region (Fig. 3b), NDA-1 expression was diminished by means of antisense technology. Two transgenic lines of hydra were established that produced a 60% (line D1) and 80% (line E11) decrease of the endogenous NDA-1 transcript, as determined by quantitative real-time PCR (Fig. 3d). Control lines originating from the same mosaic founder polyp lacking eGFP-positive cells were used to measure the effect of the transgenic interference within a conserved genomic background. Supplementary Fig. 2 shows confocal laser scanning micrographs of the foot region, illustrating reduced expression of NDA-1 in the knockdown lines. The NDA-1 knockdown animals showed no differences in mechanical-induced contractile behavior and feeding response when compared to the corresponding control lines, indicating that NDA-1 knockdown does not appear to have functional consequences regarding common behavioral responses in Hydra (Supplementary Figs. 3 and 4). As expected, the decreased expression of NDA-1 in both transgenic lines affected the spatial distribution of *Curvibacter* (Fig. 3d), resulting in a higher *Curvibacter* abundance in the head and foot compared to control lines. This suggests that neuropeptide NDA-1 in wild-type polyps contributes to the reduction of *Curvibacter* abundance of head and body compared to tentacle tissue, and prevents *Curvibacter* growth at the very basal end of foot tissue. The neuropeptide, therefore, appears to contribute to the spatial distribution of hydra's main colonizing bacteria along the body column.

Interestingly, attempts to overexpress NDA-1 ectopically in epithelial cells resulted in a lethal phenotype early after hatching, suggesting that NDA-1 may have not yet discovered functions in addition to its role in host–microbe interaction (Supplementary Fig. 5).

Other hydra neuropeptides also have antimicrobial activity. Previous works had already identified a large number of peptides

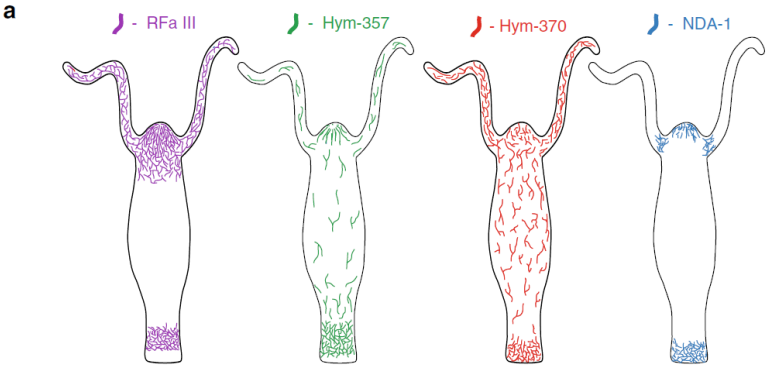

b

	Bacterial strain	RFamide III	Hym-357	Hym-370	NDA-1
		MIC in µM			
Gram +	*B. megaterium* ATCC 14581	0.7	4.4	1.8	0.4
	B. subtilis DSM 10	>500	22	4.5 – 9.0	5.8
	T. pasteurii DSM 2381	0.9	1.4	0.6	0.9
	T. collinsii DSM 14526	0.5 – 0.9	0.3	0.3	0.4–0.9
Gram –	*E. coli* K12 MG1665	461	>500	72	>14.0
	Curvibacter sp.	58.2	>500	>500	0.4
	Acinetobacter sp.	1.8	11	2.2	7.0
	Pseudomonas sp.	58.2	>500	143.6	>20.9

Fig. 4 Local distribution of expression and antibacterial activity of three neuropeptides. **a** Schematic drawing of neurons expressing RFamide III (RFa III), Hym-357, and Hym-370 along the body of hydra. **b** Antibacterial activity of the three neuropeptides. Data for Hym-357 taken from ref. [22], for Hym-370 from ref. [23], for RFamide III from refs [48, 49]

characterized as neurotransmitters or neuromodulators in hydra, although NDA-1 was not among them. In line with the discovery of NDA-1 functioning as an antimicrobial peptide, we assessed whether other, pre-identified neuropeptides could also have an impact on the bacterial microbiome. Predicted biologically active forms of hydra neuropeptides were screened in silico for potential antimicrobial activity, based on their biochemical parameters such as charge distribution, isoelectric point and amphipathicity. Three neuropeptides, representing the three major neuropeptide classes of hydra were selected: Hym-370, Hym-357, and RFamide III. Hym-370 and Hym-357 had been identified in a screen for myoactive peptides[22–25]. Rfamide III is a neuropeptide belonging to a family of FMRFamide-like peptides conserved in invertebrates and vertebrates[26–29]. Previous publications[26–30] have demonstrated that the expression patterns of these three genes are unique in that each gene is expressed in different subpopulations of neurons, forming distinct localized expression patterns along the body axis with sharp boundaries (Fig. 4a). To assess their antimicrobial activity, the neuropeptides were chemically synthesized and tested in microdilution susceptibility assays against eight bacterial species. The results showed that all three peptides had antibacterial activity (Fig. 4b). Hym-357 and Hym-370 were active against all four tested Gram-positive bacteria (*B. megaterium*, *B. subtilis*, *T. pasteurii*, and *T. collinsii*), but RFamide III was inactive against *B. subtilis*. Variation in antimicrobial activity was also observed for the four Gram-negative bacteria tested, whereby not one of the tested bacteria species was insensitive to all three (Fig. 4b). In contrast to NDA-1, none of the three peptides was active against the main colonizer *Curvibacter* sp. These results suggest that distinct nerve cells may contribute to the spatial structure of hydra's microbial community by expressing a variety of neuropeptides with specific antimicrobial activity. In contrast to the antimicrobial peptides identified in hydra so far[31–34], the neuropeptides analyzed here are active mostly against Gram-positive bacteria. Additionally, the main Gram-negative colonizer *Curvibacter* is differentially affected by the peptides.

Discussion

Here, we have shown that the composition of the microbiome in hydra, a member of the ancient animal phylum Cnidaria, is regulated by NDA-1, a neuron-secreted peptide, and possibly by other neuropeptides. Using in vivo transgenesis and in vitro antimicrobial activity assays, we have demonstrated that NDA-1 affects the hydra microbiome by inhibiting the growth of Gram-positive bacteria and of the main colonizer, the Gram-negative bacterium *Curvibacter* sp. In addition, we identified a number of previously characterized neuropeptides to have specific antimicrobial activity, adding to previous reports showing that some neuropeptides from other organisms can display direct antibacterial activity[8–13].

Microbial colonization in early hydra embryos is controlled by maternally encoded antimicrobial peptides[35]. After mid-blastula transition, zygotically expressed antimicrobial peptides take control of the microbiome. After hatching, a stable microbiome is established within 3 to 4 weeks[15]. Symbiotic microbes may be acquired by both vertical and horizontal transmission[35]. In adult hydra, stably associated microbes play a role in pathogen defense[16].

Due to similarities in amino-acid composition, amphipathic design, cationic charge and size, it has been suggested that many neuropeptides and peptide hormones may be directly involved in innate immune reactions against pathogenic intruders[36]. In mammals, neuropeptides such as substance P[37], calcitonin gene-related peptide, neuropeptide Y, vasoactive intestinal polypeptide, somatostatin and corticotropin-releasing factor, have all been suggested as participating in the bidirectional gut-brain communication[6]. However, their impact on the composition of the microbiota, or their role in interaction between this and the nervous system, are still to be assessed. Our data reveal that several neuropeptides in hydra may play roles in the bidirectional relationship between the host and its associated microbiota.

Peptides have long been recognized as important signaling molecules in the hydra peptidome[24, 25, 38]. A variety of neuropeptides have been identified with different functions within the nervous system and in the dynamic interplay between neurons and other cell types. For example, Hym-357 strongly induces both tentacle and body contraction of normal polyps but has no effect on epithelial polyps, indicating that the peptide does not work directly on muscles but presumably activates other neurons, which in turn release neurotransmitters to directly induce muscle contraction[22, 23, 25]. Many of these peptides are encoded by taxonomically restricted genes[39]. Indeed, peptides of the NDA-1 family are specific for the genus *Hydra* and are absent in other animal taxa. However, we speculate that the function of neuropeptides as regulators of a resident microbiome may be widespread in the animal kingdom.

It should be noted that the tissue covered by the microbiome is heterogeneous. Neurons are in close proximity to epithelial cells, while the secretome creates a specific milieu to harbor particular bacterial colonizers. Neuropeptides can be considered part of the secretome that influence the microbial community composition by selective antimicrobial activities. The local distribution of neurons expressing specific neuropeptides contributes to local tissue heterogeneity and associated variation in microbiome composition.

The holobiont concept implies that all components participate in establishing resilience. Cnidarians have evolved a nerve net where sensory and ganglion neurons and their processes are interspersed among the epithelial cells of both layers. We speculate that the evolutionary process that resulted in a new organ such as the nervous system was partly driven by the necessity to maintain the holobiont. The observed selective effects of neuropeptides on commensal microbes not only contribute to solve the long-standing question of how community membership in a given holobiont is maintained, but also extends the functional capacity of the nervous system in early branching metazoans: their neuron-derived antimicrobial peptides may help to establish and maintain the species-specific microbiome in a spatially controlled manner. Recognizing the relationship between the neuroimmune system and the associated microbiome may provide novel insights into a deeper understanding and improved management of a number of disorders in which the neuron-microbe dialogue is disturbed.

Methods

Chemicals. If not other stated otherwise, chemicals were obtained from Roth, Karlsruhe, Germany. All primers were obtained from MWG Eurofins, Ebersberg, Germany.

Animals used and culture conditions. Experiments were carried out using *Hydra vulgaris* AEP[40]. All laboratory-cultured strains of *H. vulgaris* AEP are available from the University of Kiel. Standardized culture medium, food (1st instar larvae of *Artemia salina*, fed 3× per week) and culture conditions are described elsewhere[41].

Identification of NDA-1 peptide and structural modeling. A fold recognition algorithm was validated with human CYP17A1 and cytochrome P450 (ProHit package, ProCeryon Biosciences GmbH, Salzburg, Austria). The X-ray structure of pancreatic colipase (PDB accession code 1N8S) produced a high score of the pair potential and the best match of cysteine-pairing; thus, this served as the template for the three-dimensional model of NDA-1. According to the alignment obtained by the fold recognition procedure, amino-acid residues were exchanged in the

template. Insertions and deletions in NDA-1 were modeled using a database-search approach included in the software package WHATIF[42].

In situ hybridization and immunostaining of NDA-1. In situ nucleotide hybridization in hydra polyps whole-mounts was performed as previously described[43]. A digoxigenin (DIG)-labeled antisense RNA probe was designed (primers NDA-1F: 5′-AACAAAATCAATTTCGCTGA-3′ and NDA-1R: 5′-TCGTCATTTA AATCATCTTC-3′) to recognize specifically the sequence of *Hydra NDA-1* gene product (GenBank accession number XM_002162825). DIG-labeled sense probes (targeting the same sequences as the antisense probes) were used as a control.

For Immunocytochemistry, polyclonal antibodies were raised against the C-terminal part of NDA-1 in rabbits. The synthetic peptide ((C)TNEDDLNDER KYFKQDK) (Genosphere Biotechnologies, Paris, France) was coupled to KLH prior to injection. The resulting polyclonal serum was affinity-purified and used for immunocytochemistry. Detection of NDA-1 protein in whole mounts was performed following standard procedures[44]. In brief, following anesthesia, polyps were fixed in 4% (v/v) paraformaldehyde for 30 min. After removal of fixative and permeabilization with 0.5% Triton X-100 in PBS, polyps were incubated in blocking solution containing 1% bovine serum albumin (BSA). NDA-1-antiserum (1:160 dilution, 5.6 ng/µL) in blocking buffer was incubated at 4 °C overnight. After four washing steps with blocking solution for 10 min each, immunostaining with NDA-1-specific rabbit serum was followed by secondary goat anti-rabbit 488 IgG antibodies (Molecular Probes, Invitrogen, Eugene, OR, USA, cat# A-11034) as described previously[45]. F-actin was stained by rhodamin-phalloidin and nuclear DNA by TO-PRO3 iodide (642/661; Molecular Probes, Invitrogen, Eugene, OR, USA, cat# T3605) as described previously[45]. The outer membrane surface of the ectodermal epithelial cells was stained by 1A10 monoclonal antibodies[46]. Confocal laser-scanning microscopy was performed using a TCS SP1 laser-scanning confocal microscope (Leica).

Recombinant expression in *E. coli*, refolding and purification of rNDA-1. A nucleotide fragment corresponding to amino-acid residues 21 to 92 of *NDA-1* was cloned into pet28a vector (Merck-Millipore/Novagen, Darmstadt, Germany) and expressed in *E. coli* BL21 as inclusion bodies. Recombinant bacteria were lysed at 0 °C with 50 mM Tris-HCl, 0.1 M NaCl, 5 mM EDTA, 0.5% (v/v) Triton-X100, 1 mM dithiothreitol (DTT), pH 8.0 using interval sonication (5 s impulse, 5 s pause) for 3 min. The suspension was centrifuged at 20,000×*g* for 10 min and after three repeated sonication/centrifugation steps the pellet (containing NDA-1) was washed with lysis buffer without Triton X-100 and DTT and stored at −20 °C. The denatured rNDA-1 was refolded by rapid dilution as follows. The inclusion body pellet was solubilized at 0 °C in solubilization buffer (8.5 M urea, 0.1 M Tris-base, 50 mM glycine, 0.1 M DTT, pH 8.0) by interval sonication for 1 min (5 s impulse, 5 s pause). Protein was concentrated by 20,000×*g* centrifugation and drop-wise diluted to a final concentration of 100 µg/mL (as estimated by A280 absorption) into refolding buffer (0.1 M Tris-base, 50 mM glycine, 10% (v/v) glycerin, 0.4 mM L-arginine, 5 mM glutathione red, 0.5 mM glutathione oxi, 1 mM EDTA, 0.2 mM PMSF, pH8.0) under moderate stirring at room temperature. The solution was stirred overnight at room temperature in the dark after which it was dialyzed (MWCO 3500, ThermoFisher Scientific (Pierce), Waltham, MA, USA) at 4 °C against 0.1 M Tris-base, 0.15 M NaCl, pH 8.0. Any precipitated protein was removed by centrifugation at 20,000×*g* for 30 min at 4 °C. The supernatant containing water-soluble rNDA-1 peptide was again dialyzed overnight at 4 °C and finally stored at 4 °C. The dialysate was further purified with two consecutive reverse phase chromatography procedures. To decrease the volume and as a pre-purification step, the dialysate was bound to a SepPak® C18 Vac 6 cc column (Waters, Eschborn, Germany) and eluted with 84% acetonitrile (ACN). The eluate was lyophilized and stored at −20 °C. The dried rNDA-1 peptide was solubilized in 0.05% trifluoroacetic acid (TFA) and bound to an Xselect® CSH C18 reverse phase HPLC column (Waters, Eschborn, Germany) after which a linear gradient of 1.2% ACN/min for 60 min was used for eluation. The peptide-containing fractions were lyophilized and solubilized in 0.05% (v/v) TFA and further analyzed for their antibacterial activity using *Bacillus megaterium* ATCC 14581 (source: American Type Culture Collection (ATCC)) in a microdilution susceptibility assay. Fractions showing a MIC < 0.46 µM were pooled and analyzed by sodium dodecyl sulfate-polyacrylamide gel electrophoresis, mass spectrometry and circular dichroism spectroscopy. The pooled fractions were aliquoted and stored at −20 °C to be further used in a microdilution susceptibility assay.

MIC determination of antibacterial neuropeptides. The following bacterial strains were used in MIC assays: *Bacillus megaterium* ATCC 14581, *Staphylococcus aureus* ATCC 12600 (both obtained from ATCC), *Bacillus subtilis* DSM 10, *Trichococcus pasteurii* DSM 2381, *Trichococcus collinsii* DSM 14526 (all three obtained from Deutsche Stammsammlung von Mikroorganismen und Zellkulturen GmbH (DSM-Braunschweig), Germany), *Escherichia coli* K12 MG1665 (donated by Dr J.C. Escalante-Semerena, MMI UW-Madison, WI, USA), and three isolates from hydra cultures: *Curvibacter* sp[16], *Acinetobacter* sp., and *Pseudomonas* sp. The latter two strains were isolated from biofilms formed in hydra culture dishes (S. Fraune, unpublished data).

Microdilution susceptibility assays were performed in 96-well microtiter plates that were pre-coated with sterile 0.1% BSA for 10 min. After removal of BSA the wells were filled with a twofold dilution series of either rNDA-1, Hym-370, Hym-357, or RFamid III peptide. The neuropeptides Hym-370 (KPNAYKGKLPI GLW-amide), Hym-357 (KPAFLFKGYKP-amide) and RFamid III (KPHLRGRF-amide) had been chemically synthesized (GenScript, Hong Kong, China) at quantities between 5–9 mg with a purity of > 95% and lyophilized peptides were dissolved in 0.05% TFA to final concentration of 10 mg/mL. Incubation with an inoculum of approximately 100 CFU per well was performed in 10 mM Na_2HPO4 buffer (pH 6.2), except for the three strains derived from hydra cultures, which were incubated in R2A media. Following overnight incubation at 37 °C (*B. megaterium*, *S. aureus*, *B. subtilis*, *E. coli*) or for 3–5 days at 18 °C (others) in a moisture chamber the MIC was determined as the lowest serial dilution showing absence of a bacterial cell pellet. Experiments were carried out in triplicates and MICs were reported as a range in case of triplicate variation.

Generation of transgenic *Hydra vulgaris* AEP polyps. Hairpin-mediated silencing of target genes in hydra was achieved as previously described[47]. For generating *NDA-1* knockdown lines, a cassette consisting of a 225-bp-long fragment of *NDA-1* and its corresponding antisense sequence, separated by a spacer of 157 bp, was cloned in the LigAF-1 vector downstream of *eGFP*. The construct was injected into *H. vulgaris* AEP embryos as previously described[40]. Founder polyps showing stable eGFP expression in a group of interstitial stem cells (i-cells) were expanded further by clonal propagation. By selecting for eGFP-expression, mass cultures of polyps without transgenic i-cells (NDA-1 control) as well as knockdown polyps expressing eGFP (NDA-1 kd) were generated. Completely transgenic NDA-1 knockdown lines could not be established, due to the low eGFP expression (a hallmark of the hairpin construct), the sophisticated structure of the nerve net with countless numbers of i-cells, and the fact that transgenic hydra start as mosaic animals with only a few transgenic cells. As a result, NDA-1 expression in the isolated lines can be variable. Thus, *NDA-1* knockdown was validated by quantitative real-time PCR using specific oligonucleotide primers (AL8F: 5′-GAGCAAGCGTTTGCATGAGC and AL8R: 5′-CTTCATCGGGTTCAGGTTCG). Reverse transcription PCR (RT-PCR) data were analyzed by conventional ΔΔCt analysis, using expression levels of hydra Elongation Factor 1α (EF1αF: 5′-GCAGTACTGGTGAGTTTGAAG and EF1αR: 5′-CTTCGCTGTATGGTGGTTCAG) and hydra β-actin (hyActinF: 5′-GAATCA GCTGGTATCCATGAAAC and hyActinR: 5′-AACATTGTCGTACCACCTGA TAG) as equilibration references. Fold-changes were normalized to control polyps of the same line (D1, E11).

To analyze the effect of *NDA-1* knockdown on abundance of *Curvibacter* sp. at different hydra body regions, the knockdown lineages D1 and E11 were each cultured with their controls as a mixed animal population. The polyps were starved for 2 days and GFP-positive knockdown animals were separated from GFP-negative control animals prior to *Curvibacter* analysis.

Spatial distribution of *Curvibacter* sp. on hydra polyps. In three to five independent experiments, combined hydra and bacterial DNA was isolated from ten polyps each that were first washed three times with sterile filtered culture medium and then divided into five body sections: tentacles, head (hypostome area without tentacles), upper body half, lower body half, and foot (peduncle). These tissue parts were subjected to the DNeasy Blood and Tissue Kit (Qiagen, Hilden, Germany) following the manufacturer's protocol to extract DNA, except that in the final step DNA was eluted in 50 µL. The amount of isolated DNA from the various body parts was standardized using quantitative reverse transcription PCR (qRT-PCR) targeting β-actin as described above. Total bacterial DNA was quantified using universal bacterial 16 S rDNA primers (Eub338F: 5′-ACTCCTACGGGAGGCAG CAG; and Eub518R: 5′-ATTACCGCGGCTGCTGG) and *Curvibacter* sp. DNA was quantified using genus-specific primers (CP_AEP1.3 F: 5′-TAGCGAGCTCTA ATACAGTTTGCTA and CP_AEP1.3 R: 5′-GGGATTTCACATCTGTCTTAC ATC). The latter experiments were performed as threefold (Fig. 3d, e) or fivefold (Fig. 3a) replicates.

Statistical analysis. Statistical analyses were performed using R software (version 3.2.3). For Fig. 3a (influence of tissue on total bacteria or *Curvibacter* sp. abundance), data were analyzed separately by generalized linear model with a gamma distribution (GLM; $n = 5$). The explanatory variable was *tissue*. The method of contrasts was used for side-by-side comparisons. *P*-values were adjusted for multiple comparisons using the false discovery rate's correction (fdr). For Fig. 3d (effect of knock-down on the expression of NDA-1) fold-change data were log transformed and a linear model with two factors (*treatment* and *line*) was used. For analysis of variance (ANOVA, $n = 3$), residuals were checked for normality by Shapiro's test, and for homoscedasticity by Levene's test. F statistics were given for global effects of factors and pairwise comparisons were performed using Tukey's honestly significant difference (HSD) test. For Fig. 3e (influence of treatment on bacterial abundance in the different tissues), data ($n = 3$) were analyzed by generalized linear model with a gamma distribution. The minimum model that fitted the data best included *tissue* and *treatment* as explanatory variables (Supplementary Table 1). χ^2 statistics were given for global effects of factors and the method of contrasts was used for side-by-side comparisons. *P*-values were adjusted for multiple comparisons using the fdr correction.

Data availability. The authors declare that the data supporting the findings of the study are available in this article and its Supporting Information files, or from the corresponding author upon request.

Received: 13 December 2016 Accepted: 13 July 2017
Published online: 26 September 2017

References

1. Ley, R. E. et al. Evolution of mammals and their gut microbes. *Science* **320**, 1647–1651 (2008). Erratum in: Science **322**, 1188 (2008).
2. Ley, R. E., Lozupone, C. A., Hamady, M., Knight, R. & Gordon, J. I. Worlds within worlds: evolution of the vertebrate gut microbiota. *Nat. Rev. Microbiol.* **6**, 776–788 (2008).
3. McFall-Ngai, M. et al. Animals in a bacterial world, a new imperative for the life sciences. *Proc. Natl Acad. Sci. USA* **110**, 3229–3236 (2013).
4. Bourne, D. G., Morrow, K. M. & Webster, N. S. Insights into the coral microbiome: underpinning the health and resilience of reef ecosystems. *Annu. Rev. Microbiol.* **70**, 317–340 (2016).
5. Webster, N. S. & Thomas, T. The sponge hologenome. *MBio* **7**, e00135–16 (2016).
6. Holzer, P. & Farzi, A. Neuropeptides and the microbiota-gut-brain axis. *Adv. Exp. Med. Biol.* **817**, 195–219 (2014).
7. Chiu, I. M. et al. Bacteria activate sensory neurons that modulate pain and inflammation. *Nature* **501**, 52–57 (2013).
8. Shimizu, M., Shigeri, Y., Yoshikawa, S. & Yumoto, N. Enhancement of antimicrobial activity of neuropeptide Y by N-terminal truncation. *Antimicrob. Agents Chemother.* **42**, 2745–2746 (1998).
9. Cutuli, M., Cristiani, S., Lipton, J. M. & Catania, A. Antimicrobial effects of α-MSH peptides. *J. Leukoc. Biol.* **67**, 233–239 (2000).
10. Allaker, R. P., Zihni, C. & Kapas, S. An investigation into the antimicrobial effects of adrenomedullin on members of the skin, oral, respiratory tract and gut microflora. *FEMS Immunol. Med. Microbiol.* **23**, 289–293 (1999).
11. Kowalska, K., Carr, D. B. & Lipkowski, A. W. Direct antimicrobial properties of substance P. *Life Sci.* **71**, 747–750 (2002).
12. Hansen, C. J., Burnell, K. & Brogden, K. A. Antimicrobial activity of substance P and neuropeptide Y against laboratory strains of bacteria and oral microorganisms. *J. Neuroimmunol.* **177**, 215–218 (2006).
13. El Karim, I. A., Linden, G. J., Orr, D. F. & Lundy, F. T. Antimicrobial activity of neuropeptides against a range of microorganisms from skin, oral, respiratory and gastrointestinal tract sites. *J. Neuroimmunol.* **200**, 11–16 (2008).
14. Bosch, T. C. G. et al. Back to the basics: cnidarians start to fire. *Trends Neurosci.* **40**, 92–105 (2017).
15. Franzenburg, S. et al. Bacterial colonization of *Hydra* hatchlings follows a robust temporal pattern. *ISME J.* **7**, 781–790 (2013).
16. Fraune, S. et al. Bacteria-bacteria interactions within the microbiota of the ancestral metazoan *Hydra* contribute to fungal resistance. *ISME J.* **9**, 1543–1556 (2015).
17. Fraune, S., Abe, Y. & Bosch, T. C. G. Disturbing epithelial homeostasis in the metazoan *Hydra* leads to drastic changes in associated microbiota. *Environ. Microbiol.* **11**, 2361–2369 (2009).
18. Martin, V. J., Littlefield, C. L., Archer, W. E. & Bode, H. R. Embryogenesis in hydra. *Biol. Bull.* **192**, 345–363 (1997).
19. Söderhäll, I., Kim, Y. A., Jiravanichpaisal, P., Lee, S. Y. & Söderhäll, K. An ancient role for a prokineticin domain in invertebrate hematopoiesis. *J. Immunol.* **174**, 6153–6160 (2005).
20. Schwentner, M. & Bosch, T. C. G. Revisiting the age, evolutionary history and species level diversity of the genus *Hydra* (Cnidaria: Hydrozoa). *Mol. Phylogenet. Evol.* **91**, 41–55 (2015).
21. Schröder, K. & Bosch, T. C. G. The origin of mucosal immunity: lessons from the holobiont Hydra. *MBio* **7**, e01184–16 (2016).
22. Yum, S. et al. A novel neuropeptide, Hym-176, induces contraction of the ectodermal muscle in *Hydra*. *Biochem. Biophys. Res. Commun.* **248**, 584–590 (1998).
23. Takahashi, T. et al. Identification of a new member of the GLWamide peptide family: physiological activity and cellular localization in cnidarian polyps. *Comp. Biochem. Physiol. B. Biochem. Mol. Biol.* **135**, 309–324 (2003).
24. Fujisawa, T. Hydra peptide project 1993–2007. *Dev. Growth Differ.* **50**(Suppl 1): S257–S268 (2008).
25. Fujisawa, T. & Hayakawa, E. Peptide signaling in Hydra. *Int. J. Dev. Biol.* **56**, 543–550 (2012).
26. Koizumi, O., Wilson, J. D., Grimmelikhuijzen, C. J. & Westfall, J. A. Ultrastructural localization of RFamide-like peptides in neuronal dense-cored vesicles in the peduncle of *Hydra*. *J. Exp. Zool.* **249**, 17–22 (1989).
27. Grimmelikhuijzen, C. J. & Westfall, J. A. The nervous systems of cnidarians. *EXS* **72**, 7–24 (1995).
28. Dürrnagel, S. et al. Three homologous subunits form a high affinity peptide-gated ion channel in *Hydra*. *J. Biol. Chem.* **285**, 11958–11965 (2010).
29. Jékely, G. Global view of the evolution and diversity of metazoan neuropeptide signaling. *Proc. Natl Acad. Sci. USA* **110**, 8702–8707 (2013).
30. Koizumi, O., Sato, N. & Goto, C. in *Coelenterate Biology 2003* 41–47 (Springer, 2004).
31. Franzenburg, S. et al. Distinct antimicrobial peptide expression determines host species-specific bacterial associations. *Proc. Natl Acad. Sci. USA* **110**, E3730–E3738 (2013).
32. Bosch, T. C. G. et al. Uncovering the evolutionary history of innate immunity: the simple metazoan *Hydra* uses epithelial cells for host defence. *Dev. Comp. Immunol.* **33**, 559–569 (2009).
33. Augustin, R. et al. Activity of the novel peptide arminin against multiresistant human pathogens shows the considerable potential of phylogenetically ancient organisms as drug sources. *Antimicrob. Agents Chemother.* **53**, 5245–5250 (2009).
34. Jung, S. et al. Hydramacin-1, structure and antibacterial activity of a protein from the basal metazoan *Hydra*. *J. Biol. Chem.* **284**, 1896–1905 (2009).
35. Fraune, S. et al. In an early branching metazoan, bacterial colonization of the embryo is controlled by maternal antimicrobial peptides. *Proc. Natl Acad. Sci. USA* **107**, 18067–18072 (2010).
36. Brogden, K. A., Guthmiller, J. M., Salzet, M. & Zasloff, M. The nervous system and innate immunity: the neuropeptide connection. *Nat. Immunol.* **6**, 558–564 (2005).
37. Grimmelikhuijzen, C. J., Balfe, A., Emson, P. C., Powell, D. & Sundler, F. Substance P-like immunoreactivity in the nervous system of hydra. *Histochemtry* **71**, 325–333 (1981).
38. Takahashi, T. et al. Systematic isolation of peptide signal molecules regulating development in hydra: LWamide and PW families. *Proc. Natl Acad. Sci. USA* **94**, 1241–1246 (1997).
39. Khalturin, K., Hemmrich, G., Fraune, S., Augustin, R. & Bosch, T. C. G. More than just orphans: are taxonomically-restricted genes important in evolution? *Trends Genet.* **25**, 404–413 (2009).
40. Hemmrich, G., Anokhin, B., Zacharias, H. & Bosch, T. C. G. Molecular phylogenetics in *Hydra*, a classical model in evolutionary developmental biology. *Mol. Phylogenet. Evol.* **44**, 281–290 (2007).
41. Lenhoff, H. M. & Brown, R. D. Mass culture of hydra: an improved method and its application to other aquatic invertebrates. *Lab. Anim.* **4**, 139–154 (1970).
42. Vriend, G. WHATIF: a molecular modeling and drug design program. *J. Mol. Graph.* **8**, 52–56 (1990).
43. Augustin, R. et al. Dickkopf related genes are components of the positional value gradient in *Hydra*. *Dev. Biol.* **296**, 62–70 (2006).
44. Wittlieb, J., Khalturin, K., Lohmann, J. U., Anton-Erxleben, F. & Bosch, T. C. G. Transgenic *Hydra* allow *in vivo* tracking of individual stem cells during morphogenesis. *Proc. Natl Acad. Sci. USA* **103**, 6208–6211 (2006).
45. Anton-Erxleben, F., Thomas, A., Wittlieb, J., Fraune, S. & Bosch, T. C. G. Plasticity of epithelial cell shape in response to upstream signals: a whole-organism study using transgenic Hydra. *Zoology (Jena)* **112**, 185–194 (2009).
46. Samoilovich, M. P., Kuznetsov, S. G., Pavlova, M. S. & Klimovich, V. B. Monoclonal antibodies against antigens of *Hydra vulgaris* and *Hydra oligactis*. *J. Evol. Biochem. Physiol.* **37**, 348–357 (2001).
47. Franzenburg, S. et al. MyD88-deficient *Hydra* reveal an ancient function of TLR signaling in sensing bacterial colonizers. *Proc. Natl Acad. Sci. USA* **109**, 19374–19379 (2012).
48. Moosler, A., Rinehart, K. L. & Grimmelikhuijzen, C. J. Isolation of four novel neuropeptides, the hydra-RFamides I-IV, from *Hydra magnipapillata*. *Biochem. Biophys. Res. Commun.* **229**, 596–602 (1996).
49. Darmer, D. et al. Three different prohormones yield a variety of Hydra-RFamide (Arg-Phe-NH2) neuropeptides in *Hydra magnipapillata*. *Biochem. J.* **332**, 403–412 (1998).

Acknowledgements

We thank Natacha Kremer for help with the statistical analysis, Alexander Klimovich for assistance in confocal microscopy and Matthias Leippe for providing the HPLC facility. This work was supported by the Deutsche Forschungsgemeinschaft (DFG) (CRC1182 "Origin and function of Metaorganisms", DFG grant BO 848/17–1, and grants from the DFG Cluster of Excellence program "Inflammation at Interfaces"). T.C.G.B. gratefully appreciates support from the Canadian Institute for Advanced Research (CIFAR).

Author contributions

R.A. and K.S. were responsible for the experimental design and contributed equally to prepare the manuscript. R.A. performed protein purification, MIC assays, qRT-PCR, and (with K.S.) immunocytochemistry. K.S. generated the constructs for transgenesis and recombinant expression in *E. coli* (with E.-M.H.), performed in situ hybridization and mechanical stimulation. A.P.M.R. performed qRT-PCR and the GSH assay. F.A.-E. was responsible for confocal microscopy. M.S. performed the phylogenetic analysis. J.G. was

responsible for the structural modeling of NDA-1. T.M.W. assisted in graphical presentation of the data and writing the manuscript. T.G.C.B. supervised the project and was the driving force behind the research concept.

Additional information

Supplementary Information accompanies this paper at doi:10.1038/s41467-017-00625-1.

Competing interests: The authors declare no competing financial interests.

Reprints and permission information is available online at http://npg.nature.com/reprintsandpermissions/

Publisher's note: Springer Nature remains neutral with regard to jurisdictional claims in published maps and institutional affiliations.

Supplementary information

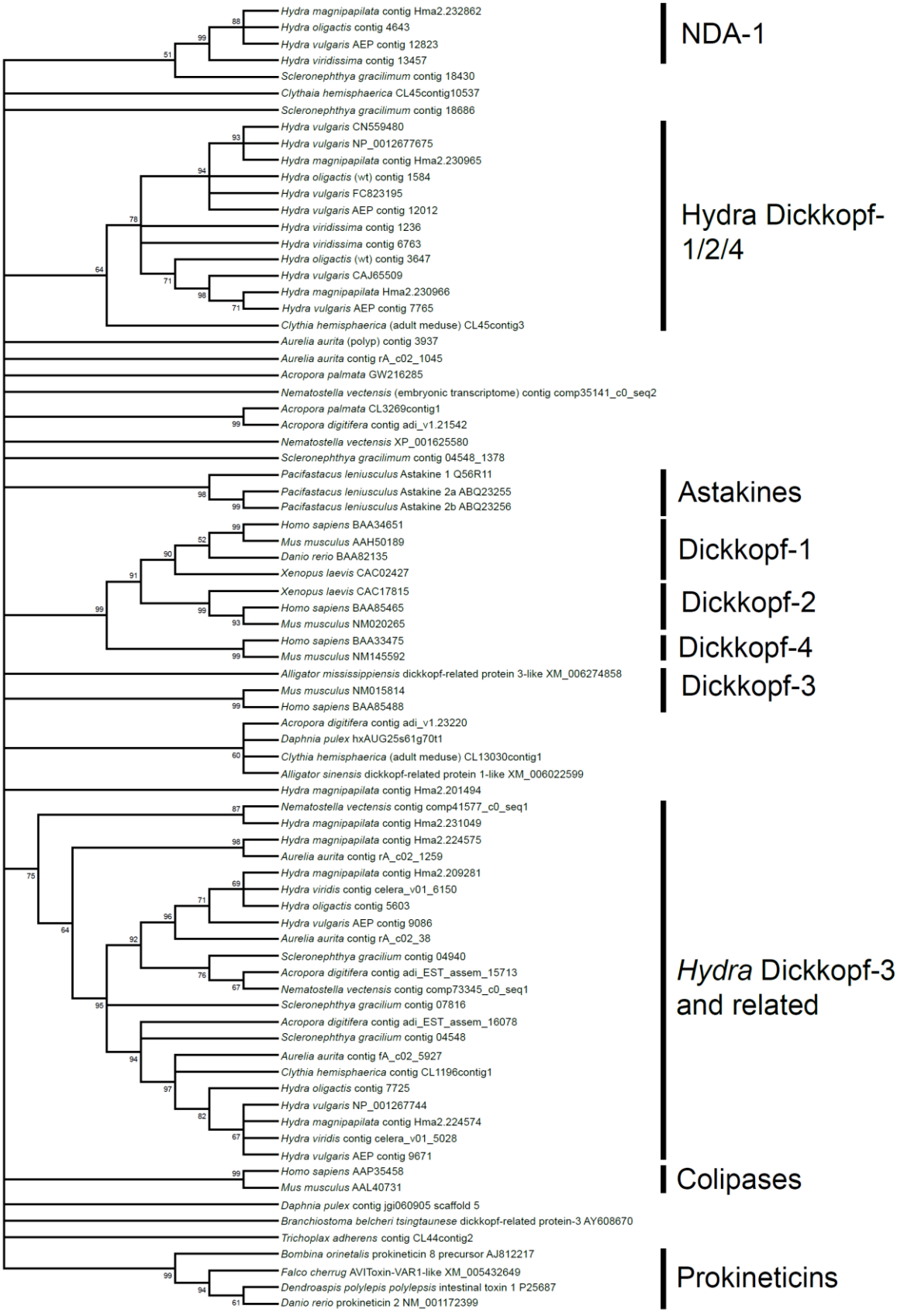

Supplementary Figure 1. Neighbour-joining phylogenetic tree of prokineticins, astakines, Dickkopf and colipase gene families showing absence of congruence between NDA-1 (at the top) and the other peptides.

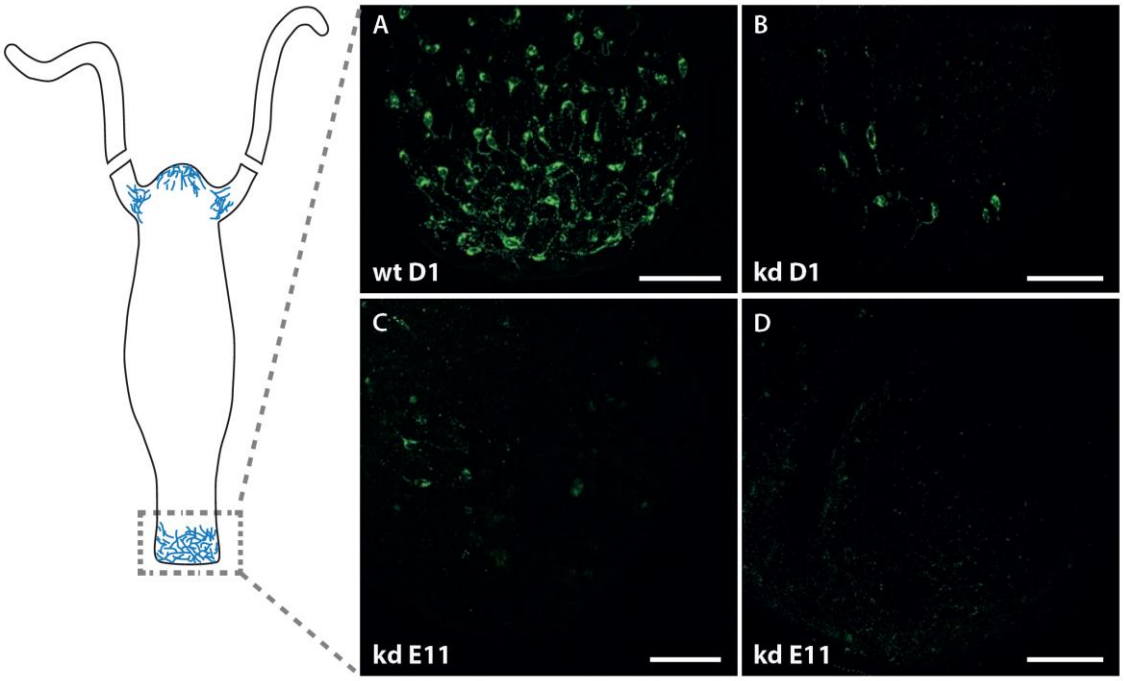

Supplementary Figure 2. Confocal laser scanning micrographs of the foot region of Hydra, stained for NDA-1 peptide by means of polyclonal antiserum. Wildtype (panel A) is compared to the transgenic knockdown lines D1 (B) and E11 (C, D), which have lower NDA-1 expression levels. Scale bars: 50 µm.

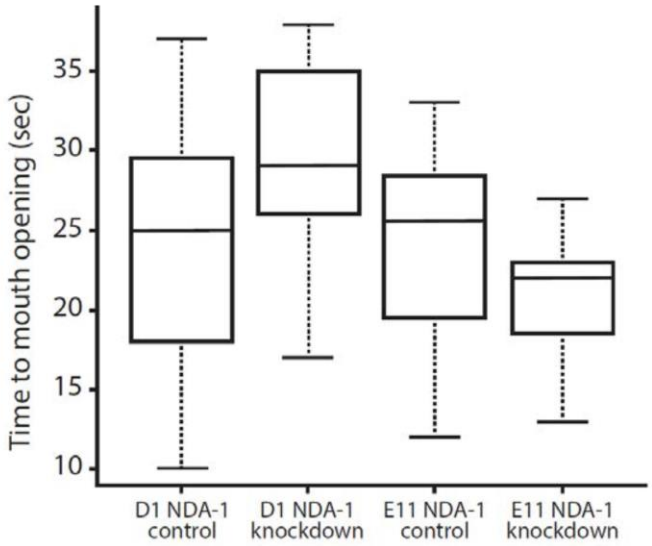

Supplementary Figure 3. Glutathione (GSH) response of NDA-1 knockdown and control polyps. The feeding response of *Hydra* can be evoked chemically using micromolar concentrations of γ-glutamil-cysteinyl-glycine (reduced glutathione, GSH), which forces the polyps to open their mouth as they do when capturing prey[1]. This GSH-induced response, like feeding behaviour, is neuron-dependent, since nerve-free animals do not open their mouth[2]. The figure shows the GSH response in 100% of NDA-1 knockdown animals after exposure to 10μM GSH. There was no statistical significant difference in time to mouth opening between NDA-1 knockdown and control animals (t-test: D1: t = -2, df = 20, p = 0.1; NDA-1 control n = 12, NDA-1 knockdown n = 13; E11: t = 1, df = 20, p = 0.2; NDA-1 control n = 12, NDA-1 knockdown n = 12). Boxes in boxplots represent the interquartile range, the line inside the box corresponds to the median, and the wiskers display the span of the data (maximun and minimum values)

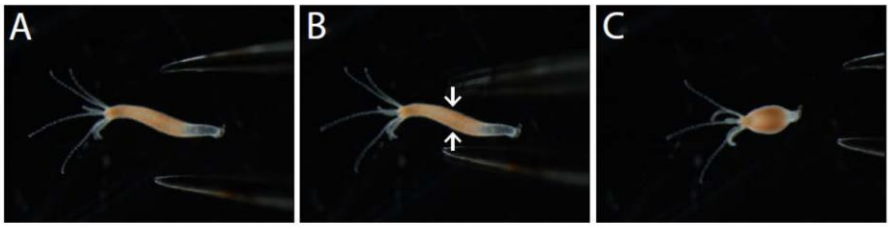

D

	D1 NDA-1 control	D1 NDA-1 knockdown	E11 NDA-1 control	E11 NDA-1 knockdown
Number of animals contracting	20 / 20	14 / 14	16 / 16	19 / 19

Supplementary Figure 4. Contractile behavior induced by mechanical stimulation.
When *Hydra* polyps are pinched with a pair of forceps, the animals response with rapid contraction of the body column[2]. Here this response to mechanical stimulation is shown. Panel A: no stimulation. Panel B: pincer stimulation as indicated by arrows. Panel C: contraction of body column. Panel D: Response of control and NDA-1 knockdown animals. There was no difference in contractile behaviour.

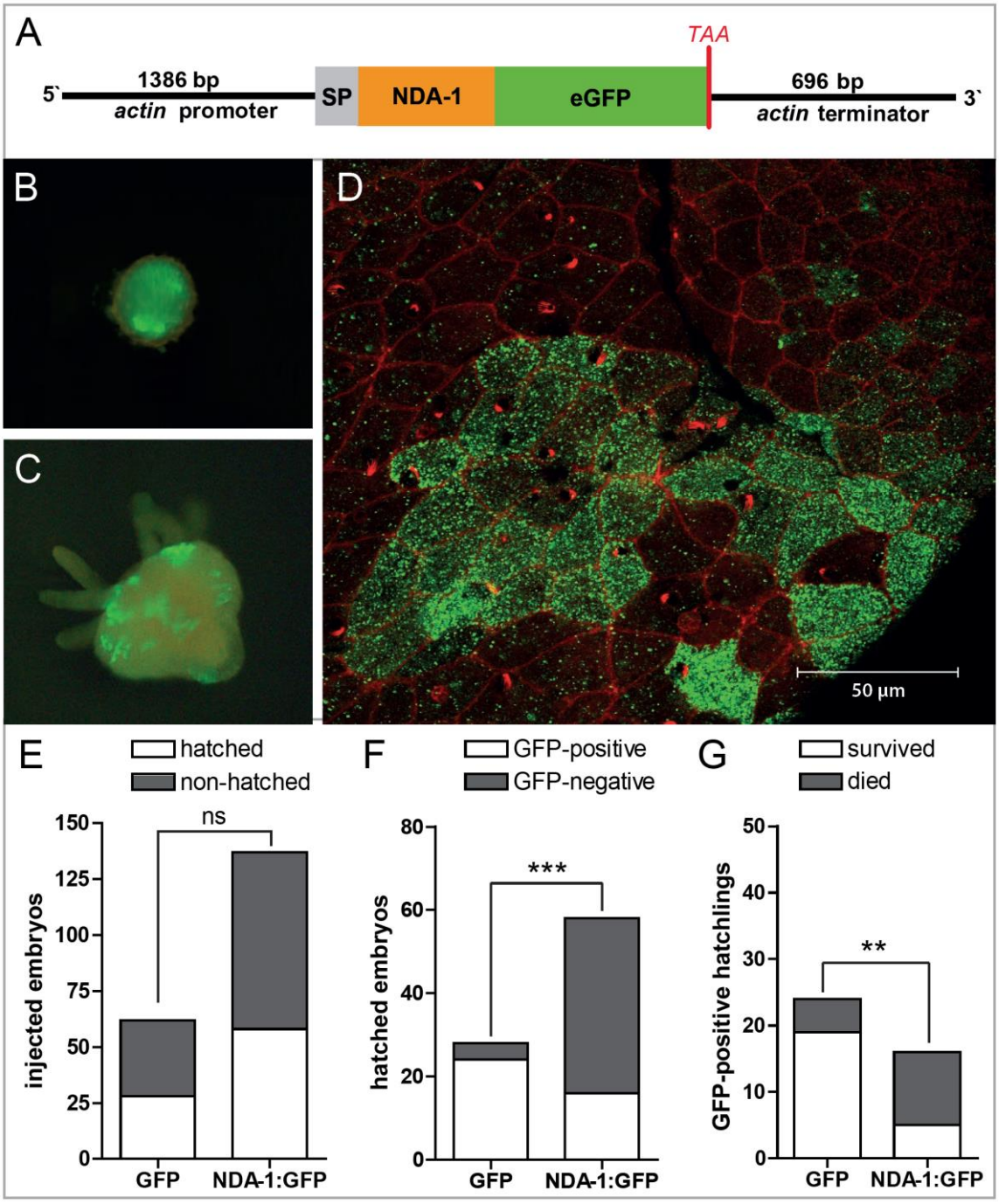

Supplementary Figure 5. Ectopic overexpression of NDA-1:eGFP.
(A) Construct used for generation of transgenic hydra overexpressing NDA-1:eGFP. **(B, C)** *In vivo* images of a transgenic *Hydra vulgaris* (AEP) embryo **(B)** and hatchling **(C)** with mosaic expression of NDA-1:eGFP. **(D)** Immunostaining detects the NDA-1:eGFP fusion protein in dense vesicles of ectodermal epithelial cells. Green, eGFP; red, rhodamin-phalloidin for F-actin. **(E)** Embryos injected with the NDA-1:eGFP construct showed no difference in hatching rate compared to embryos injected with a control construct based on the same vector lacking the NDA-1 sequence (eGFP: n=62; NDA-1:eGFP: n=137; p=0.7583, Fisher's exact test). **(F)** NDA-1:eGFP injection resulted in significantly less GFP-positive hatchlings compared to the control construct (eGFP: n=28; NDA-1:eGFP: n= 58; p<0.0001, Fisher's exact test). **(G)** Hatchlings expressing NDA-1:eGFP showed significantly reduced survival compared to hatchlings expressing eGFP only (eGFP: n= 24; NDA-1:eGFP: n=16; p=0.0036, Fisher's exact test). Notably, all surviving NDA-1:eGFP hatchlings lost their GFP-positive cells within 2-3 weeks after hatching and thus, no stable transgenic line was obtained.

Chapter III

Metabolic co-dependence drives the evolutionarily ancient *Hydra-Chlorella* symbiosis

***eLife* (2018)**: accepted 26th of May 2018

doi: 10.7554/eLife.35122

eLIFE elifesciences.org

RESEARCH ARTICLE

Metabolic co-dependence drives the evolutionarily ancient *Hydra–Chlorella* symbiosis

Mayuko Hamada[1,2†], Katja Schröder[3,4†], Jay Bathia[3,4], Ulrich Kürn[3,4], Sebastian Fraune[3,4], Mariia Khalturina[1], Konstantin Khalturin[1], Chuya Shinzato[1,5], Nori Satoh[1], Thomas CG Bosch[3,4]*

[1]Marine Genomics Unit, Okinawa Institute of Science and Technology Graduate University, Okinawa, Japan; [2]Ushimado Marine Institute, Okayama University, Okayama, Japan; [3]Interdisciplinary Research Center, Kiel Life Science, Kiel University, Kiel, Germany; [4]Zoological Institute, Kiel Life Science, Kiel University, Kiel, Germany; [5]Atmosphere and Ocean Research Institute, The University of Tokyo, Tokyo, Japan

Abstract Many multicellular organisms rely on symbiotic associations for support of metabolic activity, protection, or energy. Understanding the mechanisms involved in controlling such interactions remains a major challenge. In an unbiased approach we identified key players that control the symbiosis between *Hydra viridissima* and its photosynthetic symbiont *Chlorella* sp. A99. We discovered significant up-regulation of *Hydra* genes encoding a phosphate transporter and glutamine synthetase suggesting regulated nutrition supply between host and symbionts. Interestingly, supplementing the medium with glutamine temporarily supports in vitro growth of the otherwise obligate symbiotic *Chlorella*, indicating loss of autonomy and dependence on the host. Genome sequencing of *Chlorella* sp. A99 revealed a large number of amino acid transporters and a degenerated nitrate assimilation pathway, presumably as consequence of the adaptation to the host environment. Our observations portray ancient symbiotic interactions as a codependent partnership in which exchange of nutrients appears to be the primary driving force.
DOI: https://doi.org/10.7554/eLife.35122.001

***For correspondence:** tbosch@zoologie.uni-kiel.de

[†]These authors contributed equally to this work

Competing interests: The authors declare that no competing interests exist.

Funding: See page 27

Received: 16 January 2018
Accepted: 26 May 2018
Published: 31 May 2018

Reviewing editor: Paul G Falkowski, Rutgers University, United States

Introduction

Symbiosis has been a prevailing force throughout the evolution of life, driving the diversification of organisms and facilitating rapid adaptation of species to divergent new niches (***Moran, 2007***; ***Joy, 2013***; ***McFall-Ngai et al., 2013***). In particular, symbiosis with photosynthetic symbionts is observed in many species of cnidarians such as corals, jellyfish, sea anemones and hydra, contributing to the ecological success of these sessile or planktonic animals (***Douglas, 1994***; ***Davy et al., 2012***). Among the many animals dependent on algal symbionts, inter-species interactions between green hydra *Hydra viridissima* and endosymbiotic unicellular green algae of the genus *Chlorella* have been a subject of interest for decades (***Muscatine and Lenhoff, 1963***; ***Roffman and Lenhoff, 1969***). Such studies not only provide insights into the basic 'tool kit' necessary to establish symbiotic interactions, but are also of relevance in understanding the resulting evolutionary selective processes (***Muscatine and Lenhoff, 1965a***; ***1965b***; ***Thorington and Margulis, 1981***).

The symbionts are enclosed in the host endodermal epithelial cells within perialgal vacuoles called 'symbiosomes'. The interactions at play here are clearly metabolic: the algae depend on nutrients that are derived from the host or from the environment surrounding the host, while in return the host receives a significant amount of photosynthetically fixed carbon from the algae.

eLife digest All animals host microorganisms; some of which form 'symbiotic' relationships with their host that are mutually beneficial. For instance, the human gut shelters tens of thousands of species of bacteria that break down our food for us, and corals, jellyfish or sea anemones can extract energy directly from sunlight thanks to the algae that live inside their cells.

Hydra, a small freshwater animal, lives in a symbiotic relationship with algae called *Chlorella* that it carries inside its cells. Once an independent organism, *Chlorella* has evolved in such a way that, in nature, it cannot exist without *Hydra* anymore. In turn, the algae produce sugars to fuel the animal when it cannot get food from the environment. Yet, despite over 30 years of research, it still remains unclear how exactly the relationship between *Hydra* and *Chlorella* works, and how it came to be. Understanding how these two organisms live together could help researchers to figure out the general principles that guide symbiotic interactions.

Nitrogen is an element that is essential for life, and organisms can extract it from various sources, such as nitrates or the amino acid glutamine. Here, Hamada, Schröder et al. sequenced the entire genome of *Chlorella*. This revealed that *Chlorella* has lost someof the genes required to obtain nitrates, and to process them into nitrogen. However, the genetic analysis showed that the algae express genes that allow them to import amino acids.

In turn, analysis of the genes expressed by *Hydra* when it lives in symbiosis with *Chlorella* showed that the animal turns on genetic information needed to make glutamine. It thus seems that *Hydra* creates glutamine which *Chlorella* can import; the algae then process this amino acid to obtain the nitrogen they need. Hamada, Schröder et al. also discovered that if the environment was artificially enriched in glutamine, *Chlorella* could live on their own outside of *Hydra* for a while.

The results suggest that symbiotic relationships, such as the one between *Hydra* and *Chlorella*, were established because the organisms became dependent on each other for essential nutrients. This co-dependency is strengthened if the organisms lose the ability to produce the nutrients on their own. However, this partnership may be altered when the environment changes too much, especially if the balance of nutrients available gets tipped. For example, if seas that are normally poor in nutrients become suddenly rich in these elements, this may disrupt the existence of symbiotic organisms such as corals.

DOI: https://doi.org/10.7554/eLife.35122.002

Previous studies have provided evidence that the photosynthetic symbionts provide their host with maltose, enabling *H. viridissima* to survive periods of starvation (**Muscatine and Lenhoff, 1963**; **Muscatine, 1965**; **Roffman and Lenhoff, 1969**; **Cook and Kelty, 1982**; **Huss et al., 1994**). *Chlorella*-to-*Hydra* translocation of photosynthates is critical for polyps to grow (**Muscatine and Lenhoff, 1965b**; **Mews, 1980**; **Douglas and Smith, 1983**; **1984**). Presence of symbiotic algae also has a profound impact on hydra´s fitness by promoting oogenesis (**Habetha et al., 2003**; **Habetha and Bosch, 2005**).

Pioneering studies performed in the 1980 s (**McAuley and Smith, 1982**; **Rahat and Reich, 1984**) showed that there is a great deal of adaptation and specificity in this symbiotic relationship. All endosymbiotic algae found in a single host polyp are clonal and proliferation of symbiont and host is tightly correlated (**Bossert and Dunn, 1986**; **McAuley, 1986a**). Although it is not yet known how *Hydra* controls cell division in symbiotic *Chlorella*, *Chlorella* strain A99 is unable to grow outside its polyp host and is transmitted vertically to the next generation of *Hydra*, indicating loss of autonomy during establishment of its symbiotic relationship with this host (**Muscatine and McAuley, 1982**; **Campbell, 1990**; **Habetha et al., 2003**).

Molecular phylogenetic analyses suggest that *H. viridissima* is the most basal species in the genus *Hydra* and that symbiosis with *Chlorella* was established in the ancestral *viridissima* group after their divergence from non-symbiotic *Hydra* groups (**Martínez et al., 2010**; **Schwentner and Bosch, 2015**). A recent phylogenetic analysis of different strains of green hydra resulted in a phylogenetic tree that is topologically equivalent to that of their symbiotic algae (**Kawaida et al., 2013**), suggesting these species co-evolved as a result of their symbiotic relationship. Although our understanding of the factors that promote symbiotic relationships in cnidarians has increased (**Shinzato et al.,**

2011; *Davy et al., 2012*; *Lehnert et al., 2014*; *Baumgarten et al., 2015*; *Ishikawa et al., 2016*), very little is known about the molecular mechanisms allowing this partnership to persist over millions of years.

Recent advances in transcriptome and genome analysis allowed us to identify the metabolic interactions and genomic evolution involved in achieving the *Hydra-Chlorella* symbiotic relationship. We present here the first characterization, to our knowledge, of genetic complementarity between green *Hydra* and *Chlorella* algae that explains the emergence and/or maintenance of a stable symbiosis. We also provide here the first report of the complete genome sequence from an obligate intracellular *Chlorella* symbiont. Together, our results show that exchange of nutrients is the primary driving force for the symbiosis between *Chlorella* and *Hydra*. Subsequently, reduction of metabolic pathways may have further strengthened their codependency. Our findings provide a framework for understanding the evolution of a highly codependent symbiotic partnership in an early emerging metazoan.

Results

Discovery of symbiosis-dependent *Hydra* genes

As tool for our study we used the green hydra *H. viridissima* (*Figure 1A*) colonized with symbiotic *Chlorella* sp. strain A99 (abbreviated here as Hv_Sym), aposymbiotic *H. viridissima* from which the symbiotic *Chlorella* were removed (Hv_Apo), as well as aposymbiotic *H.viridissima,* which have been artificially infected with *Chlorella variabilis* NC64A (Hv_NC64A). The latter is symbiotic to the single-cellular protist *Paramecium* (*Karakashian and Karakashian, 1965*). Although an association between *H. viridissima* and *Chlorella* NC64A can be maintained for some time, both their growth rate (*Figure 1B*) and the number of NC64A algae per *Hydra* cell (*Figure 1—figure supplement 1*) are significantly reduced compared to the symbiosis with native symbiotic *Chlorella* A99.

H.*H. viridissima* genes involved in the symbiosis with *Chlorella* algae were identified by microarray based on the contigs of *H. viridissima* A99 transcriptome (NCBI GEO Platform ID: GPL23280). For the microarray analysis, total RNA was extracted from the polyps after light exposure for six hours. By comparing the transcriptomes of Hv_Sym and Hv_Apo, we identified 423 contigs that are up-regulated and 256 contigs that are down-regulated in presence of *Chlorella* A99 (*Figure 1C*). To exclude genes involved in oogenesis and embryogenesis, only contigs differently expressed with similar patterns in both sexual and asexual Hv_Sym were recorded. Interestingly, contigs whose predicted products had no discernible homologs in other organisms including other *Hydra* species were overrepresented in these differentially expressed contigs (Chi-squared test $p<0.001$) (*Figure 1—figure supplement 2*). Such taxonomically restricted genes (TRGs) are thought to play important roles in the development of evolutionary novelties and morphological diversity within a given taxonomic group (*Khalturin et al., 2009*; *Tautz and Domazet-Lošo, 2011*).

We further characterized functions of the differentially expressed *Hydra* genes by Gene Ontology (GO) terms (*Ashburner et al., 2000*) and found the GO term 'localization' overrepresented among up-regulated contigs (Hv_Sym > Hv_Apo), whereas the GO term 'metabolic process' was enriched among down-regulated contigs (Hv_Sym < Hv_Apo) (*Figure 1D*). More specifically, the up-regulated contigs included many genes related to 'transmembrane transporter activity', 'transmembrane transport', 'transposition', 'cilium' and 'protein binding, bridging' (*Figure 1E*). In the down-regulated contig set, the GO classes 'cellular amino acid metabolic process', 'cell wall organization or biogenesis' and 'peptidase activity' were overrepresented (*Figure 1E*). These results suggest that the *Chlorella* symbiont affects core metabolic processes and pathways in *Hydra*. Particularly, carrier proteins and active membrane transport appear to play a prominent role in the symbiosis.

As next step, we used GO terms, domain search and similarity search to further analyze the differentially expressed contigs between Hv_Sym and Hv_Apo (*Supplementary file 1*). As the genes with GO terms related to localization and transport, we identified 27 up-regulated contigs in Hv_Sym (*Table 1*). Interestingly, this gene set included a contig showing sequence similarity to the glucose transporter GLUT8 gene, which was previously reported to be up-regulated in the symbiotic state of the sea anemone *Aiptasia* (*Lehnert et al., 2014*; *Sproles et al., 2018*). Thus, a conserved mechanism may be responsible for photosynthate transport from the symbiont into the host cytoplasm across the symbiosome membrane. Further, a contig encoding a carbonic anhydrase (CA) enzyme was up-

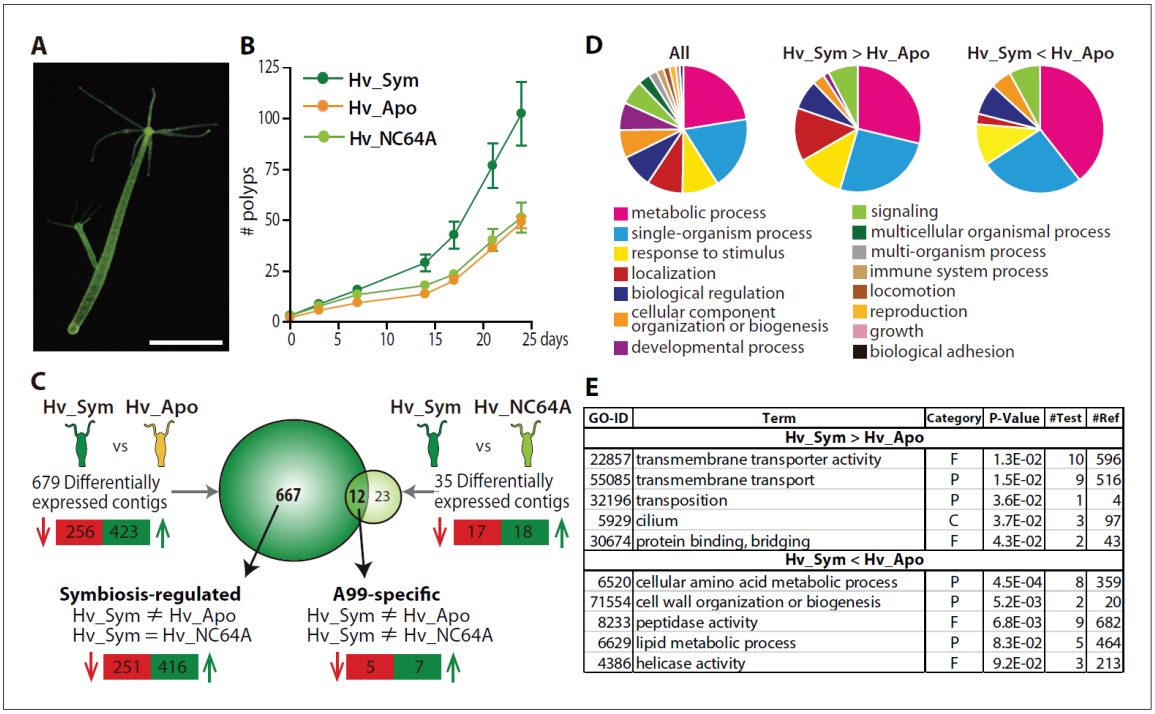

E

GO-ID	Term	Category	P-Value	#Test	#Ref
	Hv_Sym > Hv_Apo				
22857	transmembrane transporter activity	F	1.3E-02	10	596
55085	transmembrane transport	P	1.5E-02	9	516
32196	transposition	P	3.6E-02	1	4
5929	cilium	C	3.7E-02	3	97
30674	protein binding, bridging	F	4.3E-02	2	43
	Hv_Sym < Hv_Apo				
6520	cellular amino acid metabolic process	P	4.5E-04	8	359
71554	cell wall organization or biogenesis	P	5.2E-03	2	20
8233	peptidase activity	F	6.8E-03	9	682
6629	lipid metabolic process	P	8.3E-02	5	464
4386	helicase activity	F	9.2E-02	3	213

Figure 1. *Hydra* growth and differential expression of *Hydra* genes resulting from symbiosis. (**A**) *Hydra viridissima* strain A99 used for this study. Scale bar, 2 mm. (**B**) Growth rates of polyps grown with native symbiotic *Chlorella* A99 (Hv_Sym, dark green), Aposymbiotic polyps from which *Chlorella* were removed (Hv_Apo, orange) and aposymbiotic polyps reinfected with *Chlorella variabilis* NC64A (Hv_NC64A, light green). Average of the number of hydra in each experimental group (n = 6) is represented. Error bars indicate standard deviation. (**C**) Graphic representation of differentially expressed genes identified by microarray. The transcriptome of Hv_Sym is compared with that of Hv_Apo and Hv_NC64A with the number of down-regulated contigs in Hv_Sym shown in red and those up-regulated in green. Genes differentially expressed in Hv_Sym compared to both Hv_Apo and Hv_NC64A are given as 'A99-specific', those differentially expressed between Hv_A99 and Hv_Apo but not Hv_NC64A as 'Symbiosis-regulated'. (**D**) GO distribution of Biological Process at level two in all contigs (All), up-regulated contigs (Hv_Sym > Hv_Apo) and down-regulated contigs (Hv_Sym < Hv_Apo) in Hv_Sym. (**E**) Overrepresented GO terms in up-regulated contigs (Hv_Sym > Hv_Apo) and down-regulated contigs (Hv_Sym < Hv_Apo). Category, F: molecular function, C: cellular component, P: biological process. P-values, probability of Fisher's exact test. #Test, number of corresponding contigs in differentially expressed contigs. #Ref, number of corresponding contigs in all contigs.

DOI: https://doi.org/10.7554/eLife.35122.003

The following source data and figure supplements are available for figure 1:

Source data 1. GO distribution of Biological Process in all contigs (All), up-regulated contigs (up: Hv_Sym > Hv_Apo) and down-regulated contigs (down: Hv_Sym < Hv_Apo) in Hv_Sym.

DOI: https://doi.org/10.7554/eLife.35122.007

Figure supplement 1. *Chlorella* sp. A99 and *Chlorella variabilis* NC64A in *Hydra viridissima* A99.

DOI: https://doi.org/10.7554/eLife.35122.004

Figure supplement 2. Conserved genes and species-specific genes differentially expressed in symbiotic *Hydra*.

DOI: https://doi.org/10.7554/eLife.35122.005

Figure supplement 3. Glutamine synthetase (GS) genes in Cnidarians.

DOI: https://doi.org/10.7554/eLife.35122.006

regulated in Hv_Sym (***Table 1***). CA catalyzes the interconversion of HCO_3 and CO_2. Similar to the GLUT8 gene, carbonic anhydrase also appears to be up-regulated in symbiotic corals and anemones (***Weis et al., 1989***; ***Grasso et al., 2008***; ***Ganot et al., 2011***; ***Lehnert et al., 2014***). It appears plausible that for efficient photosynthesis in symbiotic algae, the host may need to convert CO_2 to the less freely diffusing inorganic carbon (HCO_3) to maintain it in the symbiosome (***Lucas and Berry, 1985***; ***Weis et al., 1989***; ***Barott et al., 2015***). We also observed up-regulation of contigs encoding

Table 1. List of differentially expressed genes between Hv_Sym and Hv_Apo, which are likely to be involved in symbiotic relationship

	Fold change				
Probename	**Hv_Sym /Hv_Apo**	**Hv_Sym_sexy /Hv_Apo**	**Hv_NC64A /Hv_Sym**	**Human_BestHit**	**blast2GO_Description**
Localization and Transport					
Hv_Sym > Hv_Apo					
rc_6788	9.87	8.00	1.01		helicase conserved c-terminal domain containing protein
rc_10246	8.26	5.15	1.82		protein
rc_6298	7.10	4.73	0.99	hypothetical protein LOC220081	protein fam194b
2268	6.96	3.58	1.26	protein Daple	viral a-type inclusion protein
10548	6.74	6.89	0.73	transient receptor potential cation channel subfamily M member three isoform d	transient receptor potential cation channel subfamily m member 3-like
rc_1290	6.44	7.18	0.99	tetratricopeptide repeat protein eight isoform B	tetratricopeptide repeat protein 8
18736	6.04	6.34	1.03	BTB/POZ domain-containing protein KCTD9	btb poz domain-containing protein kctd9-like; unnamed protein product
rc_9270	5.96	10.03	1.37	PREDICTED: hypothetical protein LOC100131693	eukaryotic translation initiation factor 4e
NPNHRC_15697	3.85	2.74	0.62		major facilitator superfamily domain-containing protein 1
290	3.68	3.73	1.32	splicing factor, arginine/ serine-rich 6	splicing arginine serine-rich 4
rc_9596	3.56	4.19	1.62	BTB/POZ domain-containing protein KCTD10	btb poz domain-containing adapter for cul3-mediated degradation protein 3
rc_6774	3.34	3.32	1.31	solute carrier family 43, member 2	large neutral amino acids transporter small subunit 4
rc_26218	3.29	2.91	0.41	sodium-dependent phosphate transport protein 2A isoform 1	sodium-dependent phosphate transport protein 2b
NPNHRC_26094	3.20	3.98	1.31	SPE-39 proteinid="T5"	spe-39 protein
9096	3.10	2.20	0.69	otoferlin isoform d	otoferlin
rc_21349	2.89	4.25	0.78	5′-AMP-activated protein kinase catalytic subunit alpha-2	5 -amp-activated protein kinase catalytic subunit alpha-2
npRC_14488	2.88	2.65	0.71	solute carrier family 2, facilitated glucose transporter member 8	solute carrier family facilitated glucose transporter member 8-like
8863	2.75	2.70	0.81	ATP-binding cassette, sub-family B, member 10 precursor	abc transporter b family protein
rc_11896	2.49	2.56	1.52	ATP-binding cassette, sub-family B, member 10 precursor	abc transporter b family member 25-like
rc_6842	2.41	3.35	1.59	hypothetical protein LOC112752 isoform 2	intraflagellar transport protein 43 homolog
5242	2.36	3.35	1.22	growth arrest-specific protein 8	growth arrest-specific protein 8
5815	2.23	2.47	0.78	plasma membrane calcium-transporting ATPase 4 isoform 4a	plasma membrane calcium atpase
8765	2.22	3.25	0.91	growth arrest-specific protein 8	growth arrest-specific protein 8
NPNH_14052	2.19	2.17	0.79	V-type proton ATPase 21 kDa proteolipid subunit isoform 2	v-type proton atpase 21 kda proteolipid subunit-like
rc_2499	2.18	2.03	1.47	endoplasmic reticulum-Golgi intermediate compartment protein three isoform a	endoplasmic reticulum-golgi intermediate compartment protein 3 isoform 2
rc_13969	2.08	3.09	0.97		major facilitator superfamily
(IPR023561) Carbonic anhydrase, alpha-class					

Table 1 continued on next page

Table 1 continued

Probename	Fold change Hv_Sym /Hv_Apo	Hv_Sym_sexy /Hv_Apo	Hv_NC64A /Hv_Sym	Human_BestHit	blast2GO_Description
rc_24825	2.49	2.38	0.83	protein tyrosine phosphatase, receptor type, G precursor	receptor-type tyrosine-protein phosphatase gamma
Cell Adhesion and extracelluar matrix					
Hv_Sym > Hv_Apo					
7915	4.01	5.09	0.94	fibrillin-2 precursor	fibrillin-1- partial
npRC_24163	glutamate3.69	3.59	1.32	semaphorin 5A precursor	rhamnospondin 1
Immunity, apoptosis and recognition					
Hv_Sym > Hv_Apo					
(IPR000157) Toll/interleukin-1 receptor homology (TIR) domain					
5168	9.28	4.92	0.61		protein; PREDICTED: uncharacterized protein LOC100893943
12749	5.13	3.35	1.26		PREDICTED: uncharacterized protein LOC100893943 [Strongylocentrotus purpuratus]
(IPR011029) DEATH-like					
6508	6.70	5.10	0.64		PREDICTED: hypothetical protein [Hydra magnipapillata]
rc_2417	5.39	2.70	1.01		nod3 partial; PREDICTED: uncharacterized protein LOC100206003
(IPR002398) Peptidase C14, caspase precursor p45					
NPNH_21275	2.36	3.53	1.18	caspase seven isoform alpha precursor	caspase d
(IPR016187) C-type lectin fold					
11411	2.93	2.98	0.75	C-type mannose receptor 2	PREDICTED: similar to predicted protein, partial [Hydra magnipapillata]
Hv_Sym < Hv_Apo					
(IPR000488) Death					
7319	0.45	0.31	1.10	probable ubiquitin carboxyl-terminal hydrolase CYLD isoform 2	ubiquitin carboxyl-terminal hydrolase cyld
(IPR001875) Death effector domain					
RC_FV81RT001CSTY	0.31	0.39	0.93	astrocytic phosphoprotein PEA-15	fadd
Chitinase					
Hv_Sym > Hv_Apo					
(IPR001223) Glycoside hydrolase, family 18, catalytic domain					
rc_4450	2.78	3.83	0.66		chitinase 2
Hv_Sym < Hv_Apo					
(IPR000726) Glycoside hydrolase, family 19, catalytic					
FPVQZVL01EAWBY	0.21	0.16	1.78		endochitinase 1-like
1028	0.23	0.18	1.47		endochitinase 1-like
Oxidative Stress Response					
Hv_Sym > Hv_Apo					
np_1276	5.99	7.16	0.78	glutaredoxin-2, mitochondrial isoform 2	cpyc type
10926	3.9	2.3	0.8	hydroxysteroid dehydrogenase-like protein 2	hydroxysteroid dehydrogenase-like protein 2

Table 1 continued on next page

Table 1 continued

Probename	Fold change Hv_Sym /Hv_Apo	Hv_Sym_sexy /Hv_Apo	Hv_NC64A /Hv_Sym	Human_BestHit	blast2GO_Description
469	2.97	3.53	0.76	cytochrome P450 3A7	cytochrome p450
FV81RT001DCTAQ	2.69	2.50	0.75	oxidoreductase NAD-binding domain-containing protein one precursor	oxidoreductase nad-binding domain-containing protein 1
696	2.30	3.24	0.69	methionine-R-sulfoxide reductase B1	selenoprotein 1; methionine-r-sulfoxide reductase b1-a-like
6572	2.23	2.15	1.06	L-xylulose reductase	l-xylulose reductase
13298	2.10	3.49	0.64	eosinophil peroxidase preproprotein	peroxidase
npRC_6975	2.04	2.77	1.42	methionine-R-sulfoxide reductase B1	selenoprotein 1; methionine-r-sulfoxide reductase b1-a-like
(IPR024079) Metallopeptidase, catalytic domain					
Hv_array_4952	4.77	13.31	0.72	meprin A subunit beta precursor	zinc metalloproteinase nas-4-like
Hv_array_rc_3992	2.66	2.23	1.27	matrix metalloproteinase seven preproprotein	matrix metalloproteinase-24-like
Hv_Sym < Hv_Apo					
RC_FWZAEML02HKSC	0.255	0.153	1.444		ascorbate peroxidase
np_14962	0.293	0.455	1.390	tryptophan 5-hydroxylase 2	phenylalanine hydroxylase
rc_4151	0.318	0.463	1.693	phenylalanine-4-hydroxylase	phenylalanine hydroxylase
2835	0.384	0.344	1.787		u1 small nuclear ribonucleoprotein 70 kda
rc_11426	0.413	0.458	1.591	short-chain dehydrogenase/ reductase family 9C member 7	uncharacterized oxidoreductase -like
FWZAEML02IC34R	0.427	0.448	1.159	aldehyde dehydrogenase 5A1 isoform two precursor	succinate-semialdehyde mitochondrial-like
FWZAEML02HKSCO	0.454	0.307	0.833		ascorbate peroxidase
(IPR004045) Glutathione S-transferase, N-terminal					
RC_FWZAEML02GGHN	0.09	0.07	1.81	hematopoietic prostaglandin D synthase	glutathione s-transferase family member (gst-7)
(IPR024079) Metallopeptidase, catalytic domain					
rc_11270	0.14	0.20	1.33	meprin A subunit beta precursor	protein; zinc metalloproteinase nas-4-like
rc_RSASM_15059	0.22	0.29	1.42		—NA—
2111	0.37	0.43	1.74	meprin A subunit beta precursor	zinc metalloproteinase nas-4-like
12451	0.50	0.39	0.78	meprin A subunit alpha precursor	zinc metalloproteinase nas-13- partial
(IPR013122) Polycystin cation channel, PKD1/PKD2					
28854	0.37	0.28	0.94	polycystin-2	receptor for egg jelly partial
15774	0.40	0.26	0.76	polycystic kidney disease protein 1-like two isoform a	protein

DOI: https://doi.org/10.7554/eLife.35122.008

proteins involved in vesicular and endosomal trafficking, such as spe-39 protein, otoferlin, protein fam194b and V-type proton ATPase 21 kda proteolipid, which may have a function in nutrition exchange between host and symbiont and maintenance of proper condition in the symbiosome. Upregulated genes also include genes encoding rhamnospondin and fibrillin, known to be involved in cell adhesion and extracellular matrix, and retention of the symbiont at the proper site in the *Hydra* cells.

Photosynthesis by symbiotic algae imposes Reactive Oxygen Species (ROS) that can damage lipids, proteins and DNA in the host cells (**Lesser, 2006**). Therefore, in symbiosis with photosynthetic organisms an appropriate oxidative stress response of the host is required for tolerance of the symbiont. Indeed, an increase of antioxidant activities in symbiotic states of cnidarians has been reported previously (**Richier et al., 2005**) and it has been suggested that ROS produced by stress could be the major trigger of symbiosis breakdown during coral bleaching (**Lesser, 2006**; **Weis, 2008**). To understand the oxidative stress response in green hydra, we searched the differentially expressed genes with the GO terms 'response to oxidative stress', 'oxidation-reduction process' and 'oxidoreductase activity'. In Hv_Sym, contigs for peroxidase, methionine-r-sulfoxide reductase/selenoprotein and glutaredoxin, which are known to be related to oxidative stress response were up-regulated (**Table 1**). On the other hand, some contigs encoding glutathione S-transferase and ascorbate peroxidase were down-regulated in Hv_Sym. In addition, two contigs encoding polycystin were down-regulated in Hv_Sym. Polycystin is an intracellular calcium release channel that is inhibited by ROS (**Montalbetti et al., 2008**) and is also down-regulated in a different strain of symbiotic green hydra (**Ishikawa et al., 2016**). In addition, six contigs encoding metalloproteinases showed differential expression between Hv_Sym and Hv_Apo. Although metalloproteinases have many functions such as cleavage of cell surface proteins and remodeling of the extracellular matrix, in a previous study they also were found to play a role in the oxidative stress response (**Császár et al., 2009**). A key antioxidant in the oxidative stress response in symbiotic cnidarians turns out to be glutathione (**Sunagawa et al., 2009**; **Meyer and Weis, 2012**). The gene encoding glutathione S-transferase was previously observed to be downregulated in corals, sea anemones, different strains of green hydra and *Paramecium* (**Kodama et al., 2014**; **Lehnert et al., 2014**; **Ishikawa et al., 2016**; **Mohamed et al., 2016**). Our study supports this view (**Table 1**) and may point to a conserved feature of oxidative stress response in algal-animal symbiosis.

Previous studies have suggested that during establishment of coral–algal symbiosis the host immune response may be partially suppressed (Weis et al., 2008; **Mohamed et al., 2016**). Our observations in *Hydra* together with previous findings in corals indicate that regulation of symbiosis by innate immunity pathways indeed may be a general feature of cnidarian symbiosis. Among the differentially expressed contigs we identified a number of genes involved in innate immunity and apoptosis. Pattern recognition receptors (PRRs) and the downstream innate immunity and apoptosis pathways are thought to play important roles in various symbiotic interactions including cnidarian-dinoflagellate symbiosis (**Davy et al., 2012**). In Hv_Sym we found two up-regulated contigs that contain a Toll/interleukin-1 receptor (TIR) domain (**Table 1**). TIR is a known PRR that is inserted in the host cell membrane and plays an important role in the innate immune system by specifically recognizing microbial-associated molecular patterns, such as flagellin, lipopolysaccharide (LPS) and peptidoglycan (**Hoving et al., 2014**). Furthermore, we found one up-regulated contig with similarity to a mannose receptor gene with C-type lectin domain (**Table 1**). This is worth noting since C-type lectin receptors bind carbohydrates and some of them are known to function as PRRs. Host lectin-algal glycan interactions have been proposed to be involved in infection and recognition of symbionts in some cnidarians including green hydra, sea anemones and corals (**Meints and Pardy, 1980**; **Lin et al., 2000**; **Wood-Charlson et al., 2006**). Interestingly, up-regulation of C-type lectin genes was also observed during onset of cnidarian–dinoflagellate symbiosis (**Grasso et al., 2008**; **Schwarz et al., 2008**; **Sunagawa et al., 2009**; **Mohamed et al., 2016**).

Furthermore, contigs encoding chitinase enzymes also were differentially expressed between Hv_Sym and Hv_Apo (**Table 1**). Chitinases are involved in degradation of chitin, which is a component of the exoskeleton of arthropods and the cell wall of fungi, bacteria and some *Chlorella* algae (**Kapaun and Reisser, 1995**), and also might play a role in host-defense systems for pathogens which have chitinous cell wall. Chitinases are classified into two glycoside hydrolase families, GH18 and GH19, with different structures and catalytic mechanisms. In Hv_Sym two contigs encoding GH18 chitinases were up-regulated, while one contig encoding a GH19 chitinase was down-regulated, suggesting that the enzymes involved in chitin degradation are sensitive to the presence or absence of symbiotic *Chlorella*.

To narrow down the number of genes specifically affected by the presence of the native symbiont *Chlorella* A99, we identified 12 contigs that are differentially expressed in symbiosis with *Chlorella* A99, but not in presence of foreign *Chlorella* NC64A (**Figure 1C** A99-specific). Independent qPCR confirmed the differential expression pattern for 10 of these genes (**Table 2**). The genes up-

Table 2. List of genes differentially expressed in Hv_Sym compared to both Hv_Apo and Hv_NC64A ('A99-specific')
Fold change of expression level determined by microarray analysis and qPCR analysis

Hv_Sym > Hv_Apo, Hv_NC64A

	Microarray		qPCR			
Probe name (gene ID)	**Sym/Apo**	**Sym/NC64A**	**Sym/Apo**	**Sym/NC64A**	**Gene annotation**	**InterProScan**
rc_13579	12.8	4.0	11.2	4.0	(Hydra specific)	
rc_12891	9.0	2.9	14.6	6.9	(Hydra viridis specific)	
27417	4.5	4.8	3.0	3.0		IPR009786 Spot_14
rc_26218	3.3	2.4	2.5	2.3	sodium-dependent phosphate transport protein	PTHR10010 Sodium-dependent phosphate transport protein 2C
1046	3.1	2.1	2.2	1.6	glutamine synthetase	

Hv_Sym < Hv_Apo, Hv_NC64A

Probe name (gene ID)	Microarray		qPCR		Gene Annotation	InterProScan
	Apo/Sym	NC64A/Sym	Apo/Sym	NC64A/Sym		
NPNHRC_26859	83.2	9.7	∞	∞	(Hydra viridis specific)	
RC_FVQRUGK01AXSJ	13.7	2.6	2.1	1.5	acetoacetyl-CoA synthetase	
rc_14793	7.2	4.1	9.4	4.8	2-isopropylmalate synthase	IPR013785 Aldolase_TIM,
FV81RT002HT2FL	2.8	2.0	3.1	1.8	histidine ammonia-lyase	IPR001106 Aromatic_Lyase IPR008948 L-Aspartase-like
NPNHRC_12201	2.7glutamate	2.3	2.6	2.5	(Hydra viridis specific)	

DOI: https://doi.org/10.7554/eLife.35122.009

The following source data available for Table 2:

Source data 1. Expression level of 'A99-specific' genes and 'Symbiosis related' genes examined by microarray and qPCR.

DOI: https://doi.org/10.7554/eLife.35122.010

regulated by the presence of the symbiont encode a Spot_14 protein, a glutamine synthetase (GS) and a sodium-dependent phosphate (Na/Pi) transport protein in addition to a *H. viridissima* specific gene (rc_12891: *Sym-1*) and a *Hydra* genus specific gene (rc_13570: *Sym-2*) (***Table 2***). *Hydra* genes down-regulated by the presence of *Chlorella* A99 were two *H. viridissima*-specific genes and three metabolic genes encoding histidine ammonia-lyase, acetoacetyl-CoA synthetase and 2-isopropylmalate synthase (***Table 2***). Of the up-regulated genes, Spot_14 is described as thyroid hormone-responsive spot 14 protein reported to be induced by dietary carbohydrates and glucose in mammals (***Tao and Towle, 1986***; ***Brown et al., 1997***). Na/Pi transport protein is a membrane transporter actively transporting phosphate into cells (***Murer and Biber, 1996***). GS plays an essential role in the metabolism of nitrogen by catalyzing the reaction between glutamate and ammonia to form glutamine (***Liaw et al., 1995***). Interestingly, out of the three GS genes *H. viridissima* contains only *GS-1* was found to be up-regulated by the presence of the symbiont (***Figure 1—figure supplement 3***). The discovery of these transcriptional responses points to an intimate metabolic exchange between the partners in a species-specific manner.

To better understand the specificity of *Hydra*´s response to the presence of the foreign symbiont, we also identified the genes differentially expressed in *Hydra* polyps hosting a non-native *Chlorella* NC64A (Hv_NC64A) compared to both polyps hosting the obligate symbiont *Chlorella* A99 (Hv_A99) and aposymbiotic Hydra (Hv_Apo). We found 19 contigs that were up-regulated and 45 contigs that were down-regulated in presence of NC64A, which strikingly did not include any genes related to immunity or oxidative stress response (***Supplementary file 1***). Instead, the differentially expressed contigs showed similarity to methylase genes involved in ubiquinone menaquinone biosynthesis and secondary metabolite synthesis such as n-(5-amino-5-carboxypentanoyl)-l-cysteinyl-d-valine synthase and non-ribosomal peptide synthase. Four differentially expressed contigs specifically up-regulated in Hv_NC64A encoded ubiquitin carboxyl-terminal hydrolases, (***Table 3***).

Table 3. List of annotated genes up-regulated in Hv_NC64A compared to Hv_Sym

Probename	Hv_NC64A/ Hv_Sym	Hv_Apo/ Hv_Sym	Hv_Sym_sexy/ Hv_Sym	Blast2GO description
rc_1623	4.57	1.64	5.98	methylase involved in ubiquinone menaquinone biosynthesis
28947	3.52	1.59	0.63	non-ribosomal peptide synthetase
1353	3.13	1.63	0.10	nuclear protein set
14347	2.69	2.40	0.54	n-(5-amino-5-carboxypentanoyl)-l -cysteinyl-d-valine synthase
SSH_397	2.67	2.39	0.50	n-(5-amino-5-carboxypentanoyl)-l -cysteinyl-d-valine synthase
RC_FWZAEML01C7BP	2.28	0.82	0.41	ubiquitin carboxyl-terminal hydrolase family protein
RC_FVQRUGK01EOXS	2.25	1.52	0.53	ubiquitin carboxyl-terminal hydrolase family protein
rc_11710	2.15	1.26	0.31	ubiquitin carboxyl-terminal hydrolase family protein
1677	2.10	1.19	0.38	ubiquitin carboxyl-terminal hydrolase family protein
rc_363	2.21	1.04	0.76	gcc2 and gcc3 family protein

DOI: https://doi.org/10.7554/eLife.35122.011

Symbiont-dependent *Hydra* genes are up-regulated by photosynthetic activity of *Chlorella A99*

To test whether photosynthetic activity of the symbiont is required for up-regulation of gene expression, Hv_Sym was either cultured under a standard 12 hr light/dark alternating regime or continuously in the dark for 1 to 4 days prior to RNA extraction (***Figure 2A***). Interestingly, four (*GS1*, *Spot14*, *Na/Pi* and *Sym-1*) of five genes specifically activated by the presence of *Chlorella* A99 showed significant up-regulation when exposed to light (***Figure 2B***), indicating the relevance of photosynthetic activity of *Chlorella*. This up-regulation was strictly dependent on presence of the algae, as in aposymbiotic Hv_Apo the response was absent (***Figure 2B***). On the other hand, symbiosis-regulated *Hydra* genes not specific for *Chlorella* A99 (***Figure 1C*** Symbiosis-regulated, ***Table 4***) appear to be not up-regulated in a light-dependent manner (***Figure 2—figure supplement 1***). These genes are involved in *Hydra´s* innate immune system (e.g. proteins containing Toll/interleukin-1 receptor domain or Death domain) or in signal transduction (C-type mannose receptor, ephrin receptor, proline-rich transmembrane protein 1, 'protein-kinase, interferon-inducible double stranded RNA dependent inhibitor, repressor of (p58 repressor)'). That particular transcriptional changes observed in *Hydra* rely solely on the photosynthetic activity of *Chlorella* A99 was confirmed by substituting the dark incubation with selective chemical photosynthesis inhibitor DCMU (Dichorophenyl-dimethylurea) (***Vandermeulen et al., 1972***), which resulted in a similar effect (***Figure 2C,D***).

Symbiont-dependent *Hydra* genes are expressed in endodermal epithelial cells and up-regulated by sugars

To further characterize the symbiont induced *Hydra* genes, we performed whole mount in situ hybridization (***Figure 3A–F***) and quantified transcripts by qPCR using templates from isolated endoderm and ectoderm (***Figure 3—figure supplement 1***), again comparing symbiotic and aposymbiotic polyps (***Figure 3G–I***). The GS-1 gene and the Spot14 gene are expressed both in ectoderm and in endoderm (***Figure 3A,B***) and both genes are strongly up-regulated in the presence of the symbiont (***Figure 3G,H***). In contrast, the Na/Pi gene was expressed only in the endoderm (***Figure 3C***) and there it was strongly up-regulated by the symbiont (***Figure 3I***). Since *Chlorella* sp. A99 colonizes endodermal epithelial cells only, the impact of algae on symbiosis-dependent genes in both the ectodermal and the endodermal layer indicates that photosynthetic products can be transported across these two tissue layers or some signals can be transduced by cell-cell communication.

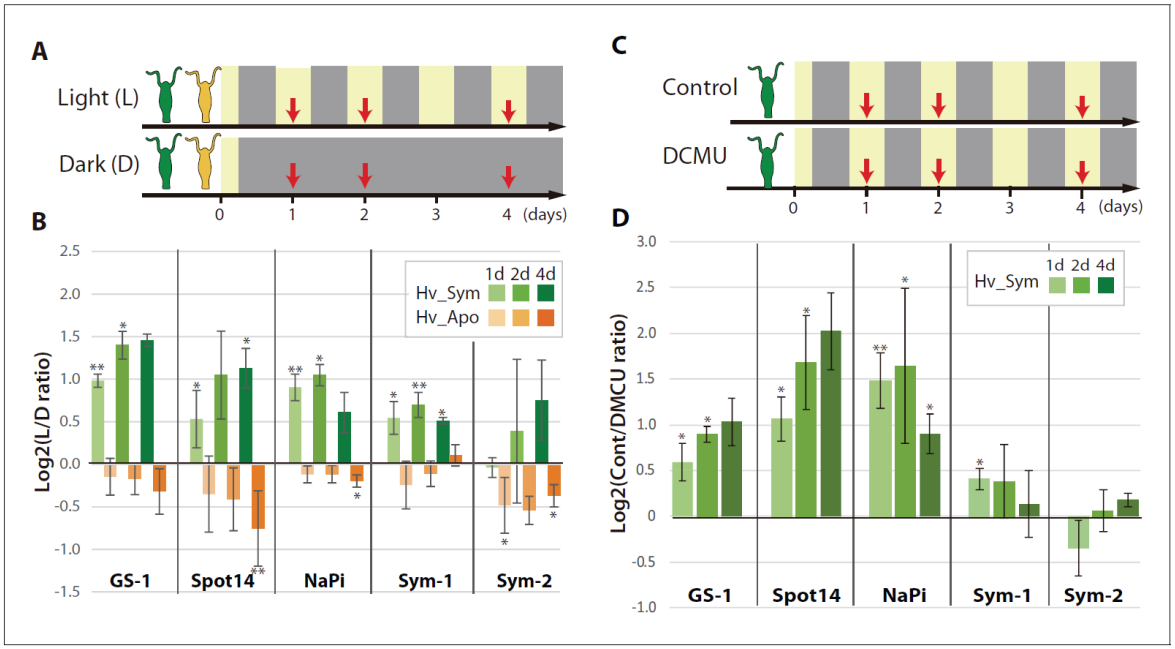

Figure 2. Differential expression of *Hydra* genes under influence of *Chlorella* photosynthesis. (**A**) Sampling scheme. Hv_Sym (green) and Hv_Apo (orange) were cultured under a standard light-dark regime (Light: L) and in continuous darkness (Dark: D), and RNA was extracted from the polyps at the days indicated by red arrows. (**B**) Expression difference of five A99-specific genes in Hv_Sym (green bars) and Hv_Apo (orange bars) between the light-dark condition and darkness. The vertical axis shows log scale (log2) fold changes of relative expression level in Light over Dark. (**C**) Sampling scheme of inhibiting photosynthesis. (**D**) Differential expression of the five A99-specific genes under conditions allowing (Control) or inhibiting photosynthesis (DCMU). The vertical axis shows log scale (log2) fold changes of relative expression level in Control over DCMU treated. T-tests were performed between Light and Dark (**B**), and DCMU and Control (**D**). For each biological replicate (n = 3) 50 hydra polyps were used for total RNA extraction. Error bars indicate standard deviation. P-value of t-test, *<0.05, **<0.01.

DOI: https://doi.org/10.7554/eLife.35122.012

The following source data and figure supplements are available for figure 2:

Figure supplement 1. Differential expression of symbiosis-dependent *Hydra* genes grown under light/dark condition and in darkness.

DOI: https://doi.org/10.7554/eLife.35122.013

Figure supplement 1—source data 1. *Hydra* genes under influence of *Chlorella* photosynthesis examined by qPCR.

DOI: https://doi.org/10.7554/eLife.35122.014

To more closely dissect the nature of the functional interaction between *Hydra* and *Chlorella* and to explore the possibility that maltose released from the algae is involved in A99-specific gene regulation, we cultured aposymbiotic polyps (Hv_Apo) for 2 days in medium containing various concentrations of maltose (***Figure 3J***). Of the five A99 specific genes, GS-1 and the Spot14 gene were up-regulated by maltose in a dose-dependent manner; the Na/Pi gene was only up-regulated in 100 mM maltose and the *Hydra* specific genes Sym-1 and Sym-2 did not show significant changes in expression by exposure to maltose (***Figure 3J***). This provides strong support for previous views that maltose excretion by symbiotic algae contributes to the stabilization of this symbiotic association (***Cernichiari et al., 1969***). When polyps were exposed to glucose instead of maltose, the genes of interest were also transcriptionally activated in a dose-dependent manner, while sucrose had no effect (***Figure 3—figure supplement 2A–D***). Exposure to low concentrations of galactose increased transcriptional activity but at high concentration it did not, indicating a substrate inhibitor effect for this sugar. That the response to glucose is similar or even higher compared to maltose after 6 hr of treatment (***Figure 3—figure supplement 2E***), suggests that *Hydra* cells transform maltose to glucose as a source of energy. In animals including cnidarians, several glucose transporters have been

Table 4. List of the genes differentially expressed between Hv_Sym and Hv_Apo
Fold change of expression level determined by microarray analysis and qPCR

Hv_Sym > Hv_Apo

Probe name (gene ID)	Microarray Sym/Apo	qPCR Sym/Apo	Gene annotation	InterProScan
5168	9.3	7.4		IPR000157 TIR_dom PTHR23097 Tumor necrosis factor receptor superfamily member
6508	6.7	2.9		IPR011029:DEATH-like_dom
11411	2.9	2.0	C-type mannose receptor 2	IPR000742 EG-like_dom IPR001304 C-type_lectin
26108	7.2	7.2	ephrin type-A receptor six isoform a	
rc_2417	5.4	3.5		IPR000488 Death_domain
rc_24563	6.1	6.7	Proline-rich transmembrane protein 1	IPR007593 CD225/Dispanin_fam PTHR14948 NG5
rc_9398	6.2	5.4	protein-kinase, interferon-inducible double stranded RNA dependent inhibitor, repressor of (P58 repressor)	PTHR11697 general transcription factor 2-related zinc finger protein

Hv_Sym < Hv_Apo

Probe name (gene ID)	Microarray Apo/Sym	qPCR Apo/Sym	Gene Annotation	InterProScan
rc_10789	2.5	3.7	endoribonuclease Dicer	IPR000999 RNase_III_dom PTHR1495 helicase-related
rc_12826	3.0	2.3	interferon regulatory factor 1	IPR001346 Interferon_reg_fact_DNA-bd_dom; IPR011991 WHTH_DNA-bd_dom PTHR11949 interferon regulatory factor
rc_8898	6.1	4.1	leucine-rich repeat-containing protein 15 isoform b	IPR001611 Leu-rich_rp PTHR24373 Toll-like receptor 9
FV81RT001CSTY	3.2	2.0	astrocytic phosphoprotein PEA-15	IPR001875 DED, IPR011029 DEATH-like_dom
RSASM_17752	4.0	2.1	CD97 antigen isoform two precursor	IPR000832 GPCR_2_secretin-like PTHR12011 vasoactive intestinal polypeptide receptor 2

DOI: https://doi.org/10.7554/eLife.35122.015

The following source data available for Table 4:

Source data 1. Expression level of 'Symbiosis related' genes examined by microarray and qPCR.

DOI: https://doi.org/10.7554/eLife.35122.016

identified (***Sproles et al., 2018***), but yet no maltose transporters. This is consistent with the view that maltose produced by the symbiont is digested to glucose in the symbiosome and translocated to the host cytoplasm through glucose transporters.

The *Chlorella* A99 genome records a symbiotic life style

To better understand the symbiosis between *H. viridissima* and *Chlorella* and to refine our knowledge of the functions that are required in this symbiosis, we sequenced the genome of *Chlorella* sp. strain A99 and compared it to the genomes of other green algae. The genome of *Chlorella* sp. A99 was sequenced to approximately 211-fold coverage, enabling the generation of an assembly comprising a total of 40.9 Mbp (82 scaffolds, N50 = 1.7 Mbp) (***Table 5***). *Chlorella* sp. A99 belongs to the family *Chlorellaceae* (***Figure 4A***) and of the green algae whose genomes have been sequenced it is most closely related to *Chlorella variabilis* NC64A (NC64A) (***Merchant et al., 2007***; ***Palenik et al., 2007***; ***Worden et al., 2009***; ***Blanc et al., 2010***; ***Prochnik et al., 2010***; ***Blanc et al., 2012***; ***Gao et al., 2014***; ***Pombert et al., 2014***). The genome size of the total assembly in strain A99 was similar to that of strain NC64A (46.2 Mb) (***Figure 4B***). By k-mer analysis (k-mer = 19), the genome size of A99 was estimated to be 61 Mbp (***Marçais and Kingsford, 2011***). Its GC content of 68%, is the highest among the green algae species recorded (***Figure 4B***). In the A99 genome, 8298 gene

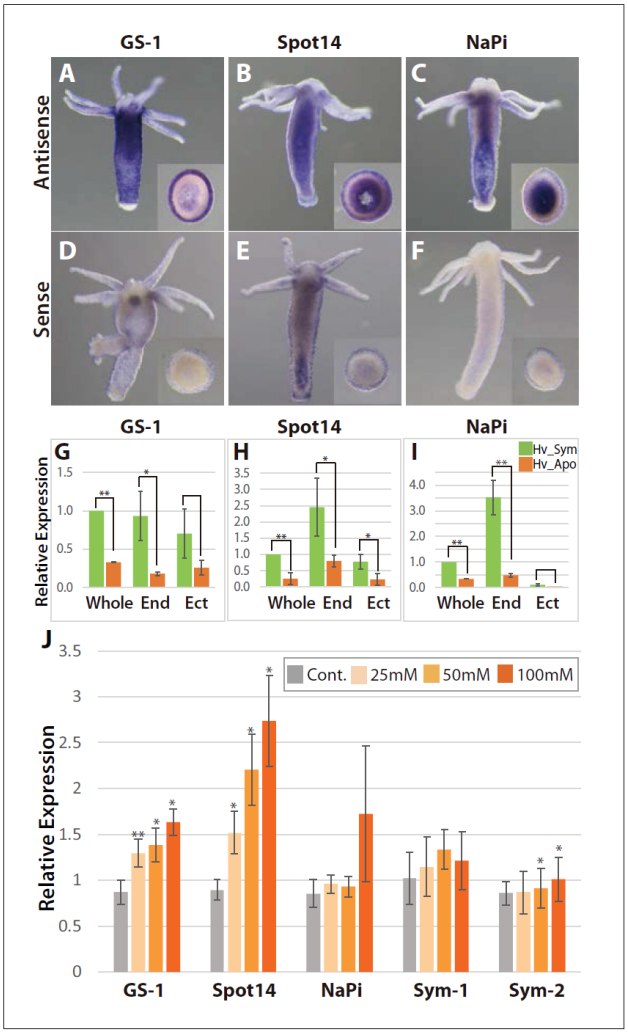

Figure 3. Spatial expression patterns of genes coding for glutamine synthetase, Spot 14 and Na/Pi-transporter. (**A-F**); Whole mount in situ hybridization using antisense (**A–C**) and sense probes (**D-F**; negative controls) for glutamine synthetase-1 (GS-1; left), Spot 14 (center) and Na/Pi-transporter (NaPi; right). Inserts show cross sections of the polyp's body. (**G–I**) Relative expression levels of whole animal (whole), isolated endoderm (End) and isolated ectoderm (Ect) tissue of Hv_Sym (green bars) and Hv_Apo (orange bars). For each biological replicate (n = 3) 10–20 hydra polyps were used for total RNA extraction of endodermal and ectodermal tissue. T-test was performed between Hv_Sym and Hv_apo. Pvalue, *<0.05, **<0.01. (**J**) Expression change of genes GS-1, Spot14, NaPi, Sym-1 and Sym-2 following exposure to 25, 50 and 100 mM maltose in Hv_Apo. For each biological replicate (n = 3) 50 hydra polyps were used for total RNA extraction The vertical axis shows log scale (log2) fold changes of relative expression level of maltose-treated over the untreated Hv_Apo control. T-test was performed between maltose-treated in each concentration and control (*: p value <0.05) and Kruskal-Wallis test (†: p value <0.05) in the series of 48 hr treatment were performed. Error bars indicate standard deviation.

DOI: https://doi.org/10.7554/eLife.35122.017

The following source data and figure supplements are available for figure 3:

Source data 1. Expression change of genes GS-1, Spot14, NaPi, Sym-1 and Sym-2 following exposure to 25, 50 and 100 mM maltose in Hv_Apo examined by qPCR.

DOI: https://doi.org/10.7554/eLife.35122.021

Figure 3 continued on next page

Figure 3 continued

Figure supplement 1. Tissue isolation of green hydra.
DOI: https://doi.org/10.7554/eLife.35122.018
Figure supplement 2. Effects of sugars on *Hydra* growth.
DOI: https://doi.org/10.7554/eLife.35122.019
Figure supplement 2—source data 1. Effects in presence of maltose, glucose, sucrose and galactose on gene expression of GS-1, Spot14 and NaPi in Hv_Apo examined by qPCR.
DOI: https://doi.org/10.7554/eLife.35122.020

models were predicted. As shown in ***Figure 4C***, about 80% of these predicted genes have extensive sequence similarity to plant genes, while 13% so far have no similarity to genes of any other organisms (***Figure 4C***). It is also noteworthy that 7% of the A99 genes are similar to genes of other kingdoms but not to *Hydra*, indicating the absence of gene transfer from *Hydra* to the symbiont genome (***Figure 4C***).

The *Chlorella* A99 genome provides evidences for extensive nitrogenous amino acid import and an incomplete nitrate assimilation pathway

Several independent lines of evidence demonstrate that nitrogen limitation and amino-acid metabolism have a key role in the *Chlorella–Hydra* symbiosis and that symbiotic *Chlorella* A99 depends on glutamine provided by its host (***Rees, 1986***; ***McAuley, 1987a***; ***1987b***; ***McAuley, 1991***; ***Rees, 1991***;***1989***). To identify *Chlorella* candidate factors for the development and maintenance of the symbiotic life style, we therefore used the available genome information to assess genes potentially involved in amino acid transport and the nitrogen metabolic pathway.

When performing a search for the Pfam domain 'Aa_trans' or 'AA_permease' to find amino acid transporter genes in the A99 genome, we discovered numerous genes containing the Aa_trans domain (***Table 6A***). In particular, A99 contains many orthologous genes of amino acid permease 2 and of transmembrane amino acid transporter family protein (solute carrier family 38, sodium-coupled neutral amino acid transporter), as well as NC64A (***Table 6B***, ***Supplementary file 2***). Both of these gene products are known to transport neutral amino acids including glutamine. This observation is supporting the view that import of amino acids is an essential feature for the symbiotic way of life of *Chlorella*.

In symbiotic organisms, loss of genes often occurs due to the strictly interdependent relationship (***Ochman and Moran, 2001***; ***Wernegreen, 2012***), raising the possibility that *Chlorella* A99 might have lost some essential genes. To test this hypothesis, we searched the *Chlorella* A99 genome for genes conserved across free-living green algae *Coccomyxa subellipsoidea* C169 (C169), *Chlamydomonas reinhardtii* (Cr) and *Volvox carteri* (Vc). In a total of 9851 C169 genes, we found 5701 genes to be conserved in Cr and Vc (***Supplementary file 3***). Of these, 238 genes did not match to any gene models and genomic regions in *Chlorella* A99 and thus were considered as gene loss candidates. Interestingly, within these 238 candidates, genes with the GO terms 'transport' in biological

Table 5. Summary of sequence data for assembling *Chlorella* sp. A99 genome sequences

Number of reads	85469010	
Number of reads assembled	61838513	
Number of bases	17398635102	
	Scaffolds	Contigs
Total length of sequence	40934037	40687875
Total number of sequences	82	7455
Maximum length of sequence	4003385	171868
N50	1727419	12747
GC contents (%)	68.07%	69.95%

DOI: https://doi.org/10.7554/eLife.35122.023

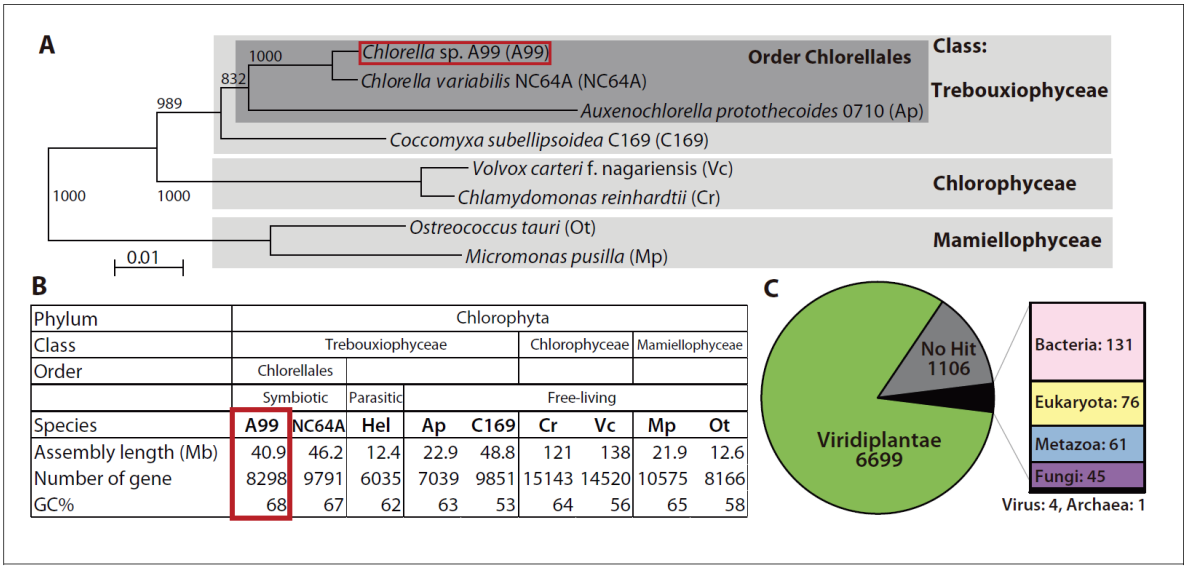

Phylum	Chlorophyta								
Class	Trebouxiophyceae					Chlorophyceae		Mamiellophyceae	
Order	Chlorellales								
	Symbiotic		Parasitic	Free-living					
Species	A99	NC64A	Hel	Ap	C169	Cr	Vc	Mp	Ot
Assembly length (Mb)	40.9	46.2	12.4	22.9	48.8	121	138	21.9	12.6
Number of gene	8298	9791	6035	7039	9851	15143	14520	10575	8166
GC%	68	67	62	63	53	64	56	65	58

Figure 4. Comparison of key features deduced from the *Chlorella* A99 genome with other green algae. (**A**) Phylogenetic tree of eight genome sequenced chlorophyte green algae including *Chlorella* sp. A99. The NJ tree is based on sequences of the 18S rRNA gene, ITS1, 5.8S rRNA gene, ITS2 and 28S rRNA gene. (**B**) Genomic features and taxonomy of the sequenced chlorophyte green algae. Hel: *Helicosporidium* sp. ATCC50920. (**C**) The proportion of similarity of *Chlorella* A99 gene models to those of other organisms.

DOI: https://doi.org/10.7554/eLife.35122.022

process and 'transporter activity' in molecular function were overrepresented (***Figure 5***). In particular, the 28 genes annotated to these GO terms encoded nitrate transporter, urea transporter and molybdate transporter, which are known to be involved in nitrogen metabolism (***Table 7***). Beside ammonium, nitrate and urea are major nitrogen sources for plants, whereas molybdate is a co-factor of the nitrate reductase, an important enzyme in the nitrate assimilation pathway. These transporter genes are conserved across green algae including *Chlorella* NC64A (***Sanz-Luque et al., 2015***; ***Gao et al., 2014***) and appear to be lost in the *Chlorella* A99 genome.

In nitrogen assimilation processes, plants usually take up nitrogen in the form of nitrate (NO_3^-) via nitrate transporters (NRTs) or as ammonium (NH_4^+) via ammonium transporters (AMT) (***Figure 6A***). In higher plants, two types of nitrate transporters, NRT1 and NRT2, have been identified (***Krapp et al., 2014***). Some NRT2 require nitrate assimilation-related component 2 (NAR2) to be

Table 6. Amino acid transporter genes in *Chlorella* sp. A99 (A99), *Chlorella variabilis NC64A* (NC64A), *Coccomyxa subellipsoidea* C-169 (C169), *Volvox carteri* (Vc), *Micromonas pusilla* (Mp) and *Ostreococcus tauri* (Ot) and *Chlamydomonas reinhardtii* (Cr)

A. The number of Pfam domains related to amino acids transport

Pfam domain name	A99	NC64A	c169	Cr	Vc	Mp	Ot
Aa_trans	30	38	21	9	7	9	8
AA_permease	4	6	15	5	6	1	1

B. Ortholog groups including Aa_trans domain containing genes overrepresented in symbiotic *Chlorella*

Ortholog group ID: Gene annotation	A99	NC64A	c169	Cr	Vc	Mp	Ot
OG0000040: amino acid permease 2	12	12	6	3	1	0	0
OG0000324: transmembrane amino acid transporter family protein (solute carrier family 38, sodium-coupled neutral amino acid transporter)	6	7	1	2	1	0	0

DOI: https://doi.org/10.7554/eLife.35122.024

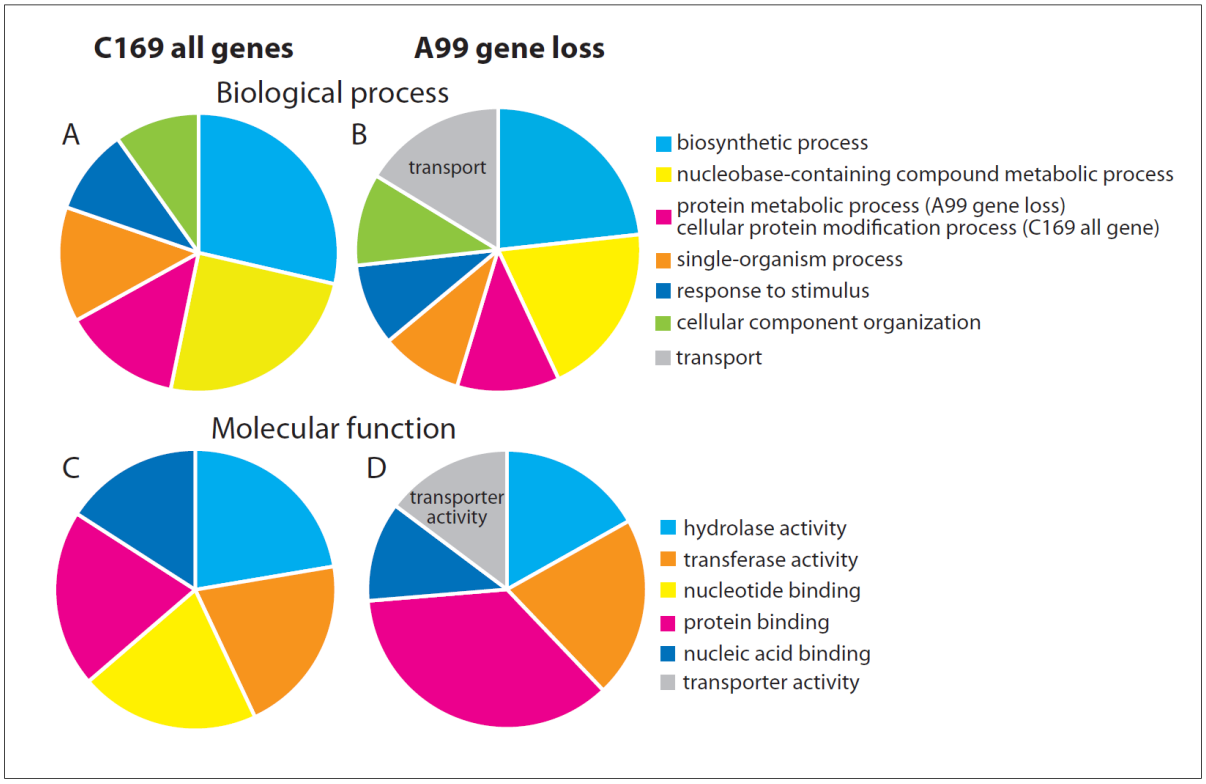

Figure 5. Genes missing in the genome of *Chlorella* A99. Functional categorization of genes present in *Coccomyxa subellipsoidea* C169 (**A**, **C**) and genes missing in *Chlorella* A99 (**B**, **D**) by GO terms using Bast2GO. Multilevel pie charts show enrichment of GO' Biological Process' terms (**A**, **B**) and GO 'Molecular Function' terms (**C**, **D**) on the lowest level, which cover at least 10% of the total amount of annotated sequences.

DOI: https://doi.org/10.7554/eLife.35122.025

The following source data is available for figure 5:

Source data 1. Functional categorization of genes present in *Coccomyxa subellipsoidea* C169 (C169_all) and genes missing in Chlorella A99 (A99 gene loss) by GO terms' Biological Process' terms and 'Molecular Function' on the lowest level, which cover at least 10% of the total amount of annotated sequences.

DOI: https://doi.org/10.7554/eLife.35122.026

functional (***Quesada et al., 1994***). NO_3^- is reduced to nitrite by nitrate reductase (NR), NO_2^- is transported to the chloroplast by nitrate assimilation-related component1 (NAR1), and NO_2^- is reduced to NH_4^+ by nitrite reductase (NiR). NH_4^+ is incorporated into glutamine (Gln) by glutamine synthetase (GS), and Gln is incorporated into glutamate (Glu) by NADH-dependent glutamine amide-2-oxoglutarate aminotransferase (GOGAT), also known as glutamate synthase. This pathway is highly conserved among plants and all of its major components, including NRT1 and NRT2, NAR1 and NAR2, NR, NiR, AMT, GOGAT and GS, are present in the 10 green algae species that have been genome-sequenced so far (with the exception of NRT1, which is absent in *Micromonas pusilla*) (***Sanz-Luque et al., 2015***). In *Symbiodinium*, the photosynthetic symbiont of marine invertebrates, all these components of the nitrogen assimilation pathway were also observed (***Supplementary file 4***) (***Shoguchi et al., 2013***; ***Lin et al., 2015***; ***Aranda et al., 2016***; ***Sproles et al., 2018***).

Based on the annotation by Sanz-Luque et al. (***Sanz-Luque et al., 2015***), we searched these nitrogen assimilation genes in the *Chlorella* A99 genome, using ortholog grouping and a reciprocal BLAST search using the protein sequences from other green algae (***Figure 6B***, ***Supplementary file 5***). As expected, the *Chlorella* A99 genome contains many homologues of the genes involved in

Table 7. List of *Coccomyxa subellipsoidea* C169 (C169) genes, which are present in *Chlamydomonas reinhardtii* and *Volvox carteri*, but missing in the genome of *Chlorella* A99

UniProt ID in C169	Description
F1DPL8_9CHLO	ATP synthase F0 subunit 6 (mitochondrion)
F1DPL7_9CHLO	cytochrome c oxidase subunit 3 (mitochondrion)
I0YZU4_9CHLO	equilibrative nucleoside transporter 1
I0Z311_9CHLO	equilibrative nucleoside transporter family
I0YZC9_9CHLO	high affinity nitrate transporter
I0Z2L2_9CHLO	hypothetical protein COCSUDRAFT_28432
I0YJ99_9CHLO	hypothetical protein COCSUDRAFT_34498
I0YKQ1_9CHLO	hypothetical protein COCSUDRAFT_45098
I0YYD3_9CHLO	hypothetical protein COCSUDRAFT_65897
I0YYP5_9CHLO	importin-4 isoform X1
I0YQQ1_9CHLO	low-CO2-inducible membrane
I0YJD4_9CHLO	MFS transporter
I0YTY0_9CHLO	molybdate transporter 2
F1DPM0_9CHLO	NADH dehydrogenase subunit 3 (mitochondrion)
F1DPM4_9CHLO	NADH dehydrogenase subunit 6 (mitochondrion)
F1DPM8_9CHLO	NADH dehydrogenase subunit 9 (mitochondrion)
I0Z357_9CHLO	plasma membrane phosphate transporter Pho87
I0Z9Y1_9CHLO	pre translocase subunit
I0YPT2_9CHLO	transcription and mRNA export factor ENY2-like
I0Z976_9CHLO	transport SEC23
I0Z3Q6_9CHLO	tyrosine-specific transport -like isoform X1
I0YXU9_9CHLO	urea active transporter
I0YRT0_9CHLO	urea active transporter
I0YRL4_9CHLO	urea-proton symporter DUR3
I0YUF9_9CHLO	urea-proton symporter DUR3
I0YJS6_9CHLO	urea-proton symporter DUR3
I0YQ78_9CHLO	urea-proton symporter DUR3-like
I0YIH7_9CHLO	Zip-domain-containing protein

DOI: https://doi.org/10.7554/eLife.35122.027

nitrogen assimilation in plants including genes encoding NRT1, NAR1, NR, AMT, GS and GOGAT (***Figure 6B***). Intriguingly, our systematic searches failed to identify representative genes for NRT2, NAR2 and NiR in the *Chlorella* A99 genome (***Figure 6B***). We confirmed the absence of the NRT2 and NiR genes by PCR using primers designed for the conserved regions of these genes and which failed to produce a product with genomic DNA as a template (***Figure 6—figure supplement 1***). Due to the weak sequence conservation of the NAR2 gene in the three algae genomes, PCR of that gene was not performed. Taken together, our observations indicate that *Chlorella* A99 algae appears to lack NRT2, NAR2 and NiR.

Since in many fungi, cyanobacteria and algae species, nitrate assimilation genes are known to act in concert and a gene cluster of NR and NiR genes is conserved between different green algae (***Sanz-Luque et al., 2015***), we next investigated the level of genomic clustering of the nitrate assimilation pathway genes in the *Chlorella* genome. Comparing the genomes of NC64A and C169 revealed the presence of a cluster of NR and NiR genes (***Figure 6C***). In NC64A, two NRT2 genes, together with genes for NAR2, NR and NiR are clustered on scaffold 21. In C169, one of the NR genes and NiR are clustered together, whereas the second NR gene is separate. Interestingly, analysis of the sequences around the NR gene in the *Chlorella* A99 genome provided no evidence for the

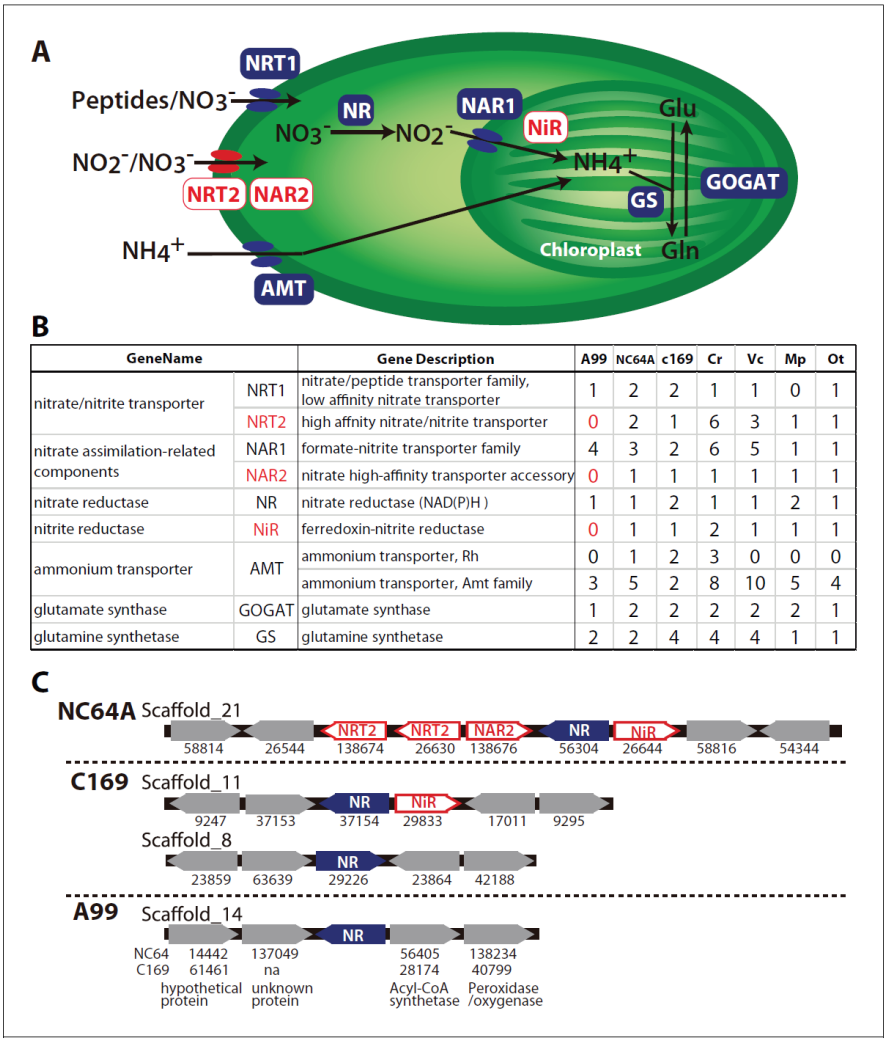

GeneName		Gene Description	A99	NC64A	c169	Cr	Vc	Mp	Ot
nitrate/nitrite transporter	NRT1	nitrate/peptide transporter family, low affinity nitrate transporter	1	2	2	1	1	0	1
	NRT2	high affnity nitrate/nitrite transporter	0	2	1	6	3	1	1
nitrate assimilation-related components	NAR1	formate-nitrite transporter family	4	3	2	6	5	1	1
	NAR2	nitrate high-affinity transporter accessory	0	1	1	1	1	1	1
nitrate reductase	NR	nitrate reductase (NAD(P)H)	1	1	2	1	1	2	1
nitrite reductase	NiR	ferredoxin-nitrite reductase	0	1	1	2	1	1	1
ammonium transporter	AMT	ammonium transporter, Rh	0	1	2	3	0	0	0
		ammonium transporter, Amt family	3	5	2	8	10	5	4
glutamate synthase	GOGAT	glutamate synthase	1	2	2	2	2	2	1
glutamine synthetase	GS	glutamine synthetase	2	2	4	4	4	1	1

Figure 6. Nitrogen assimilation pathways in *Chlorella* A99. (**A**) Schematic diagram of the nitrogen assimilation pathway in plants showing the function of nitrate transporters NRT1 (peptides/nitrate transporter) and NRT2 (nitrate/nitrite transporter), nitrate assimilation-related components NAR1 and NAR2, nitrate reductase NR, nitrite reductase NiR, ammonium transporter AMT, glutamate synthetase GOGAT and glutamine synthetase GS. Genes shown in red boxes (NRT2, NAR2 and NiR) were not found in the *Chlorella* sp. A99 genome. (**B**) Table showing the number of nitrogen assimilation genes in *Chlorella* sp. A99 (**A99**), *Chlorella variabilis* NC64A (NC64A), *Coccomyxa subellipsoidea* C169 (C169), *Volvox carteri f. nagariensis* (Vc), *Chlamydomonas reinhardtii* (Cr), *Ostreococcus tauri* (Ot) *and Micromonas pusilla* (Mp). (**C**) Gene clusters of nitrate assimilation genes around the shared NR genes (blue) in the genomes of NC64A, C169 and A99. Red boxes show nitrate assimilation genes absent in A99 and gray boxes depict other genes. Numbers below the boxes are JGI protein IDs of NC64A and C169. Numbers below the genes of A99 are JGI protein IDs of the best hit genes in NC64A and C169 and their gene name.

DOI: https://doi.org/10.7554/eLife.35122.028

The following figure supplement is available for figure 6:

Figure supplement 1. PCR of nitrate assimilation genes.

DOI: https://doi.org/10.7554/eLife.35122.029

presence of a co-localized NiR gene or any other nitrate assimilation genes, nor any conserved gene synteny to NC64A and C169 (***Figure 6C***). Therefore, our comparative genomic analyses points to an incomplete and scattered nitrogen metabolic pathway in symbiotic *Chlorella* A99, which lacks essential transporters and enzymes for nitrate assimilation as well as the clustered structure of nitrate assimilation genes.

Supplementing the medium with glutamine allows temporary in vitro growth of symbiotic *Chlorella* A99

The absence of genes essential for nitrate assimilation in the *Chlorella* A99 genome (***Figure 6***) is consistent with its inability to grow outside the *Hydra* host cell (***Habetha and Bosch, 2005***) and indicates that *Chlorella* symbionts are dependent on metabolites provided by their host. We hypothesized that *Chlorella* is unable to use nitrite and ammonium as a nitrogen source, and that it relies on *Hydra* assimilating ammonium to glutamine to serve as the nitrogen source. To test this hypothesis and to examine utilization of nitrogen compounds of A99, we isolated *Chlorella* A99 from Hv_Sym and cultivated it in vitro using modified bold basal medium (BBM) (***Nichols and Bold, 1965***) containing the same amount of nitrogen in the form of NO_3^-, NH_4^+, Gln or casamino acids (***Figure 7***). As controls, *Chlorella variabilis* NC64A (NC64A) isolated from Hv_NC64A and free-living C169 were used. To confirm that the cultured A99 is not contamination, we amplified and sequenced the genomic region of the 18S rRNA gene by PCR (***Figure 7—figure supplement 1***) and checked this against the genomic sequence of A99. Kamako et al. reported that free-living alga *Chlorella vulgaris* Beijerinck var. *vulgaris* grow in media containing only inorganic nitrogen compounds as well as in media containing casamino acids as a nitrogen source, while NC64A required amino acids for growth (***Kamako et al., 2005***). Consistent with these observations, C169 grew in all tested media and NC64A grew in media containing casamino acids and Gln, although its growth rate was quite low in presence of NH_4^+ and NO_3^- (***Figure 7***). Remarkably, *Chlorella* A99 increased in cell number for up to 8 days in media containing casamino acids and Gln (***Figure 7***). Similar to NC64A, A99 did not grow in presence of NH_4^+ and NO_3^-. The growth rates of both A99 and NC64A were higher in medium containing a mixture of amino acids (casamino acids) than the single amino acid Gln. In contrast to NC64A, A99 could not be cultivated permanently in casamino acids or glutamine supplemented medium, indicating that additional growth factors are necessary to maintain in

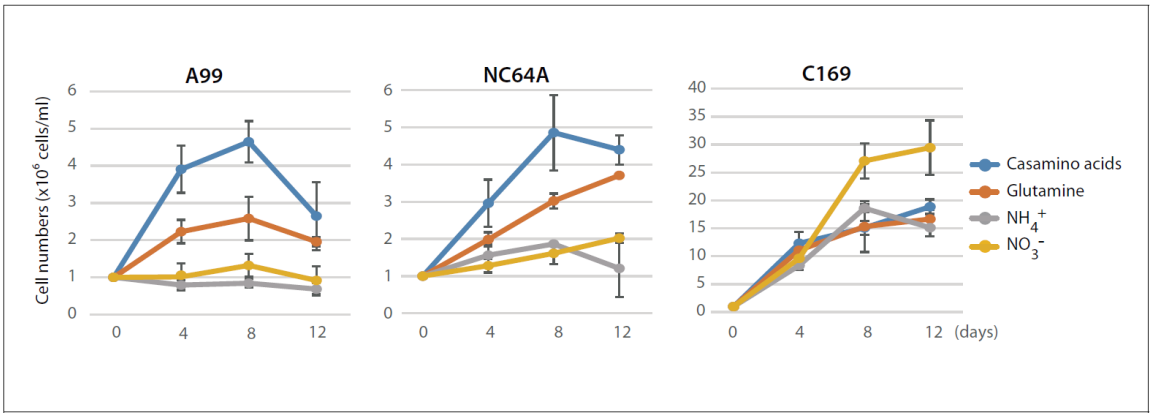

Figure 7. Growth of green algae in presence of various nitrogen sources. The growth rate of *Chlorella* A99 (A99), *Chlorella variabilis* NC64A (NC64A) and *Coccomyxa subellipsoidea* C-169 (C169) by in vitro culture was assessed for different nitrogen sources with casamino acids (blue), glutamine (orange), ammonium (gray) and nitrate (yellow). Mean number of algae per ml were determined at 4, 8, 12 days after inoculation with 10^6 cell/ml. Error bars indicate standard deviation.

DOI: https://doi.org/10.7554/eLife.35122.030

The following figure supplement is available for figure 7:

Figure supplement 1. PCR of 18S rRNA genes in cultured algae.

DOI: https://doi.org/10.7554/eLife.35122.031

vitro growth of this obligate symbiont. Thus, although in vitro growth of A99 can be promoted by adding Glu and amino acids to the medium, A99 cannot be cultured permanently in this enriched medium, indicating that other host derived factors remain to be uncovered.

Discussion

Metabolic co-dependence in *Hydra-Chlorella* symbiosis

Sequencing of the *Chlorella* A99 genome in combination with the transcriptome analyses of symbiotic, aposymbiotic and NC64A-infected *H. viridissima* polyps has enabled the identification of genes with specific functions in this symbiotic partnership. The *Hydra-Chlorella* symbiosis links carbohydrate supply from the photosynthetic symbiont to glutamine synthesis by the host. Characteristics of the symbiont genome obviously reflect its adaptation to this way of life, including an increase in amino acid transporters and degeneration of the nitrate assimilation pathway. This conclusion is based on six observations: (i) Expression of some genes including GS-1, Spot 14 and NaPi is specifically up-regulated in the presence of *Chlorella* A99 (***Figure 1C***, ***Table 2***), and (ii) they are induced by both, photosynthetic activity of *Chlorella* and by supplying exogenous maltose or glucose (***Figures 2*** and ***3J***, ***Figure 3—figure supplement 2***). Maltose produced by the symbiont is likely to be digested to glucose in symbiosome and translocated to the host cytoplasm through glucose transporters (***Figure 8A***). Upregulation of a GLUT8 gene in the symbiotic state of green hydra may reflect activation of sugar transport (***Table 1***). These results indicate that maltose release by photosynthesis of the symbiont enhances nutrition supply including glutamine by the host (***Figure 8A***). (iii) Symbiotic *Chlorella* A99 cannot be cultivated in vitro in medium containing a single inorganic nitrogen source (***Figure 7***). Since medium containing glutamine supports in vitro growth of A99, this organism appears to depend on glutamine provided by the *Hydra* host. (iv) The genome of *Chlorella* A99 contains multiple amino acid transporter genes (***Table 6***), but lacks genes involved in nitrate assimilation (***Figure 6***), pointing to amino acids as main source of nitrogen and a degenerated nitrate assimilation pathway. As for ammonium, which is one of the main nitrogen sources in plants, previous studies have reported the inability of symbiotic algae to take up ammonium because of the low perialgal pH (pH 4–5) that stimulates maltose release (***Douglas and Smith, 1984***; ***Rees, 1989***; ***McAuley, 1991***; ***Dorling et al., 1997***). Since *Chlorella* apparently cannot use nitrite and ammonium as a nitrogen source, it seems that *Hydra* has to assimilate ammonium to glutamine and provides it to *Chlorella* A99 (***Figure 8A***).

(v) While polyps with native symbiont *Chlorella* A99 grew faster than aposymbiotic ones, symbiosis with foreign algae NC64A had no effect on the growth of polyps at all (***Figure 1B***). (vi) *Hydra* endodermal epithelial cells host significantly fewer NC64A algae than A99 (***Figure 1—figure supplement 1***) providing additional support for the view of a tightly regulated codependent partnership in which exchange of nutrients appears to be the primary driving force. Previous studies have reported that symbiotic *Chlorella* in green hydra releases significantly larger amounts of maltose than NC64A (***Mews and Smith, 1982***; ***Rees, 1989***). In addition, Rees reported that *Hydra* polyps containing high maltose releasing algae had a high GS activity, whereas aposymbiotic *Hydra* or *Hydra* with a low maltose releasing algae had lower GS activity (***Rees, 1986***). Although the underlying mechanism of how maltose secretion and transportation from *Chlorella* is regulated is still unclear, the amount of maltose released by the symbiont could be an important symbiont-derived driver or stabilizer of the *Hydra–Chlorella* symbiosis.

More general lessons for animal-algal symbiosis

Transcriptome comparison between symbiotic and aposymbiotic *H. viridissima* demonstrated that symbiosis-regulated genes are involved in oxidative stress response and innate immunity. The fact that PRRs and apoptosis-related genes, are also differentially expressed in a number of other symbiotic cnidarians (***Table 1***), suggests innate immunity as conserved mechanism involved in controlling the development and maintenance of stable symbiotic interactions. Furthermore, the exchange of nitrogenous compounds and photosynthetic products between host and symbiont observed here in the *Hydra-Chlorella* symbiosis is also observed in marine invertebrates such as corals, sea anemones and giant clams associated with *Symbiodinium* algae (***Figure 8B,C***). Despite these similarities, however, there are also conspicuous differences among symbiotic cnidarians in particular with respect to

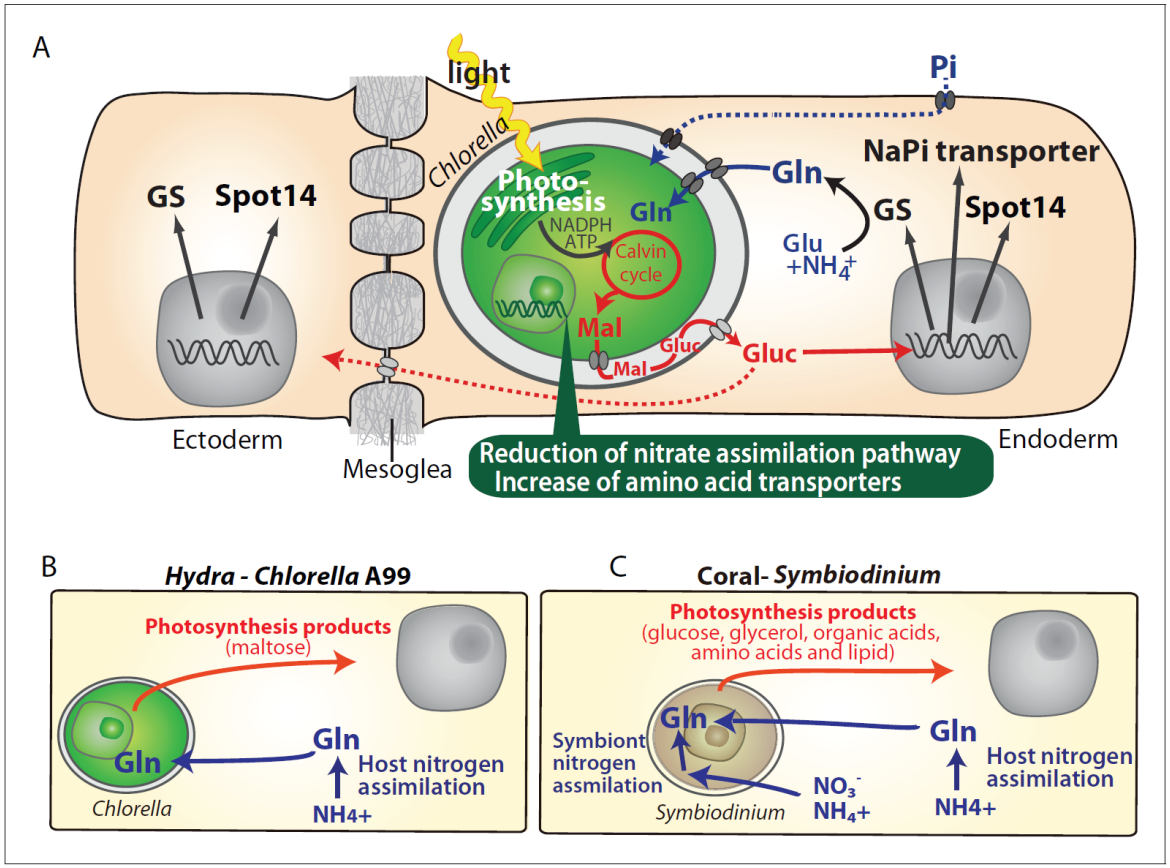

Figure 8. Molecular interactions in the symbiosis of cnidarians. (**A**) Summary of symbiotic interactions between *Hydra* and *Chlorella* A99. During light conditions, *Chlorella* A99 performs photosynthesis and produces maltose (Mal), which is secreted into the *Hydra* symbiosome where it is possibly digested to glucose (Gluc), shown in red. The sugar induces expression of *Hydra* genes encoding glutamine synthetase (GS), Na/Pi transporter (NaPi) and Spot14. GS catalyzes the condensation of glutamate (Glu) and ammonium (NH_4^+) to form glutamine (Gln), which is used by *Chlorella* as a nitrogen source. Since the sugar also up-regulates the NaPi gene, which controls intracellular phosphate levels, it might be involved in the supply of phosphorus to *Chlorella* as well (blue broken line). The sugar is transported to the ectoderm (red broken line) and there induces the expression of GS and Spot14. In the *Chlorella* A99 genome, degeneration of the nitrate assimilation system and an increase of amino acid transporters was observed (green balloon). (**B, C**) Comparison between *Hydra-Chlorella* symbiosis and coral-*Symbiodinium* symbiosis. Red indicates transfer of photosynthesis products from the symbiont to the host, and blue indicates transfer of nitrogen sources from the host to the symbiont. While the host organisms *Hydra* and coral can assimilate NH_4^+ to Gln (**B, C**), assimilation of inorganic nitrogen by *Symbiodinidium* plays an important role for the symbiotic system in coral (**C**).
DOI: https://doi.org/10.7554/eLife.35122.032

the nutrients provided by the symbiont to the host. For example, symbiotic *Chlorella* algae in green hydra, *Paramecium* and fresh water sponges provide their photosynthetic products in form of maltose and glucose (***Figure 8B***) (***Brown and Nielsen, 1974***; ***Wilkinson, 1980***; ***Kamako and Imamura, 2006***). In contrast, *Symbiodinium* provides glucose, glycerol, organic acids, amino acids as well as lipids to its marine hosts (***Figure 8C***) (***Muscatine and Cernichiari, 1969***; ***Lewis and Smith, 1971***; ***Trench, 1971***; ***Kellogg and Patton, 1983***). A former transcriptome analysis of amino acid biosynthetic pathways suggested that *Symbiodinium* can synthesize almost all amino acids (***Shinzato et al., 2014***). Gene loss in cysteine synthesis pathway in the coral host *Acropora digitifera* seems to reflect the dependency on the amino acids provided by the *Symbiodinium* symbiont (***Shinzato et al., 2011***). In contrast to *Symbiodinium* which can assimilate inorganic nitrogen such as nitrate and

ammonium (**Lipschultz and Cook, 2002**; **Grover et al., 2003**; **Tanaka et al., 2006**; **Yellowlees et al., 2008**), the symbiotic *Chlorella* algae in *Hydra* and *Paramecium* can only use amino acids as a nitrogen source (**Figure 6**) (**Kamako et al., 2005**).

In efforts to explain the metabolic efficiency of nitrogen use in symbiotic organisms, two models have been proposed: the 'nitrogen conservation' and the 'nitrogen recycling' hypothesis. The nitrogen conservation hypothesis suggests that photosynthetic carbon compounds from the symbiont are used preferentially by the host respiration, which reduces catabolism of nitrogenous compounds (**Rees and Ellard, 1989**; **Szmant et al., 1990**; **Wang and Douglas, 1998**). The 'nitrogen recycling' hypothesis suggests that symbionts assimilate nitrogenous waste (ammonium) of the host into valuable, organic compounds, which then are translocated back to the host (**Figure 8C** Symbiont nitrogen assimilation) (**Lewis and Smith, 1971**; **Muscatine and Porter, 1977**; **Falkowski et al., 1993**; **Wang and Douglas, 1998**). Our observation that in symbiotic green hydra many genes involved in amino acid metabolism are down-regulated (**Figure 1E**) is consistent with the assumption of reduction of amino acid consumption by respiration.

In addition to the nitrogen recycling hypothesis, it has been proposed that also corals, sea anemones, *Paramecium* and green hydra hosts can assimilate ammonium into amino acids (**Figure 8B,C** Host nitrogen assimilation) (**Miller and Yellowlees, 1989**; **Rees, 1989**; **Szmant et al., 1990**; **Rees, 1991**; **Wang and Douglas, 1998**; **Lipschultz and Cook, 2002**). Ammonia assimilation by the host implies that the host controls the nitrogen status to regulate metabolism of the symbionts, which may be involved in controlling the number of symbionts within the host cell. For organisms such as corals living in oligotrophic sea, inorganic nitrogen assimilation and recycling may be necessary to manage the nitrogen sources efficiently. In contrast, for *Hydra* and *Paramecium* living in a relatively nutrient-rich environment may be advantageous in terms of metabolic efficiency that the symbiont abandons its ability to assimilate inorganic nitrogen and specializes in the supply of photosynthetic carbohydrate to the host.

Genome evolution in symbiotic *Chlorella* sp. A99

Metabolic dependence of symbionts on host supply occasionally results in genome reduction and gene loss. For example, symbiotic *Buchnera* bacteria in insects are missing particular genes in essential amino acid pathways (**Shigenobu et al., 2000**; **Hansen and Moran, 2011**). The fact that the corresponding genes of the host are up-regulated in the bacteriocyte, indicates complementarity and syntrophy between host and symbiont. Similarly, in *Chlorella* A99 the nitrogen assimilation system could have been lost as a result of continuous supply of nitrogenous amino acids provided by *Hydra*.

Compared to *Chlorella* NC64A, the closest relative to *Chlorella* A99 among the genome-sequenced algae, genome size and total number of genes in *Chlorella* A99 were found to be smaller (**Figure 4B**). Although both A99 and NC64A cannot be cultivated using inorganic nitrogen sources (**Figure 7**) (**Kamako et al., 2005**), NC64A, unlike A99, obtains all major nitrogen assimilation genes and their cluster structure on the chromosome (**Figure 6**) (**Sanz-Luque et al., 2015**). NR and NiR activities were found to be induced by nitrate in free-living *Chlorella*, but not in *Chlorella* NC64A, indicating mutations in the regulatory region (**Kamako et al., 2005**). Considering the phylogenetic position of NC64A and the symbiotic *Chlorella* of green hydra (**Kawaida et al., 2013**), the disability of nitrate assimilation in A99 and NC64A seems to have evolved independently, suggesting convergent evolution in a similar symbiotic environment.

Although our findings indicate that genome reduction in *Chlorella* A99 is more advanced than in *Chlorella* NC64A, genome size and total number of genes do not differ much between the Trebouxiophyceae (A99, NC64A and C169) (**Figure 4B**). By contrast, the parasitic algae *Helicosporidium* and *Auxochlorella* have significantly smaller genome sizes and number of genes indicating extensive genome reduction (**Gao et al., 2014**; **Pombert et al., 2014**). The apparently unchanged complexity of the *Chlorella* A99 genome suggests a relatively early stage of this symbiotic partnership. Thus, gene loss in metabolic pathways could occur as a first step of genome reduction in symbionts caused by the adaptation to continuous nutrient supply from the host. Taken together, our study suggests metabolic-codependency as the primary driving force in the evolution of symbiosis between *Hydra* and *Chlorella*.

Materials and methods

Key resources table

Reagent type (species) or resource	Designation	Source or reference	Identifiers	Additional information
Strain, strain background (*Hydra viridissima* A99)	*Hydra viridissima* A99	PMID: 16351895		
Strain, strain background (*Chlorella* sp. A99)	*Chlorella* sp. A99	PMID: 16351895	NCBI BioProject ID: PRJNA412448	
Strain, strain background (*Chlorella variabilis* NC64A)	*Chlorella variabilis* NC64A	Microbial Culture Collection at the National Institute for Environmental Studies	NIES-2541	
Strain, strain background (*Coccomyxa subellipsoidea* C-169)	*Coccomyxa subellipsoidea* C-169	Microbial Culture Collection at the National Institute for Environmental Studies	NIES-2166	
Strain, strain background (*Chlamydomonas reinhardtii*)	*Chlamydomonas reinhardtii*	Microbial Culture Collection at the National Institute for Environmental Studies	NIES-2235	
Commercial assay or kit	TruSeq DNA LT Sample Prep Kit	Illumina	FC-121–2001	
Commercial assay or kit	Nextera Mate Pair Sample Preparation Kit	Illumina	FC-132–1001	
Commercial assay or kit	Miseq reagent kit v3	Illumina	MS-102–3003	
Commercial assay or kit	HiSeq SBS kit v4	Illumina	FC-401–4003	
Commercial assay or kit	BigDye Terminator v3.1 Cycle Sequencing Kit	Thermo Fisher Scientific	4337454	
Commercial assay or kit	4 × 44K *Hydra viridissima* A99 Custom-Made Microarray	Agilent Technologies	NCBI GEO Platform ID: GPL23280	
Commercial assay or kit	GE Hybridization Kit and GE Wash Pack	Agilent Technologies	5188–5242, 5188–5327	
Commercial assay or kit	High Sensitivity DNA Kit	Agilent Technologies	5067–4626	
Commercial assay or kit	RNA6000 nano kit	Agilent Technologies	5067–1511	
Commercial assay or kit	Low Input Quick Amp Labeling Kit	Agilent Technologies	5190–2305	
Commercial assay or kit	PureLink RNA Mini Kit	Thermo Fisher Scientific	12183018A	
Commercial assay or kit	Fermentas First Strand cDNA Synthesis Kit	Thermo Fisher Scientific	K1621	
Chemical compound, drug	Trizol reagent	Thermo Fisher Scientific	15596026	
Chemical compound, drug	AmpliTaq Gold 360 Master Mix	Thermo Fisher Scientific	4398901	
Chemical compound, drug	ISOPLANT II	Nippon Gene	316–04153	
Chemical compound, drug	GoTaq qPCR Master Mix	Promega	A6002	
Chemical compound, drug	KOD FX Neo	TOYOBO	KFX-201	
Software, algorithm	Feature Extraction Software	Agilent Technologies	RRID:SCR_014963	
Software, algorithm	Newbler	454 Life Sciences, Roche Diagnostics	RRID:SCR_011916	
Software, algorithm	SSPACE	PMID: 21149342	RRID:SCR_005056	
Software, algorithm	GapCloser	PMID: 23587118	RRID:SCR_015026	
Software, algorithm	NCBI BLAST	PMID: 2231712	RRID:SCR_004870	
Software, algorithm	CEGMA	PMID: 17332020	RRID:SCR_015055	

Continued on next page

Continued

Reagent type (species) or resource	Designation	Source or reference	Identifiers	Additional information
Software, algorithm	Augustus: Gene Prediction	PMID: 16845043	RRID:SCR_008417	
Software, algorithm	Blast2GO	PMID: 16081474	RRID:SCR_005828	
Software, algorithm	Hmmer	PMID: 9918945	RRID:SCR_005305	
Software, algorithm	CLUSTALX2	PMID: 17846036	RRID:SCR_002909	
Software, algorithm	BioEdit	Nucleic Acid Symposium Series 41, 95–98	RRID:SCR_007361	
Software, algorithm	Njplot	Biochimie 78, 364–369	NA	
Software, algorithm	OrthoFinder	PMID: 26243257	NA	

Biological materials and procedures

Experiments were carried out with the Australian *Hydra viridissima* strain A99, which was obtained from Dr. Richard Campbell, Irvine. Polyps were maintained at 18°C on a 12 hr light/dark cycle and fed with *Artemia* two or three times a week. Aposymbiotic (algae free) polyps were obtained by photobleaching using 5 µM DCMU (3-(3,4-dichlorophenyl)−1,1-dimethylurea) as described before (***Pardy, 1976***; ***Habetha et al., 2003***). Experiments were carried out with polyps starved for 3–6 days. Isolation of endodermal layer and ectodermal layer was performed as described by Kishimoto et al. (***Kishimoto et al., 1996***). Symbiotic *Chlorella* were isolated as described before by Muscatine and McAuley (***Muscatine, 1983***; ***McAuley, 1986***). *Chlorella variabilis* NC64A (NIES-2541), *Coccomyxa subellipsoidea* C-169 (NIES-2166) and *Chlamydomonas reinhardtii* (NIES-2235) were obtained from the Microbial Culture Collection at the National Institute for Environmental Studies (Tsukuba, Japan).

Nucleic acid preparation

Total RNA of *Hydra* was extracted by use of the Trizol reagent and PureLink RNA Mini Kit (Thermo Fisher Scientific) after lysis and removal of algae by centrifugation. The genomic DNA of green algae was extracted using ISOPLANT II (Nippon Gene, Tokyo, Japan) following DNase I treatment to degrade contaminant DNA. Quantity and quality of DNA and RNA were checked by NanoDrop (Thermo Scientific Inc., Madison, USA) and BioAnalyzer (Agilent Technologies, Santa Clara, USA).

Microarray analysis

Total RNA for synthesis of cRNA targets was extracted from about 100 green hydra for each experimental group. Experiments were carried out using three biological replicates. cRNA labeled with cyanine-3 were synthesized from 400 ng total *Hydra* RNA using a Low Input Quick Amp Labeling Kit for one color detection (Agilent Technologies). A set of fluorescently labeled cRNA targets was employed in a hybridization reaction with 4 × 44K Custom-Made *Hydra viridissima* Microarray (Agilent Technologies) contributing a total of 43,222 transcripts that was built by mRNA-seq data (NCBI GEO Platform ID: GPL23280) (***Bosch et al., 2009***). Hybridization and washing were performed using the GE Hybridization Kit and GE Wash Pack (Agilent Technologies) after which the arrays were scanned on an Agilent Technologies G2565BA microarray scanner system with SureScan technology following protocols according to the manufacturer's instructions. The intensity of probes was extracted from scanned microarray images using Feature Extraction 10.7 software (Agilent Technologies). All algorithms and parameters used in this analysis were used with default conditions. Background-subtracted signal-intensity values (gProcessedSignal) generated by the Feature Extraction software were normalized using the 75th percentile signal intensity among the microarray. Those genes differentially expressed between two samples were determined by average of fold change (cut of >2.0) and Student's t-test ($p<0.1$). The data series are accessible at NCBI GEO under accession number GSE97633.

Quantitative real time RT-PCR

Total RNA was extracted from 50 green hydra polyps for each biological replicate independently. For reverse transcription of total RNA First Strand cDNA Synthesis Kit (Fermentas, Ontario, Canada)

was used. Real-time PCR was performed using GoTaq qPCR Master Mix (Promega, Madison, USA) and ABI Prism 7300 (Applied Biosystems, Foster City, USA). All qPCR experiments were performed in duplicate with three biological replicates each. Values were normalized using the expression of the tubulin alpha gene. Primers used for these experiments are listed in ***Supplementary file 6A***.

Whole mount in situ hybridization

Expression patterns of specific *Hydra* genes were detected by whole mount in situ hybridization with digoxigenin (DIG)-labelled RNA probes. Specimens were fixed in 4% paraformaldehyde. Hybridization signal was visualized using anti-DIG antibodies conjugated to alkaline phosphatase and NBT/BCIP staining solution (Roche). DIG-labeled sense probes (targeting the same sequences as the antisense probes) were used as a control. Primers used for these experiments are listed in ***Supplementary file 6B***.

Genome sequencing and gene prediction

For genome sequencing of *Chlorella* sp. A99, *Chlorella* sp. A99 was isolated from *H. viridissima* A99 and genomic DNA was extracted. Paired-end library (insert size: 740 bp) and mate-pair libraries (insert size: 2.2 and 15.2 kb) were made using Illumina TruSeq DNA LT Sample Prep Kit and Nextera Mate Pair Sample Preparation Kit respectively (Illumina Inc., San Diego, USA), following the manufacturer's protocols. Genome sequencing was performed using Illumina Miseq and Hiseq 2000 platforms. Sequence reads were assembled using Newbler Assembler version 2.8 (Roche, Penzberg, Germany) and subsequent scaffolding was performed by SSPACE (***Boetzer et al., 2011***). Gaps inside the scaffolds were closed with the paired-end and mate-pair data using GapCloser of Short Oligonucleotide Analysis Package (***Luo et al., 2012***). To overcome potential assembly errors arising from tandem repeats, sequences that aligned to another sequence by more than 50% of the length using blastn (1e-50) were removed from the assembly. The completeness of the genome was evaluated using CEGMA v2.4 (Core Eukaryotic Genes Mapping Approach) based on mapping of the 248 most highly conserved core eukaryotic genes (CEGs) on the assembled genome (***Parra et al., 2007***). The completeness of complete and partial CEGs in the A99 scaffolds was 80 and 88%, respectively. The fraction of repetitive sequences was 12%. Gene model was predicted by AUGUSTUS 3.0.1 using model parameters for NC64A (***Stanke et al., 2006***). This Whole Genome Shotgun project has been deposited at DDBJ/ENA/GenBank under the accession PCFQ00000000 (BioProject ID: PRJNA412448). Genome sequences and gene models are also accessible at the website of OIST Marine Genomics Unit Genome Project (http://marinegenomics.oist.jp/chlorellaA99/viewer/info?project_id=65).

Analysis of genes in *Hydra viridissima* and *Chlorella*

Annotation of transcriptome contigs and prediction of gene models was performed by use of BLAST, Gene Ontology (***Ashburner et al., 2000***) and blast2go (***Conesa et al., 2005***). To examine the conservation of *H. viridissima* contigs among metazoans, homology searches by blastx (evalue 1E-5) were performed using protein databases obtained from NCBI for *Drosophila melanogaster* and *Homo sapiens*, from the JGI genome portal (http://genome.jgi.doe.gov/) for *Branchiostoma floridae*, *Nematostella vectensis*, from Echinobase (http://www.echinobase.org/EchinoBase/) for *Strongylocentrotus pupuratus*, from Compagen for *Hydra magnipapillata*, and from the OIST marine genomics Genome browser ver.1.1 (http://marinegenomics.oist.jp/coral/viewer/info?project_id=3) for *Acropora digitifera*.

For comparative analysis of gene models of *Chlorella* sp. A99 and other algae, domain searches against the Pfam database (Pfam-A.hmm) were performed using HMMER (***Eddy, 1998***; ***Finn et al., 2016***), and ortholog gene grouping was done using OrthoFinder (***Emms and Kelly, 2015***). The sequences of the reference genes and genomes were obtained from the database of the JGI genome portal for *Chlorella variabilis* NC64A, *Coccomyxa subellipsoidea* C-169, *Volvox carteri*, *Micromonas pusilla*, and *Ostreococcus tauri*, from NCBI for *Auxenochlorella protothecoides* 0710, from Phytozome (http://phytozome.jgi.doe.gov/pz/portal.html) for *Chlamydomonas reinhardtii*, from OIST Marine Genomics (http://marinegenomics.oist.jp/symb/viewer/info?project_id=21) for *Symbiodinium minutum*, *Symbiodinium kawagutti* genome, from Dinoflagellate Resources (http://web.malab.cn/symka_new/) for *Symbiodinium kawagutti* and Reefgenomics (http://reefgenomics.org/)

for *Symbiodinium microadriaticum*) (**Merchant et al., 2007**; **Palenik et al., 2007**; **Worden et al., 2009**; **Blanc et al., 2010**; **Prochnik et al., 2010**; **Blanc et al., 2012**)

Nitrogen assimilation genes in *Chlorella* A99 were identified by orthologous gene groups and reciprocal blast searches. The number of genes for nitrate assimilation genes, glutamine synthetase and glutamate synthetase, and clustering of such genes were systematically reported by (**Sanz-Luque et al., 2015**). We used these data as reference for searches of nitrogen assimilation genes, and further nitrogen assimilation genes were searched by Kyoto Encyclopedia of Genes and Genomes (KEGG) pathway (**Kanehisa and Goto, 2000**). JGI genome browsers of *Chlorella variabilis* NC64A and *Coccomyxa subellipsoidea* C-169 were also used for retrieving genes and checking gene order on the scaffolds.

Phylogenetic analysis

For a phylogenetic tree of chlorophyte green algae, the sequences of 18S rRNA gene, ITS1, 5.8S rRNA gene, ITS2 and 28S rRNA gene were obtained from scaffold20 of *Chlorella* A99 genome sequence, and from NCBI nucleotide database entries for *Chlorella variabilis* NC64A (FM205849.1), *Auxenochlorella protothecoides* 0710 (NW_011934479.1), *Coccomyxa subellipsoidea* C169 (AGSI01000011.1), *Volvox carteri* f. nagariensis (NW_003307662.1), *Chlamydomonas reinhardtii* (FR865576.1), *Ostreococcus tauri* (GQ426340.1) and *Micromonas pusilla* (FN562452.1). Multiple alignments were produced with CLUSTALX (2.1) with gap trimming (**Larkin et al., 2007**). Sequences of poor quality that did not well align were deleted using BioEdit (**Hall, 1999**). Phylogenetic analyses were performed using the Neighbor-Joining method by CLUSTALX with the default parameters (1000 bootstrap tests and 111 seeds). Representative phylogenetic trees were drawn by using NJ plot (**Perrière and Gouy, 1996**).

PCR amplification of nitrate assimilation genes in green algae

Primers were designed based on the conserved region of the NRT2 gene, NiR and NR genes (positive control) identified by comparison of genes from *Chlorella variabilis* NC64A (NC64A), *Coccomyxa subellipsoidea* C169 (C169), and *Chlamydomonas reinhardtii* (Cr) which belongs to Chlorophyceae class of green algae. Primers for NAR2 could not be designed because of insufficient conservation. As positive controls, amplicons were produced for NR of all the green algae examined and of NRT2 and NiR from NC64A, C169 and Cr, after which their sequences were checked. KOD FX Neo (TOYOBO, Tokyo, Japan) was used under the following conditions: an initial denaturation phase (94˚C for 120 s) followed by 36 cycles of (98˚C for 30 s, 69˚C for 100 s) for NiR, (98˚C for 30 s, 58˚C for 30 s and 68˚C for 210 s) for NRT2 and (98˚C for 30 s, 59˚C for 30 s and 68˚C for 60 s) for NR. In each case, 10 ng gDNA was used as a template. The primers used are described in **Supplementary file 6C**. PCR products were sequenced to confirm amplification of the target genes using ABI PRISM 3100 Genetic Analyzer (Thermo Fisher Scientific Inc., Madison, USA) using BigDye Terminator v3.1 Cycle Sequencing Kit (Thermo Fisher Scientific).

In vitro culture of algae

To isolate symbiotic algae, polyps were quickly homogenized in 0.25% sodium dodecyl sulfate (SDS) solution and centrifuged at 3000 g for 1 min. The pellet was resuspended in 0.05% SDS and centrifuged at 500 g for 5 min. Isolated A99, NC64A and C169 were washed by sterilized Bold Basal Medium (**Bischoff and Bold, 1963**) modified by the addition of 0.5% glucose, 1.2 mg/L vitamine B1 (Thiaminhydrochloride), 0.01 mg/L vitamine B12 (Cyanocobalamin) (**Supplementary file 7**) and incubated for two days in modified Bold Basal Medium with 50 mg/l ampicillin and streptomycin. The algae were cultivated in 5 ml of modified Bold Basal Medium (BBM) with the same amount of nitrogen (2.9 mM $NaNO_3$, NH_4Cl, glutamine or 426 mg/l casamino acids) and 5 mg/l Carbendazim (antifungal) with fluorescent illumination (12 hr light, 12 hr dark) at 20˚C. Mean numbers of algae per ml were calculated from three tubes enumerated at 4, 8, and 12 days after inoculation with 10^6 cell/sml using a hemocytometer. After cultivation, gDNA was isolated from the A99 cultured in Gln-containing BBM and casamino acid-containing BBM and A99 was isolated from green hydra directly. A partial genomic region of the 18S rRNA gene was amplified by PCR and sequenced to confirm absence of contamination by other algae. PCR was performed using AmpliTaq Gold (Thermo Fisher

Scientific). Sequencing was performed as described above. The primers used are described in ***Supplementary file 6D***.

Acknowledgements

We thank Trudy Wassenaar for critical reading the text and for discussion. We also thank the DNA Sequencing Section, IT Section and Kanako Hisata in the Okinawa Institute of Science and Technology (OIST) for excellent technical support. The computations for this work were partially performed on the NIG supercomputer at the ROIS National Institute of Genetics. We are thankful to Angela Douglas for sustained exchanges and discussions on symbiosis in hydra and two anonymous referees for their constructive comments on a previous version of this manuscript. This work was supported in part by JSPS KAKENHI Grant-in-Aid for Young Scientists (B) 25840132 and Scientific Research (C) 15K07173 to MH. and by the Deutsche Forschungsgemeinschaft (DFG) (CRC1182 'Origin and Function of Metaorganisms'). TCGB. gratefully appreciates support from the Canadian Institute for Advanced Research (CIFAR).

Additional information

Funding

Funder	Grant reference number	Author
Japan Society for the Promotion of Science	Young Scientists (B) 25840132	Mayuko Hamada
Japan Society for the Promotion of Science	Scientific Research (C) 15K07173	Mayuko Hamada
Deutsche Forschungsgemeinschaft	CRC1182	Thomas CG Bosch

The funders had no role in study design, data collection and interpretation, or the decision to submit the work for publication.

Author contributions

Mayuko Hamada, Conceptualization, Formal analysis, Funding acquisition, Investigation, Visualization, Writing—original draft; Katja Schröder, Formal analysis, Investigation, Visualization, Writing—review and editing; Jay Bathia, Formal analysis, Investigation, Writing—review and editing; Ulrich Kürn, Formal analysis, Investigation; Sebastian Fraune, Resources, Writing—review and editing; Mariia Khalturina, Investigation, Writing—review and editing, Library preparation and genome sequencing; Konstantin Khalturin, Chuya Shinzato, Formal analysis, Writing—review and editing; Nori Satoh, Supervision, Project administration, Writing—review and editing; Thomas CG Bosch, Conceptualization, Supervision, Funding acquisition, Writing—original draft, Writing—review and editing

Author ORCIDs

Mayuko Hamada http://orcid.org/0000-0001-7306-2032
Katja Schröder http://orcid.org/0000-0003-1158-2598
Sebastian Fraune http://orcid.org/0000-0002-6940-9571
Konstantin Khalturin http://orcid.org/0000-0003-4359-2993
Chuya Shinzato http://orcid.org/0000-0001-7843-3381
Nori Satoh https://orcid.org/0000-0002-4480-3572
Thomas CG Bosch http://orcid.org/0000-0002-9488-5545

Decision letter and Author response

Decision letter https://doi.org/10.7554/eLife.35122.064
Author response https://doi.org/10.7554/eLife.35122.065

Additional files

Supplementary files

- Supplementary file 1. Results of microarray analysis and list of differentially expressed genes. Gene expression of green hydra with native symbiotic *Chlorella* A99 (Hv_Sym), that in sexual phase (Hv_Sym_sexy), aposymbiotic polyps from which symbiotic *Chlorella* were removed (Hv_Apo) and aposymbiotic polyps reinfected with *Chlorella variabilis* NC64A (Hv_NC64A) were compared.
DOI: https://doi.org/10.7554/eLife.35122.033
- Supplementary file 2. (A) Ortholog groups of Aa_trans containing protein in *Chlorella variabilis NC64A* (NC64A), *Coccomyxa subellipsoidea* C-169 (C169), *Chlamydomonas reinhardtii* (Cr), *Volvox carteri* (Vc), *Micromonas pusilla* (Mp) and *Ostreococcus tauri* (Ot). (B) Blast best hit genes of *Arabidopsis thaliana* in *Chlorella* sp. A99 genes belonging to OG0000040 and OG0000324.
DOI: https://doi.org/10.7554/eLife.35122.034
- Supplementary file 3. List of *Coccomyxa subellipsoidea* C169 (C169) and their BLAST best hit genes in *Chlamydomonas reinhardtii* (Cr), *Volvox carteri* (Vc) and *Chlorella* A99 (A99) gene model and genome scaffolds.
DOI: https://doi.org/10.7554/eLife.35122.035
- Supplementary file 4. Sequence ID of nitrogen assimilation genes in *Symbiodinium*.
DOI: https://doi.org/10.7554/eLife.35122.036
- Supplementary file 5. Sequence ID of nitrogen assimilation genes in *Chlorella variabilis NC64A* (NC64A), *Coccomyxa subellipsoidea* C-169 (C169), *Volvox carteri* (Vc), *Micromonas pusilla* (Mp) and *Ostreococcus tauri* (Ot) and *Chlamydomonas reinhardtii* (Cr).
DOI: https://doi.org/10.7554/eLife.35122.037
- Supplementary file 6. Primers used in this study, for quantitative real time RT-PCR. (A), in situ hybridization probes (B), PCR amplification of nitrogen assimilation genes in green algae (C) and PCR amplification of 18S ribosomal DNA gene in green algae (D).
DOI: https://doi.org/10.7554/eLife.35122.038
- Supplementary file 7. Composition of modified Bold's Basal Medium for one liter (pH. 7).
DOI: https://doi.org/10.7554/eLife.35122.039
- Transparent reporting form
DOI: https://doi.org/10.7554/eLife.35122.040

Data availability

Microarray information and the data series are accessible at NCBI GEO under accession number GPL23280 and GSE97633 respectively. All the results of microarray analysis are included in Supplementary Table 1. The Whole Genome Shotgun project of Chlorella sp. A99 has been deposited at DDBJ/ENA/GenBank under the accession PCFQ00000000 (BioProject ID: PRJNA412448). Genome sequences and gene models are also accessible at the website of OIST Marine Genomics Unit Genome Project (http://marinegenomics.oist.jp/chlorellaA99/viewer/info?project_id=65). All data generated by qPCR are included in Source Data: Figure2, Figure2 - Figure supplement 1, Source Data: Figure3, Source Data: Figure3 - Figure Supplement 2 and Source Data: Table 2, Table 4

The following datasets were generated:

Author(s)	Year	Dataset title	Dataset URL	Database, license, and accessibility information
Mayuko Hamada	2018	Chlorella sp. A99 genome sequence and gene models	http://marinegenomics.oist.jp/chlorellaA99/viewer/info?project_id=65	Publicly available at OIST Marine Genomics Unit (Chlorella sp. A99)
Mayuko Hamada	2018	Chlorella sp. A99 genome sequence	http://www.ncbi.nlm.nih.gov/bioproject/412448	Publicly available at NCBI BioProject (Accession no: PCFQ00000000)
Fraune S, Bosch TC	2017	Agilent-029560 Hydra viridissima transcriptome-based custom microarray	https://www.ncbi.nlm.nih.gov/geo/query/acc.cgi?acc=GPL23280	Publicly available at the NCBI Gene Expression Omnibus

				(accession no: GPL23280)
Fraune S, Kürn U, Bosch TC	2017	Identification of genes involved in symbiosis of green hydra and Chlorella	https://www.ncbi.nlm.nih.gov/geo/query/acc.cgi?acc=GSE97633	Publicly available at the NCBI Gene Expression Omnibus (accession no: GSE97633)

The following previously published datasets were used:

Author(s)	Year	Dataset title	Dataset URL	Database, license, and accessibility information
Blanc G, Duncan G, Agarkova I, Borodovsky M, Gurnon J, Kuo A, Lindquist E, Lucas S, Pangilinan J, Polle J, Salamov A, Terry A, Yamada T, Dunigan DD, Grigoriev IV, Claverie JM, Van Etten JL	2010	The Chlorella variabilis NC64A genome reveals adaptation to photosymbiosis, coevolution with viruses, and cryptic sex	https://genome.jgi.doe.gov/ChlNC64A_1/ChlNC64A_1.home.html	Publicly available at JGI MycoCosm (Chlorella variabilis NC64A)
Blanc G, Agarkova I, Grimwood J, Kuo A, Brueggeman A, Dunigan DD, Gurnon J, Ladunga I, Lindquist E, Lucas S, Pangilinan J, Proschold T, Salamov A, Schmutz J, Weeks D, Yamada T, Lomsadze A, Borodovsky M, Claverie JM, Grigoriev IV, Van Etten JL	2012	The genome of the polar eukaryotic microalga Coccomyxa subellipsoidea reveals traits of cold adaptation	https://genome.jgi.doe.gov/Coc_C169_1/Coc_C169_1.home.html	Publicly available at JGI MycoCosm (Coccomyxa subellipsoidea C-169 v2.0)
Prochnik SE, Umen J, Nedelcu AM, Hallmann A, Miller SM, Nishii I, Ferris P, Kuo A, Mitros T, Fritz-Laylin LK, Hellsten U, Chapman J, Simakov O, Rensing SA, Terry A, Pangilinan J, Kapitonov V, Jurka J, Salamov A, Shapiro H, Schmutz J, Grimwood J, Lindquist E, Lucas S, Grigoriev IV, Schmitt R, Kirk D, Rokhsar DS	2010	Genomic analysis of organismal complexity in the multicellular green alga Volvox carteri	https://phytozome.jgi.doe.gov/pz/portal.html#!info?alias=Org_Vcarteri	Publicly available at JGI Phytozome (Volvox carteri v2.1)
Merchant SS, Prochnik SE, Vallon O, Harris EH, Karpowicz SJ, Witman, GB, Terry A, Salamov, A, Fritz-Laylin LK, Marechal-Drouard L, Marshall WF, Qu LH, Nelson DR, Sanderfoot AA, Spalding MH, Kapitonov VV, Ren Q, Ferris P, Lindquist	2007	The Chlamydomonas genome reveals the evolution of key animal and plant functions	http://phytozome.jgi.doe.gov/pz/portal.html	Publicly available at JGI Phytozome (Chlamydomonas reinhardtii v5.5)

E, Shapiro H, Lucas SM, Grimwood J, Schmutz J, Cardol P, Cerutti H, Chanfreau G, Chen CL, Cognat V, Croft MT, Dent R, Dutcher S, Fernandez E, Fukuzawa H, Gonzalez-Ballester D, Gonzalez-Halphen D, Hallmann A, Hanikenne M, Hippler M, Inwood W, Jabbari K, Kalanon M, Kuras R, Lefebvre PA, Lemaire SD, Lobanov AV, Lohr M, Manuell A, Meier I, Mets L, Mittag M, Mittelmeier T, Moroney JV, Moseley J, Napoli C, Nedelcu AM, Niyogi K, Novoselov SV, Paulsen IT, Pazour G, Purton S, Ral JP, Riano-Pachon DM, Riekhof W, Rymarquis L, Schroda M, Stern D, Umen J, Willows R, Wilson N, Zimmer SL, Allmer J, Balk J, Bisova K, Chen CJ, Elias M, Gendler K, Hauser C, Lamb MR, Ledford H, Long JC, Minagawa J, Page MD, Pan J, Pootakham W, Roje S, Rose A, Stahlberg E, Terauchi AM, Yang P, Ball S, Bowler C, Dieckmann CL, Gladyshev VN, Green P, Jorgensen R, Mayfield S, Mueller-Roeber B, Rajamani S, Sayre RT, Brokstein P, Dubchak I, Goodstein D, Hornick L, Huang YW, Jhaveri J, Luo Y, Martinez D, Ngau WC, Otillar B, Poliakov A, Porter A, Szajkowski L, Werner G, Zhou, K, Grigoriev IV, Rokhsar DS, Grossman AR				
Worden AZ, Lee JH, Mock T, Rouze P, Simmons MP, Aerts AL, Allen AE, Cuvelier ML, Derelle E, Everett MV, Foulon E, Grimwood J, Gundlach H, Henrissat B,	2009	Green evolution and dynamic adaptations revealed by genomes of the marine picoeukaryotes Micromonas	https://genome.jgi.doe.gov/MicpuC2/MicpuC2.home.html	Publicly available at JGI MycoCosm (Micromonas pusilla CCMP1545)

Napoli C, McDonald SM, Parker MS, Rombauts S, Salamov A, Von Dassow P, Badger JH, Coutinho PM, Demir E, Dubchak I, Gentemann C, Eikrem W, Gready JE, John U, Lanier W, Lindquist EA, Lucas S, Mayer KF, Moreau H, Not F, Otillar R, Panaud O, Pangilinan J, Paulsen I, Piegu B, Poliakov A, Robbens S, Schmutz J, Toulza E, Wyss T, Zelensky A, Zhou K, Armbrust EV, Bhattacharya D, Goodenough UW, Van de Peer Y, Grigoriev IV				
Palenik B, Grimwood J, Aerts A, Rouze P, Salamov A, Putnam N, Dupont C, Jorgensen R, Derelle E, Rombauts S, Zhou K, Otillar R, Merchant SS, Podell S, Gaasterland T, Napoli C, Gendler K, Manuell A, Tai V, Vallon O, Piganeau G, Jancek S, Heijde M, Jabbari K, Bowler C, Lohr M, Robbens S, Werner G, Dubchak I, Pazour GJ, Ren Q, Paulsen I, Delwiche C, Schmutz J, Rokhsar D, Van de Peer Y, Moreau H, Grigoriev IV	2007	The tiny eukaryote Ostreococcus provides genomic insights into the paradox of plankton speciation	https://genome.jgi.doe.gov/Ostta4221_3/Ostta4221_3.home.html	Publicly available at JGI MycoCosm (Ostreococcus tauri RCC4221 v3.0)
Finn RD, Coggill P, Eberhardt RY, Eddy SR, Mistry J, Mitchell AL, Potter SC, Punta M, Qureshi M, Sangrador-Vegas A, Salazar GA, Tate J, Bateman A	2016	The Pfam protein families database: towards a more sustainable future. Nucleic Acids Res. 44, D279-285. 10.1093/nar/gkv1344.	ftp://ftp.ebi.ac.uk/pub/databases/Pfam/releases/Pfam31.0/	Available to download at the ftp site. (dataset name: Pfam-A.hmm)

References

Aranda M, Li Y, Liew YJ, Baumgarten S, Simakov O, Wilson MC, Piel J, Ashoor H, Bougouffa S, Bajic VB, Ryu T, Ravasi T, Bayer T, Micklem G, Kim H, Bhak J, LaJeunesse TC, Voolstra CR. 2016. Genomes of coral dinoflagellate symbionts highlight evolutionary adaptations conducive to a symbiotic lifestyle. *Scientific Reports* **6**:39734. DOI: https://doi.org/10.1038/srep39734, PMID: 28004835

Ashburner M, Ball CA, Blake JA, Botstein D, Butler H, Cherry JM, Davis AP, Dolinski K, Dwight SS, Eppig JT, Harris MA, Hill DP, Issel-Tarver L, Kasarskis A, Lewis S, Matese JC, Richardson JE, Ringwald M, Rubin GM, Sherlock G. 2000. Gene ontology: tool for the unification of biology. *Nature Genetics* **25**:25–29. DOI: https://doi.org/10.1038/75556

Barott KL, Venn AA, Perez SO, Tambutté S, Tresguerres M. 2015. Coral host cells acidify symbiotic algal microenvironment to promote photosynthesis. *PNAS* **112**:607–612. DOI: https://doi.org/10.1073/pnas.1413483112, PMID: 25548188

Baumgarten S, Simakov O, Esherick LY, Liew YJ, Lehnert EM, Michell CT, Li Y, Hambleton EA, Guse A, Oates ME, Gough J, Weis VM, Aranda M, Pringle JR, Voolstra CR. 2015. The genome of *Aiptasia*, a sea anemone model for coral symbiosis. *PNAS* **112**:11893–11898. DOI: https://doi.org/10.1073/pnas.1513318112, PMID: 26324906

Bischoff HW, Bold HC. 1963. *Some Soil Algae From Enchanted Rock and Related Algal Species*. Austin: University of Texas.

Blanc G, Agarkova I, Grimwood J, Kuo A, Brueggeman A, Dunigan DD, Gurnon J, Ladunga I, Lindquist E, Lucas S, Pangilinan J, Pröschold T, Salamov A, Schmutz J, Weeks D, Yamada T, Lomsadze A, Borodovsky M, Claverie JM, Grigoriev IV, et al. 2012. The genome of the polar eukaryotic microalga coccomyxa subellipsoidea reveals traits of cold adaptation. *Genome Biology* **13**:R39. DOI: https://doi.org/10.1186/gb-2012-13-5-r39, PMID: 22630137

Blanc G, Duncan G, Agarkova I, Borodovsky M, Gurnon J, Kuo A, Lindquist E, Lucas S, Pangilinan J, Polle J, Salamov A, Terry A, Yamada T, Dunigan DD, Grigoriev IV, Claverie JM, Van Etten JL. 2010. The *chlorella variabilis* NC64A genome reveals adaptation to photosymbiosis, coevolution with viruses, and cryptic sex. *The Plant Cell* **22**:2943–2955. DOI: https://doi.org/10.1105/tpc.110.076406, PMID: 20852019

Boetzer M, Henkel CV, Jansen HJ, Butler D, Pirovano W. 2011. Scaffolding pre-assembled contigs using SSPACE. *Bioinformatics* **27**:578–579. DOI: https://doi.org/10.1093/bioinformatics/btq683, PMID: 21149342

Bosch TC, Augustin R, Anton-Erxleben F, Fraune S, Hemmrich G, Zill H, Rosenstiel P, Jacobs G, Schreiber S, Leippe M, Stanisak M, Grötzinger J, Jung S, Podschun R, Bartels J, Harder J, Schröder JM. 2009. Uncovering the evolutionary history of innate immunity: the simple metazoan Hydra uses epithelial cells for host defence. *Developmental & Comparative Immunology* **33**:559–569. DOI: https://doi.org/10.1016/j.dci.2008.10.004, PMID: 19013190

Bossert P, Dunn KW. 1986. Regulation of intracellular algae by various strains of the symbiotic Hydra viridissima. *Journal of Cell Science* **85**:187–195. PMID: 3793792

Brown JA, Nielsen PJ. 1974. Transfer of photosynthetically produced carbohydrate from endosymbiotic chlorellae to *Paramecium bursaria*. *The Journal of Protozoology* **21**:569–570. DOI: https://doi.org/10.1111/j.1550-7408.1974.tb03702.x, PMID: 4214362

Brown SB, Maloney M, Kinlaw WB. 1997. "Spot 14" protein functions at the pretranslational level in the regulation of hepatic metabolism by thyroid hormone and glucose. *Journal of Biological Chemistry* **272**:2163–2166. DOI: https://doi.org/10.1074/jbc.272.4.2163, PMID: 8999918

Campbell RD. 1990. Transmission of symbiotic algae through sexual reproduction in hydra: movement of algae into the oocyte. *Tissue and Cell* **22**:137–147. DOI: https://doi.org/10.1016/0040-8166(90)90017-4, PMID: 18620296

Cernichiari E, Muscatine L, Smith DC. 1969. Maltose excretion by the symbiotic algae of Hydra viridis. *Proceedings of the Royal Society B: Biological Sciences* **173**:557–576. DOI: https://doi.org/10.1098/rspb.1969.0077

Conesa A, Götz S, García-Gómez JM, Terol J, Talón M, Robles M. 2005. Blast2GO: a universal tool for annotation, visualization and analysis in functional genomics research. *Bioinformatics* **21**:3674–3676. DOI: https://doi.org/10.1093/bioinformatics/bti610, PMID: 16081474

Cook CB, Kelty MO. 1982. Glycogen, protein, and lipid content of green, aposymbiotic, and nonsymbiotic hydra during starvation. *Journal of Experimental Zoology* **222**:1–9. DOI: https://doi.org/10.1002/jez.1402220102

Császár NBM, Seneca FO, van Oppen MJH. 2009. Variation in antioxidant gene expression in the scleractinian coral Acropora millepora under laboratory thermal stress. *Marine Ecology Progress Series* **392**:93–102. DOI: https://doi.org/10.3354/meps08194

Davy SK, Allemand D, Weis VM. 2012. Cell biology of cnidarian-dinoflagellate symbiosis. *Microbiology and Molecular Biology Reviews* **76**:229–261. DOI: https://doi.org/10.1128/MMBR.05014-11, PMID: 22688813

Dorling M, McAuley PJ, Hodge H. 1997. Effect of pH on growth and carbon metabolism of maltose-releasing *Chlorella* (Chlorophyta). *European Journal of Phycology* **32**:19–24. DOI: https://doi.org/10.1080/09541449710001719335

Douglas A, Smith DC. 1984. The green hydra symbiosis. VIII. mechanisms in symbiont regulation. *Proceedings of the Royal Society B: Biological Sciences* **221**:291–319. DOI: https://doi.org/10.1098/rspb.1984.0035

Douglas AE, Smith DC. 1983. *The Cost of Symbionts to the Host in the Green Hydra Symbiosis*. Berlin: W. DeGriiyter and Co.

Douglas AE. 1994. *Symbiotic Interactions*. Oxford; New York: Oxford University Press.

Eddy SR. 1998. Profile hidden markov models. *Bioinformatics* **14**:755–763. DOI: https://doi.org/10.1093/bioinformatics/14.9.755, PMID: 9918945

Emms DM, Kelly S. 2015. OrthoFinder: solving fundamental biases in whole genome comparisons dramatically improves orthogroup inference accuracy. *Genome Biology* **16**:157. DOI: https://doi.org/10.1186/s13059-015-0721-2, PMID: 26243257

Falkowski PG, Dubinsky Z, Muscatine L, McCloskey L. 1993. Population control in symbiotic corals. *BioScience* **43**:606–611. DOI: https://doi.org/10.2307/1312147

Finn RD, Coggill P, Eberhardt RY, Eddy SR, Mistry J, Mitchell AL, Potter SC, Punta M, Qureshi M, Sangrador-Vegas A, Salazar GA, Tate J, Bateman A. 2016. The pfam protein families database: towards a more

sustainable future. *Nucleic Acids Research* **44**:D279–D285. DOI: https://doi.org/10.1093/nar/gkv1344, PMID: 26673716

Ganot P, Moya A, Magnone V, Allemand D, Furla P, Sabourault C. 2011. Adaptations to endosymbiosis in a cnidarian-dinoflagellate association: differential gene expression and specific gene duplications. *PLoS Genetics* **7**:e1002187. DOI: https://doi.org/10.1371/journal.pgen.1002187, PMID: 21811417

Gao C, Wang Y, Shen Y, Yan D, He X, Dai J, Wu Q. 2014. Oil accumulation mechanisms of the oleaginous microalga chlorella protothecoides revealed through its genome, transcriptomes, and proteomes. *BMC Genomics* **15**:582. DOI: https://doi.org/10.1186/1471-2164-15-582, PMID: 25012212

Grasso LC, Maindonald J, Rudd S, Hayward DC, Saint R, Miller DJ, Ball EE. 2008. Microarray analysis identifies candidate genes for key roles in coral development. *BMC Genomics* **9**:540. DOI: https://doi.org/10.1186/1471-2164-9-540, PMID: 19014561

Grover R, Maguer J-F, Allemand D, Ferrier-Pagés C. 2003. Nitrate uptake in the scleractinian coral *Stylophora pistillata*. *Limnology and Oceanography* **48**:2266–2274 . DOI: https://doi.org/10.4319/lo.2003.48.6.2266

Habetha M, Anton-Erxleben F, Neumann K, Bosch TC. 2003. The Hydra viridis/Chlorella symbiosis. growth and sexual differentiation in polyps without symbionts. *Zoology* **106**:101–108. DOI: https://doi.org/10.1078/0944-2006-00104, PMID: 16351895

Habetha M, Bosch TC. 2005. Symbiotic Hydra express a plant-like peroxidase gene during oogenesis. *Journal of Experimental Biology* **208**:2157–2165. DOI: https://doi.org/10.1242/jeb.01571, PMID: 15914659

Hall TA. 1999. BioEdit: a user-friendly biological sequence alignment editor and analysis program for windows 95/98/NT. *Nucleic Acid Symposium Series* **41**:95–98.

Hansen AK, Moran NA. 2011. Aphid genome expression reveals host-symbiont cooperation in the production of amino acids. *Proceedings of the National Academy of Sciences* **108**:2849–2854. DOI: https://doi.org/10.1073/pnas.1013465108, PMID: 21282658

Hoving JC, Wilson GJ, Brown GD. 2014. Signalling C-type lectin receptors, microbial recognition and immunity. *Cellular Microbiology* **16**:185–194. DOI: https://doi.org/10.1111/cmi.12249, PMID: 24330199

Huss VAR, Holweg C, Seidel B, Reich V, Rahat M, Kessler E. 1994. There is an ecological basis for host/symbiont specificity in chlorella/Hydra symbioses. *Endocytobiosis and Cell Research* **10**:35–46.

Ishikawa M, Yuyama I, Shimizu H, Nozawa M, Ikeo K, Gojobori T. 2016. Different endosymbiotic interactions in two Hydra species reflect the evolutionary history of endosymbiosis. *Genome Biology and Evolution* **8**:2155–2163. DOI: https://doi.org/10.1093/gbe/evw142, PMID: 27324918

Joy JB. 2013. Symbiosis catalyses niche expansion and diversification. *Proceedings of the Royal Society B: Biological Sciences* **280**:20122820. DOI: https://doi.org/10.1098/rspb.2012.2820

Kamako S, Imamura N. 2006. Effect of Japanese paramecium bursaria extract on photosynthetic carbon fixation of symbiotic algae. *The Journal of Eukaryotic Microbiology* **53**:136–141. DOI: https://doi.org/10.1111/j.1550-7408.2005.00084.x, PMID: 16579816

Kamako S-ichiro, Hoshina R, Ueno S, Imamura N. 2005. Establishment of axenic endosymbiotic strains of Japanese Paramecium bursaria and the utilization of carbohydrate and nitrogen compounds by the isolated algae. *European Journal of Protistology* **41**:193–202. DOI: https://doi.org/10.1016/j.ejop.2005.04.001

Kanehisa M, Goto S. 2000. KEGG: kyoto encyclopedia of genes and genomes. *Nucleic Acids Research* **28**:27–30. DOI: https://doi.org/10.1093/nar/28.1.27, PMID: 10592173

Kapaun E, Reisser W. 1995. A chitin-like glycan in the cell wall of a chlorella sp. (Chlorococcales, chlorophyceae). *Planta* **197**:577–582. DOI: https://doi.org/10.1007/BF00191563

Karakashian SJ, Karakashian MW. 1965. Evolution and symbiosis in the genus *Chlorella* and related algae. *Evolution* **19**:368–377 . DOI: https://doi.org/10.1111/j.1558-5646.1965.tb01728.x

Kawaida H, Ohba K, Koutake Y, Shimizu H, Tachida H, Kobayakawa Y. 2013. Symbiosis between Hydra and chlorella: molecular phylogenetic analysis and experimental study provide insight into its origin and evolution. *Molecular Phylogenetics and Evolution* **66**:906–914. DOI: https://doi.org/10.1016/j.ympev.2012.11.018, PMID: 23219706

Kellogg RB, Patton JS. 1983. Lipid droplets, medium of energy exchange in the symbiotic Anemone condylactis gigantea: a model coral polyp. *Marine Biology* **75**:137–149. DOI: https://doi.org/10.1007/BF00405996

Khalturin K, Hemmrich G, Fraune S, Augustin R, Bosch TC. 2009. More than just orphans: are taxonomically-restricted genes important in evolution? *Trends in Genetics* **25**:404–413. DOI: https://doi.org/10.1016/j.tig.2009.07.006, PMID: 19716618

Kishimoto Y, Murate M, Sugiyama T. 1996. Hydra regeneration from recombined ectodermal and endodermal tissue. I. Epibolic ectodermal spreading is driven by cell intercalation. *Journal of Cell Science* **109**:763–772. PMID: 8718667

Kodama Y, Suzuki H, Dohra H, Sugii M, Kitazume T, Yamaguchi K, Shigenobu S, Fujishima M. 2014. Comparison of gene expression of Paramecium bursaria with and without chlorella variabilis symbionts. *BMC Genomics* **15**:183. DOI: https://doi.org/10.1186/1471-2164-15-183, PMID: 24612690

Krapp A, David LC, Chardin C, Girin T, Marmagne A, Leprince AS, Chaillou S, Ferrario-Méry S, Meyer C, Daniel-Vedele F. 2014. Nitrate transport and signalling in Arabidopsis. *Journal of Experimental Botany* **65**:789–798. DOI: https://doi.org/10.1093/jxb/eru001, PMID: 24532451

Larkin MA, Blackshields G, Brown NP, Chenna R, McGettigan PA, McWilliam H, Valentin F, Wallace IM, Wilm A, Lopez R, Thompson JD, Gibson TJ, Higgins DG. 2007. Clustal W and clustal X version 2.0. *Bioinformatics* **23**:2947–2948. DOI: https://doi.org/10.1093/bioinformatics/btm404, PMID: 17846036

Lehnert EM, Mouchka ME, Burriesci MS, Gallo ND, Schwarz JA, Pringle JR. 2014. Extensive differences in gene expression between symbiotic and aposymbiotic cnidarians. *G3: Genes|Genomes|Genetics* **4**:277–295. DOI: https://doi.org/10.1534/g3.113.009084

Lesser MP. 2006. Oxidative stress in marine environments: biochemistry and physiological ecology. *Annual Review of Physiology* **68**:253–278. DOI: https://doi.org/10.1146/annurev.physiol.68.040104.110001, PMID: 16460273

Lewis DH, Smith DC. 1971. The autotrophic nutrition of symbiotic marine coelenterates with special reference to hermatypic corals. I. Movement of photosynthetic products between the symbionts. *Proceedings of the Royal Society B: Biological Sciences* **178**:111–129. DOI: https://doi.org/10.1098/rspb.1971.0055

Liaw SH, Kuo I, Eisenberg D. 1995. Discovery of the ammonium substrate site on glutamine synthetase, a third cation binding site. *Protein Science* **4**:2358–2365. DOI: https://doi.org/10.1002/pro.5560041114, PMID: 8563633

Lin KL, Wang JT, Fang LS. 2000. Participation of glycoproteins on zooxanthellal cell walls in the establishment of a symbiotic relationship with the Sea Anemone, aiptasia pulchella. *Zoological Studies* **39**:172–178.

Lin S, Cheng S, Song B, Zhong X, Lin X, Li W, Li L, Zhang Y, Zhang H, Ji Z, Cai M, Zhuang Y, Shi X, Lin L, Wang L, Wang Z, Liu X, Yu S, Zeng P, Hao H, et al. 2015. The Symbiodinium kawagutii genome illuminates dinoflagellate gene expression and coral symbiosis. *Science* **350**:691–694. DOI: https://doi.org/10.1126/science.aad0408, PMID: 26542574

Lipschultz F, Cook CB. 2002. Uptake and assimilation of 15N-ammonium by the symbiotic sea anemones Bartholomea annulata and Aiptasia pallida: conservation versus recycling of nitrogen. *Marine Biology* **140**:489–502 . DOI: https://doi.org/10.1007/s00227-001-0717-1

Lucas WJ, Berry JA. 1985. Inorganic carbon transport in aquatic photosynthetic organisms. *Physiologia Plantarum* **65**:539–543. DOI: https://doi.org/10.1111/j.1399-3054.1985.tb08687.x

Luo R, Liu B, Xie Y, Li Z, Huang W, Yuan J, He G, Chen Y, Pan Q, Liu Y, Tang J, Wu G, Zhang H, Shi Y, Liu Y, Yu C, Wang B, Lu Y, Han C, Cheung DW, et al. 2012. SOAPdenovo2: an empirically improved memory-efficient short-read de novo assembler. *GigaScience* **1**:18. DOI: https://doi.org/10.1186/2047-217X-1-18

Martínez DE, Iñiguez AR, Percell KM, Willner JB, Signorovitch J, Campbell RD. 2010. Phylogeny and biogeography of Hydra (Cnidaria: Hydridae) using mitochondrial and nuclear DNA sequences. *Molecular Phylogenetics and Evolution* **57**:403–410. DOI: https://doi.org/10.1016/j.ympev.2010.06.016

Marçais G, Kingsford C. 2011. A fast, lock-free approach for efficient parallel counting of occurrences of k-mers. *Bioinformatics* **27**:764–770. DOI: https://doi.org/10.1093/bioinformatics/btr011

McAuley PJ, Smith DC. 1982. The green Hydra symbiosis. V. Stages in the intracellular recognition of algal symbionts by digestive cells. *Proceedings of the Royal Society B: Biological Sciences* **216**:7–23. DOI: https://doi.org/10.1098/rspb.1982.0058

McAuley PJ. 1986. Isolation of viable uncontaminated *chlorella* from green hydra1. *Limnology and Oceanography* **31**:222–224 . DOI: https://doi.org/10.4319/lo.1986.31.1.0222

McAuley PJ. 1986a. The cell cycle of symbiotic Chlorella. III. Numbers of algae in green hydra digestive cells are regulated at digestive cell division. *Journal of cell science* **85**:63–71.

McAuley PJ. 1987a. Nitrogen limitation and amino-acid metabolism of Chlorella symbiotic with green hydra. *Planta* **171**:532–538. DOI: https://doi.org/10.1007/BF00392303

McAuley PJ. 1987b. Quantitative estimation of movement of an amino acid from host to *Chlorella* symbionts in green hydra. *The Biological Bulletin* **173**:504–512. DOI: https://doi.org/10.2307/1541696, PMID: 29320223

McAuley PJ. 1991. Amino acids as a nitrogen source for Chlorella symbiotic with green hydra. In: Williams R. B, Cornelius P. F. S, Hughes R. G, Robson E. A (Eds). *Coelenterate Biology: Recent Research on Cnidaria and Ctenophora: Proceedings of the Fifth International Conference on Coelenterate Biology, 1989*. Dordrecht: Springer Netherlands. p. 369–376 . DOI: https://doi.org/10.1007/978-94-011-3240-4_53

McFall-Ngai M, Hadfield MG, Bosch TC, Carey HV, Domazet-Lošo T, Douglas AE, Dubilier N, Eberl G, Fukami T, Gilbert SF, Hentschel U, King N, Kjelleberg S, Knoll AH, Kremer N, Mazmanian SK, Metcalf JL, Nealson K, Pierce NE, Rawls JF, et al. 2013. Animals in a bacterial world, a new imperative for the life sciences. *PNAS* **110**:3229–3236. DOI: https://doi.org/10.1073/pnas.1218525110, PMID: 23391737

Meints RH, Pardy RL. 1980. Quantitative demonstration of cell surface involvement in a plant-animal symbiosis: lectin inhibition of reassociation. *Journal of Cell Science* **43**:239–251. PMID: 7419619

Merchant SS, Prochnik SE, Vallon O, Harris EH, Karpowicz SJ, Witman GB, Terry A, Salamov A, Fritz-Laylin LK, Maréchal-Drouard L, Marshall WF, Qu LH, Nelson DR, Sanderfoot AA, Spalding MH, Kapitonov VV, Ren Q, Ferris P, Lindquist E, Shapiro H, et al. 2007. The Chlamydomonas genome reveals the evolution of key animal and plant functions. *Science* **318**:245–250. DOI: https://doi.org/10.1126/science.1143609, PMID: 17932292

Mews LK, Smith DC. 1982. The green Hydra symbiosis. VI. What is the role of maltose transfer from alga to animal? proceedings of the royal society of London. *Series B: Biological Sciences* **216**:397–413. DOI: https://doi.org/10.1098/rspb.1982.0083

Mews LK. 1980. The green hydra symbiosis. III. The biotrophic transport of carbohydrate from alga to animal. *Proceedings of the Royal Society B: Biological Sciences* **209**:377–401. DOI: https://doi.org/10.1098/rspb.1980.0101

Meyer E, Weis VM. 2012. Study of cnidarian-algal symbiosis in the "omics" age. *The Biological Bulletin* **223**:44–65. DOI: https://doi.org/10.1086/BBLv223n1p44, PMID: 22983032

Miller DJ, Yellowlees D. 1989. Inorganic nitrogen uptake by symbiotic marine cnidarians: a critical review. *Proceedings of the Royal Society B: Biological Sciences* **237**:109–125. DOI: https://doi.org/10.1098/rspb.1989.0040

Mohamed AR, Cumbo V, Harii S, Shinzato C, Chan CX, Ragan MA, Bourne DG, Willis BL, Ball EE, Satoh N, Miller DJ. 2016. The transcriptomic response of the coral *Acropora digitifera* to a competent *Symbiodinium* strain: the symbiosome as an arrested early phagosome. *Molecular Ecology* **25**:3127–3141. DOI: https://doi.org/10.1111/mec.13659, PMID: 27094992

Montalbetti N, Cantero MR, Dalghi MG, Cantiello HF. 2008. Reactive oxygen species inhibit polycystin-2 (TRPP2) cation channel activity in term human syncytiotrophoblast. *Placenta* **29**:510–518. DOI: https://doi.org/10.1016/j.placenta.2008.02.015, PMID: 18417208

Moran NA. 2007. Symbiosis as an adaptive process and source of phenotypic complexity. *PNAS* **104**:8627–8633. DOI: https://doi.org/10.1073/pnas.0611659104, PMID: 17494762

Murer H, Biber J. 1996. Molecular mechanisms of renal apical na/phosphate cotransport. *Annual Review of Physiology* **58**:607–618. DOI: https://doi.org/10.1146/annurev.ph.58.030196.003135, PMID: 8815811

Muscatine L, Cernichiari E. 1969. Assimilation of photosynthetic products of zooxanthellae by a reef coral. *The Biological Bulletin* **137**:506–523. DOI: https://doi.org/10.2307/1540172, PMID: 28368714

Muscatine L, Lenhoff HM. 1963. Symbiosis: on the role of algae symbiotic with Hydra. *Science* **142**:956–958. DOI: https://doi.org/10.1126/science.142.3594.956, PMID: 17753799

Muscatine L, Lenhoff HM. 1965a. Symbiosis of Hydra and algae. I. Effects of some environmental cations on growth of symbiotic and aposymbiotic Hydra. *The Biological Bulletin* **128**:415–424. DOI: https://doi.org/10.2307/1539903

Muscatine L, Lenhoff HM. 1965b. Symbiosis of Hydra and algae. II. Effects of limited food and starvation on growth of symbiotic and aposymbiotic Hydra. *The Biological Bulletin* **129**:316–328. DOI: https://doi.org/10.2307/1539848

Muscatine L, McAuley PJ. 1982. Transmission of symbiotic algae to eggs of green Hydra. *Cytobios* **33**:111–124. PMID: 7105843

Muscatine L, Porter JW. 1977. Reef corals: mutualistic symbioses adapted to Nutrient-Poor environments. *BioScience* **27**:454–460. DOI: https://doi.org/10.2307/1297526

Muscatine L. 1965. Symbiosis of Hydra and algae—III. Extracellular products of the algae. *Comparative Biochemistry and Physiology* **16**:77–92. DOI: https://doi.org/10.1016/0010-406X(65)90165-9, PMID: 4379313

Muscatine L. 1983. *Hydra: Research Methods*. New York: Plenum Press.

Nichols HW, Bold HC. 1965. Trichosarcina polymorpha Gen. et sp. nov. *Journal of Phycology* **1**:34–38. DOI: https://doi.org/10.1111/j.1529-8817.1965.tb04552.x

Ochman H, Moran NA. 2001. Genes lost and genes found: evolution of bacterial pathogenesis and symbiosis. *Science* **292**:1096–1099. DOI: https://doi.org/10.1126/science.1058543, PMID: 11352062

Palenik B, Grimwood J, Aerts A, Rouzé P, Salamov A, Putnam N, Dupont C, Jorgensen R, Derelle E, Rombauts S, Zhou K, Otillar R, Merchant SS, Podell S, Gaasterland T, Napoli C, Gendler K, Manuell A, Tai V, Vallon O, et al. 2007. The tiny eukaryote Ostreococcus provides genomic insights into the paradox of plankton speciation. *PNAS* **104**:7705–7710. DOI: https://doi.org/10.1073/pnas.0611046104, PMID: 17460045

Pardy RL. 1976. The morphology of green Hydra endosymbionts as influenced by host strain and host environment. *Journal of Cell Science* **20**:655–669. PMID: 178679

Parra G, Bradnam K, Korf I. 2007. CEGMA: a pipeline to accurately annotate core genes in eukaryotic genomes. *Bioinformatics* **23**:1061–1067. DOI: https://doi.org/10.1093/bioinformatics/btm071, PMID: 17332020

Perrière G, Gouy M. 1996. WWW-query: an on-line retrieval system for biological sequence banks. *Biochimie* **78**:364–369. DOI: https://doi.org/10.1016/0300-9084(96)84768-7, PMID: 8905155

Pombert JF, Blouin NA, Lane C, Boucias D, Keeling PJ. 2014. A lack of parasitic reduction in the obligate parasitic green alga Helicosporidium. *PLoS Genetics* **10**:e1004355. DOI: https://doi.org/10.1371/journal.pgen.1004355, PMID: 24809511

Prochnik SE, Umen J, Nedelcu AM, Hallmann A, Miller SM, Nishii I, Ferris P, Kuo A, Mitros T, Fritz-Laylin LK, Hellsten U, Chapman J, Simakov O, Rensing SA, Terry A, Pangilinan J, Kapitonov V, Jurka J, Salamov A, Shapiro H, et al. 2010. Genomic analysis of organismal complexity in the multicellular green alga Volvox carteri. *Science* **329**:223–226. DOI: https://doi.org/10.1126/science.1188800, PMID: 20616280

Quesada A, Galván A, Fernández E. 1994. Identification of nitrate transporter genes in Chlamydomonas reinhardtii. *The Plant Journal* **5**:407–419. DOI: https://doi.org/10.1111/j.1365-313X.1994.00407.x, PMID: 8180624

Rahat M, Reich V. 1984. Intracellular infection of aposymbiotic Hydra viridis by a foreign free-living chlorella sp.: initiation of a stable symbiosis. *Journal of Cell Science* **65**:265–277. PMID: 6715427

Rees TAV, Ellard FM. 1989. Nitrogen conservation and the green Hydra symbiosis. *Proceedings of the Royal Society B: Biological Sciences* **236**:203–212. DOI: https://doi.org/10.1098/rspb.1989.0021

Rees TAV. 1986. The green Hydra symbiosis and ammonium I. the role of the host in ammonium assimilation and its possible regulatory significance. *Proceedings of the Royal Society B: Biological Sciences* **229**:299–314. DOI: https://doi.org/10.1098/rspb.1986.0087

Rees TAV. 1989. The green Hydra symbiosis and Ammonium II. ammonium assimilation and release by freshly isolated symbionts and cultured algae. *Proceedings of the Royal Society B: Biological Sciences* **235**:365–382. DOI: https://doi.org/10.1098/rspb.1989.0005

Rees TAV. 1991. Are symbiotic algae nutrient deficient? *Proceedings of the Royal Society B: Biological Sciences* **243**:227–233. DOI: https://doi.org/10.1098/rspb.1991.0036

Richier S, Furla P, Plantivaux A, Merle PL, Allemand D. 2005. Symbiosis-induced adaptation to oxidative stress. *Journal of Experimental Biology* **208**:277–285. DOI: https://doi.org/10.1242/jeb.01368, PMID: 15634847

Roffman B, Lenhoff HM. 1969. Formation of polysaccharides by Hydra from substrates produced by their endosymbiotic algae. *Nature* **221**:381–382. DOI: https://doi.org/10.1038/221381a0, PMID: 4387768

Sanz-Luque E, Chamizo-Ampudia A, Llamas A, Galvan A, Fernandez E. 2015. Understanding nitrate assimilation and its regulation in microalgae. *Frontiers in Plant Science* **6**:899. DOI: https://doi.org/10.3389/fpls.2015.00899, PMID: 26579149

Schwarz JA, Brokstein PB, Voolstra C, Terry AY, Manohar CF, Miller DJ, Szmant AM, Coffroth MA, Medina M. 2008. Coral life history and symbiosis: functional genomic resources for two reef building caribbean corals, Acropora palmata and Montastraea faveolata. *BMC Genomics* **9**:97. DOI: https://doi.org/10.1186/1471-2164-9-97, PMID: 18298846

Schwentner M, Bosch TC. 2015. Revisiting the age, evolutionary history and species level diversity of the genus Hydra (Cnidaria: hydrozoa). *Molecular Phylogenetics and Evolution* **91**:41–55. DOI: https://doi.org/10.1016/j.ympev.2015.05.013, PMID: 26014206

Shigenobu S, Watanabe H, Hattori M, Sakaki Y, Ishikawa H. 2000. Genome sequence of the endocellular bacterial symbiont of aphids Buchnera sp. APS.. *Nature* **407**:81–87. DOI: https://doi.org/10.1038/35024074, PMID: 10993077

Shinzato C, Inoue M, Kusakabe M. 2014. A snapshot of a coral "holobiont": a transcriptome assembly of the scleractinian coral, porites, captures a wide variety of genes from both the host and symbiotic zooxanthellae. *PLoS ONE* **9**:e85182. DOI: https://doi.org/10.1371/journal.pone.0085182, PMID: 24454815

Shinzato C, Shoguchi E, Kawashima T, Hamada M, Hisata K, Tanaka M, Fujie M, Fujiwara M, Koyanagi R, Ikuta T, Fujiyama A, Miller DJ, Satoh N. 2011. Using the Acropora digitifera genome to understand coral responses to environmental change. *Nature* **476**:320–323. DOI: https://doi.org/10.1038/nature10249, PMID: 21785439

Shoguchi E, Shinzato C, Kawashima T, Gyoja F, Mungpakdee S, Koyanagi R, Takeuchi T, Hisata K, Tanaka M, Fujiwara M, Hamada M, Seidi A, Fujie M, Usami T, Goto H, Yamasaki S, Arakaki N, Suzuki Y, Sugano S, Toyoda A, et al. 2013. Draft assembly of the Symbiodinium minutum nuclear genome reveals dinoflagellate gene structure. *Current Biology* **23**:1399–1408. DOI: https://doi.org/10.1016/j.cub.2013.05.062, PMID: 23850284

Sproles AE, Kirk NL, Kitchen SA, Oakley CA, Grossman AR, Weis VM, Davy SK. 2018. Phylogenetic characterization of transporter proteins in the cnidarian-dinoflagellate symbiosis. *Molecular Phylogenetics and Evolution* **120**:307–320. DOI: https://doi.org/10.1016/j.ympev.2017.12.007, PMID: 29233707

Stanke M, Keller O, Gunduz I, Hayes A, Waack S, Morgenstern B. 2006. AUGUSTUS: ab initio prediction of alternative transcripts. *Nucleic Acids Research* **34**:W435–W439. DOI: https://doi.org/10.1093/nar/gkl200, PMID: 16845043

Sunagawa S, Wilson EC, Thaler M, Smith ML, Caruso C, Pringle JR, Weis VM, Medina M, Schwarz JA. 2009. Generation and analysis of transcriptomic resources for a model system on the rise: the sea anemone Aiptasia pallida and its dinoflagellate endosymbiont. *BMC Genomics* **10**:258. DOI: https://doi.org/10.1186/1471-2164-10-258, PMID: 19500365

Szmant AM, Ferrer LM, FitzGerald LM. 1990. Nitrogen excretion and O:n ratios in reef corals: evidence for conservation of nitrogen. *Marine Biology* **104**:119–127. DOI: https://doi.org/10.1007/BF01313165

Tanaka Y, Miyajima T, Koike I, Hayashibara T, Ogawa H. 2006. Translocation and conservation of organic nitrogen within the coral-zooxanthella symbiotic system of Acropora pulchra, as demonstrated by dual isotope-labeling techniques. *Journal of Experimental Marine Biology and Ecology* **336**:110–119. DOI: https://doi.org/10.1016/j.jembe.2006.04.011

Tao TY, Towle HC. 1986. Coordinate regulation of rat liver genes by thyroid hormone and dietary carbohydrate. *Annals of the New York Academy of Sciences* **478**:20–30. DOI: https://doi.org/10.1111/j.1749-6632.1986.tb15518.x, PMID: 3467640

Tautz D, Domazet-Lošo T. 2011. The evolutionary origin of orphan genes. *Nature Reviews Genetics* **12**:692–702. DOI: https://doi.org/10.1038/nrg3053, PMID: 21878963

Thorington G, Margulis L. 1981. Hydra viridis: transfer of metabolites between Hydra and symbiotic algae. *The Biological Bulletin* **160**:175–188. DOI: https://doi.org/10.2307/1540911, PMID: 6164406

Trench RK. 1971. The physiology and biochemistry of zooxanthellae symbiotic with marine coelenterates. I. The assimilation of photosynthetic products of zooxanthellae by two marine coelenterates. *Proceedings of the Royal Society B: Biological Sciences* **177**:225–235. DOI: https://doi.org/10.1098/rspb.1971.0024

Vandermeulen JH, Davis ND, Muscatine L. 1972. The effect of inhibitors of photosynthesis on zooxanthellae in corals and other marine invertebrates. *Marine Biology* **16**:185–191. DOI: https://doi.org/10.1007/BF00346940

Wang J, Douglas AE. 1998. Nitrogen recycling or nitrogen conservation in an alga-invertebrate symbiosis? *The Journal of Experimental Biology* **201**:2445–2453. PMID: 9679106

Weis VM, Smith GJ, Muscatine L. 1989. A ?CO2 supply? mechanism in Zooxanthellate cnidarians: role of carbonic anhydrase. *Marine Biology* **100**:195–202. DOI: https://doi.org/10.1007/BF00391958

Weis VM. 2008. Cellular mechanisms of cnidarian bleaching: stress causes the collapse of symbiosis. *Journal of Experimental Biology* **211**:3059–3066. DOI: https://doi.org/10.1242/jeb.009597, PMID: 18805804

Wernegreen JJ. 2012. Endosymbiosis. *Current Biology* **22**:R555–R561. DOI: https://doi.org/10.1016/j.cub.2012.06.010, PMID: 22835786

Wilkinson CR. 1980. Nutrient translocation from green algal symbionts to the freshwater sponge Ephydatia fluviatilis. *Hydrobiologia* **75**:241–250. DOI: https://doi.org/10.1007/BF00006488

Wood-Charlson EM, Hollingsworth LL, Krupp DA, Weis VM. 2006. Lectin/glycan interactions play a role in recognition in a coral/dinoflagellate symbiosis. *Cellular Microbiology* **8**:1985–1993. DOI: https://doi.org/10.1111/j.1462-5822.2006.00765.x, PMID: 16879456

Worden AZ, Lee JH, Mock T, Rouzé P, Simmons MP, Aerts AL, Allen AE, Cuvelier ML, Derelle E, Everett MV, Foulon E, Grimwood J, Gundlach H, Henrissat B, Napoli C, McDonald SM, Parker MS, Rombauts S, Salamov A, Von Dassow P, et al. 2009. Green evolution and dynamic adaptations revealed by genomes of the marine picoeukaryotes Micromonas. *Science* **324**:268–272. DOI: https://doi.org/10.1126/science.1167222, PMID: 19359590

Yellowlees D, Rees TA, Leggat W. 2008. Metabolic interactions between algal symbionts and invertebrate hosts. *Plant, Cell & Environment* **31**:679–694. DOI: https://doi.org/10.1111/j.1365-3040.2008.01802.x, PMID: 18315536

Chapter IV

Symbiotic algae in *Hydra viridissima* contribute to shape the bacterial microbiota in a light-dependent manner

Authors

Katja Schröder[1*], Sebastian Fraune[1*], Mayuko Hamada[2, 3], Ulrich Kürn[1], Friederike Anton-Erxleben[1], Sven Künzel[4] and Thomas C. G. Bosch[1]

Affiliations

[1] Zoological Institute and Interdisciplinary Research Center Kiel Life Science, Kiel University, Kiel, Germany

[2] Marine Genomics Unit, Okinawa Institute of Science and Technology Graduate University, Okinawa, Japan

[3] Ushimado Marine Institute, Okayama University, Okayama, Japan

[4] Max-Planck Institute for Evolutionary Biology, 24306 Plön, Germany

* These authors contributed equally to this work.

***manuscript**: in preparation*

Abstract

Different species of the freshwater polyp *Hydra* are colonized by a distinct, species-specific bacterial community. In addition to bacteria, the species *Hydra viridissima* also hosts photosynthetic endosymbiotic *Chlorella* algae. The bacterial microbiota and the endosymbiotic *Chlorella algae* have been independently shown to benefit the hydra host in terms of antifungal resistance, starvation tolerance and reproduction. In contrast, it is largely unknown whether the photosythetic algae, which reside in the endodermal epithelium of *Hydra viridissima,* influences the extracellularly located bacterial community. This study aimed to evaluate differences in bacterial community composition associated with the presence or absence of photosynthetic algae. 16S rRNA sequencing and fluorescent *in situ* hybridization (FISH) analysis were used to characterize bacterial microbiota of *Hydra viridissima*. The bacterial community composition differed significantly between symbiotic and algae-free polyps indicating that the *Chlorella* algae affect the resident microbiota. Furthermore, in presence of algal endosymbionts the bacterial microbiota differed significantly between light and darkness suggesting an effect of *Chlorella*'s photosynthetic activity on the bacterial community composition. Taken together, we show that the endosymbiotic algae contribute to shape the *Hydra viridissima*-specific microbiota in light-dependent manner. Furthermore, our findings suggest that green hydra can serve as model for understanding mutualistic interactions in tripartite interkingdom associations.

Introduction

All multicellular animals are hosts to microbial communities consisting of mutualistic, commensal, opportunistic and pathogenic microorganisms referred to as the microbiota (Lederberg and McCray, 2001). Research of the last two decades supports the assumption that microbial symbioses have fundamentally important impacts on host biology (Russell et al., 2014). Numerous studies have shown that the host-specific microbiota plays a pivotal role in the maturation and training of the mammalian immune system (Belkaid and Hand, 2014) and provides the host with metabolic functions that are not encoded in its own genome (Sommer and Bäckhed, 2013). In addition to these well-known functions there is accumulating evidence that the microbiota also affects traits such as development and behavior, which were previously believed to be exclusively under host control (Koropatnick et al., 2004; Rawls et al., 2004; Bates et al., 2006; Sharon et al., 2010; Sampson and Mazmanian, 2015; Shikuma et al., 2016; Murillo-Rincon et al., 2017). These integral host-microbe relationships have led to a

conceptualization of multicellular organisms as 'holobionts' or synonymously 'metaorganisms', which displays the multipartite entity of a host and its associated microbial communities (Zilber-Rosenberg and Rosenberg, 2008; Bosch and McFall-Ngai, 2011; McFall-Ngai et al., 2013; Bordenstein and Theis, 2015). The holobiont or metaorganism concept considers the dynamic microbiota as an integral part of the functionality of the host organism itself and therefore, the holobiont is posited to form a unit of natural selection (Zilber-Rosenberg and Rosenberg, 2008).

Like all animals, the freshwater polyp *Hydra* is colonized by a distinct microbiota, which inhabits the glycocalyx covering the polyp's ectodermal epithelium and provides antifungal immunity to the host (Fraune and Bosch, 2007; Fraune et al., 2015). The bacterial community composition is specific for any given *Hydra* species and mirrors the phylogenetic relationship of their hosts (Fraune and Bosch, 2007; Franzenburg et al., 2013), a pattern termed phylosymbiosis (Brucker and Bordenstein, 2013). Species-specific antimicrobial peptides, which are controlled by the stem cell transcription factor FoxO, are involved in shaping *Hydra*'s microbiota, which is remarkably stable over time (Fraune and Bosch, 2007; Franzenburg et al., 2013; Mortzfeld et al., 2018).

In the green hydra, *Hydra viridissima*, long-term persisting mutualistic associations involve not only the animal host and its bacterial colonizers, but also unicellular photosynthetic algae of the genus *Chlorella*, which reside intracellularly at the basal part of the endodermal epithelial cells. All *Chlorella* algae found in a single polyp are clonal and passed to the next generation of *Hydra* by vertical transmission (Muscatine and McAuley, 1982). A recent phylogenetic analysis of six different green hydra strains and their symbiotic *Chlorella* algae revealed that the phylogenetic trees of the *Hydra* hosts and the algal symbionts are congruent indicating that they share a long co-evolutionary history (Kawaida et al., 2013). While mutualistic host-bacteria interactions in *Hydra* have come into focus only in the last decade, the intimate endosymbiotic relationsship between the *Hydra* and *Chlorella* has been subject of research for more than 50 years (Muscatine and Lenhoff, 1963; Muscatine, 1965; Muscatine and Lenhoff, 1965; Muscatine et al., 1975; Thorington and Margulis, 1981; McAuley, 1986; McAuley and Darrah, 1990).

Although algae-free *H. viridissima* have never been reported in nature (Muscatine and McAuley, 1982; Habetha et al., 2003), green hydra can be artificially deprived of their endosymbionts by various means (Pardy, 1976; Habetha et al., 2003). These so-called aposymbiotic polyps show the same morphology as symbiotic animals and can be easily

maintained under laboratory conditions, thereby providing a useful experimental tool for comparison of genetically identical polyps with and without *Chlorella* algae. Indeed, it was shown that symbiotic animals have a significant competitive advantage during periods of starvation due to maltose provided by the photosynthetic algae (Muscatine and Lenhoff, 1963, 1965; Roffman and Lenhoff, 1969; Huss et al., 1993; Habetha et al., 2003). Furthermore, the endosymbiont has severe impact on sexual reproduction in *H. viridissima* by promoting oogenesis (Habetha et al., 2003). In contrast to the hydra host, the symbiotic *Chlorella* algae are unable to grow independently outside the host indicating loss of autonomy during establishment of the intimate endosymbiotic relationship (Muscatine, 1965; Park et al., 1967; Habetha et al., 2003). Indeed, genome sequencing of the symbiotic *Chlorella sp.* A99 revealed a degenerated nitrate assimilation pathway and thus, the alga depends on the hydra host in terms of nitrogen supply *(Hamada et al., 2018).*

While our understanding of the green hydra was shaped by many decades of research on the binary interactions in host–algal endosymbiosis, efforts to understand the role of bacterial symbionts in the *H. viridissima* holobiont have been sporadic. In the 1980s two authors reported the discovery of bacteria associated with *H. viridissima* (Margulis et al., 1978; Wilkerson, 1980). While Wilkerson observed extracellularly located bacteria colonizing the ectodermal epithelial surface, Margulis and co-workers identified intracellular bacteria in endodermal epithelial cells of some, but not all *H. viridissima* strains. A more recent comparative analysis of the microbiota among seven different *Hydra* species revealed that the bacterial community in symbiotic *H. viridissima* is dominated by bacteria of the *Alcaligenaceae* family (Franzenburg et al., 2013). However, the microbiota of aposymbiotic *H. viridissima* as well as the localization of the bacteria were not analyzed in that study.

In their intracellular habitat each *Chlorella* symbiont is enclosed within an individual perialgal vacuolar membrane termed ‘symbiosome’ (Muscatine et al., 1975; Jolley and Smith, 1978). This anatomy requires adaptation of the host to allow transport of normally excreted inorganic nutrients such as CO_2 and phosphate into the symbiosome. In parallel *Hydra* receives maltose as well as low amounts of glucose and glycolic acid from the endosymbiont (Muscatine et al., 1967; Cernichiari et al., 1969). Thus, the presence of the endosymbiont affects the metabolic state of the host, which may involve changes in the extracellular microenvironment. Based on this assumption, we characterized the microbiota of aposymbiotic and symbiotic *H. viridissima* to elucidate whether the presence of photosynthetic *Chlorella* algae affects the bacterial community composition.

Here, we demonstrate that the extracellularly located bacterial communities differ between *H. viridissima* with and without endosymbiotic *Chlorell*a algae. Furthermore, we show that the microbiota in symbiotic polyps undergoes significant diurnal fluctuations in light-dependent manner. Thus, our experiments indicate a role for the photosynthetic endosymbiont in shaping the bacterial microbiota in the green hydra holobiont.

Results

The *H. viridissima* ectodermal epithelium harbors intracellular and extracellular bacteria

Depending on the investigated *Hydra* species, bacteria were located intracellularly in the endodermal (Margulis et al., 1978) or ectodermal epithelium (Fraune and Bosch, 2007) as well as extracellularly in the glycocalyx that overlies the ectodermal epithelium (Wilkerson, 1980; Fraune et al., 2015). To obtain information on the localization of the bacterial community in *H. viridissima* we performed fluorescent *in situ* hybridization (FISH) analysis. To examine whether bacteria inhabit the glycocalyx of *H. viridissima*, polyps were exposed to a brief hypertonic salt wash, a treatment that does not injure the animals, but leads to shedding of the glycocalyx and extracellular bacteria attached to it (Böttger et al., 2012; Fraune et al., 2015). The supernatant was subsequently fixed onto a filter membrane and subjected to FISH analysis using an Alexa Fluor 488-labeled EUB338 universal eubacterial probe (Amann et al., 1990) and a Cy3-labeled phylospecific probe for OTU (*Rhodoferax* sp.). Epifluorescence microscopy uncovered that morphologically heterogeneous bacteria colonize the ectodermal epithelial surface of *H. viridissima* (**Figure 1A**). *A* rod-shaped bacterium was identified as *Rhodoferax* sp., which appears to be the dominant member of the extracellularly located bacterial community (**Figure 1B and C**). In addition, we performed FISH analysis on paraffin-embedded tissue sections to search for intracellularly located bacteria. Indeed, EUB338-positive bacteria were detected within the ectodermal epithelial cells, while the endodermal cells of symbiotic polyps exclusively harbor algal cells and respectively, no endosymbionts in aposymbiotic animals (**Figure 1D and E**). FISH analyses were performed on symbiotic and aposymbiotic *H. viridissima* revealing that both harbor intra- and extracellularly located bacteria with no obvious differences detectable (**Figure 1F**).

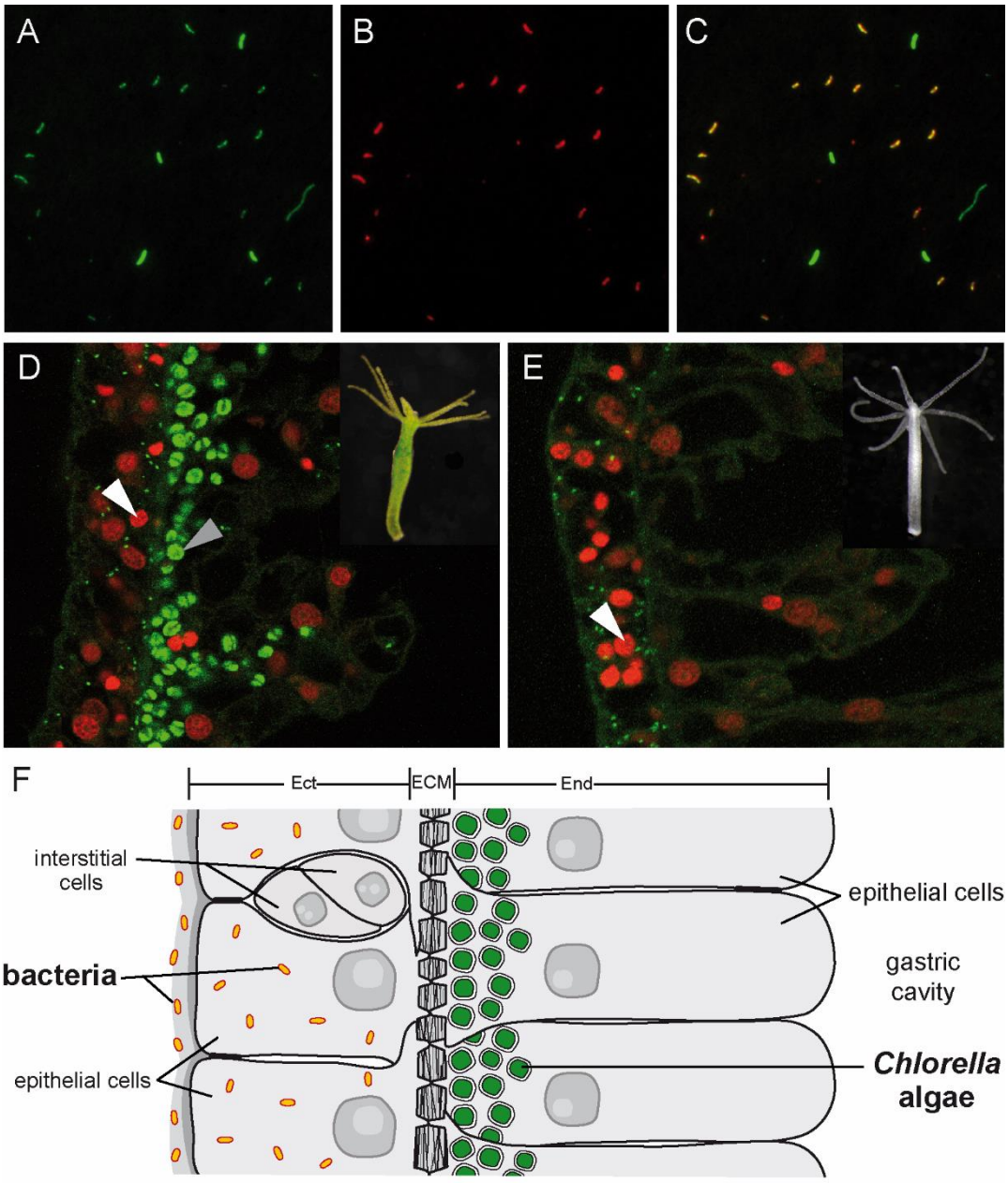

Figure 1. Fluorescence *in-situ* hybridization (FISH) analyses of bacteria colonizing *Hydra viridissima*. Bacteria removed from the ectodermal epithelial surface were stained with the eubacterial oligonucleotide probe EUB338 (A) and a phylotype-specific probe for OTU 138 (*Rhodoferax* sp.) (B). Overlay images indicating the specifically labeled bacteria in yellow (C). FISH analysis of longitudinal sections of symbiotic (D) and aposymbiotic (E) *H. viridissima* using EUB338. Bacteria (green) are located within epithelial cells of the ectodermal layer, while *Chlorella* algae are present at the base of endodermal epithelial cells (green auto-fluorescence, gray arrow head). Nuclear DNA was counterstained by TO-PRO®-3 (red, white arrow head). (F) Scheme showing a longitudinal section of a symbiotic *H. viridissima* polyp. The body wall is organized as an epithelial bilayer with an intervening extracellular matrix (ECM). Ect, ectodermal epithelium; End, endodermal epithelium.

Bacterial community profiles differ between symbiotic and aposymbiotic polyps

To examine whether the presence of the *Chlorella* endosymbiont affects the bacterial community composition in *H. viridissima*, we co-cultivated symbiotic and aposymbiotic polyps for four weeks according to standard procedure in a 12 h light-12 h dark cycle. Following that period total DNA was isolated from symbiotic and aposymbiotic polyps after 12 h light as well as after 12 h darkness and subsequently subjected to 454 sequencing of the bacterial microbiota. Six biological replicates (n=6) were conducted per time point. Chimeric sequences and *Chlorella* sp. chloroplast sequences in samples of symbiotic *H. viridissima were removed in silico.* For inter-sample comparisons, sequences were rarified to 3000 reads grouped into operational taxonomic units (OTUs) at a ≥ 97% sequence identity threshold and classified by RDP classifier.

The analysis of the 16S rRNA gene sequences revealed that the microbiota of both symbiotic and aposymbiotic *H viridissima* is dominated by one single OTU (OTU 116) belonging to the *Alcaligenaceae* family of the *Betaproteobacteria*. Within the bacterial community of symbiotic and aposymbiotic polyps OTU 116 represented in average by 96.8% and 97.4% of the sequence reads, respectively. According to our FISH analyses, the microbiota colonizing the extracellular glycocalyx of *H. viridissima* was dominated by OTU 138 belonging to *Rhodoferax* sp., a member of the *Comamonadaceae* family of the *Betaproteobacteria*. This indicates that OTU 116 inhabits another niche within the hydra host, which is not accessible to the hypertonic salt wash removing the glycocalyx. Therefore, OTU 116 displays a putative candidate for the intracellular bacteria inhabiting the ectodermal epithelium (**Figure 1D-F**).

However, the predominance of a single DNA template is known to limit the effectiveness of PCR-based 16S rRNA gene profiling by masking the presence of less abundant bacterial 16S sequences and thus, may result in under-estimation of diversity (Green and Minz, 2005). The problem is well known from arthropods harboring endosymbiotic bacteria (Chandler et al., 2011; Gofton et al., 2015; Simhadri et al., 2017; Greay et al., 2018) and can generally be overcome by the use of a blocking primer (Vestheim and Jarman, 2008). However, to employ this methodology, the sequence of the dominant DNA must be known prior sequencing, which was not the case in our study. Since OTU 116 was not affected by the presence or absence of *Chlorella* algae (ANOVA, $p = 0.22$), we decided to remove the OTU from the data set prior to further sequence analysis to identify bacterial phylotypes that differ in abundance between symbiotic and aposymbiotic *H. viridissima*.

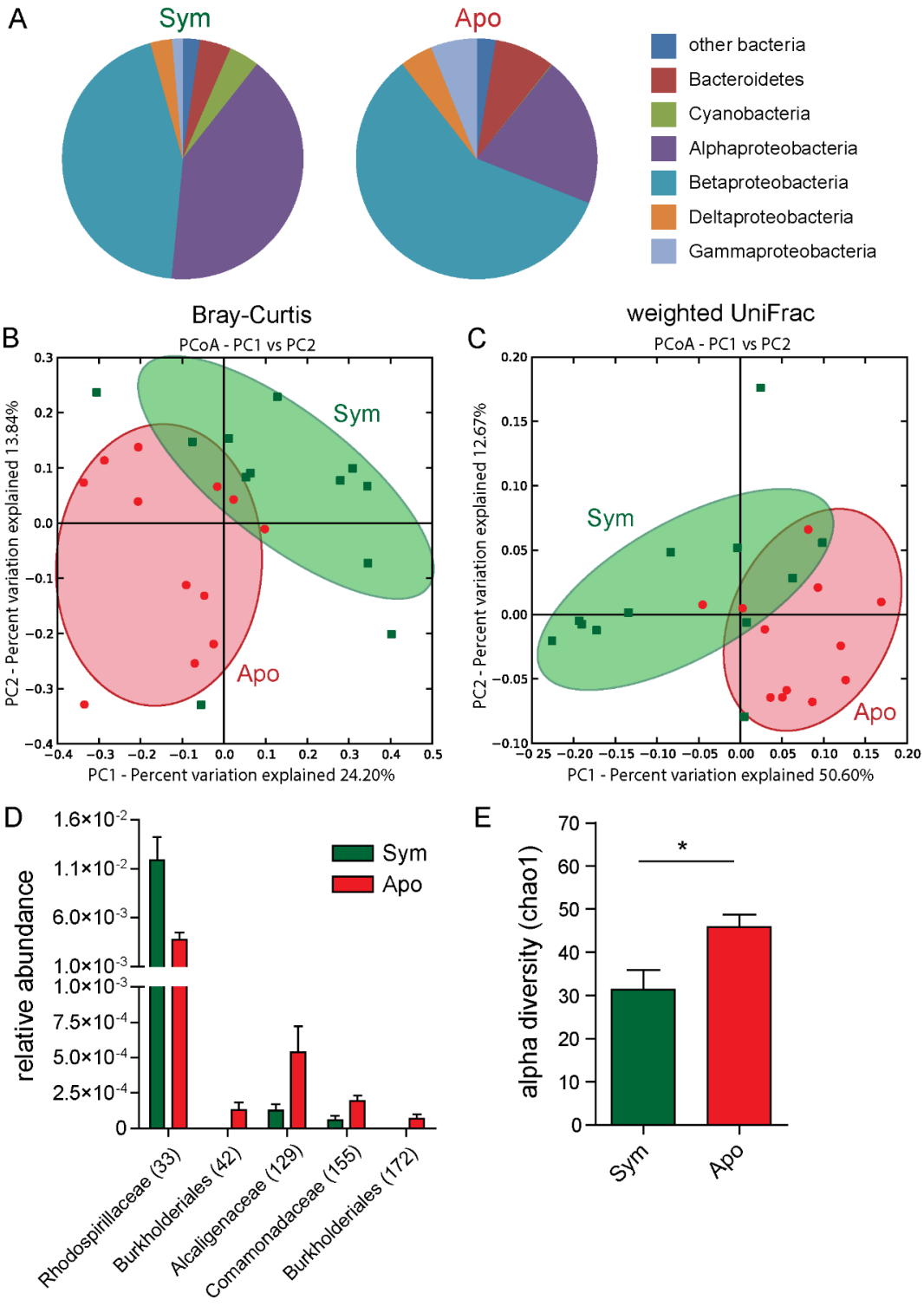

Figure 2. Bacterial community composition in symbiotic and aposymbiotic polyps.
(A) Pie diagrams representing the mean relative abundances of bacteria on phylum and class levels in symbiotic and aposymbiotic *H. viridissima*. The dominant OTU 116 was removed from the analysis. (B) Bacterial communities of symbiotic and aposymbiotic polyps were clustered using principal coordinate analysis (PCoA) of the Bray-Curtis (B) and weighted UniFrac (C) distance matrices. The percent variation explained by the principle coordinates is indicated at the axes. (D) Relative abundance of OTUs significantly differed between symbiotic and aposymbiotic polyps (ANOVA, $p<0,05$) (E) Alpha-diversity (Chao1) of symbiotic and aposymbiotic polyps. Statistics were carried out using *t*-test, * $p<0,05$, ** $p<0,01$, *** $p<0,001$.

The 16S rRNA sequence analysis of the remaining bacterial communities revealed significant differences between symbiotic and aposymbiotic *H. viridissima*. The bacterial community of symbiotic polyps was dominated by two major classes, the *Alphaproteobacteria* and *Betaproteobacteria*. In comparison, the microbiota of aposymbiotic animals showed a significant decrease in the relative abundance of *Alphaproteobacteria* (ANOVA, p = 0,009) and *Cyanobacteria* (ANOVA, p = 0,053), while the fraction of *Betaproteobacteria* was increased (**Figure 2A**). To analyze the effect of symbiotic algae on the bacterial composition in more detail we performed principal coordinate analysis using six different beta diversity metrics (**Figure 2B and C, Table 1**). Using the nonparametric statistical method Adonis, five distance metrics revealed significant clustering of the bacterial communities of symbiotic and aposymbiotic polyps (**Table 1**), with the highest effect size using the weighted unifrac metric. Here, approximately 24% (Adonis: R2 = 0.24, p = 0.002) of the variation in bacterial composition can be explained by the presence and absence of the algae symbiont. Further, we identified individual bacterial OTUs contributing to the differential community composition. The significant decrease in the fraction of *Alphaproteobacteria* in aposymbiotic *H. viridissima* was attributed mainly to OTU 33 (*Rhodospirallaceae*), while the increase in relative abundance of the *Betaproteobacteria* four members of (OTU 42, 129, 155 and 172) (**Figure 2D**).

Table 1. Statistical analysis comparing the bacterial colonization of symbiotic (Sym) and aposymbiotic (Apo) *H. viridissima.*

		Adonis		
	metric	**R^2**	**p-value**	
Apo vs. Sym	Abund Jaccard	0.11	0.002	**
	Binary Jaccard	0.07	0.011	*
	Bray-Curtis	0.12	0.002	**
	Pearson	0.15	0.015	*
	Unweighted UniFrac	0.07	0.070	
	Weighted UniFrac	0.24	0.002	**

Alpha diversity was measured using the Chao1 metric showed higher bacterial diversity in aposymbiotic polyps compared to symbiotic *H. viridissima* (**Figure 2E**). Taken together, these data uncover significant differences in the bacterial community composition between symbiotic and aposymbiotic *H. viridissima* indicating that the presence of the photosynthetic algae influences the bacterial microbiota.

In symbiotic polyps bacterial community profiles differ between light and darkness

To explore whether the bacterial community composition in *H. viridissima* varies between day and night, we compared the microbiota of symbiotic and aposymbiotic polyps after 12 h light and 12 h darkness (**Figure 3A**). Interestingly, the bacterial community composition differed significantly between symbiotic and aposymbiotic polyps in the 12 h light phase (**Figure 3B and D, Table 2**), but not in darkness (**Figure 3C and E, Table 2**).

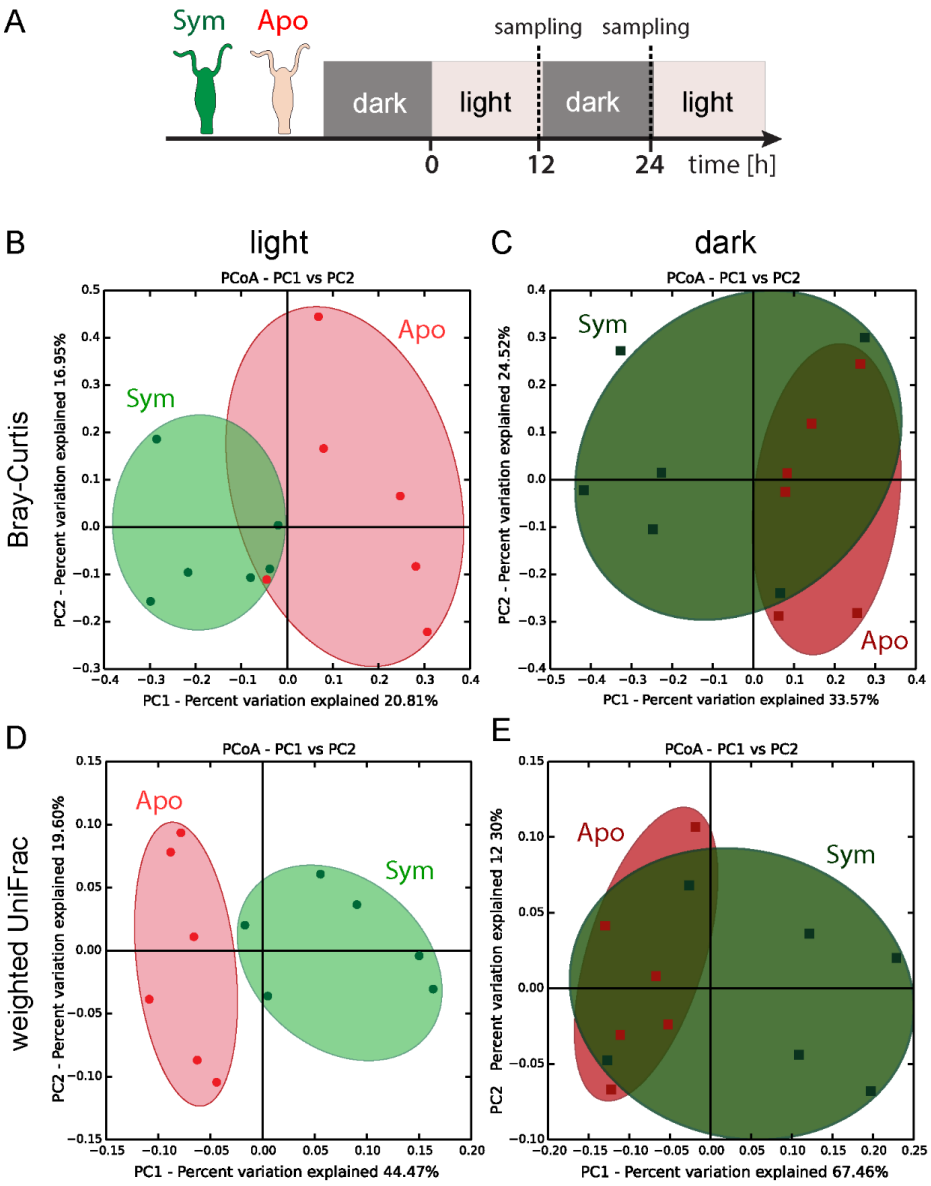

Figure 3. Comparison of the bacterial communities in symbiotic and aposymbiotic *H. viridissima* during 12 h light and 12 h darkness.
(A) Experimental setup. Symbiotic and aposymbiotic polyps were cocultured for 4 weeks under a 12 h light-dark rhythm. Samples were taken at the end of the 12 h light period and at the end of the 12 h dark period. Bacterial communities were clustered using principal coordinate analysis (PCoA) of the Bray-Curtis (B and C) and weighted UniFrac (D and E) distance matrices. The percent variation explained by the principle coordinates is indicated at the axes.

Table 2. Statistical analysis comparing bacterial colonization of symbiotic (Sym) and aposymbiotic (Apo) *H. viridissima* after 12 h light and 12 h darkness.

		Adonis		
	metric	**R^2**	**p-value**	
Apo vs. Sym light	Abund Jaccard	0.14	0.017	*
	Binary Jaccard	0.10	0.186	
	Bray-Curtis	0.16	0.009	**
	Pearson	0.25	0.012	*
	Unweighted UniFrac	0.12	0.109	
	Weighted UniFrac	0.33	0.005	**
Apo vs. Sym dark	Abund Jaccard	0.11	0.259	
	Binary Jaccard	0.11	0.161	
	Bray-Curtis	0.18	0.068	
	Pearson	0.12	0.316	
	Unweighted UniFrac	0.09	0.414	
	Weighted UniFrac	0.33	0.027	*

To further characterize the differences in the microbiota composition during light and dark phases, we compared the 12 h light samples and the 12 h dark samples of symbiotic animals with each other (**Figure 4A and C**). The same analysis was conducted on the samples of aposymbiotic animals (**Figure 4B and D**). Strikingly, the bacterial community composition in symbiotic polyps differed significantly between the light and dark period, while this phenomenon was not observed in aposymbiotic animals (**Figure 4A-D, Table 3**). Individual OTUs responding to the daily 12 h light-dark rhythm in symbiotic polyps belong to the bacterial phyla *Alphaproteobacteria* (OTU 33 and 91), *Betaproteobacteria* (OTU 170) and *Bacteroidetes* (OTU 55) (**Figure 4E**). While OTU 55 (*Cytophagaceae*) and OTU 170 (*Limnobacter*) decrease in their relative abundance during the light period, members of the *Alphaproteobacteria* (OTU 33 and 91) show a substantial increase. Interestingly, many members of the *Rhodospirillaceae* (OTU 33) as well as the *Rhodobacteraceae* family (OTU 91) are known to be photosynthetic (Baldani et al., 2014; Pujalte et al., 2014).

We have previously shown that the bacterial diversity (alpha diversity, Chao1) in symbiotic polyps was significantly reduced compared to aposymbiotic animals (**Figure 2E**). Separate analysis of the two sampling time points (12 h light, 12 h dark) revealed that the bacterial diversity in aposymbiotic animals is constant during light-dark cycle. In contrast, the previously observed decreased bacterial diversity in symbiotic polyps can be clearly attributed to 12 h darkness (**Figure 4F**), while during light the bacterial diversity is comparable to aposymbiotic animals (**Figure 4F**).

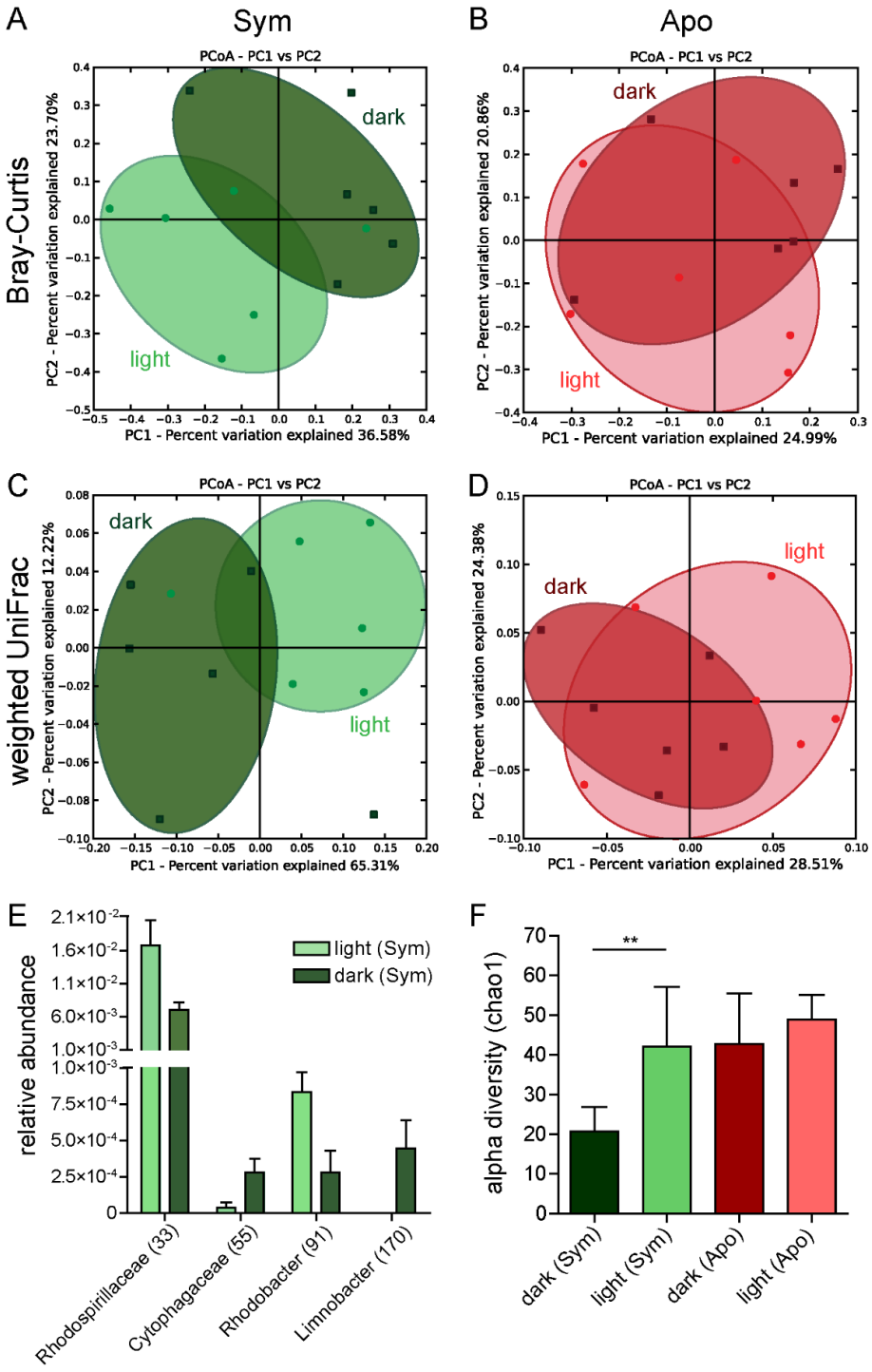

Figure 4. Comparison of bacterial communities during 12 h light and 12 h darkness in symbiotic and aposymbiotic *H. viridissima*.

Bacterial communities were clustered using principal coordinate analysis (PCoA) of the Bray-Curtis (A and B) and weighted UniFrac (C and D) distance matrices. The percent variation explained by the principle coordinates is indicated at the axes. (E) Relative abundance of OTUs that significantly differ between light and dark condition in symbiotic polyps (ANOVA, p<0,05). (F) Alpha diversity estimated by Chao1 in symbiotic and aposymbiotic polyps during dark and light conditions. Statistics were carried out using *t*-test, * p<0,05, ** p<0,01, *** p<0,001.

Table 3. Statistical analysis comparing the bacterial colonization after 12 h darkness and 12 h light of symbiotic (Sym) and aposymbiotic (Apo) *H. viridissima.*

		Adonis		
	metric	**R^2**	**p-value**	
light vs. dark Sym	Abund Jaccard	0.25	0.009	**
	Binary Jaccard	0.15	0.038	*
	Bray-Curtis	0.20	0.027	*
	Pearson	0.18	0.110	
	Unweighted UniFrac	0.23	0.029	*
	Weighted UniFrac	0.25	0.063	
light vs. dark Apo	Abund Jaccard	0.11	0.244	
	Binary Jaccard	0.12	0.081	
	Bray-Curtis	0.11	0.267	
	Pearson	0.08	0.479	
	Unweighted UniFrac	0.15	0.060	
	Weighted UniFrac	0.12	0.190	

In summary, we conclude from these experiments that the microbial shift observed in symbiotic polyp during light is linked to the presence of photosynthetic *Chlorella* algae, because aposymbiotic polyps did not differ significantly in their microbiota during light and darkness.

Absence of intracellular bacteria does not affect diurnal fluctuations in the microbiota

Besides an extracellularly located bacterial community inhabiting the glycocalyx, *H. viridissima* also harbors intracellular bacteria in the ectodermal epithelial cells (**Figure 1D-F**). Many, if not most, intracellular symbionts are vertically transmitted to the host's offspring (Bright and Bulgheresi, 2010), e.g. endosymbiotic *Chlorella* are well known to be maternally inherited to the next generation of *H. viridissima* (Muscatine and McAuley, 1982; Campbell, 1990). Thus, we were wondering if such an intimate relationship also exists between *H. viridissima* and the intracellular bacteria. To investigate, whether the intracellular bacteria are transmitted to the next generation of *H. viridissima*, embryos of symbiotic polyps were collected and allowed to hatch. In contrast to the *Chlorella* alga, which was successfully transmitted to the next generation, the intracellular bacteria were not found in any polyp of the *H. viridissima* F_1 generation and thus, were neither transmitted vertically nor horizontally acquired from the environment.

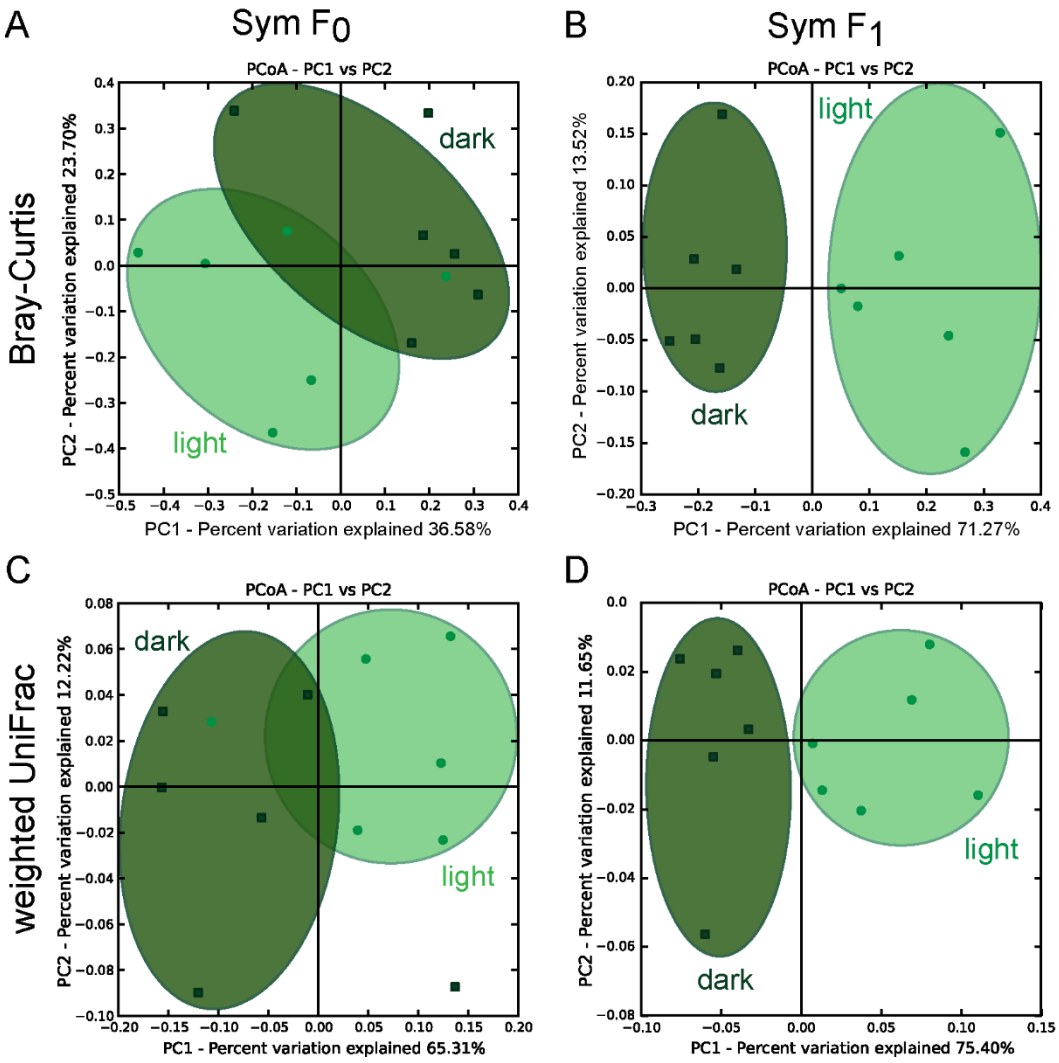

Figure 5. Comparison of bacterial communities during 12 h light and 12 h darkness in symbiotic *H. viridissima* with (Sym F_0) and without (Sym F_1) intracellular bacteria.
Bacterial communities during 12 h light-dark rhythm were clustered using principal coordinate analysis (PCoA) of the Bray-Curtis (B) and weighted UniFrac (C) distance matrices. The percent variation explained by the principle coordinates is indicated at the axes.

As mentioned before, the effectiveness of our previous 16S rRNA profiling approach was limited by the high abundance of a member of the *Alcaligenaceae* (OTU 116), which is likely to be represented by the intracellular bacteria. Since these are not present in the *H. viridissima* F_1 generation, we decided to use this newly established line for another 16S rRNA profiling. *H. viridissima* F_1 polyps maintained under a 12 h light-dark cycle and samples were taken at the end of the 12 h light period and after 12 h darkness respectively. Six biological replicates of each sampling time point were subjected to 16S rRNA microbiota profiling *via* sequencing on the Illumina MiSeq platform. Indeed, the microbial community of *H. viridissima* F_1 was not dominated by an *Alcaligenaceae* bacterium, which is consistent with our hypothesis that OTU 116 displays *the intracellular bacteria detected in the*

ectodermal epithelial cells of the F_0 generation. Principle coordinate analysis (PCoA) using six different beta diversity metrics revealed that symbiotic polyps of *H. viridissima* F_1 generation show significant differences in the bacterial community composition during light and dark phases (**Figure 5B and D, Table 4**), which is in line with our previous analysis of the *H. viridissima* founder polyps (F_0) (**Figure 5A and C**). These results indicate that the shift in the microbiota of symbiotic polyps during the light period is independent of the presence or absence of the intracellular bacteria in the ectodermal epithelium of *H. viridissima*.

Table 4. Statistical analysis comparing the bacterial colonization at 12 h and 24 h in symbiotic *H. viridissima* F_1 under normal light-dark cycle (12 h light vs. 24 h dark) and under constant darkness (12 h dark vs. 24 h dark).

		Adonis		
	metric	**R^2**	**p-value**	
12 h light vs. 24 h dark	Abund Jaccard	0.39	0.011	*
	Binary Jaccard	0.18	0.005	**
	Bray-Curtis	0.62	0.002	**
	Pearson	0.94	0.001	***
	Unweighted UniFrac	0.20	0.007	**
	Weighted UniFrac	0.62	0.004	**
12 h dark vs. 24 h dark	Abund Jaccard	0.40	0.006	**
	Binary Jaccard	0.25	0.002	**
	Bray-Curtis	0.27	0.023	*
	Pearson	0.34	0.030	*
	Unweighted UniFrac	0.26	0.006	**
	Weighted UniFrac	0.31	0.017	*

Diurnal fluctuations in the microbiota of symbiotic polyps are light-dependent

Since aposymbiotic polyps did not differ significantly in their microbiota during light and darkness (**Figure 4B and D, Table 3**), we concluded that photosynthesis of *Chlorella* algae is involved in the microbial shift observed in symbiotic polyps during light. In a previous work we have shown that the photosynthetic activity of *Chlorella* algae involves transcriptional changes in *H. viridissima* including up-regulation of a phosphate transporter and glutamine synthetase, which are proposed to have a function in nutrition exchange between host and symbiont (Hamada et al., 2018). Hence, it is likely that the photosynthetic activity of *Chlorella* influences the metabolic state of the host and leads to changes in the microenvironment, which in turn may affect the bacterial microbiota.

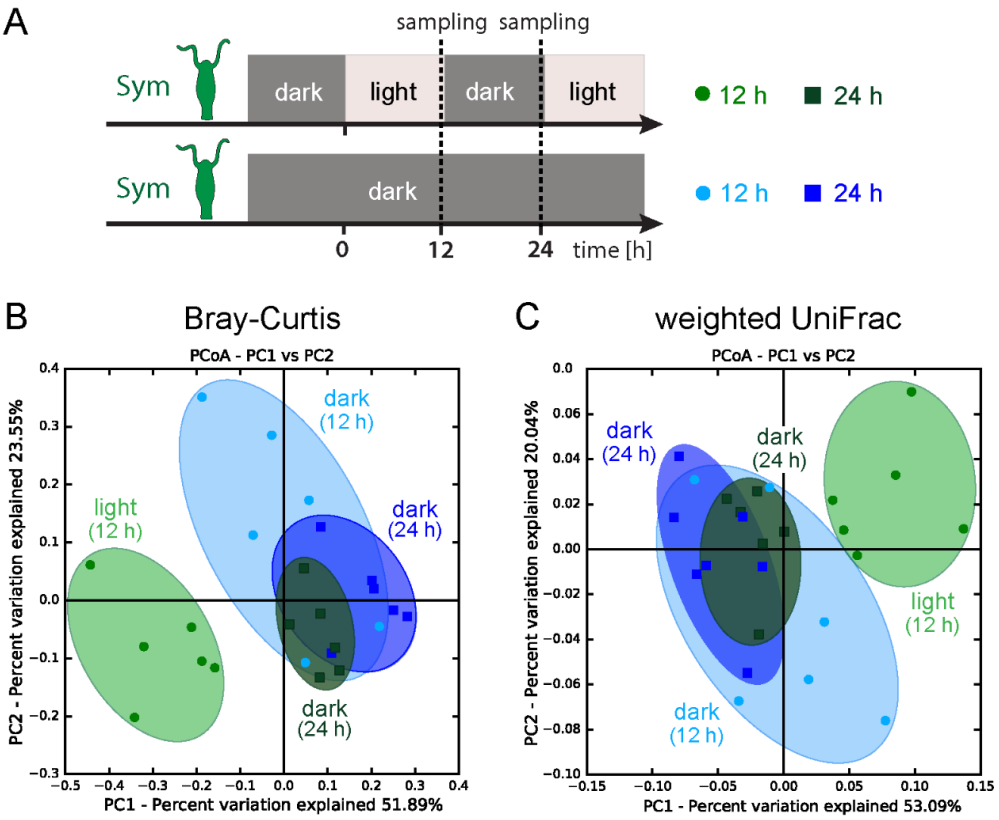

Figure 6. Comparison of bacterial communities under normal light-dark cycle and in constant darkness in symbiotic *H. viridissima*.
(A) Experimental setup. Symbiotic polyps were cultured under a 12 h light-dark cycle or maintained at constant darkness. Bacterial communities after 12 h and 24 h were clustered using principal coordinate analysis (PCoA) of the Bray-Curtis (B) and weighted UniFrac (C) distance matrices. The percent variation explained by the principle coordinates is indicated at the axes.

To exclude the possibility that the diurnal fluctuations in the microbial composition of symbiotic polyps are driven by light-independent circadian rhythm, *H. viridissima* F_1 polyps were split into two cohorts with one cultivated under a normal 12 h light-dark cycle and the other one maintained at constant darkness for 2 days. Sampling was done at the second day simoutaneously in both batches at two time points; after 12 h in light ('12 h light') or darkness ('12 h dark') respectively as well as after the subsequent dark period ('24 h dark') (**Figure 6A**). Six biological replicates of each sampling time point were subjected to 16S rRNA microbiota profiling *via* sequencing on the Illumina MiSeq platform. PCoA using six different beta diversity metrics shows that the shift in microbial community composition of symbiotic *H. viridissima* occurs only in the presence of light and was not detected in symbiotic polyps maintained in constant darkness (**Figure 6B and C, Table 4**). However, it is noticeable that the samples of polyps kept in darkness during the day ('12 h dark') clearly show a higher dispersion than the 24 h dark samples (**Figure 6B and C**). This may indicate that light-independent mechanisms may be also involved in the microbial shift in symbiotic polyps.

In summary, our study shows that the bacterial community of *H. viridissima* shows diurnal light-dependent fluctuations in presence of the endosymbiotic *Chlorella* algae, but not in aposymbiotic animals.

Discussion

In recent years, biologists have developed a growing appreciation for complex host-symbiont interactions. Symbiosis research traditionally focused on bipartite host-microbe interactions such as the *squid-Vibrio fisheri* symbiosis, while tripartite and multipartite associations have received less attention. However, it is becoming evident that long-term symbiotic persistence is prevalent not only in two-party interactions, but also in more complex systems such as reef-building corals. Corals represent a complex tripartite interkingdom symbiosis involving the coral polyp, eukaryotic endosymbiotic algae of the genus *Symbiodinium*, and a vast array of intracellular and extracellular bacterial colonizers (Rohwer et al., 2002; Lema et al., 2012). The documented decline in coral reef ecosystems worldwide (Carpenter et al., 2008) gives researchers a new urgency to understand how stability and breakdown (‘*coral bleaching*’) of these tripartite symbiosis is influenced by changing environmental conditions. When investigating coral bleaching most researchers have initially focused on the loss of the algal symbionts, which correlates with declining coral health. However, with the discovery that diseased or bleached corals harbor different bacterial communities than healthy ones (Perez, 2006; Ritchie, 2006; Bourne et al., 2008; Reis et al., 2009; Sunagawa et al., 2009), the coral holobiont was recognized as a tripartite association. Since then bacterial diversity in corals has been extensively studied and putative functions of the coral microbiota have been proposed including pathogen defense (Rohwer et al., 2002; Shnit-Orland and Kushmaro, 2009) and the supply and cycling of nutrients (Lesser et al., 2004; Wegley et al., 2007). Nevertheless, compared to the well-studied coral-algal symbiosis, the current understanding of the coral-bacterial partnership is still limited and even less for algal-bacterial interactions. However, it has become clear that corals need to be studied as holobionts to fully assess the contribution of each partner to coral bleaching and elucidate their role in adaptation to environmental stress.

Given the toolkit available for studying symbiotic interactions in the model organism *Hydra* (Augustin et al., 2012; Bosch, 2012), the green hydra, *H. viridissima*, offers a promising system for deciphering the underlying mechanisms in tripartite associations comprising a

cnidarian host, an endosymbiotic photosynthetic algae and a stably associated bacterial microbiota.

The present study has revealed a unique aspect of this tripartite interkingdom symbiosis. We show for the first time, to our knowledge, that the photosynthetic activity of endosymbiotic algae can modulate the bacterial community of *H. viridissima* in a light-dependent manner. Yet, we lack any mechanistic understanding of the interaction between the endodermally located intracellular algae and the extracellularly residing bacteria that inhabit the mucus-like layer of the ectodermal glycocalyx (Fraune et al., 2015). However, although the *Chlorella* photobiont and the bacterial microbiota colonize separate niches in the *H. viridissima* holobiont it seems likely that the photosynthetic activity of the endosymbiotic algae can influence microenvironmental physicochemical parameters such as pH and oxygen level. Therefore, the photosynthetic endosymbiont may modify the properties of microbial habitat, which is supported by studies in corals indicating that the mucus of some corals cycles from being fully-oxygenated during photosynthesis of the coral endosymbiont *Symbiodinium* to anaerobic at night when respiration rates exceed oxygenesis (Carlton and Richardson, 1995; Kuhl et al., 1995; Brown and Bythell, 2005). Furthermore, *Symbiodinium* endosymbionts were shown to influence the microbial community structure by release of complex carbon-containing secretions including dimethylsulfoniopropionate (Raina et al., 2009, 2010). Besides being directly affected by photosynthesis products, the microbial niche may also be modified due to photosynthesis-induced changes in host metabolism. Indeed, photosynthetic activity of *Chlorella* has been shown to involve transcriptional changes not only in endoderm of *H. viridissima*, but also in the ectoderm that gives rise to the microbial habitat, the glycocalyx (Hamada et al., 2018).

Another question that arises from our results is, whether the light-dependent diurnal fluctuations of the bacterial microbiota play the physiological role in green hydra or rather display a by-product of the endosymbiosis with the photosynthetic *Chlorella* alga. We have previously shown that *Hydra*'s microbiota provides resistance against the filamentous fungi *Fusarium* sp. and thus, is considered as an integral part of polyp's immune system (Fraune et al., 2015). Interestingly, multiple aspects of pathogenesis in filamentous fungi are regulated in a light-dependent manner including the production of asexual spores and the synthesis of secondary metabolites such as mycotoxins (Bayram et al., 2008; Avalos and Estrada, 2010; Kim et al., 2011). Therefore, diurnal fluctuations in the bacterial community composition in *Hydra* may represent an adaptation to maximize antifungal defense at times when pathogen

invasion is most likely to occur. Indeed, many immune functions have been shown to be regulated in diurnal manner (reviewed in (Arjona et al., 2012; Scheiermann et al., 2013)), a phenomenon observed not only in mammals, but also in flies and plants (McDonald and Rosbash, 2001; Lee and Edery, 2008; Roden and Ingle, 2009; Wang et al., 2011; Stone et al., 2012).

Interestingly, the fluctuations observed in *Hydra*'s bacterial microbiota are not controlled by the endogenous circadian rhythm of the host, since they do not occur in aposymbiotic animals. Instead, the diurnal microbial shift depends on the presence of the intracellular algae as well as on light. Taken together, our results indicate that the photosynthetic activity of the *Chlorella* endosymbiont is involved in shaping the bacterial microbiota of *H. viridissima*. However, currently it is unknown whether the light-dependent microbial shift in green hydra plays a physiological role and has functional consequences for the holobiont phenotype. Further research is required to elucidate if this phenomenon occurs in other tripartite symbioses such as corals and may increase our knowledge on the forces that structure microbial communities.

Materials and Methods

Animals husbandry

Experiments were carried out with the Australian *Hydra viridissima* strain A99, which was obtained from Dr. Richard Campbell, Irvine. Aposymbiotic (algae free) polyps were obtained by photobleaching using 5 µM 3-(3,4-dichlorophenyl)-1,1-dimethylurea (DCMU) as described before (Habetha et al., 2003) and subsequently cultivated for more than one year prior to the start of the experiments. All animals were cultivated at constant temperature (18 °C), light conditions (12 h / 12 h light/dark rhythm) and culture medium (0.28 mM $CaCl_2$, 0.33 mM $MgSO_4$, 0.5 mM $NaHCO_3$ and 0.08 mM KCO_3) according to the standard procedure (Lenhoff and Brown, 1970). Four weeks before DNA isolation symbiotic and aposymbiotic animals were co-cultivated and fed three times per week with freshly hatched *Artemia salina*. Prior to gDNA extraction polyps were starved for 72 h.

FISH analysis of bacterial colonizers

For isolation of glycocalyx-attached bacteria, *H. viridissima* polyps were washed in 500 µl phophate buffered saline for 2 min. The supernatant was transferred to a new tube and

fixed by adding 500 µl 8% paraformaldehyde for 60 min. Afterwards, the supernatant was filtered through a white polycarbonate membrane filter (pore size: 0.2 µm). The filter was washed by 10 ml sterile H_2O and air-dried.

For whole-mount FISH analysis polyps were relaxed in 2% urethane/ culture medium for 2 min and fixed in 4% paraformaldehyde / culture medium for 16 h at 4 °C. Paraffin sections (15 µm) were prepared as previously described (Fröbius et al., 2003) and incubated for 60 min at 46 °C in blocking solution (10% formamide, 0,9 M NaCl, 0,02 M TrisHCl, 1x Denhardt's, 100 µg/ml heparin, 0,01% SDS) prior to hybridization procedure.

Hybridization of filters and paraffin sections was conducted as previously described (Manz et al., 1992) with *10% formamide* and 90 min hybridization time. Monofluorescently labeled ribosomal RNA (rRNA)-targeted oligonucleotide probes were used: positive control, universal eubacterial probe EUB338 5′-GCTGCCTCCCGTAGGAGT-3′, and negative control, EUB338 antisense probe non-EUB338 5′-ACTCCTACGGGAGGCAGC-3′. The phylotype-specific oligonucleotide probe for OTU 138 (*Rhodoferax* sp.) was designed using the computational tool Primrose 2.17 (Ashelford, 2002). Probes were 5′ end-labeled with either Alexa Fluor 488 (Life Technologies GmbH) (green fluorescence) or Cy3 (Life Technologies GmbH) (red fluorescence). Nuclear staining in paraffin sections was done by TO-PRO®-3 (Invitrogen).

TEM microscopy

For transmission electron microscopy animals were embedded in Agar 100 resin (Agar Scientific, Ltd.). Ultrathin sections were contrasted with 2.5% uranyl acetate for 5 min and lead citrate solution (freshly prepared from lead acetate and sodium citrate) for 2 min and were analyzed using a Tecnai™ G2 Spirit BioTWIN transmission electron microscope (FEI Company).

DNA extraction

For each biological replicate (n=6) combined hydra and bacterial DNA was isolated from ten polyps. Animals were washed three times in sterile filtered (0.2 µm) culture medium and subsequently ruptured in buffer ALT (Qiagen) by using a 23G syringe. Algae were removed by centrifugation. Suspensions were centrifuged three times at 350 g for 2 min. After each centrifugation step supernatant was transferred to new tube. The gDNA was extracted from the third supernatant using the DNeasy Blood & Tissue Kit (Qiagen) with elution performed in 50 µl AE buffer. The extracted DNA was stored at -20 °C until sequencing.

Sequencing of 16S rRNA genes

For sequencing of the bacterial 16S rRNA genes, the variable regions 1 and 2 (V1V2) were amplified using the universal forward primer V2_B_Pyro_27F (5'-CTATGCGCCTTGCCAGCCCGCTCAG*TC***AGAGTTTGATCCTGGCTCAG**-3') which consists of the 454 FLX Amplicon primer B (underlined), a two base linker (italics) and the universal 16S primer 27F (bold) and the barcoded reverse primer V2_A_338R (5'-CGTATCGCCTCCCTCGCGCCATCAGNNNNNNNNNN*CA***TGCTGCCTCCCGTAGG**AGT-3') which contains the 454 FLX Amplicon primer A (underlined), a sample specific 10-mer barcode (N's), a two base linker (italics) and the universal 16S primer 338R (bold). 25 µl PCR reactions were performed using the Phusion® Hot-Start II DNA polymerase (Finnzymes, Espoo, Finland) following the manufacturer's instructions. PCR conditions consisted of an initial denaturation step (98 °C, 30 sec) followed by 30 cycles of denaturation (98 °C, 9 sec), annealing (55 °C, 30 sec) and elongation (72 °C, 20 sec). PCR was terminated by a final elongation of 72 °C for 10 min. All reactions were performed in duplicates, which were combined after PCR. PCR products were extracted from agarose-gels with the Qiagen MinElute Gel Extraction Kit and quantified with the Quant-iT™ dsDNA BR Assay Kit on a NanoDrop 3300 Fluorometer. Equimolar amounts of purified PCR product were pooled and further purified using Ampure Beads (Agencourt). A sample of each library was run on an Agilent Bioanalyzer prior to emulsion PCR and sequencing as recommended by Roche. Amplicon libraries were subsequently sequenced on a 454 GS-FLX using Titanium sequencing chemistry.

Sequencing of 16S rRNA genes by MiSeq Illumina

Prior to sequencing the variable regions 1 and 2 (V1V2) of the bacterial 16S rRNA genes were amplified according to a previously established protocol using the primers 27F and 338R (Rausch et al., 2016). For bacterial 16S rRNA profiling paired-end sequencing of 2x300 bp was performed on the Illumina MiSeq platform.

16S rRNA gene sequence analysis

16S rRNA gene amplicon sequence analysis was conducted using the Qiime 1.8.0 package (Madigan et al., 1984). Using the sequence fasta-file, a quality file and a mapping file which assigned the 10 nt barcodes to the corresponding sample as input, the sequences were analyzed using the following parameters: length between 300 and 400 bp, no ambiguous bases and no mismatch to the primer sequence. Chimeric sequences were identified using Chimera Slayer (Haas et al., 2011) and verified manually before removal from the data set. Putative

chimeric sequences, which were present in at least two independent samples, were retained. Reads assigned to chloroplasts of the algal endosymbiont were removed *in silico*. Sequences were rarified to the lowest number of reads in the dataset, which was 3000 reads. Subsequently, sequences were grouped into operational taxonomic units (OTUs) at a ≥ 97% sequence identity threshold and classified by RDP classifier. Bacterial community analyses including six beta-diversity measures, statistical analysis of clustering (using the statistical methods adonis) and principal coordinate analysis (PCoA) were carried out using Qiime 1.8.0 package (Caporaso et al., 2010). Alpha diversity was calculated using the Chao1 metric implemented in Qiime.

Acknowledgments

We thank Benedikt Mortzfeld for his assistance in MiSeq library preparation. This work was funded by the Deutsche Forschungsgemeinschaft (DFG) through grants from the DFG Cluster of Excellence programs “The Future Ocean” and “Inflammation at Interfaces". MH was supported by JSPS grant KAKENHI (no.25840132).

References

Amann RI, Krumholz L and Stahl DA (1990) Fluorescent-oligonucleotide probing of whole cells for determinative, phylogenetic, and environmental studies in microbiology. *J. Bacteriol.* **172**(2). 762–770. doi:10.1128/jb.172.2.762-770.1990.

Arjona A, Silver AC, Walker WE and Fikrig E (2012) Immunity’s fourth dimension: Approaching the circadian-immune connection. *Trends Immunol.*, 607–612. doi:10.1016/j.it.2012.08.007.

Ashelford KE (2002) PRIMROSE: a computer program for generating and estimating the phylogenetic range of 16S rRNA oligonucleotide probes and primers in conjunction with the RDP-II database. *Nucleic Acids Res.* **30**(15). 3481–3489. doi:10.1093/nar/gkf450.

Augustin R, Fraune S, Franzenburg S and Bosch TCG (2012) Where simplicity meets complexity: Hydra, a model for host-microbe interactions. *Adv. Exp. Med. Biol.* **710**. 71–81. doi:10.1007/978-1-4419-5638-5_8.

Avalos J and Estrada AF (2010) Regulation by light in Fusarium. *Fungal Genet. Biol.*, 930–938. doi:10.1016/j.fgb.2010.05.001.

Baldani JI, Videira SS, Dos Santos Teixeira KR, Reis VM, De Oliveira ALM, Schwab S, et al. (2014) The family Rhodospirillaceae. *The Prokaryotes: Alphaproteobacteria and Betaproteobacteria*, 533–618. doi:10.1007/978-3-642-30197-1_300.

Bates JM, Mittge E, Kuhlman J, Baden KN, Cheesman SE and Guillemin K (2006) Distinct signals from the microbiota promote different aspects of zebrafish gut differentiation. *Dev. Biol.* **297**(2). 374–86. doi:10.1016/j.ydbio.2006.05.006.

Bayram Ö, Krappmann S, Ni M, Jin WB, Helmstaedt K, Valerius O, et al. (2008) VelB/VeA/LaeA complex coordinates light signal with fungal development and secondary metabolism. *Science (80-.).* **320**(5882). 1504–1506. doi:10.1126/science.1155888.

Belkaid Y and Hand TW (2014) Role of the microbiota in immunity and inflammation. *Cell*, 121–141. doi:10.1016/j.cell.2014.03.011.

Bordenstein SR and Theis KR (2015) Host biology in light of the microbiome: Ten principles of holobionts and hologenomes. *PLoS Biol.* **13**(8). e1002226. doi:10.1371/journal.pbio.1002226.

Bosch TCG (2012) Understanding complex host-microbe interactions in Hydra. *Gut Microbes*, 345–351. doi:10.4161/gmic.20660.

Bosch TCG and McFall-Ngai MJ (2011) Metaorganisms as the new frontier. *Zoology* **114**(4). 185–190.

Böttger A, Doxey AC, Hess MW, Pfaller K, Salvenmoser W, Deutzmann R, et al. (2012) Horizontal gene transfer contributed to the evolution of extracellular surface structures: the freshwater polyp Hydra is covered by a complex fibrous cuticle containing glycosaminoglycans and proteins of the PPOD and SWT (sweet tooth) families. *PLoS One* **7**(12). e52278. doi:10.1371/journal.pone.0052278.

Bourne D, Iida Y, Uthicke S and Smith-Keune C (2008) Changes in coral-associated microbial communities during a bleaching event. *ISME J.* **2**(4). 350–363. doi:10.1038/ismej.2007.112.

Bright M and Bulgheresi S (2010) A complex journey: Transmission of microbial symbionts. *Nat. Rev. Microbiol.*, 218–230. doi:10.1038/nrmicro2262.

Brown BE and Bythell JC (2005) Perspectives on mucus secretion in reef corals. *Mar. Ecol. Prog. Ser.*, 291–309. doi:10.3354/meps296291.

Brucker RM and Bordenstein SR (2013) The hologenomic basis of speciation: gut bacteria cause hybrid lethality in the genus Nasonia. *Science* **341**(6146). 667–9. doi:10.1126/science.1240659.

Campbell RD (1990) Transmission of symbiotic algae through sexual reproduction in hydra: Movement of algae into the oocyte. *Tissue Cell* **22**(2). 137–147. doi:10.1016/0040-8166(90)90017-4.

Caporaso JG, Kuczynski J, Stombaugh J, Bittinger K, Bushman FD, Costello EK, et al. (2010) QIIME allows analysis of high-throughput community sequencing data. *Nat. Methods* **7**(5). 335–6. doi:10.1038/nmeth.f.303.

Carlton RG and Richardson LL (1995) Oxygen and sulfide dynamics in a horizontally migrating cyanobacterial mat: Black band disease of corals. *FEMS Microbiol. Ecol.* **18**(2). 155–162. doi:10.1016/0168-6496(95)00052-C.

Carpenter KE, Abrar M, Aeby G, Aronson RB, Banks S, Bruckner A, et al. (2008) One-third of reef-building corals face elevated extinction risk from climate change and local impacts. *Science (80-.).* **321**(5888). 560–563. doi:10.1126/science.1159196.

Cernichiari E, Muscatine L and Smith DC (1969) Maltose Excretion by the Symbiotic Algae of Hydra viridis. *Proc. R. Soc. B Biol. Sci.* **173**(1033). 557–576. doi:10.1098/rspb.1969.0077.

Chandler JA, Lang J, Bhatnagar S, Eisen JA and Kopp A (2011) Bacterial communities of diverse Drosophila species: Ecological context of a host-microbe model system. *PLoS Genet.* **7**(9). e1002272. doi:10.1371/journal.pgen.1002272.

Franzenburg S, Walter J, Künzel S, Wang J, Baines JF, Bosch TCG, et al. (2013) Distinct antimicrobial peptide expression determines host species-specific bacterial associations. *Proc. Natl. Acad. Sci. U. S. A.* **110**(39). E3730-8. doi:10.1073/pnas.1304960110.

Fraune S, Anton-Erxleben F, Augustin R, Franzenburg S, Knop M, Schröder K, et al. (2015) Bacteria-bacteria interactions within the microbiota of the ancestral metazoan Hydra contribute to fungal resistance. *ISME J.* **9**(7). 1543–56. doi:10.1038/ismej.2014.239.

Fraune S and Bosch TCG (2007) Long-term maintenance of species-specific bacterial microbiota in the basal metazoan Hydra. *Proc. Natl. Acad. Sci.* **104**(32). 13146–13151. doi:10.1073/pnas.0703375104.

Fröbius AC, Genikhovich G, Kürn U, Anton-Erxleben F and Bosch TCG (2003) Expression of developmental genes during early embryogenesis of Hydra. *Dev. Genes Evol.* **213**(9). 445–455. doi:10.1007/s00427-003-0344-6.

Gofton AW, Oskam CL, Lo N, Beninati T, Wei H, McCarl V, et al. (2015) Inhibition of the endosymbiont "Candidatus Midichloria mitochondrii" during 16S rRNA gene profiling reveals potential pathogens in Ixodes ticks from Australia. *Parasites and Vectors* **8**(1). 345. doi:10.1186/s13071-015-0958-3.

Greay TL, Gofton AW, Paparini A, Ryan UM, Oskam CL and Irwin PJ (2018) Recent insights into the tick microbiome gained through next-generation sequencing. *Parasites and Vectors* **11**(1). 12. doi:10.1186/s13071-017-2550-5.

Green SJ and Minz D (2005) Suicide polymerase endonuclease restriction, a novel technique for enhancing PCR amplification of minor DNA templates. *Appl. Environ. Microbiol.* **71**(8). 4721–4727. doi:10.1128/AEM.71.8.4721-4727.2005.

Haas BJ, Gevers D, Earl AM, Feldgarden M, Ward D V., Giannoukos G, et al. (2011) Chimeric 16S rRNA sequence formation and detection in Sanger and 454-pyrosequenced PCR amplicons. *Genome Res.* **21**(3). 494–504. doi:10.1101/gr.112730.110.

Habetha M, Anton-Erxleben F, Neumann K and Bosch TCG (2003) The Hydra viridis / Chlorella symbiosis. Growth and sexual differentiation in polyps without symbionts. *Zoology* **106**(2). 101–108.

Hamada M, Schröder K, Bathia J, Kürn U, Fraune S, Khalturina M, et al. (2018) Metabolic co-dependence drives the evolutionarily ancient Hydra–Chlorella symbiosis. *Elife* **7**. doi:10.7554/eLife.35122.

Huss V a. R, Holweg C, Seidel B, Reich V, Rahat M and Kessler E (1993) There is an ecological basis for host/symbiont specificity in Chlorella/Hydra symbioses. *Endocytobiosis Cell Res.* **10**(1). 35–46.

Jolley E and Smith DC (1978) The green hydra symbiosis: I. Isolation, culture and characteristics of the Chlorella symbiont of 'European' Hydra viridis. *New Phytol.* **81**(3). 637–645. doi:10.1111/j.1469-8137.1978.tb01637.x.

Kawaida H, Ohba K, Koutake Y, Shimizu H, Tachida H and Kobayakawa Y (2013) Symbiosis between hydra and chlorella: Molecular phylogenetic analysis and experimental study provide insight into its origin and evolution. *Mol. Phylogenet. Evol.* **66**(3). 906–914. doi:10.1016/j.ympev.2012.11.018.

Kim H, Ridenour JB, Dunkle LD and Bluhm BH (2011) Regulation of stomatal tropism and infection by light in cercospora zeae-maydis: Evidence for coordinated host/pathogen responses to photoperiod? *PLoS Pathog.* **7**(7). e1002113. doi:10.1371/journal.ppat.1002113.

Koropatnick TA, Engle JT, Apicella MA, Stabb E V, Goldman WE and McFall-Ngai MJ (2004) Microbial factor-mediated development in a host-bacterial mutualism. *Science (80-.).* **306**(5699). 1186–1188. doi:10.1126/science.1102218.

Kuhl M, Cohen Y, Dalsgaard T, Jorgensen BB and Revsbech NP (1995) Microenvironment and photosynthesis of zooxanthellae in scleractinian corals studied with microsensors for O2, pH and light. *Mar. Ecol. Prog. Ser.* **117**(1–3). 159–177. doi:10.3354/meps117159.

Lederberg BJ and McCray AT (2001) ' Ome Sweet ' Omics-- A Genealogical Treasury of Words. *Sci.* **15**(7). 8.

Lee JE and Edery I (2008) Circadian Regulation in the Ability of Drosophila to Combat Pathogenic Infections. *Curr. Biol.* **18**(3). 195–199. doi:10.1016/j.cub.2007.12.054.

Lema KA, Willis BL and Bourneb DG (2012) Corals form characteristic associations with symbiotic nitrogen-fixing bacteria. *Appl. Environ. Microbiol.* **78**(9). 3136–3144. doi:10.1128/AEM.07800-11.

Lenhoff HM and Brown RD (1970) Mass culture of hydra: an improved method and its application to other aquatic invertebrates. *Lab. Anim.* **4**(1). 139–154. doi:10.1258/002367770781036463.

Lesser MP, Mazel CH, Gorbunov MY and Falkowski PG (2004) Discovery of symbiotic nitrogen-fixing cyanobacteria in corals. *Science (80-.).* **305**(5686). 997–1000. doi:10.1126/science.1099128.

Madigan M, Cox SS and Stegeman RA (1984) Nitrogen fixation and nitrogenase activities in members of the family Rhodospirillaceae. *J. Bacteriol.* **157**(1). 73–8.

Manz W, Amann R, Ludwig W, Wagner M and Schleifer KH (1992) Phylogenetic oligonucleotide probes for the major subclassesof Proteobacteria - problems and solutions. *Syst. Appl. Microbiol.* **15**. 593–600.

Margulis L, Thorington G, Berger B and Stolz J (1978) Endosymbiotic bacteria associated with the intracellular green algae ofHydra viridis. *Curr. Microbiol.* **1**(4). 227–232. doi:10.1007/BF02602848.

McAuley PJ (1986) The cell cycle of symbiotic Chlorella. III. Numbers of algae in green hydra digestive cells are regulated at digestive cell division. *J. Cell Sci.* **85**. 63–71.

McAuley PJ and Darrah PR (1990) Regulation of numbers of symbiotic Chlorella by density-dependent division. *Philos. Trans. - R. Soc. London, B* **329**(1252). 55–63. doi:10.1098/rstb.1990.0149.

McDonald MJ and Rosbash M (2001) Microarray analysis and organization of circadian gene expression in Drosophila. *Cell* **107**(5). 567–578. doi:10.1016/S0092-8674(01)00545-1.

McFall-Ngai M, Hadfield MG, Bosch TCG, Carey H V, Domazet-Lošo T, Douglas AE, et al. (2013) Animals in a bacterial world, a new imperative for the life sciences. *Proc. Natl. Acad. Sci. U. S. A.* **110**(9). 3229–36. doi:10.1073/pnas.1218525110.

Mortzfeld BM, Taubenheim J, Fraune S, Klimovich A V and Bosch TCG (2018) Stem Cell Transcription Factor FoxO Controls Microbiome Resilience in Hydra. *Front. Microbiol.* **9**. 629. doi:10.3389/fmicb.2018.00629.

Murillo-Rincon AP, Klimovich A, Pemöller E, Taubenheim J, Mortzfeld B, Augustin R, et al. (2017) Spontaneous body contractions are modulated by the microbiome of Hydra. *Sci. Rep.* **7**(1). 15937. doi:10.1038/s41598-017-16191-x.

Muscatine L (1965) Symbiosis of hydra and algae—III. Extracellular products of the algae. *Comp. Biochem. Physiol.* **16**(1). 77–92. doi:10.1016/0010-406X(65)90165-9.

Muscatine L, Cook CB, Pardy RL and Pool RR (1975) Uptake, recognition and maintenance of symbiotic Chlorella by Hydra viridis. *Symp. Soc. Exp. Biol.* (29). 175–203.

Muscatine L, Karakashian SJ and Karakashian MW (1967) Soluble extracellular products of algae symbiotic with a ciliate, a sponge and a mutant hydra. *Comp. Biochem. Physiol.* **20**(1). 1–12. doi:10.1016/0010-406X(67)90720-7.

Muscatine L and Lenhoff HM (1963) Symbiosis: On the role of algae symbiotic with hydra. *Science (80-.).* **142**(3594). 956–958. doi:10.1126/science.142.3594.956.

Muscatine L and Lenhoff HM (1965) Symbiosis of Hydra and Algae. II. Effects of Limited Food and Starvation on Growth of Symbiotic and Aposymbiotic Hydra. *Biol. Bull.* **129**(2). 316. doi:10.2307/1539848.

Muscatine L and McAuley PJ (1982) Transmission of symbiotic algae to eggs of green hydra. *Cytobios* **33**(130). 111–124.

Pardy RL (1976) The production of aposymbiotic hydra by the photodestruction of green hydra zoochlorellae. *Biol. Bull.* **151**(1). 225–235. doi:10.2307/1540716.

Park HD, Greenblatt CL, Mattern CFT and Merril CR (1967) Some relationships between Chlorohydra, its symbionts and some other chlorophyllous forms. *J. Exp. Zool.* **164**(2). 141–161. doi:10.1002/jez.1401640203.

Perez S (2006) Nitric oxide and cnidarian bleaching: an eviction notice mediates breakdown of a symbiosis. *J. Exp. Biol.* **209**(14). 2804–2810. doi:10.1242/jeb.02309.

Pujalte MJ, Lucena T, Ruvira MA, Arahal DR and Macián MC (2014) The family Rhodobacteraceae. *The Prokaryotes: Alphaproteobacteria and Betaproteobacteria*, 439–512. doi:10.1007/978-3-642-30197-1_377.

Raina J-B, Dinsdale EA, Willis BL and Bourne DG (2010) Do the organic sulfur compounds DMSP and DMS drive coral microbial associations? *Trends Microbiol.* **18**(3). 101–108. doi:10.1016/j.tim.2009.12.002.

Raina JB, Tapiolas D, Willis BL and Bourne DG (2009) Coral-associated bacteria and their role in the biogeochemical cycling of sulfur. *Appl. Environ. Microbiol.* **75**(11). 3492–3501. doi:10.1128/AEM.02567-08.

Rausch P, Basic M, Batra A, Bischoff SC, Blaut M, Clavel T, et al. (2016) Analysis of factors contributing to variation in the C57BL/6J fecal microbiota across German animal facilities. *Int. J. Med. Microbiol.* **306**(5). 343–355. doi:10.1016/j.ijmm.2016.03.004.

Rawls JF, Samuel BS and Gordon JI (2004) Gnotobiotic zebrafish reveal evolutionarily conserved responses to the gut microbiota. *Proc. Natl. Acad. Sci. U. S. A.* **101**(13). 4596–601. doi:10.1073/pnas.0400706101.

Reis AMM, Araújo SD, Moura RL, Francini-Filho RB, Pappas G, Coelho AMA, et al. (2009) Bacterial diversity associated with the Brazilian endemic reef coral Mussismilia braziliensis. *J. Appl. Microbiol.* **106**(4). 1378–1387. doi:10.1111/j.1365-2672.2008.04106.x.

Ritchie KB (2006) Regulation of microbial populations by coral surface mucus and mucus-associated bacteria. *Mar. Ecol. Prog. Ser.* **322**. 1–14. doi:10.3354/meps322001.

Roden LC and Ingle RA (2009) Lights, Rhythms, Infection: The Role of Light and the Circadian Clock in Determining the Outcome of Plant-Pathogen Interactions. *PLANT CELL ONLINE* **21**(9). 2546–2552. doi:10.1105/tpc.109.069922.

Roffman B and Lenhoff HM (1969) Formation of polysaccharides by hydra from substrates produced by their endosymbiotic algae. *Nature* **221**(5178). 381–2.

Rohwer F, Seguritan V, Azam F and Knowlton N (2002) Diversity and distribution of coral-associated bacteria. *Mar. Ecol. Prog. Ser.* **243**. 1–10. doi:10.3354/meps243001.

Russell JA, Dubilier N and Rudgers JA (2014) Nature's microbiome: Introduction. *Mol. Ecol.*, 1225–1237. doi:10.1111/mec.12676.

Sampson TR and Mazmanian SK (2015) Control of brain development, function, and behavior by the microbiome. *Cell Host Microbe*, 565–576. doi:10.1016/j.chom.2015.04.011.

Scheiermann C, Kunisaki Y and Frenette PS (2013) Circadian control of the immune system. *Nat. Rev. Immunol.*, 190–198. doi:10.1038/nri3386.

Sharon G, Segal D, Ringo JM, Hefetz A, Zilber-Rosenberg I and Rosenberg E (2010) Commensal bacteria play a role in mating preference of Drosophila melanogaster. *Proc. Natl. Acad. Sci.* **107**(46). 20051–20056. doi:10.1073/pnas.1009906107.

Shikuma NJ, Antoshechkin I, Medeiros JM, Pilhofer M and Newman DK (2016) Stepwise metamorphosis of the tubeworm Hydroides elegans is mediated by a bacterial inducer and MAPK signaling. *Proc. Natl. Acad. Sci.* **113**(36). 10097–10102. doi:10.1073/pnas.1603142113.

Shnit-Orland M and Kushmaro A (2009) Coral mucus-associated bacteria: A possible first line of defense. *FEMS Microbiol. Ecol.* **67**(3). 371–380. doi:10.1111/j.1574-6941.2008.00644.x.

Simhadri RK, Fast EM, Guo R, Schultz MJ, Vaisman N, Ortiz L, et al. (2017) The Gut Commensal Microbiome of Drosophila melanogaster Is Modified by the Endosymbiont Wolbachia. *mSphere* **2**(5). e00287-17. doi:10.1128/mSphere.00287-17.

Sommer F and Bäckhed F (2013) The gut microbiota--masters of host development and physiology. *Nat. Rev. Microbiol.* **11**(4). 227–38. doi:10.1038/nrmicro2974.

Stone EF, Fulton BO, Ayres JS, Pham LN, Ziauddin J and Shirasu-Hiza MM (2012) The circadian clock protein timeless regulates phagocytosis of bacteria in Drosophila. *PLoS Pathog.* **8**(1). e1002445. doi:10.1371/journal.ppat.1002445.

Sunagawa S, DeSantis TZ, Piceno YM, Brodie EL, DeSalvo MK, Voolstra CR, et al. (2009) Bacterial diversity and White Plague Disease-associated community changes in the Caribbean coral Montastraea faveolata. *ISME J.* **3**(5). 512–21. doi:10.1038/ismej.2008.131.

Thorington G and Margulis L (1981) Hydra viridis: transfer of metabolites between Hydra and symbiotic algae. *Biol. Bull.* **160**(1). 175–188. doi:10.2307/1540911.

Vestheim H and Jarman SN (2008) Blocking primers to enhance PCR amplification of rare sequences in mixed samples - A case study on prey DNA in Antarctic krill stomachs. *Front. Zool.* **5**(1). 12. doi:10.1186/1742-9994-5-12.

Wang W, Barnaby JY, Tada Y, Li H, Tör M, Caldelari D, et al. (2011) Timing of plant immune responses by a central circadian regulator. *Nature* **470**(7332). 110–115. doi:10.1038/nature09766.

Wegley L, Edwards R, Rodriguez-Brito B, Liu H and Rohwer F (2007) Metagenomic analysis of the microbial community associated with the coral Porites astreoides. *Environ. Microbiol.* **9**(11). 2707–2719. doi:10.1111/j.1462-2920.2007.01383.x.

Wilkerson FP (1980) Bacterial symbionts on green hydra and their effect on phosphate uptake. *Microb. Ecol.* **6**(1). 85–92. doi:10.1007/BF02020377.

Zilber-Rosenberg I and Rosenberg E (2008) Role of microorganisms in the evolution of animals and plants: The hologenome theory of evolution. *FEMS Microbiol. Rev.*, 723–735. doi:10.1111/j.1574-6976.2008.00123.x.

General discussion

Hydra's gastric cavity – digestion in absence of bacterial symbionts

A surprising finding in the present study was that *Hydra*'s gastric cavity appears to be devoid of a stable bacterial community. While the digestive tract of many animals, in particular mammals, is colonized by a large and complex microbiota that complements the metabolic capacities of the host, *Hydra* seems to pursue a feeding strategy independent of the aid of bacterial symbionts.

In contrast to most multicellular animals, digestion in *Hydra* occurs extra- and intracellularly. The mouth opening is used for both, food uptake and excretion of waste products and thus, there is a two-way flow in the sac-like gastric cavity. Gland cells secrete proteolytic enzymes, while peristalsis, segmentation movements and cilia of the endodermal cells are stirring up the food and break it into small pieces (Shimizu et al., 2004). Finally, endodermal epithelial cells phagocytize food particles and digestion is completed intracellularly. Notably, the apical surface of the endodermal cells does not exhibit a glycocalyx or a mucus gel, which may be more of a hindrance than a help in fulfilling their phagocytic task.

Taken together, stationary phagocytes lining the gastric cavity, the absence of a mucus layer, digestive movements and a relatively fast transit time of 6-9 hours that typify *Hydra*'s digestive physiology may be unfavorable to microbial growth. An additional attribute that may hinder microbial colonization includes the high expression levels of several AMP families in endodermal epithelium (Augustin et al., 2009a, 2009b; Bosch et al., 2009; Jung et al., 2009; Franzenburg et al., 2013).

Notably, *Hydra* is not unique in lacking a resident gut microbiota. For instance, in a parasitic horsehair worm (Hudson and Floate, 2007), sawfly larvae (Whittome et al., 2007), walking sticks (Shelomi et al., 2013), a saprophagous fly (Šustr et al., 2014), certain ants (Sanders et al., 2017) and a broad diversity of caterpillar species (Hammer et al., 2017) microbial symbionts were found to be generally absent or present only in low numbers in the digestive tract. A symbiont-independent feeding strategy may release *Hydra* and others from constraints imposed on animals that depend on gut symbionts. Engaging in mutualisms involves also costs (Frederickson et al., 2012; Nougué et al., 2015; Simonsen et al., 2017) such as nutrient competition between the host and the microbes (Gaskins et al., 2002), the risk of gut microbes becoming pathogenic (Broderick et al., 2009; Young et al., 2017) and exploitation of a hospitable gut environment by foodborne pathogens.

Nevertheless, *Hydra* polyps harbor a specific bacterial communities in the glycocalyx covering the ectodermal surface of the polyp. Although not contributing to digestion, *Hydra*'s microbiota has significant impact on host fitness by providing antifungal immunity (Fraune et al., 2015). A recent study demonstrated that the bacterial microbiota modulates the spontaneous contraction behaviour (Murillo-Rincon et al., 2017) and also the feeding response of *Hydra* (Murillo, Klimovich, Bosch, *in prep.*). Intriguingly, in the absence of bacteria the feeding response of the polyps is significantly shortened. Thus, although not assisting in digestion, *Hydra*'s bacterial microbiota may still be critically involved in the feeding process by regulating the polyp's behaviour.

Hydra's glycocalyx – a prototype of mucosal interfaces?

The mammalian gut harbors the largest and most diverse microbial communities of the body. Intriguingly, its surface is only lined by a single cell layer, which is covered by an extensive glycocalyx and a mucus gel. The extraordinary task of maintaining tolerance to the beneficial microbiota and innocuous food antigens, while at the same time combating occasionally incoming pathogens, is pursued by the mucosal immune system. Both, immunological and physical barriers regulate the spatial organization of the microbiota, which is crucial for intestinal homeostasis (Johansson and Hansson, 2016). In the large intestine the mucus is organized in two distinct layers; an outer loose layer representing the habitat of the microbiota and an adherent inner layer, which is impervious to the bacteria and thus, forms a barrier preventing excessive immune activation in the healthy gut (Johansson et al., 2008, 2011; Johansson and Hansson, 2016). Furthermore, the antibacterial lectin RegIIIγ was shown to play a crucial role in the spatial segregation between the microbiota and the host epithelium in the small intestine (Vaishnava et al., 2011; El Aidy et al., 2012).

The ancient metazoan *Hydra* is colonized by species-specific bacterial communities that are remarkably stable and provide antifungal immunity to their host. Instead of harbouring the symbiotic microbes in the gastric cavity, *Hydra* hosts its bacterial colonizers on the surface of the ectodermal epithelium facing the aquatic environment. More precisely, the ectodermal epithelium is covered by a multilayered glycocalyx and the bacteria inhabit the outer mucus-like layer, but were never observed to penetrate the inner glycocalyx layers. The present work provides the first evidence, that the dual function of mucus as a habitat and a barrier can be traced back to ancestral metazoans and thus, may display a conserved feature. Compared to mammalian mucus gels ranging in thickness from 10 µm in the eye up to 700 µm in the

mammalian large intestine (Linden et al., 2008), *Hydra*'s glycocalyx appears relatively small extending ~1.5 µm from the cell surface. However, considering that the entire *Hydra* polyp is composed only of an epithelial bilayer and mucus regeneration is metabolically costly, the glycocalyx appears to be at an appropriate ratio.

Given that metazoan evolution took place in an environment dominated by microorganisms, it is likely that immune systems evolved as much to manage and exploit beneficial microbes as to fend off harmful ones. Launching an immune response comes at a cost, consuming extra resources and energy. Between efficiency and cost, metazoans are driven to evolve immune mechanisms and strategies to achieve a dynamic balance within the holobiont (Huang et al., 2011). Toward this goal, early-emerging metazoans have used their single-cell epithelia to develop an effective innate immune system to detect and control microbial colonization. The ability to produce a multi-functional mucus gel as an interface between the epithelium and the external environment was an important evolutionary step and the emerge of mucin-like protein can be traced back to the begin of metazoan evolution (Lang et al., 2007, 2016). However, over the past 560 million years of vertebrate evolution, additional and complex mechanisms of mucosal defenses have evolved. Early vertebrates, such as fish, originated in aquatic environments and therefore their skin represents an mucosal surface that harbours mucus-producing cells, lacks keratinization, and is built from living epithelial cells that are in direct contact with the water. Strikingly, it was found that the skin of fish shares key features of mammalian mucosal immune responses (Salinas et al., 2011; Gomez et al., 2013; Xu et al., 2013). Thus, regardless of the phylogenetic origin and tissue localization, mucosal immunity may operate under the guidance of primordially conserved principles.

The mucus of fish skin contains a rich repertoire of immune-related substances including lectins, protease-inhibitors, enzymes such as peroxidases, proteases and lysozyme, as well as numerous AMPs (Ross et al., 2000; Watanabe et al., 2009; Guardiola et al., 2014; Esteban and Cerezuela, 2015; Cordero et al., 2016). Strikingly, in the present many of these molecules have been identified as putative components of *Hydra*'s glycocalyx (chapter I, Table 1). However, these proteins are awaiting future validation and follow-up experiments to elucidate their potential role in host defense and regulation of the microbiota.

Taken together, the present study demonstrated that the ectodermal epithlium of the ancient metazoan *Hydra* is covered by a mucus-like layer that represents a barrier and the habitat for the bacterial microbiota. Furthermore, a mass spectrometry analysis of the mucus-like layer identified among others mucin-like proteins, putative AMPs and lectins,

which are important components of both, the skin mucus of fish (Dash et al., 2018) and the mucus of the mammalian intestine (Chairatana and Nolan, 2017). Thus, although *Hydra* appears to be a 'scaled-down' model in terms of epithelial cell types, magnitude of the mucus layer, diversity of the microbiota and the lack of adaptive immunity, the polyp seems to share many innate immune components with the vertebrate 'mucosome' (the combined host- and microbe-derived components present in the mucus). Furthermore, *Hydra*'s body wall is built up by a single-layered epithelium of unipotent stem cells that continuously self-renew, rapidly close wounds and provide a protective physical barrier. Key players of *Hydra*'s innate immune system such as TLR-signaling and AMPs were shown to be not only involved in pathogen defense, but also play a critical role in selecting the resident microbiota (Franzenburg et al., 2012, 2013). Similarly, the mammalian intestinal epithelium is composed of a single cell layer with a high turnover rate and displays a crucial regulator of gut homeostasis by acting as a physical barrier and as a coordinating hub for immune defense and crosstalk between bacteria and the host. As an aquatic organism, *Hydra* lives in a medium where microorganisms thrive more than in the air and thus, the mucosal surface of the ectodermal epithelium may face similar obstacles to those encountering vertebrate mucosal tissues. As an evolutionary ancient metazoan, *Hydra* can provide insights into the basic molecular toolkit required for establishment and maintenance of a holobiont and has been proven to be a valuable model to analyze host-microbe interactions in the last decade. Its 'scaled-down' complexity together with the availability of transgenic and germ-free polyps as well as the cultivability of most bacterial colonizers displays the precise strength of the model organism, which may allow to decipher the mechanisms in more complex systems such as the mammalian gut.

An ancient role for the nervous system in host-microbe interactions

AMPs are ancient molecules of the innate immune system that act in both host defense and regulation of the resident microbiota (Salzman et al., 2010; Bevins and Salzman, 2011; Vaishnava et al., 2011; Franzenburg et al., 2013). In the present study it was shown that antimicrobial activity is not restricted to epithelium-derived peptides, but also a feature of several neuropeptides in the ancient metazoan *Hydra*. Indeed, an additional function as anti-infective molecules has been hypothesized for some neuropeptides due to their similarities with AMPs in size, amino-acid composition, cationic charge and amphipathic design (Brogden et al., 2005). In mammals, neuropeptides such as substance P, calcitonin gene-related peptide, vasoactive intestinal polypeptide (VIP), and neuropeptide Y were shown to possess *in vitro*

antimicrobial activities against *E. coli* and *Pseudomonas aeruginosa* (El Karim et al., 2008) comparable with those reported for α-defensin (Lundy et al., 2008). However, the *in vivo* significance of neuropeptide-derived antimicrobial activity has not been addressed so far.

As a part of this thesis, it was demonstrated that the antimicrobial neuropeptide NDA-1 regulates the spatial distribution of *Curvibacter* sp., the main bacterial colonizer. In *Hydra*, the bacterial habitat is formed by the mucus-like layer of the glycocalyx covering the ectodermal epithelium. Notably, neurons are interspersed among the epithelial cells and their secreted products likely contribute to the 'mucosome' (the combined host- and microbe-derived components present in the mucus), which creates a specific habitat for a distinct microbia. The local distribution of *Hydra*'s neurons, which express specific sets of neuropeptides may lead to local heterogeneity of the mucosome and thus, regulate the microbial community composition along the polyp's body axis. Further investigations are required to address the arising question how the spatial organization of *Hydra*'s microbiota is connected to their function.

Interestingly, attempts to overexpress NDA-1 ectopically in epithelial cells resulted in a lethal phenotype early after hatching, suggesting that, in addition to its role in spatial organization of *Hydra*'s microbiota, NDA-1 has other not yet discovered functions. Indeed, pleiotropic functions have been consistently reported for both neuropeptides and AMPs revealing that these two groups of molecules share more than antimicrobial activity. For instance, immune cells themselves produce neuropeptides in response to inflammatory signals and these neuropeptides act in an autocrine/paracrine manner through their specific receptors, which are also expressed on macrophages, microglia and neutrophils (Gonzalez-Rey and Delgado, 2007; Smith, 2008). Most neuropeptides show a clear anti-inflammatory profile and thus, participate in the maintenance of immune tolerance (Gonzalez-Rey and Delgado, 2007). Similarly, some AMPs were also shown to function as potent immune regulators by acting as chemokines, modulating TLR-dependent inflammatory responses, and promoting wound healing (Nakatsuji and Gallo, 2012). Taken together, both neuropeptides and AMPs appear to have additional functions as immune-modulatory cytokine-like factors. Furthermore, it has been shown recently that some AMPs are implicated in sleep regulation (Dissel et al., 2015) and long-term memory (Barajas-Azpeleta et al., 2018) in *Drosophila*, suggesting that AMPs have not exclusively immune-related functions, but may also act as neuromodulators in the nervous system.

Although traditionally the immune and the nervous systems have been considered to be independent, today there is compelling evidence that they are integrally connected and use a

common biochemical language for intra- and inter-system communication. For instance, neuropeptide receptors are expressed on immune cells (Sternberg, 2006; Gonzalez-Rey and Delgado, 2007; Smith, 2008; Gonzalez-Rey et al., 2010), while TLRs are present on neurons of the enteric nervous system (Barajon et al., 2009; Anitha et al., 2012) and on neurons, microglial cells and astrocytes of the brain (van Noort and Bsibsi, 2009; Arroyo et al., 2011; Mallard, 2012). While the immune system-microbiota alliance has been acknowledged soon after realizing the tremendous impact of microbes on host physiology, the idea that the microbiota influences the nervous system and *vice versa* came into focus comparatively late. Nevertheless, today a large body of evidence has accumulated indicating that the microbiota is required for normal development and function of the nervous system including cognitive, emotional and behavioral processes (Cryan and Dinan, 2012; Forsythe and Kunze, 2012; Sharon et al., 2016). Although most studies have been performed in rodents, there is also evidence coming from invertebrates. For instance, in *Drosophila melanogaster* a member of the gut microbiota modulates mate choice (Sharon et al., 2010) and in *C. elegans* recognition of pathogenic bacteria secondary metabolites by neurons triggers avoidance behavior to reduces the ingestion of pathogens (Meisel et al., 2014). In *Hydra* the spontaneous contractile behavior (Murillo-Rincon et al., 2017) and the feeding response (Murillo, Klimovich, Bosch, *in prep.*) are influenced by the microbiota suggesting that the bidirectional communication between the nervous system and the microbiota is an ancient feature throughout the metazoan lineage (Klimovich and Bosch, 2018). Furthermore, the finding that *Hydra*'s neuropeptides possess antimicrobial activity and regulate the bacterial community composition in a spatially-controlled manner extends the functional capacity of the nervous system in early-branching metazoans to innate immunity.

All multicellular organisms are holobionts that evolved in a world dominated by microorganisms. Thus, it can be speculated that the evolutionary process that resulted in the emerge of the nervous system was partly driven by the necessity to maintain homeostasis within the holobiont. Both, the immune system and the nervous system constantly survey the external and internal environments and orchestrate appropriate responses to a plethora of cues. It is hardly imaginable that two such vital systems can work isolated from one another without jeopardizing homeostasis of the holobiont. Indeed, today there is compelling evidence evidence that the immune system and the nervous are not self-regulated, but participate in a multifaceted bidirectional communication system involving neural, immune, endocrine, and metabolic signaling, which is reflected in the concept of the 'microbiota-gut-brain axis' (Stilling et al., 2014; Carabotti et al., 2015).

Almost 35 years ago Edwin Blalock first proposed that the immune system acts as a sensory organ and should be considered as our ‘sixth’ sense (Blalock, 1984, 2005; Blalock and Smith, 2007; Kipnis, 2018). Taking into account that the microbiota is inextricably connected to an organism’s health, the ‘invention’ of a sensory system that continously monitors the bacterial composition, localization and behavior appears to be a logic consequence. Thus, with the microbiota-gut-brain axis Blalock’s metaphor in part has become reality.

The green hydra holobiont – untangling a tripartite relationship

Endosymbiosis, in which one partner lives within the cells of a larger host organism, is the most intimate form of symbiosis. The establishment of an endosymbiotic relationship is typically driven by complementation of the host's metabolic capabilities by the endosymbiont, thereby enabling the holobiont to exploit vacant ecological niches and occupy new environments that otherwise would be inaccessible (Hoffmeister and Martin, 2003; Archibald, 2009; Douglas, 2009; Wernegreen, 2012). Algal endosymbiosis is widely present among eukaryotes including many protists and invertebrates such as Porifera and Cnidaria. Symbiosis research traditionally focused on bipartite interactions such as the coral-*Symbiodinium* association. However, with the discovery that diseased or bleached corals harbor different bacterial communities than healthy ones (Perez, 2006; Ritchie, 2006; Bourne et al., 2008; Reis et al., 2009; Sunagawa et al., 2009), researchers have developed a growing appreciation of the coral holobiont as a complex tripartite interkingdom symbiosis. The documented decline in coral reef ecosystems worldwide (Carpenter et al., 2008) gives researchers a new urgency to understand the underlying mechanisms of these tripartite associations and which factors lead to their breakdown (‘*coral bleaching*’).

In the present study the *H. viridissima* holobiont was used to investigate symbiotic interactions in a tripartite cnidarian–algal–bacterial model system. Genome sequencing of the photosynthetic *Chlorella* sp. A99 revealed a degenerated nitrate assimilation pathway and a large number of amino acid transporters indicating that the alga depends on the import of host-derived amino acids as a nitrogen source. Indeed, *in vitro* growth of otherwise obligate symbiotic *Chlorella* was supported by supplementing the medium with glutamine, but not with the inorganic nitrogen compounds ammonium and nitrite. Microarray transcriptional profiling of the hydra host identified, among others, a glutamine synthetase that is specifically up-regulated by the photosynthetic activity of *Chlorella* as well as by supplying exogenous maltose or glucose. These results indicate a metabolic co-dependence between *H. viridissima* and

Chlorella. The algae provide the photosynthetic product maltose or glucose to *Hydra*, which in turn up-regulates the glutamine synthetase expression to supply the endosymbiont with a suitable nitrogen source.

Pioneering studies in the 1980s showed that there is a great deal of adaptation and specificity in the *Hydra-Chlorella* symbiosis and suggested that distinct physiological requirements must be fulfilled by both partners for successful establishment of a stable endosymbiosis (McAuley and Smith, 1982; Rahat and Reich, 1984). The results of the present study support this view. On one hand, an alga that does not secrete maltose or glucose will not be efficiently supplied with glutamine by *H. viridissima*. On the other hand, the secretion of photosynthesis products may not induce glutamine synthesis in *Hydra* species outside the *viridissima* group. The *H. viridissima* genome project is under way and will most likely provide further insights into the molecular toolkit that enables the members of the *viridissima* species group to establish and stably maintain endosymbiosis with *Chlorella* algae, but not other *Hydra* species. A previous study reported that seven strains of *Chlorella* algae, which were originally symbiotic with other invertebrates, formed stable associations with the European strain of green hydra (Douglas and Smith, 1984). However, it is not clear to what extent these associations resemble the physiological relationship of *H. viridissima* and its native *Chlorella* endosymbiont. In the present study aposymbiotic animals of the Australian *H. viridissima* A99 strain were infected with NC64A, the endosymbiont of the protist *Paramecium* (Karakashian and Karakashian, 1965). Although, *H. viridissima* and *Chlorella* NC64A formed a stable association, these polyps showed a significantly reduced growth rate and number of algae per cell compared to the symbiosis with native *Chlorella* A99. Furthermore, these polyps were never observed to form oocytes suggesting that sexual reproduction of *Hydra* is blocked in the presence of a foreign endosymbiont and thus, the *Hydra*-NC64A association may represent an evolutionary dead end (Hamada and Schröder, *unpublished data*).

A potential focal point for further study is the question how maintenance of a stable symbiont / host cell ratio is achieved in the *Hydra-Chlorella* symbiosis. Besides a mechanism directly interfering with algal mitosis, several studies indicated that the algal division rate might be regulated by the availability of host-derived inorganic nutrients such as nitrogen (McAuley, 1986, 1987; McAuley and Muscatine, 1986; Rees, 1986, 1989, 1990a, 1990b; Rees and Ellard, 1989; Rees et al., 1989). The present study demonstrated that aposymbiotic polyps cultured in maltose supplemented media show a dose-dependent up-regulation of the glutamine synthetase gene. Furthermore, previous studies have reported that the native *Chlorella* symbiont releases

significantly larger amounts of maltose than *Chlorella variabilis* NC64A (Mews and Smith, 1982; Rees, 1989). Indeed, *H. viridissima,* which have been artificially infected with NC64A algae showed a significantly reduced growth rate and number of algae per cell compared to the symbiosis with native *Chlorella* A99. Taken together, these results provide strong support for previous views that restriction of nitrogen supply may be an essential element in the host's control over the algae and that the amount of maltose released by symbiotic algae contributes to the stabilization of the symbiotic association (Cernichiari et al., 1969). However, *Chlorella* A99 could not be cultivated permanently in media containing glutamine or casamino acids, indicating that the obligate symbiont requires additional growth factors from *Hydra*, which may add another level of control to the host.

Apart from the metabolic interactions between *Hydra* and *Chlorella* A99, another aspect investigated in the present study was the influence of photosynthetic algae on the bacterial microbiota of *H. viridissima*. Interestingly, the *Chlorella* endosymbiont appears to shape the bacterial community composition in *H. viridissima* in a light-dependent manner. The diurnal fluctuations of the microbiota are independent of the host's endogenous circadian rhythm, because they do not occur in aposymbiotic animals and diminish in symbiotic animals subjected to darkness for 48 hours. Instead, the diurnal microbial shift seem to depend on the photosynthetic activity of the *Chlorella* endosymbiont. How the intracellular algae residing in the endoderm influence the extracellular bacteria colonizing the ectodermal surface is unknown. One can speculate that *Chlorella*'s photosynthetic activity may affect the microbiota by changing microenvironmental physicochemical parameters such as pH and oxygen level in the bacterial habitat represented by the mucus-like layer of the glycocalyx. Indeed, some studies indicate that the mucus of some corals cycles from being fully-oxygenated during photosynthesis of the coral endosymbiont *Symbiodinium* to anaerobic at night when respiration rates exceed oxygenesis (Carlton and Richardson, 1995; Kuhl et al., 1995; Brown and Bythell, 2005). Another possibility is that the microbial niche is modified due to photosynthesis-induced changes in host metabolism. Microarray analysis has shown that the photosynthetic activity of *Chlorella* involves transcriptional changes not only in endoderm of *H. viridissima*, but also in the ectoderm indicating that photosynthetic products can be transported across the two tissue layers or some signals are transduced by cell-cell communication. Thus, although photosynthesis is occurring in the endodermal epithelium, it may affect the ectoderm-derived bacterial habitat. Furthermore, microalgae are well-known to produce a wide range of secondary metabolites including antibacterial compounds (Amaro et al., 2011; Falaise et al., 2016). Indeed, the *Chlorella* A99 genome contains some genes with similarity to non-ribosomal

peptide synthetases (NRPS) (Hamada, *unpublished data*). NRPS are large multienzyme machineries that assemble numerous peptides with large structural and functional diversity including antibiotics such as vancomycin and the β-lactam-containing penicillins and cephalosporins. However, the function of *Chlorella*'s NRPS and their transcriptional regulation in terms of light- or photosynthesis-dependency requires further investigations.

Another question that arises from the results of this study is whether the light-dependent diurnal fluctuations of the bacterial microbiota play a physiological role in green hydra or rather display a by-product of the photosynthetic activity of *Chlorella*. One function of *Hydra*'s microbiota is to provide resistance against the filamentous fungi *Fusarium* sp. (Fraune et al., 2015). Interestingly, multiple aspects of pathogenesis in filamentous fungi are regulated in a light-dependent manner including the production of asexual spores and the synthesis of secondary metabolites such as mycotoxins (Bayram et al., 2008; Avalos and Estrada, 2010; Kim et al., 2011). Therefore, one may speculate that diurnal fluctuations in the bacterial community composition may represent an adaptation to maximize host defense at times when pathogen invasion is most likely to occur. Indeed, many immune functions have been shown to be regulated in diurnal manner (reviewed in (Arjona et al., 2012; Scheiermann et al., 2013)), a phenomenon observed not only in mammals, but also in flies and plants (McDonald and Rosbash, 2001; Lee and Edery, 2008; Roden and Ingle, 2009; Wang et al., 2011; Stone et al., 2012).

In summary, the finding that intracellular algae shape the bacterial microbiota of *H. viridissima* in a light-dependent manner adds a new aspect to our knowledge on the forces that structure microbial communities in tripartite interkingdom associations. Further research is required to address the questions whether the light-dependent microbial fluctuations have functional consequences for the holobiont phenotype and whether this phenomenon also occurs in other tripartite symbioses such as corals. Interestingly, a recent study in the anthozoan *Aptasia* revealed that the presence of endosymbiontic *Symbiodinium* algae is associated with dramatic changes in the host's endogenous behavioral and transcriptional rhythms and suggesting that the endosymbiont is setting pace of the rhythmicity in body and tentacle contraction (Sorek et al., 2018). However, the authors did not look for changes in the bacterial microbiota.

References

Amaro HM, Guedes AC and Malcata FX (2011) Antimicrobial activities of microalgae : an invited review. In "Science against microbial pathogens: communicating current research and technological advances" Méndez-Vilas A. (ed) Formatex. , 1272–1280.

Anitha M, Vijay-Kumar M, Sitaraman S V., Gewirtz AT and Srinivasan S (2012) Gut microbial products regulate murine gastrointestinal motility via toll-like receptor 4 signaling. *Gastroenterology* **143**(4). 1006–1016.e4. doi:10.1053/j.gastro.2012.06.034.

Archibald JM (2009) The Puzzle of Plastid Evolution. *Curr. Biol.*, R81–R88. doi:10.1016/j.cub.2008.11.067.

Arjona A, Silver AC, Walker WE and Fikrig E (2012) Immunity's fourth dimension: Approaching the circadian-immune connection. *Trends Immunol.*, 607–612. doi:10.1016/j.it.2012.08.007.

Arroyo DS, Soria JA, Gaviglio EA, Rodriguez-Galan MC and Iribarren P (2011) Toll-like receptors are key players in neurodegeneration. *Int. Immunopharmacol.*, 1415–1421. doi:10.1016/j.intimp.2011.05.006.

Augustin R, Anton-Erxleben F, Jungnickel S, Hemmrich G, Spudy B, Podschun R, et al. (2009a) Activity of the novel peptide arminin against multiresistant human pathogens shows the considerable potential of phylogenetically ancient organisms as drug sources. *Antimicrob. Agents Chemother.* **53**(12). 5245–50. doi:10.1128/AAC.00826-09.

Augustin R, Siebert S and Bosch TCG (2009b) Identification of a kazal-type serine protease inhibitor with potent anti-staphylococcal activity as part of Hydra's innate immune system. *Dev. Comp. Immunol.* **33**(7). 830–7. doi:10.1016/j.dci.2009.01.009.

Avalos J and Estrada AF (2010) Regulation by light in Fusarium. *Fungal Genet. Biol.*, 930–938. doi:10.1016/j.fgb.2010.05.001.

Barajas-Azpeleta R, Wu J, Gill J, Welte R, Seidel C, McKinney S, et al. (2018) Antimicrobial peptides modulate long-term memory. *PLoS Genet.* **14**(10). e1007440. doi:10.1371/journal.pgen.1007440.

Barajon I, Serrao G, Arnaboldi F, Opizzi E, Ripamonti G, Balsari A, et al. (2009) Toll-like receptors 3, 4, and 7 are expressed in the enteric nervous system and dorsal root ganglia. *J. Histochem. Cytochem.* **57**(11). 1013–1023. doi:10.1369/jhc.2009.953539.

Bayram Ö, Krappmann S, Ni M, Jin WB, Helmstaedt K, Valerius O, et al. (2008) VelB/VeA/LaeA complex coordinates light signal with fungal development and secondary metabolism. *Science (80-.).* **320**(5882). 1504–1506. doi:10.1126/science.1155888.

Beutler B (2004) Innate immunity: an overview. *Mol. Immunol.* **40**(12). 845–59.

Bevins CL and Salzman NH (2011) The potter's wheel: the host's role in sculpting its microbiota. *Cell. Mol. Life Sci.* **68**(22). 3675–3685. doi:10.1007/s00018-011-0830-3.

Blalock JE (1984) The immune system as a sensory organ. *J. Immunol.* **132**(3). 1067–70.

Blalock JE (2005) The immune system as the sixth sense. *J. Intern. Med.*, 126–138. doi:10.1111/j.1365-2796.2004.01441.x.

Blalock JE and Smith EM (2007) Conceptual development of the immune system as a sixth sense. *Brain. Behav. Immun.* **21**(1). 23–33. doi:10.1016/j.bbi.2006.09.004.

Bosch TCG, Augustin R, Anton-Erxleben F, Fraune S, Hemmrich G, Zill H, et al. (2009) Uncovering the evolutionary history of innate immunity: The simple metazoan Hydra uses epithelial cells for host defence. *Dev. Comp. Immunol.* **33**(4). 559–569.

Bourne D, Iida Y, Uthicke S and Smith-Keune C (2008) Changes in coral-associated microbial communities during a bleaching event. *ISME J.* **2**(4). 350–363. doi:10.1038/ismej.2007.112.

Broderick NA, Robinson CJ, McMahon MD, Holt J, Handelsman J and Raffa KF (2009) Contributions of gut bacteria to Bacillus thuringiensis-induced mortality vary across a range of Lepidoptera. *BMC Biol.* **7**(1). 11. doi:10.1186/1741-7007-7-11.

Brogden KA, Guthmiller JM, Salzet M and Zasloff M (2005) The nervous system and innate immunity: the neuropeptide connection. *Nat. Immunol.* **6**(6). 558–64. doi:10.1038/ni1209.

Brown BE and Bythell JC (2005) Perspectives on mucus secretion in reef corals. *Mar. Ecol. Prog. Ser.*, 291–309. doi:10.3354/meps296291.

Carabotti M, Scirocco A, Maselli MA and Severi C (2015) The gut-brain axis: interactions between enteric microbiota, central and enteric nervous systems. *Ann. Gastroenterol.* **28**(2). 203–209.

Carlton RG and Richardson LL (1995) Oxygen and sulfide dynamics in a horizontally migrating cyanobacterial mat: Black band disease of corals. *FEMS Microbiol. Ecol.* **18**(2). 155–162. doi:10.1016/0168-6496(95)00052-C.

Carpenter KE, Abrar M, Aeby G, Aronson RB, Banks S, Bruckner A, et al. (2008) One-third of reef-building corals face elevated extinction risk from climate change and local impacts. *Science (80-.).* **321**(5888). 560–563. doi:10.1126/science.1159196.

Cernichiari E, Muscatine L and Smith DC (1969) Maltose Excretion by the Symbiotic Algae of Hydra viridis. *Proc. R. Soc. B Biol. Sci.* **173**(1033). 557–576. doi:10.1098/rspb.1969.0077.

Chairatana P and Nolan EM (2017) Defensins, lectins, mucins, and secretory immunoglobulin A: microbe-binding biomolecules that contribute to mucosal immunity in the human gut. *Crit. Rev. Biochem. Mol. Biol.*, 45–56. doi:10.1080/10409238.2016.1243654.

Cordero H, Cuesta A, Meseguer J and Esteban MA (2016) Characterization of the gilthead seabream (*Sparus aurata* L.) immune response under a natural lymphocystis disease virus outbreak. *J. Fish Dis.* **39**(12). 1467–1476. doi:10.1111/jfd.12481.

Cryan JF and Dinan TG (2012) Mind-altering microorganisms: the impact of the gut microbiota on brain and behaviour. *Nat. Rev. Neurosci.* **13**(10). 701–12. doi:10.1038/nrn3346.

Dash S, Das SK, Samal J and Thatoi HN (2018) Epidermal mucus, a major determinant in fish health: a review. *Iran. J. Vet. Res.* **19**(2). 72–81.

Dissel S, Seugnet L, Thimgan MS, Silverman N, Angadi V, Thacher P V., et al. (2015) Differential activation of immune factors in neurons and glia contribute to individual differences in resilience/vulnerability to sleep disruption. *Brain. Behav. Immun.* **47**. 75–85. doi:10.1016/j.bbi.2014.09.019.

Douglas A and Smith DC (1984) The Green Hydra Symbiosis. VIII. Mechanisms in Symbiont Regulation. *Proc. R. Soc. B Biol. Sci.* **221**(1224). 291–319. doi:10.1098/rspb.1984.0035.

Douglas AE (2009) The microbial dimension in insect nutritional ecology. *Funct. Ecol.*, 38–47. doi:10.1111/j.1365-2435.2008.01442.x.

El Aidy S, Van Baarlen P, Derrien M, Lindenbergh-Kortleve DJ, Hooiveld G, Levenez F, et al. (2012) Temporal and spatial interplay of microbiota and intestinal mucosa drive establishment of immune homeostasis in conventionalized mice. *Mucosal Immunol.* **5**(5). 567–579. doi:10.1038/mi.2012.32.

El Karim IA, Linden GJ, Orr DF and Lundy FT (2008) Antimicrobial activity of neuropeptides against a range of micro-organisms from skin, oral, respiratory and gastrointestinal tract sites. *J. Neuroimmunol.* **200**(1). 11–16. doi:10.1016/j.jneuroim.2008.05.014.

Esteban MÁ and Cerezuela R (2015) Fish mucosal immunity: Skin. *Mucosal Heal. Aquac.*, 67–92. doi:10.1016/B978-0-12-417186-2.00004-2.

Falaise C, François C, Travers MA, Morga B, Haure J, Tremblay R, et al. (2016) Antimicrobial compounds from eukaryotic microalgae against human pathogens and diseases in aquaculture. *Mar. Drugs*, 159. doi:10.3390/md14090159.

Forsythe P and Kunze WA (2012) Voices from within: gut microbes and the CNS. *Cell. Mol. Life Sci.* **70**(1). 55–69. doi:10.1007/s00018-012-1028-z.

Franzenburg S, Fraune S, Künzel S, Baines JF, Domazet-Loso T and Bosch TCG (2012) MyD88-deficient Hydra reveal an ancient function of TLR signaling in sensing bacterial colonizers. *Proc. Natl. Acad. Sci. U. S. A.* **109**(47). 19374–9. doi:10.1073/pnas.1213110109.

Franzenburg S, Walter J, Künzel S, Wang J, Baines JF, Bosch TCG, et al. (2013) Distinct antimicrobial peptide expression determines host species-specific bacterial associations. *Proc. Natl. Acad. Sci. U. S. A.* **110**(39). E3730-8. doi:10.1073/pnas.1304960110.

Fraune S, Anton-Erxleben F, Augustin R, Franzenburg S, Knop M, Schröder K, et al. (2015) Bacteria-bacteria interactions within the microbiota of the ancestral metazoan Hydra contribute to fungal resistance. *ISME J.* **9**(7). 1543–56. doi:10.1038/ismej.2014.239.

Frederickson ME, Ravenscraft A, Miller GA, Arcila Hernández LM, Booth G and Pierce NE (2012) The Direct and Ecological Costs of an Ant-Plant Symbiosis. *Am. Nat.* **179**(6). 768–778. doi:10.1086/665654.

Gaskins HR, Collier CT and Anderson DB (2002) Antibiotics as growth promotants: Mode of action. *Anim. Biotechnol.* **13**(1). 29–42. doi:10.1081/ABIO-120005768.

Gerbe F, Legraverend C and Jay P (2012) The intestinal epithelium tuft cells: specification and function. *Cell. Mol. Life Sci.* **69**(17). 2907–17. doi:10.1007/s00018-012-0984-7.

Gomez D, Sunyer JO and Salinas I (2013) The mucosal immune system of fish: the evolution of tolerating commensals while fighting pathogens. *Fish Shellfish Immunol.* **35**(6). 1729–39. doi:10.1016/j.fsi.2013.09.032.

Gonzalez-Rey E and Delgado M (2007) Anti-inflammatory neuropeptide receptors: new therapeutic targets for immune disorders? *Trends Pharmacol. Sci.*, 482–491. doi:10.1016/j.tips.2007.07.001.

Gonzalez-Rey E, Ganea D and Delgado M (2010) Neuropeptides: Keeping the balance between pathogen immunity and immune tolerance. *Curr. Opin. Pharmacol.*, 473–481. doi:10.1016/j.coph.2010.03.003.

Guardiola FA, Cuesta A, Abellán E, Meseguer J and Esteban MA (2014) Comparative analysis of the humoral immunity of skin mucus from several marine teleost fish. *Fish Shellfish Immunol.* **40**(1). 24–31. doi:10.1016/j.fsi.2014.06.018.

Hammer TJ, Janzen DH, Hallwachs W, Jaffe SP and Fierer N (2017) Caterpillars lack a resident gut microbiome. *Proc. Natl. Acad. Sci. U. S. A.* **114**(36). 9641–9646. doi:10.1073/pnas.1707186114.

Hoffmeister M and Martin W (2003) Interspecific evolution: Microbial symbiosis, endosymbiosis and gene transfer. *Environ. Microbiol.*, 641–649. doi:10.1046/j.1462-2920.2003.00454.x.

Huang S, Wang X, Yan Q, Guo L, Yuan S, Huang G, et al. (2011) The evolution and regulation of the mucosal immune complexity in the basal chordate amphioxus. *J. Immunol.* **186**(4). 2042–55. doi:10.4049/jimmunol.1001824.

Hudson AJ and Floate KD (2007) Further Evidence for the Absence of Bacteria in Horsehair Worms (Nematomorpha: Gordiidae). *J. Parasitol.* **95**(6). 1545–1547. doi:10.2307/40606764.

Johansson MEV and Hansson GC (2016) Immunological aspects of intestinal mucus and mucins. *Nat. Rev. Immunol.*, 639–649. doi:10.1038/nri.2016.88.

Johansson ME V, Ambort D, Pelaseyed T, Schütte A, Gustafsson JK, Ermund A, et al. (2011) Composition and functional role of the mucus layers in the intestine. *Cell. Mol. Life Sci.* **68**(22). 3635–41. doi:10.1007/s00018-011-0822-3.

Johansson ME V, Phillipson M, Petersson J, Velcich A, Holm L and Hansson GC (2008) The inner of the two Muc2 mucin-dependent mucus layers in colon is devoid of bacteria. *Proc. Natl. Acad. Sci. U. S. A.* **105**(39). 15064–9. doi:10.1073/pnas.0803124105.

Jung S, Dingley AJ, Augustin R, Anton-Erxleben F, Stanisak M, Gelhaus C, et al. (2009) Hydramacin-1, structure and antibacterial activity of a protein from the basal metazoan Hydra. *J. Biol. Chem.* **284**(3). 1896–905. doi:10.1074/jbc.M804713200.

Karakashian SJ and Karakashian MW (1965) Evolution and symbiosis in the genus chlorella and related algae. *Evolution (N. Y).* **19**(3). 368–377. doi:10.2307/2406447.

Kim H, Ridenour JB, Dunkle LD and Bluhm BH (2011) Regulation of stomatal tropism and infection by light in cercospora zeae-maydis: Evidence for coordinated host/pathogen responses to photoperiod? *PLoS Pathog.* **7**(7). e1002113. doi:10.1371/journal.ppat.1002113.

Kipnis J (2018) Immune system: The "seventh sense". *J. Exp. Med.* **215**(2). 397–398. doi:10.1084/jem.20172295.

Klimovich A V. and Bosch TCG (2018) Rethinking the Role of the Nervous System: Lessons From the Hydra Holobiont. *BioEssays*, 1800060. doi:10.1002/bies.201800060.

Kuhl M, Cohen Y, Dalsgaard T, Jorgensen BB and Revsbech NP (1995) Microenvironment and photosynthesis of zooxanthellae in scleractinian corals studied with microsensors for O2, pH and light. *Mar. Ecol. Prog. Ser.* **117**(1–3). 159–177. doi:10.3354/meps117159.

Lang T, Hansson GC and Samuelsson T (2007) Gel-forming mucins appeared early in metazoan evolution. *Proc. Natl. Acad. Sci. U. S. A.* **104**(41). 16209–14. doi:10.1073/pnas.0705984104.

Lang T, Klasson S, Larsson E, Johansson MEV, Hansson GC and Samuelsson T (2016) Searching the evolutionary origin of epithelial mucus protein components – mucins and FCGBP. *Mol. Biol. Evol.* msw066. doi:10.1093/molbev/msw066.

Lee J, Mo J-H, Katakura K, Alkalay I, Rucker AN, Liu Y-T, et al. (2006) Maintenance of colonic homeostasis by distinctive apical TLR9 signalling in intestinal epithelial cells. *Nat. Cell Biol.* **8**(12). 1327–1336. doi:10.1038/ncb1500.

Lee JE and Edery I (2008) Circadian Regulation in the Ability of Drosophila to Combat Pathogenic Infections. *Curr. Biol.* **18**(3). 195–199. doi:10.1016/j.cub.2007.12.054.

Linden SK, Sutton P, Karlsson NG, Korolik V and McGuckin MA (2008) Mucins in the mucosal barrier to infection. *Mucosal Immunol.*, 183–197. doi:10.1038/mi.2008.5.

Lundy FT, Nelson J, Lockhart D, Greer B, Harriott P and Marley JJ (2008) Antimicrobial activity of truncated α-defensin (human neutrophil peptide (HNP)-1) analogues without disulphide bridges. *Mol. Immunol.* **45**(1). 190–193. doi:10.1016/j.molimm.2007.04.018.

Mallard C (2012) Innate Immune Regulation by Toll-Like Receptors in the Brain. *ISRN Neurol.* **2012**. 1–19. doi:10.5402/2012/701950.

McAuley PJ (1986) Uptake of amino acids by cultured and freshly isolated symbiotic Chlorella. *New Phytol.* **104**(3). 415–427. doi:10.1111/j.1469-8137.1986.tb02909.x.

McAuley PJ (1987) Nitrogen limitation and amino-acid metabolism of Chlorella symbiotic with green hydra. *Planta* **171**(4). 532–538. doi:10.1007/BF00392303.

McAuley PJ and Muscatine L (1986) The cell cycle of symbiotic Chlorella. IV. DNA content of algae slowly increases during host starvation of green hydra. *J. Cell Sci.* **85**. 73–84.

McAuley PJ and Smith DC (1982) The Green Hydra Symbiosis. V. Stages in the Intracellular Recognition of Algal Symbionts by Digestive Cells. *Proc. R. Soc. B Biol. Sci.* **216**(1202). 7–23. doi:10.1098/rspb.1982.0058.

McDonald MJ and Rosbash M (2001) Microarray analysis and organization of circadian gene expression in Drosophila. *Cell* **107**(5). 567–578. doi:10.1016/S0092-8674(01)00545-1.

Mews LK and Smith DC (1982) The Green Hydra Symbiosis. VI. What is the Role of Maltose Transfer from Alga to Animal? *Proc. R. Soc. B Biol. Sci.* **216**(1205). 397–413. doi:10.1098/rspb.1982.0083.

Mukherji A, Kobiita A, Ye T and Chambon P (2013) Homeostasis in intestinal epithelium is orchestrated by the circadian clock and microbiota cues transduced by TLRs. *Cell* **153**(4). 812–827. doi:10.1016/j.cell.2013.04.020.

Murillo-Rincon AP, Klimovich A, Pemöller E, Taubenheim J, Mortzfeld B, Augustin R, et al. (2017) Spontaneous body contractions are modulated by the microbiome of Hydra. *Sci. Rep.* **7**(1). 15937. doi:10.1038/s41598-017-16191-x.

Nakatsuji T and Gallo RL (2012) Antimicrobial Peptides: Old Molecules with New Ideas. *J. Invest. Dermatol.* **132**(3). 887–895. doi:10.1038/jid.2011.387.

Nougué O, Gallet R, Chevin L-M and Lenormand T (2015) Niche Limits of Symbiotic Gut Microbiota Constrain the Salinity Tolerance of Brine Shrimp. *Am. Nat.* **186**(3). 390–403. doi:10.1086/682370.

Perez S (2006) Nitric oxide and cnidarian bleaching: an eviction notice mediates breakdown of a symbiosis. *J. Exp. Biol.* **209**(14). 2804–2810. doi:10.1242/jeb.02309.

Rahat M and Reich V (1984) Intracellular infection of aposymbiotic Hydra viridis by a foreign free-living Chlorella sp.: initiation of a stable symbiosis. *J. Cell Sci.* **65**. 265–77.

Rakoff-Nahoum S, Paglino J, Eslami-Varzaneh F, Edberg S and Medzhitov R (2004) Recognition of commensal microflora by toll-like receptors is required for intestinal homeostasis. *Cell* **118**(2). 229–241. doi:10.1016/j.cell.2004.07.002.

Rees TAV (1990a) The green hydra symbiosis and ammonium III. Characteristics of ammonium release by a high maltose-releasing symbiotic strain of Chlorella. *Proc. R. Soc. B Biol. Sci.* **242**(1305). 249–253. doi:10.1098/rspb.1990.0131.

Rees TAV (1990b) The green hydra symbiosis and ammonium IV. Methylammonium uptake by freshly isolated symbionts and cultured algae; evidence for low-ammonium concentration in the perialgal space. *Proc. R. Soc. B Biol. Sci.* **242**(1305). 255–259. doi:10.1098/rspb.1990.0132.

Rees TAV and Ellard FM (1989) Nitrogen conservation and the green hydra symbiosis. *Proc. - R. Soc. London, B* **236**(1283). 203–212. doi:10.1098/rspb.1989.0021.

Rees TA V. (1986) The Green Hydra Symbiosis and Ammonium I. The Role of the Host in Ammonium Assimilation and its Possible Regulatory Significance. *Proc. R. Soc. B Biol. Sci.* **229**(1256). 299–314. doi:10.1098/rspb.1986.0087.

Rees TA V. (1989) The Green Hydra Symbiosis and Ammonium II. Ammonium Assimilation and Release by Freshly Isolated Symbionts and Cultured Algae. *Proc. R. Soc. B Biol. Sci.* **235**(1281). 365–382. doi:10.1098/rspb.1989.0005.

Rees TA V., Shah N and Stewart GR (1989) Glutamine synthetase isoforms in the green hydra symbiosis. *New Phytol.* **111**(4). 621–623. doi:10.1111/j.1469-8137.1989.tb02355.x.

Reis AMM, Araújo SD, Moura RL, Francini-Filho RB, Pappas G, Coelho AMA, et al. (2009) Bacterial diversity associated with the Brazilian endemic reef coral Mussismilia braziliensis. *J. Appl. Microbiol.* **106**(4). 1378–1387. doi:10.1111/j.1365-2672.2008.04106.x.

Ritchie KB (2006) Regulation of microbial populations by coral surface mucus and mucus-associated bacteria. *Mar. Ecol. Prog. Ser.* **322**. 1–14. doi:10.3354/meps322001.

Roden LC and Ingle RA (2009) Lights, Rhythms, Infection: The Role of Light and the Circadian Clock in Determining the Outcome of Plant-Pathogen Interactions. *PLANT CELL ONLINE* **21**(9). 2546–2552. doi:10.1105/tpc.109.069922.

Ross NW, Firth KJ, Wang A, Burka JF and Johnson SC (2000) Changes in hydrolytic enzyme activities of naive Atlantic salmon Salmo salar skin mucus due to infection with the salmon louse Lepeophtheirus salmonis and cortisol implantation. *Dis. Aquat. Organ.* **41**(1). 43–51. doi:10.3354/dao041043.

Salinas I, Zhang Y-A and Sunyer JO (2011) Mucosal immunoglobulins and B cells of teleost fish. *Dev. Comp. Immunol.* **35**(12). 1346–65. doi:10.1016/j.dci.2011.11.009.

Salzman NH, Hung K, Haribhai D, Chu H, Karlsson-Sjöberg J, Amir E, et al. (2010) Enteric defensins are essential regulators of intestinal microbial ecology. *Nat. Immunol.* **11**(1). 76–83. doi:10.1038/ni.1825.

Sanders JG, Lukasik P, Frederickson ME, Russell JA, Koga R, Knight R, et al. (2017) Dramatic differences in gut bacterial densities correlate with diet and habitat in rainforest ants. *Integr. Comp. Biol.*, 705–722. doi:10.1093/icb/icx088.

Scheiermann C, Kunisaki Y and Frenette PS (2013) Circadian control of the immune system. *Nat. Rev. Immunol.*, 190–198. doi:10.1038/nri3386.

Sharon G, Sampson TR, Geschwind DH and Mazmanian SK (2016) The Central Nervous System and the Gut Microbiome. *Cell*, 915–932. doi:10.1016/j.cell.2016.10.027.

Sharon G, Segal D, Ringo JM, Hefetz A, Zilber-Rosenberg I and Rosenberg E (2010) Commensal bacteria play a role in mating preference of Drosophila melanogaster. *Proc. Natl. Acad. Sci.* **107**(46). 20051–20056. doi:10.1073/pnas.1009906107.

Shelomi M, Lo WS, Kimsey LS and Kuo CH (2013) Analysis of the gut microbiota of walking sticks (Phasmatodea). *BMC Res. Notes* **6**(1). 368. doi:10.1186/1756-0500-6-368.

Shimizu H, Koizumi O and Fujisawa T (2004) Three digestive movements in Hydra regulated by the diffuse nerve net in the body column. *J. Comp. Physiol. A* **190**(8). 623–30. doi:10.1007/s00359-004-0518-3.

Simonsen AK, Dinnage R, Barrett LG, Prober SM and Thrall PH (2017) Symbiosis limits establishment of legumes outside their native range at a global scale. *Nat. Commun.* **8**. 14790. doi:10.1038/ncomms14790.

Smith EM (2008) Neuropeptides as signal molecules in common with leukocytes and the hypothalamic-pituitary-adrenal axis. *Brain. Behav. Immun.* **22**(1). 3–14. doi:10.1016/j.bbi.2007.08.005.

Sorek M, Schnytzer Y, Waldman Ben-Asher H, Caspi VC, Chen CS, Miller DJ, et al. (2018) Setting the pace: Host rhythmic behaviour and gene expression patterns in the facultatively symbiotic cnidarian Aiptasia are determined largely by Symbiodinium. *Microbiome* **6**(1). 83. doi:10.1186/s40168-018-0465-9.

Sternberg EM (2006) Neural regulation of innate immunity: A coordinated nonspecific host response to pathogens. *Nat. Rev. Immunol.*, 318–328. doi:10.1038/nri1810.

Stilling RM, Dinan TG and Cryan JF (2014) Microbial genes, brain & behaviour - epigenetic regulation of the gut-brain axis. *Genes, Brain Behav.* **13**(1). 69–86. doi:10.1111/gbb.12109.

Stone EF, Fulton BO, Ayres JS, Pham LN, Ziauddin J and Shirasu-Hiza MM (2012) The circadian clock protein timeless regulates phagocytosis of bacteria in Drosophila. *PLoS Pathog.* **8**(1). e1002445. doi:10.1371/journal.ppat.1002445.

Sunagawa S, DeSantis TZ, Piceno YM, Brodie EL, DeSalvo MK, Voolstra CR, et al. (2009) Bacterial diversity and White Plague Disease-associated community changes in the Caribbean coral Montastraea faveolata. *ISME J.* **3**(5). 512–21. doi:10.1038/ismej.2008.131.

Šustr V, Stingl U and Brune A (2014) Microprofiles of oxygen, redox potential, and pH, and microbial fermentation products in the highly alkaline gut of the saprophagous larva of Penthetria holosericea (Diptera: Bibionidae). *J. Insect Physiol.* **67**. 64–69. doi:10.1016/j.jinsphys.2014.06.007.

Vaishnava S, Yamamoto M, Severson KM, Ruhn KA, Yu X, Koren O, et al. (2011) The Antibacterial Lectin RegIII Promotes the Spatial Segregation of Microbiota and Host in the Intestine. *Science (80-.).* **334**(6053). 255–258. doi:10.1126/science.1209791.

van Noort JM and Bsibsi M (2009) Toll-like receptors in the CNS: implications for neurodegeneration and repair. *Prog. Brain Res.*, 139–148. doi:10.1016/S0079-6123(09)17509-X.

Wang W, Barnaby JY, Tada Y, Li H, Tör M, Caldelari D, et al. (2011) Timing of plant immune responses by a central circadian regulator. *Nature* **470**(7332). 110–115. doi:10.1038/nature09766.

Watanabe Y, Tateno H, Nakamura-Tsuruta S, Kominami J, Hirabayashi J, Nakamura O, et al. (2009) The function of rhamnose-binding lectin in innate immunity by restricted binding to Gb3. *Dev. Comp. Immunol.* **33**(2). 187–97. doi:10.1016/j.dci.2008.08.008.

Wernegreen JJ (2012) Endosymbiosis. *Curr. Biol.* **22**(14). R555–R561. doi:10.1016/J.CUB.2012.06.010.

Whittome B, Graham RI and Levin DB (2007) Preliminary examination of gut bacteria from Neodiprion abietis (Hymenoptera: Diprionidae) larvae. *J. Entomol. Soc. Ontario* **138**. 49–63.

Williams JM, Duckworth CA, Burkitt MD, Watson AJM, Campbell BJ and Pritchard DM (2015) Epithelial Cell Shedding and Barrier Function. *Vet. Pathol.* **52**(3). 445–455. doi:10.1177/0300985814559404.

Xu Z, Parra D, Gómez D, Salinas I, Zhang Y-A, von Gersdorff Jørgensen L, et al. (2013) Teleost skin, an ancient mucosal surface that elicits gut-like immune responses. *Proc. Natl. Acad. Sci. U. S. A.* **110**(32). 13097–102. doi:10.1073/pnas.1304319110.

Young BC, Wu C-H, Gordon NC, Cole K, Price JR, Liu E, et al. (2017) Severe infections emerge from the microbiome by adaptive evolution. *doi.org* 116681. doi:10.1101/116681.

List of publications

Publications

Hamada M*, **Schröder K***, Bathia J, Kürn U, Fraune S, Khalturina M, Khalturin K, Shinzato C, Satoh N, Bosch TCG (2018) "Metabolic co-dependence drives the evolutionarily ancient *Hydra–Chlorella* symbiosis*"* ***eLife*** 7:e35122. doi: 10.7554/eLife.35122.

Augustin R*, **Schröder K***, Murillo-Rincón AP, Fraune S, Anton-Erxleben F, Herbst EM, Wittlieb J, Schwentner M, Grötzinger J, Wassenaar TM, Bosch TCG (2017). "A secreted antibacterial neuropeptide shapes the microbiome of *Hydra"* ***Nature Communications.*** 8:698. doi: 10.1038/s41467-017-00625-1.

Bosch TCG, Klimovich A, Domazet-Lošo T, Gründer S, Holstein TW, Jékely G, Miller DJ, Murillo-Rincón AP, Rentzsch F, Richards GS, **Schröder K**, Technau U, Yuste R (2017) Back to the Basics: Cnidarians Start to Fire. ***Trends Neurosci.***, 92–105. doi:10.1016/j.tins.2016.11.005.

Schröder K, Bosch TCG (2016). "The origin of mucosal immunity: lessons from the holobiont *Hydra"* ***mBio***. 7:e01184–16. doi: 10.1128/mBio.01184-16

Fraune S, Anton-Erxleben F, Augustin R, Franzenburg S, Knop M, **Schröder K**, Willoweit-Ohl D, Bosch TCG (2015) "Bacteria-bacteria interactions within the microbiota of the ancestral metazoan *Hydra* contribute to fungal resistance" ***The ISME Journal***. 9:1543–1556. doi: 10.1038/ismej.2014.239.

McMillan DGG, Ferguson SA, Dey D, **Schröder K**, Aung HL, Carbone V, Attwood GT, Ronimus RS, Meier T, Cook GM (2011) "A_1A_o-ATP synthase of *Methanobrevibacter ruminantium* couples sodium ions for ATP synthesis under physiological conditions*"* ***Journal of Biological Chemistry***. 286:39882–39892. doi:10.1074/jbc.M111.281675.

Manuscripts

Schröder K*, Fraune S*, Hamada M, Kürn U, Anton-Erxleben F, Künzel S, Bosch TCG. Symbiotic algae in *Hydra viridissima* contribute to shape the host-specific microbiota in a light-dependent manner. (*in preparation*)

(* These authors contributed equally to the work.)

Acknowledgements

An erster Stelle bedanke ich mich herzlich bei Prof. Thomas Bosch für die Betreuung mit den vielen inspirierenden, motivierenden und kritischen Diskussionen. Darüber hinaus möchte ich mich für das von Vertrauen und Wertschätzung geprägte Verhältnis bedanken. Auch nachdem mein Weg in die Medizin führte, konnte ich mir deiner Unterstützung immer sicher sein. Danke!

Für die ausgezeichnete wissenschaftliche Betreuung dieser Arbeit gilt mein besonderer Dank Dr. René Augustin und Dr. Sebastian Fraune, die mir mit großem Fachwissen stets motivierend zur Seite standen. Vielen Dank für die Diskussionen zu Experimenten und Manuskripten, die entscheidend zu dieser Arbeit beigetragen haben. René, danke, dass ich mich jederzeit auf deine Hilfe bei allen wissenschaftlichen und nicht-wissenschaftlichen Problemen verlassen konnte. Sebastian, danke, dass du immer ein offenes Ohr für all meine Fragen hattest und dir stets die Zeit genommen hast sie zu beantworten. Dein Rat hat mich stets vorangebracht.

Im Rahmen dieser Doktorarbeit habe ich die Bachelor-Arbeiten von Carina Kreutzer und Jessica Zimmermann betreut, denen ich für ihre Unterstützung im Glykokalyx-Projekt danken möchte. Mein Dank gebührt zudem Dr. Christian Treitz und Prof. Andreas Tholey für die massenspektrometrische Analyse der Glykokalyx sowie Santiago Insua für die Unterstützung bei der Analyse der Transkriptomdaten. Dr. Andrea Murillo-Rincón, Dr. Trudy Wassenaar und Prof. Joachim Grötzinger danke ich für die Zusammenarbeit im NDA-1 Projekt, sowie Dr. Ulrich Kürn für die Unterstützung im „Green Hydra“-Projekt. Mein besonderer Dank gilt an dieser Stelle Dr. Mayuko Hamada für die enge und fruchtbare Zusammenarbeit über 9000 km Entfernung.

Insbesondere möchte ich mich bei Dr. Friederike Anton-Erxleben für ihre exzellente Unterstützung bei den mikroskopischen Analysen und die anregenden Diskussionen bedanken. Antje Thomas möchte ich meinen Dank für die kompetente Hilfe bei der Herstellung histologischer Präparate aussprechen. Eva-Maria Herbst, Doris Willoweit-Ohl und Maria Franck danke ich für die technische und organisatorische Unterstützung im Labor. Großer Dank gebührt außerdem Jörg Wittlieb für die Transfektion zahlreicher *Hydra*-Embryonen und die netten Gespräche im Hydra-Raum, die lange Arbeitstage oft kürzer gemacht haben. Besonders hervorheben möchte ich zudem meinen Büro-‚Homie‘ Javier López und Dr. Cleo Pietschke, die mich durch die Zeit der Doktorarbeit begleitet haben und den Labor-Alltag immer zu einem großen Spaß gemacht haben. Anika Hintz danke ich für ihre großartige Unterstützung in allen bürokratischen Angelegenheiten, vor allem beim ‚final countdown‘, und für die Freundschaft, die uns verbindet.

Darüber hinaus bedanke ich mich herzlich bei allen weiteren Mitarbeitern der Arbeitsgruppe für die angenehme, offene Arbeitsatmosphäre und das kollegiale Miteinander. Ihr alle habt die Jahre während meiner Doktorarbeit zu einer ganz besonderen Zeit gemacht!

Von Herzen bedanke ich mich bei Max Brück, Dr. Christina Lange, Jessica Zimmermann und Carina Kreutzer. Unsere Wege haben sich alle irgendwann in der AG Bosch gekreuzt und aus Kollegen wurden gute Freunde, die auch in schwierigen Zeiten immer für mich da waren.

Mein größter Dank gebührt meiner Familie, insbesondere meinen Eltern, die mir diesen Bildungsweg ermöglicht haben und mich jederzeit in meinen Entscheidungen unterstützt haben.

Erklärung

Hiermit erkläre ich, dass ich die vorliegende Dissertation nach den Regeln guter wissenschaftlicher Praxis eigenständig verfasst und keine anderen als die angegebenen Hilfsmittel und Quellen benutzt habe. Dabei habe ich keine Hilfe, außer der wissenschaftlichen Beratung durch meinen Doktorvater Prof. Dr. Dr. h.c. Thomas C. G. Bosch in Anspruch genommen.

Des Weiteren erkläre ich, dass ich noch keinen Promotionsversuch unternommen habe und mir kein akademischer Grad entzogen wurde.

Teile dieser Arbeit wurden bereits veröffentlicht.

Kiel, den 20.12.2018

_____

Katja Schröder